FORSCHUNGSZENTRUM JÜLICH GmbH

Institut für Chemie und Dynamik der Geosphäre 4: Erdöl und Geochemie

The Fate of Oil and Gas in a Constrained Natural System – Implications from the Bakken Petroleum System

Gary Patrick Albert Muscio

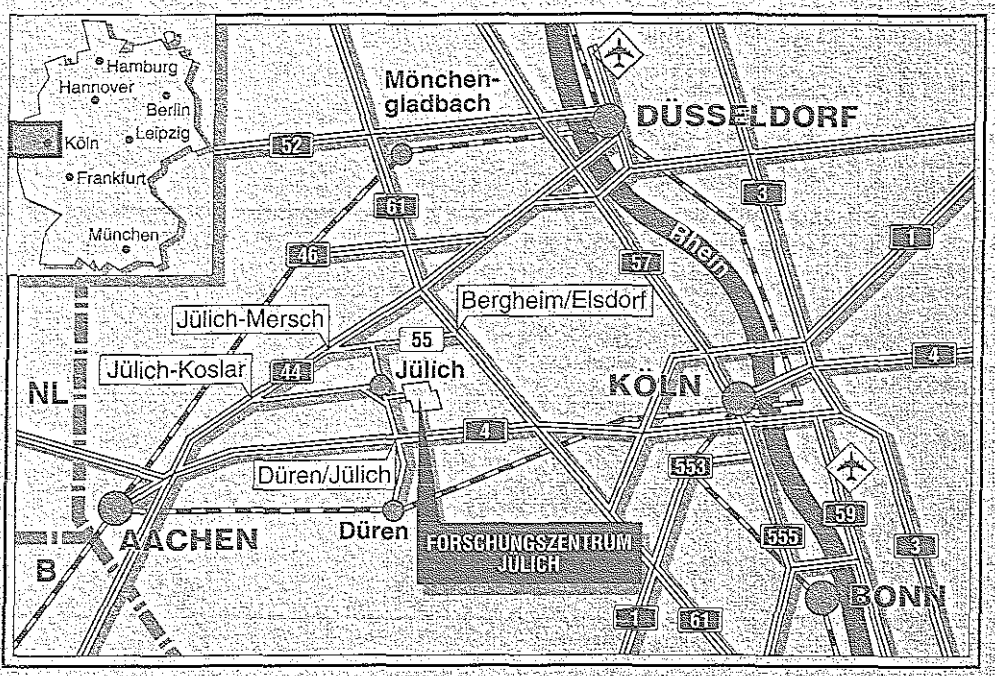

Berichte des Forschungszentrums Jülich ; 3094
ISSN 0944-2952
Institut für Chemie und Dynamik der Geosphäre 4 : Erdöl und Geochemie Jül-3094
D 82 (Diss. RWTH Aachen)

Zu beziehen durch : Forschungszentrum Jülich GmbH · Zentralbibliothek
D-52425 Jülich · Bundesrepublik Deutschland
Telefon : 02461/61-6102 · Telefax : 02461/61-6103 · Telex : 833556-70 kfa d

The Fate of Oil and Gas in a Constrained Natural System – Implications from the Bakken Petroleum System

Gary Patrick Albert Muscio

TABLE OF CONTENTS

Acknowledgements

It is virtually impossible to thank and acknowledge everybody who contributed to the completion of this dissertation.

Firstly, I would like to thank Dr. Brian Horsfield for suggesting the PhD project and for his guidance and supervision throughout the study. I am also very grateful to Prof. Dietrich H. Welte and Prof. Monika Wolf for reviewing the dissertation and their invaluable help during its completion.

The present study would not have been possible without the sponsorship by Conoco Inc., U.S.A. I wish to thank Carolyn Thompson-Rizer and Eric Michael from Conoco, Ponca City for providing valuable information on the Bakken petroleum system and Lung-Chuan Kuo, Janina Rafalska, John Davies and Roger Woods for taking care of Brian and me during our stay in Ponca City.
I also appreciated the help of Dan Burggraf from Conoco, Houston during the initial stage of the study.

I am indebted to Julie LeFever of the Wilson M. Laird Core and Sample Library of the North Dakota Geological Survey for providing the samples and data pertaining to the Bakken Shale.

I would also like to express my gratitude to all the scientists and technicians at KFA for their assistance and support in the analysis of the samples and interpretation of the data.

Christian Zwach and Michael Erdmann from KFA contributed to the present study during numerous stimulating discussions not only on scientific issues. Thank you very much for the good time we had together.

I am very grateful to Juraj Francú (Geological Survey Brno, Czech Republic) for performing the XRD analyses and to Math Kohnen (KSEPL, Rijswijk, The Netherlands) for carbon isotope analyses.

Zusammenfassung

Einleitung und Zielsetzung

Die Prozesse und Phänomene der natürlichen Bildung und Migration von Erdöl und Erdgas laufen während der Katagenese sowohl zeitlich als auch räumlich zu großen Teilen parallel zueinander ab und prägen die Eigenschaften und das Verteilungsmuster der Kohlenwasserstoffe in den Speichergesteinen. Die Entwicklung von quantitativen geochemischen Modellen, die in der Lage sind, diese Prozesse zu charakterisieren, führte zu einem besseren Verständnis der Erdölgenese und -migration. Trotzdem ist es in hohem Maße erforderlich, anhand eines *natürlichen* Erdölsystems umfassend und detailliert Einblick zu gewinnen in die Zusammensetzung des organischen Materials, in Phasenbeziehungen (Sediment-phase/Fluidphase), sowie in die rheologischen Eigenschaften des Kohlenwasserstoffbildungs- und Transportsystems, um die Prozesse der Bildung, Migration und Speicherung von Erdöl und Erdgas besser zu verstehen. Diese Vorgabe setzt natürlich voraus, daß das ausgewählte Untersuchungsgebiet ein integriertes System darstellt, welches alle Prozesse umfaßt vom Einsetzen der Genese der Kohlenwasserstoffe bis zu ihrer Speicherung.
Das Bakken-Erdölsystem des Williston Basin (U.S.A./Kanada) besitzt Attribute, die es als ein derartiges integriertes System auszeichnen:

1. Das weitgespannte Reifegradspektrum des Bakken Shale, der sich in einen oberen und unteren Tonsteinhorizont gliedert, umfaßt alle Stadien der Katagenese vom Einsetzen der Kohlenwasserstoffgenese über deren Hauptphase bis zum Ende. Infolgedessen sind entsprechende Muttergesteinsproben geprägt durch progressive Kohlenwasserstoffgenese und -expulsion.
2. Mutter- und Speichergestein sind räumlich sehr eng miteinander vergesellschaftet, so daß das Bakken-Erdöl keiner sekundären Migration im strengen Sinne unterworfen war. Des weiteren liegen viele Anhaltspunkte dafür vor, daß das Bakken-Erdölsystem ein "isoliertes" System darstellt, welches nicht von Ölen fremder Herkunft beeinflußt worden ist. Klüfte dienen als Speichermedium für Bakken-Erdöl (Meissner, 1978; Finch, 1969). Bohrlochmessungen ergaben, daß der Porenraum des Bakken-Muttergesteins mit in-situ gebildeten Kohlenwasserstoffen gesättigt ist und daß der hohe Sättigungsgrad zu Überdrücken führt (Meissner, 1978). Jedoch sind sowohl der Ursprung dieser Überdrucksituation als auch ihre beckenweite Ausdehnung noch umstritten.
3. Das Kerogen weist im gesamten Untersuchungsgebiet eine sehr gleichförmige Zusammensetzung auf, so daß Einflüsse auf das Verhalten der Erdölgenese und -migration infolge von Faziesunterschieden vernachlässigbar sind. Zusätzlich erlaubt dieser Umstand den direkten Vergleich der natürlichen Reifeserie mit der im Labor künstlich erzeugten Reifesequenz.
4. Aus bisherigen Veröffentlichungen steht eine umfassende Datenbasis zur Verfügung.

Die Muttergesteinsproben, die ausschließlich Bohrkernen entnommen wurden, sowie die Rohölproben wurden in der vorliegenden Studie einer eingehenden Untersuchung und Analytik unterworfen mit der Zielsetzung, folgende Aspekte zu beleuchten:

- Entwicklung der Erdöl- und Erdgasgenese in Abhängigkeit der Reifezunahme.
- Primäre Migration und Verteilung von Rohöl in einem eingeschränkten natürlichen System.
- Vorkommen und Entstehung von Gasen in unreifen Muttergesteinen.
- Vergleich der natürlichen Reifesequenz mit simulierten Reifungsexperimenten im Labor.

Analysenmethoden

Der Analysengang begann zunächst mit der TOC-Bestimmung und Rock-Eval-Analyse der Muttergesteinsproben, die zusammen mit den Ergebnissen der organischen Petrologie Aufschluß gaben über Reife und Kerogentyp. Es konnte bestätigt werden, daß der Kerogentyp II deutlich vorherrscht und daß sich das Reifespektrum des vorliegenden Probensatzes von 0.3 bis 1.6% R_o erstreckt. Die umfassende Charakterisierung sowohl des Kerogens als auch der flüchtigen Komponenten ermöglichte es, die Probenanzahl für weitere detailliertere Analysen auf ein repräsentatives Maß zu reduzieren. Dieser ausgewählte Probensatz wurde einer breitgefächerten organisch-geochemischen, petrophysikalischen und mineralogischen Analytik unterzogen.
Mittels der MSSV-Technik (Horsfield et al., 1989) wurden sowohl die Pyrolyse-Gaschromatographie, die Thermovaporisation-Gaschromatographie als auch die künstlichen Reifungsexperimente durchgeführt. Zusätzlich wurde das thermisch mobilisierte Material massenspektrometrisch untersucht und seine Isotopenzusammensetzung ($\delta^{13}C$) ermittelt. Das Kerogen wurde außerdem mittels Infrarotspektroskopie analysiert. Ausgesuchte Proben wurden mit der Flow Blending Methode extrahiert und die Lösungsmittelextrakte sowie die Rohölproben danach in ihre Fraktionen aufgetrennt, bevor diese gaschromatographisch als auch gaschromatographisch-massenspektrometrisch untersucht wurden. Petrophysikalische Untersuchungen umfaßten die Bestimmung der Permeabilität an ausgesuchten Kernproben und die experimentelle Simulation der Erdölgenese unter lithostatischem Druck. Schließlich wurde an einer Auswahl von Proben Röntgendiffraktometrie durchgeführt.

Analysenergebnisse

Die quantitative Auswertung der Pyrolyse-Gaschromatogramme hat gezeigt, daß das Kerogen des Bakken Shale ein Erscheinungsbild hat, das typisch ist für liptinitreiche marine Muttergesteine (überwiegend Paraffine, untergeordnet Aromaten). Die Pauschalzusammensetzung ändert sich nicht signifikant mit fortschreitender Reifung. Ein deutlicher Rückgang im Gehalt an Monoaromaten zwischen 0.57% und 0.68% R_o könnte jedoch gegen einen einheitlichen Kerogentyp und für das Vorhandensein von mindestens zwei verschiedenen Kerogentypen sprechen.
Mehrere Komponentengruppen der Lösungsmittelextrakte offenbaren zum einen Maximalausbeuten und zum anderen eine hohe Variabilität für einzelne Bohrungen innerhalb des Reifeintervals 0.8% bis 1.0%R_o, nämlich Gesamtextraktausbeute, sowie Ausbeute der gesättigten und aromatischen Kohlenwasserstofffraktion. Dabei hat der obere Bakken Shale einer Bohrung stets geringere Gehalte der jeweiligen Komponentengruppen als der untere Bakken Shale. Dieser Befund könnte anzeigen, daß beide Schichtglieder in bezug auf Expulsion und Migration

unterschiedliche Eigenschaften haben. Das Verteilungsmuster der n-Alkane (Dominanz von C_{12-18}) ist einheitlich über das gesamte Reifespektrum und zeigt keine Bevorzugung von ungeradzahligen n-Alkanen.
Der Gehalt einzelner Biomarkerverbindungen der gesättigten Kohlenwasserstofffraktion und deren Verhältnisse zueinander verdeutlichten, daß sowohl die Rohölproben, als auch der Großteil der Lösungsmittelextrakte der Muttergesteinsproben das Stadium erhöhter thermischer Überprägung erreicht haben.
Die Isotopenzusammensetzung der Gasfraktion (C_{1-5}) der thermisch mobilisierbaren Kohlenwasserstoffe hat gezeigt, daß diese thermogener und nicht biogener Natur ist. Die Gaskonzentration zeigt eine gute Korrelation mit dem TOC-Gehalt bei geringreifen Proben (< 0.8%R_o). Oberhalb von 0.8% R_o scheint der Bakken Shale sein Rückhaltevermögen für Gas verloren zu haben und das flüchtige organische Material, vorzugsweise die n-Alkane, ist beträchtlichen Fraktionierungsprozessen unterworfen. Die residuale Ölphase ist relativ angereichert an Methylzyklohexan, aber abgereichert im bezug auf leichtere Alkylzykloalkane (Methylzyklopentan und Dimethylzyklopentan). Weiterhin offenbart das thermisch mobilisierbare organische Material der reifen (>0.6% R_o) Proben hohe Gehalte an Zykloalkanen (Methylzyklohexan) und Aromaten (alkylierte Naphthaline) trotz des stark paraffinischen Erscheinungsbildes des entsprechenden Kerogens (>0.6%R_o).
Die Messung der Bakken Shale-Permeabilität für Wasser als Durchflußmedium ergab sehr niedrige Werte (nanoDarcy-Bereich). Die Ergebnisse für Proben unterschiedlicher Reife offenbarten keine gesetzmäßige Abhängigkeit vom Grad der Kerogenumwandlung.

Diskussion und Interpretation

Berechnungen zur Massenbilanz (Cooles et al., 1986), die an Bakken Shale-Proben, die ein Reifespektrum von 0.3% bis 1.1% R_o abdecken, durchgeführt wurden, haben gezeigt, daß das Hauptstadium der Erdölbildung in einer sehr frühen Phase der Katagenese (ca. 0.4% bis 0.8% R_o) stattfand. Somit ist das Kohlenwasserstoffbildungspotential in den Beckenbereichen, wo z.Zt. Bakken-Erdöl gefördert wird (> 0.8% R_o), schon weitgehend erschöpft. Jedoch geben die Massenbilanzierungen auch Anlaß zur Vermutung, daß im Laufe der natürlichen Reifung und Erdölgenese inerter Kohlenstoff gebildet worden ist, der sich kumulativ im residualen Kerogen angereichert hat. Die aromatischen Verbindungen, die in relativ hohen Konzentrationen in der flüchtigen Phase auftreten, könnten infolge von Kondensationsprozessen in das inerte Kerogen eingebaut worden sein. Dieser Fall würde dazu führen, daß bei entsprechenden Massenbilanzierungen der Grad der Kerogenumwandlung überschätzt werden würde.
Obwohl der Bakken Shale nach der chemischen und petrologischen Pauschalzusammensetzung typisch marines Kerogen enthält, besitzt dieses eine molekulare Struktur, die in der Lage ist, verstärkt gasförmige Kohlenwasserstoffe zu produzieren. Dabei hat das künstliche Aufheizen von unreifen Proben im geschlossenen System gezeigt, daß das Bakken-Kerogen unter experimentellen Bedingungen schon bei relativ geringer thermischer Belastung vorzugsweise Gas generiert. Dieses ungewöhnlich hohe Gasbildungspotential könnte in Zusammenhang stehen mit der Tatsache, daß das unreife Kerogen zu einem großen Anteil aus diaromatischen Karotenoidstrukturen besteht, als deren biologische Vorläufer grüne photosynthetische

Schwefelbakterien angenommen werden. Da die niedrigmolekularen Kohlenwasserstoffe in für diese Art Muttergesteine ungewöhnlichen hohen Konzentrationen vorkommen, könnten sie bei der Expulsion eine bedeutende Rolle spielen, und zwar in Form der Lösung der hochmolekularen Verbindungen in leichten Kohlenwasserstoffen und der diffusiven Migration.
Die Reifebestimmung der Bakken-Rohöle mittels molekularer Reifeparameter (Aromaten, Biomarker) ergab relativ hohe Werte. Die Werte, die normalerweise den Reifegrad der Erdölabgabe (Expulsion) aus dem Muttergestein anzeigen, liegen jenseits der Hauptphasen von Genese und Expulsion im Bakken-Erdölsystem. Unter der Voraussetzung, daß die molekularen Reifeparameter durch die Expulsion nicht fraktioniert worden sind, könnte die Diskrepanz anzeigen, daß die Öle im Anschluß an die Hauptphase der Genese und Expulsion einer weiteren Reifung unterlagen.
Die Hauptphase der Kerogenumwandlung wird begleitet von einer sehr effizienten Erdölexpulsion. Bereits bei 0.6% R_o ist das Maximum an Expulsionseffizienz (95%) erreicht. Dieser äußerst effiziente Transport der neu gebildeten Kohlenwasserstoffe setzt natürlich voraus, daß entsprechende Migrationsbahnen und -mechanismen zur Verfügung stehen. Im Gegensatz zum weitverbreiteten Phasenflußmodell als dem dominierenden Expulsionsmechanismus für TOC-reiche, dichte Muttergesteine, bietet der Bakken Shale Anhaltspunkte dafür, daß der Mechanismus des diffusiven Transportes in großem Maße beteiligt ist an der raschen und effizienten Expulsion von Kohlenwasserstoffen aus den Bakken Shale-Muttergesteinen. Dabei kommt es zu Fraktionierungen auf molekularer Ebene. Das gut ausgebildete und durchgängige Kerogennetzwerk könnte als geeignete Expulsions-/Migrationsbahn dienen. Eine solch effiziente Abgabe der generierten Kohlenwasserstoffe von den Bakken Shale-Horizonten an die liegenden und hangenden Schichten spricht dafür, daß die letzteren den eigentlichen Speicher darstellen, und daß das verallgemeinerte Postulat eines "In-Situ"-Reservoirs (Price & LeFever, 1992) in Frage gestellt werden muß. Im Falle des mittleren Siltsteines der Bakken Formation bieten Literaturdaten (z.B. LeFever et al., 1991) deutliche Hinweise dafür, daß dieser Horizont, der vom oberen und unteren Bakken Shale begrenzt wird, durchaus die entsprechenden petrophysikalischen Eigenschaften (erhöhte Porosität und Permeabilität) besitzt, die ihn als geeignetes Reservoir auszeichnen würden.
Es hat sich gezeigt, daß die natürliche und die künstliche Reifesequenz sowohl qualitative als auch quantitative Gemeinsamkeiten aufweisen. Die Verwendung von Parametern, die eine reifegradspezifische Entwicklung zeigen, ließ eine Unterteilung der *simulierten* Reifeserie in Reifezonen zu. Diese Reifezonierung ermöglichte eine Kalibrierung des *natürlichen* Systems. Somit konnte die molekulare Zusammensetzung von natürlichen Produkten in Abhängigkeit der Reife vorhergesagt und bestimmt werden, in welchem Ausmaß und in welcher Phase der Reifung Expulsions- und Migrationseffekte eine Rolle gespielt haben.

Die Bewertung und Interpretation der Resultate der vorliegenden Arbeit hat ergeben, daß die Kombination aus frühzeitiger, effizienter Expulsion und anschließender In-Situ-Reifung ausschlaggebend war für die Ausprägung des Bakken-Erdöls zu einem ausgesprochenen Leichtöl. Dies wurde zusätzlich durch die eingeengte Geometrie des Bakken-Erdölsystems begünstigt, in dem lateral und vor allem vertikal nur sehr kurze Migrationsbahnen zur Verfügung standen und dadurch das Muttergestein und Erdöl in bezug auf Versenkungs- und Temperaturgeschichte die gleiche Entwicklung durchliefen.

Das Schicksal des Bakken-Erdöls in Abhängigkeit von der Zeit sowie die räumlichen Umverteilungsprozesse werden auf der Basis der Ergebnisse der vorliegenden Studie in einem 4-Phasen-Modell erläutert:

Die **erste Phase** umfaßt die effiziente und frühzeitig abgeschlossene Abgabe der neu gebildeten Kohlenwasserstoffe aus dem Bakken-Muttergestein an das Liegende und Hangende. Die Unterschiede in der Pauschalzusammensetzung zwischen Muttergesteinsextrakten (asphaltenhaltig) und Bakken-Rohölen (nahezu asphaltenfrei) sind vermutlich auf einen komponentenspezifischen Fraktionierungsprozeß zurückzuführen, in dessen Ablauf mobile, relativ unpolare Fraktionen (gesättigte Kohlenwasserstoffe, Aromaten und Harze) das Muttergestein verlassen, während hochmolekulare Asphaltene zurückbleiben. Diese an Asphaltenen arme Erdölphase wird dann in einem Reservoir gespeichert. Dazu stehen der lokal begrenzte Sanish Sandstone (Finch, 1969; Meissner, 1978) und der beckenweit vorhandene mittlere Siltstein zur Verfügung. Die guten Reservoireigenschaften des letzten (LeFever et al., 1991) sprechen dafür, daß dieses Sediment das eigentliche Bakkenreservoir darstellt.

Die **zweite Phase** beginnt, nachdem das Hauptstadium der Genese und Expulsion beendet ist, die Versenkung und die damit einhergehende Reifung jedoch noch andauern. In diesem Post-Genese/-Expulsionsstadium wird das Bakken-Rohöl einer In-Situ-Reifung unterworfen, die seine Zusammensetzung deutlich ändert. Hohe Werte für aromatische Reifeparameter zeigen dies an. Zusätzlich gibt es Anhaltspunkte dafür, daß das Gas-Öl-Verhältnis (GOR) aufgrund von bereits einsetzenden Crack-Reaktionen zu höheren Werten hin verschoben wird. Alle diese Phänomene werden dadurch unterstützt, daß die Migrationsbahnen im Bakken-Erdölsystem stark eingeengt sind.

Die thermische Ausdehnung der gespeicherten Öle im Zuge der fortschreitenden Reifung stellt den wichtigsten Prozeß der **dritten Phase** dar. Hierbei nimmt die spezifische Dichte des Öls infolge der Temperaturzunahme ab, aber das Volumen nimmt zu. Wenn diese thermische Ausdehnung nicht kompensiert wird durch eine Verringerung der mechanischen Kompaktion (Auflastdruck) und/oder durch eine Zunahme der Permeabilität, dann erfolgt eine Druckzunahme im System. Dieses Phänomen wird durch die begrenzte Reservoirkapazität des mittleren Siltsteines verstärkt. Das ist damit zu erklären, daß eine Volumeneinheit dieses Gesteins gute bis sehr gute Reservoireigenschaften besitzt, das beckenweite *Gesamt*volumen an mittlerem Silstein jedoch aufgrund der geringen Mächtigkeit relativ klein ist. Eine Massenbilanz für das Gesamtvolumen an generiertem Bakken-Rohöl (Webster, 1984; Price & LeFever, 1994) und den potentiell verfügbaren Porenraum im mittleren Siltstein (LeFever et al., 1991) könnte anzeigen, daß tatsächlich eine deutliche Diskrepanz zwischen Speicherkapazität und Ölaufkommen besteht. Ein derartiges Konzept setzt natürlich voraus, daß der laterale und vertikale Bewegungsspielraum für das Öl stark eingeengt ist.

In der **vierten Phase**, die direkt an die dritte Phase anschließt, erfolgt aufgrund des Druckanstieges im Reservoir (thermische Ausdehnung) und seines begrenzten Speichervolumens eine Migration des Erdöls vom mittleren Siltstein zurück in das Muttergestein. Ein derartiger Prozeß könnte die erhöhten Gehalte an Lösungsmittelextrakten in einzelnen Bohrungen der post-genetischen Zone des Untersuchungsgebietes erklären. Sowohl die Pauschal- als auch die molekulare Zusammensetzung der entsprechenden Kohlenwasserstoffphasen (Rohöl bzw. Bitumen) liefern deutliche Hinweise für einen derartigen Vorgang. Die unterschiedlichen Verteilungsmuster für Asphaltene und Harze in den Bohrungen mit erhöhten Lösungs-

mittelextrakten könnten auch durch das Schema der Reimprägnation erklärt werden. Demgemäß werden die Asphaltene im Muttergestein zurückgehalten und sind Teil des residualen Extrakts, während die mobileren Harze sowie die gesättigte und aromatische Fraktion als Teil des Rohöls den Bakken Shale zunächst verlassen (erste Phase), um dann später im Anschluß an die dritte Phase wieder in das Muttergestein zurückzukehren. Eine auf der Grundlage dieses Konzeptes durchgeführte Massenbilanzierung für die Fraktionen der Lösungsmittelextrakte ergab, daß in einer Bohrung 70% des Bitumens auf den Prozeß der Reimprägnation zurückzuführen ist.

Aufgrund dieser Theorie kann angenommen werden, daß die gegenwärtige Überdrucksituation im Bakken-Erdölsystem ein lokal begrenztes Phänomen darstellt und nicht auf einen beckenweiten Maßstab extrapoliert werden kann. Das Druckverhalten wird gesteuert durch die Qualität des Reservoirs (Speicherkapazität) im Liegenden und Hangenden und der eingeengten Geometrie des Erdölsystems bzgl. weiträumiger lateraler und vertikaler Migrationswege.

Abstract

When petroleum is produced from its reservoir at present day, it has already been submitted to a complex array of natural processes, which have left their imprint on its chemical and physical properties. These processes involve the generation of petroleum in its source rock as a function of thermal evolution, and its migration to the reservoir. In order to achieve a better understanding of the effects that these processes have on the nature and occurrence of petroleum, it is crucial to investigate a study area that represents an integrated system encompassing all processes from the beginning of crude oil formation to entrapment. The Bakken Shale petroleum system of the Williston Basin (U.S.A./Canada) appears to fulfil these requirements as it covers a broad range of maturity incorporating all stages of catagenesis, and source and reservoir are closely associated, i.e. Bakken petroleum has not been submitted to long secondary migration routes. Combined with a basinwide uniformity in kerogen type, the latter feature constrains the broad scope of potential influences, and therefore the Bakken petroleum system is an ideal candidate to study petroleum generation, its expulsion and migration under natural conditions.

By using a selected set of wells/core samples which were considered to be representative for the entire Bakken petroleum system based on comprehensive screening analyses on both kerogen and bitumen, the present study focussed on the following principal aspects: (1) Evolution of petroleum generation as a function of maturation; (2) Primary migration and distribution of crude oil in a constrained natural system; (3) Occurrence of gas in the immature zone; (4) Evaluation of the natural maturity series with simulation experiments.

Mass balance calculations on Bakken Shale samples have revealed that the main phase of petroleum formation took place very early during catagenesis (ca. 0.4% to 0.8% R_o) and that its potential has already been realized in those areas of the basin which currently produce from the Bakken reservoirs. Expulsion efficiencies appear to be very high as well, whereby diffusion of hydrocarbons via a well-developed and continuous organic matter network may have played an important role, as suggested by compound-specific fractionation effects encountered especially in n-alkane products. Such efficient removal of petroleum from the shale units indicates that formations over- and underlying the Bakken Shale may represent the principal reservoirs and that the generalized postulate of an in-source reservoir has to be reconsidered. The hypothesized process of reimpregnation of petroleum from the reservoir back into the source rock system may account for locally occurring high concentrations of solvent extractable organic matter in Bakken Shales. The absence of a typical oil generation curve during the main stage of crude oil formation may elucidate that abnormally high reservoir pressures encountered in the Bakken Formation are not a basinwide phenomenon, but may be restricted to local areas.

The discrepancy between the maturity of peak expulsion and the maturity of crude oils based on molecular parameters implies that the high-quality, light oil character is controlled by significant post-generation and post-expulsion in-situ thermal alteration. This process was supported by the restricted lateral and vertical migration ranges in the Bakken petroleum system.

Despite being classified as a typical hydrogen-rich kerogen from bulk chemistry and petrology, the Bakken Shale shows an enhanced capability of generating gaseous hydrocarbons throughout maturation. At low levels of thermal evolution (< 0.7% R_o), the gas apparently is adsorbed on the organic matter. The coincidence of decreasing gas yields with the main phase of hydrocarbon expulsion suggests that low-molecular-weight compounds play a vital role in expulsion mechanisms in that high-molecular-weight species are dissolved in the light products and removed via diffusive transport.

The natural and artificial maturity sequences both have quantitative and qualitative features in common. The maturity related evolution of individual ratios in the residues of both lab and natural systems allow the calibration of the latter in terms of maturity zones. This approach is useful for the compositional prediction of natural products in the absence of expulsion and migration effects.

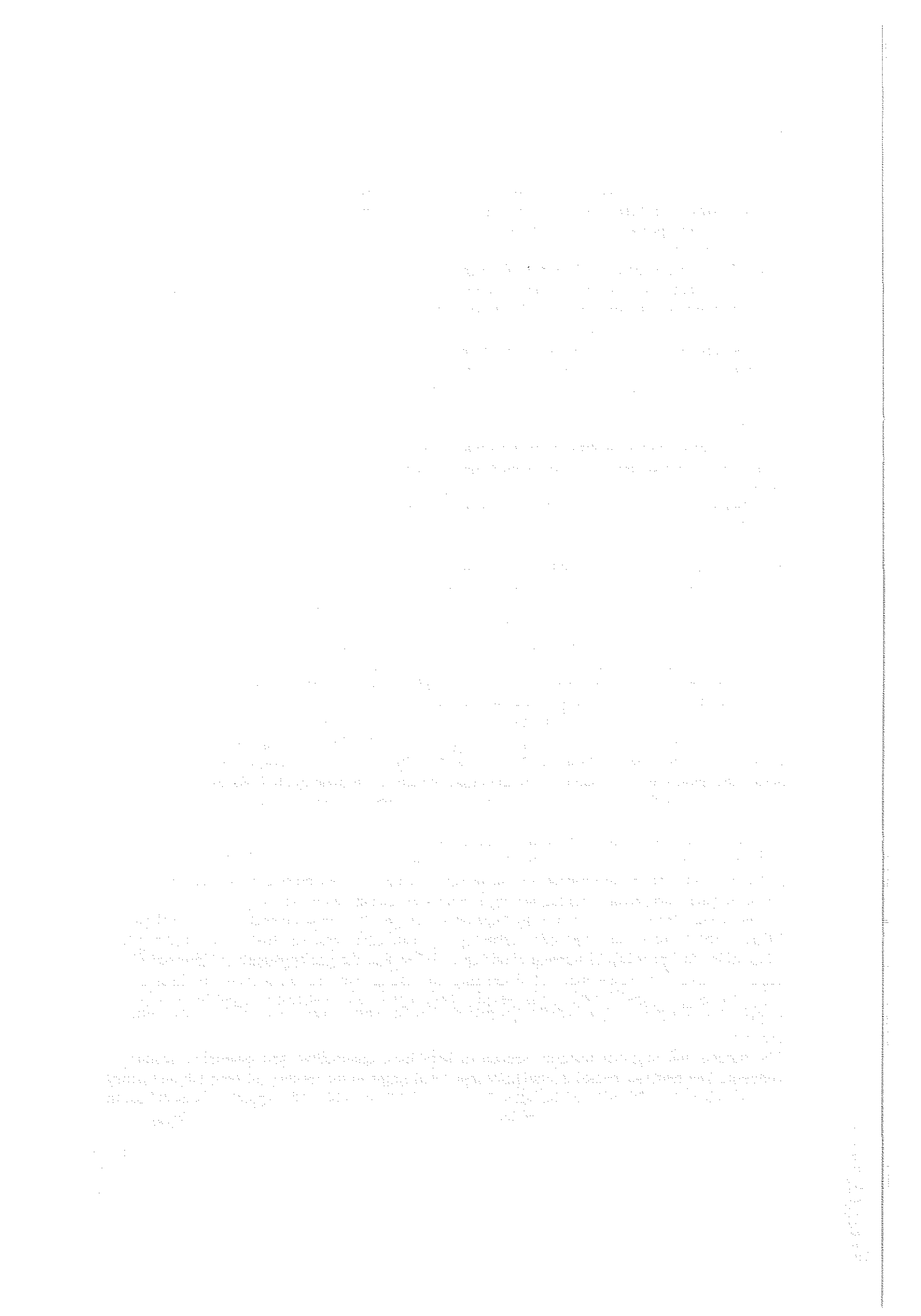

List of Abbreviations Used in Text

ARO	aromatic hydrocarbon fraction
ASP	asphaltenes
BZ	benzene
CPI	carbon preference index
DMCP	dimethylcyclopentane
DTF	Devonian Three Forks
GC	gas chromatography
GC-MS	gas chromatography-mass spectrometry
GOR	gas-oil ratio
HI	Rock-Eval hydrogen index
IR	infrared
lBK	lower Bakken Shale
LHCPI	light hydrocarbon preference index
LP	Lodgepole Formation
mBK	middle Bakken member
MCH	methylcyclohexane
MCP	methylcyclopentane
MPI-1	methylphenanthrene index 1
MPLC	medium pressure liquid chromatography
MPR-3	methylphenanthrene ratio 3
MPX	meta-/paraxylene
MSSV	micro scale sealed vessel
NMR	nuclear magnetic resonance
OI	Rock-Eval oxygen index
PEE	petroleum expulsion efficiency
PGI	petroleum generation index
py-gc	pyrolysis-gas chromatography
REE	relative expulsion efficiency
RES	resins
SAT	saturated hydrocarbon fraction
T	toluene
t'vap-gc	thermovaporisation-gas chromatography
t'vap-gc-IR-MS	thermovaporisation-gas chromatography-isotope ratio-mass spectrometry
t'vap-gc-MSD	thermovaporisation-gas chromatography-mass specific detection
TMB	1,2,3,4-tetramethylbenzene
TNR-2	trimethylnaphthalene ratio 2
TOC	total organic carbon
uBK	upper Bakken Shale
XRD	x-ray diffraction analysis

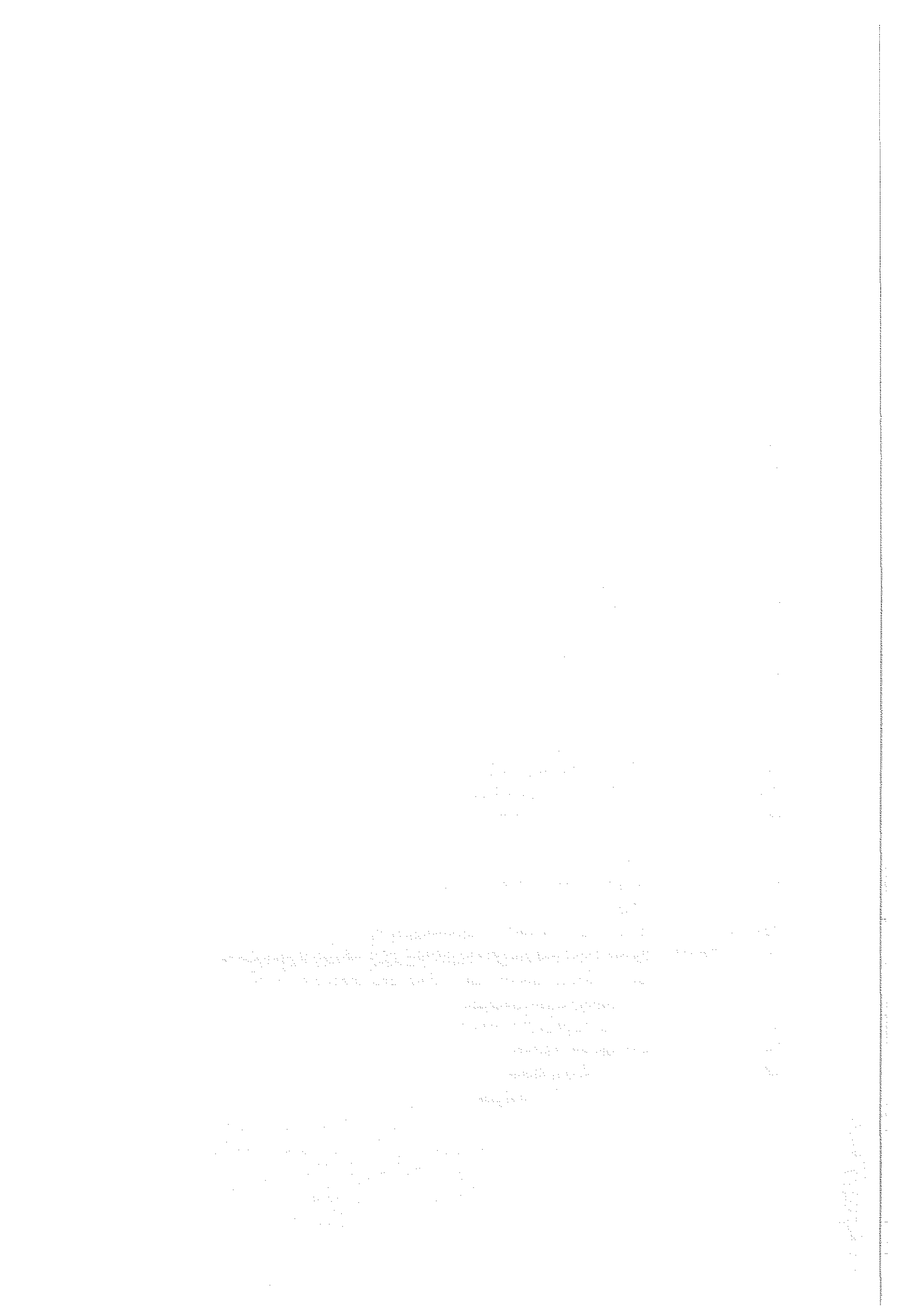

1 Introduction

The fate of petroleum from its source to its trap encompasses a complex array of natural processes. *Generation* of petroleum involving cracking and disproportionation reactions forms products which have compositional characteristics inherited from the type and quality as well as maturity of the source rock's organic matter. When the petroleum phase leaves the source rock system during *expulsion* and *primary migration*, the crude oil may be submitted to considerable compositional fractionations - even on a molecular level - as a result of the type of migration mechanism involved, differences in mobility and solubility (gas vs. oil), as well as rock-fluid interactions. The phase behaviour of the petroleum as well as rock-fluid interactions also play a significant role during the final stage of *secondary migration* and entrapment of the oil and leave their imprints on composition and quality of the petroleum that is produced from an oil field.

In recent years, remarkable progress in the understanding of each of these processes has been achieved as a result of different approaches: Detailed and comprehensive studies on petroleum systems worldwide using advanced organic geochemical analyses enabled the generation of oil and gas to be related to different source rock kerogen types and depositional environments, respectively (Louis & Tissot, 1967; Tissot et al., 1971; Cooles et al., 1986) and to decipher compositional fractionation effects associated with primary migration (Mackenzie et al., 1983; Leythaeuser et al., 1984; Price, 1989). Experimental devices and concepts were developed in the laboratory in order to simulate generation and migration in nature (Lewan et al., 1979; Lafargue et al., 1990). Quantitative and qualitative product prediction was one of the major goals of the latter approach. Closed-system conditions were chosen for these artificial maturation experiments in order to provide insight into kerogen maturation, bitumen formation and petroleum expulsion. It is assumed that the closed-system artificial maturation technique is able to mimic processes in nature, i.e. that reaction pathways in the laboratory system are the same as in nature and that only reaction rates are increased during the simulation (Horsfield et al., 1989).

Finally, input from natural systems and laboratory systems were utilized for the computer-aided numerical simulation (modeling) of generation and migration processes during basin subsidence (Welte & Yükler, 1981).

Although the petroleum industry has benefitted from the latter two approaches in that they helped to reduce the risk of exploring for oil and gas, the quality and applicability of such models is highly dependent on the results which are derived from examination of natural systems. Hence, it is crucial to improve the understanding of the natural processes occurring in petroleum systems and the quality of the natural models deduced thereof. As recently pointed out by Tissot & Ungerer (1990), further information on organic matter composition, primary migration mechanisms and hydrocarbon redistribution in the reservoir is therefore needed to gain an improved insight into the interplay of petroleum generation, migration and entrapment. Clearly, the selection of an appropriate study area which encompasses certain requirements is crucial in order to address the interrelated aspects as laid out above. In most study areas, there are too many factors and processes interfering each other which reduce the control of the investigator on the system: Very often, the organic matter content of the source rock is affected by variations in input material (both in composition and amount) during sedimentation. This feature can significantly change the petroleum generation potential of a given source rock unit across the basin. The presence of multiple petroleum systems which are hydraulically connected complicates

unequivocal oil-source correlation. On the other hand, if the chosen study area does not represent a complete catagenetic sequence, then maturity related effects cannot be investigated. Finally, the examination of a petroleum system at present time normally gives insight only into a discrete, static stage (i.e. maturity interval) of the dynamic assemblage of processes associated with the formation and accumulation of petroleum which covers 10's to 100's of millions of years. Therefore, it is of fundamental importance that the selected study area represents an integrated system, in which all processes from beginning of crude oil formation to entrapment are encountered. This scheme is depicted in Fig. 1.

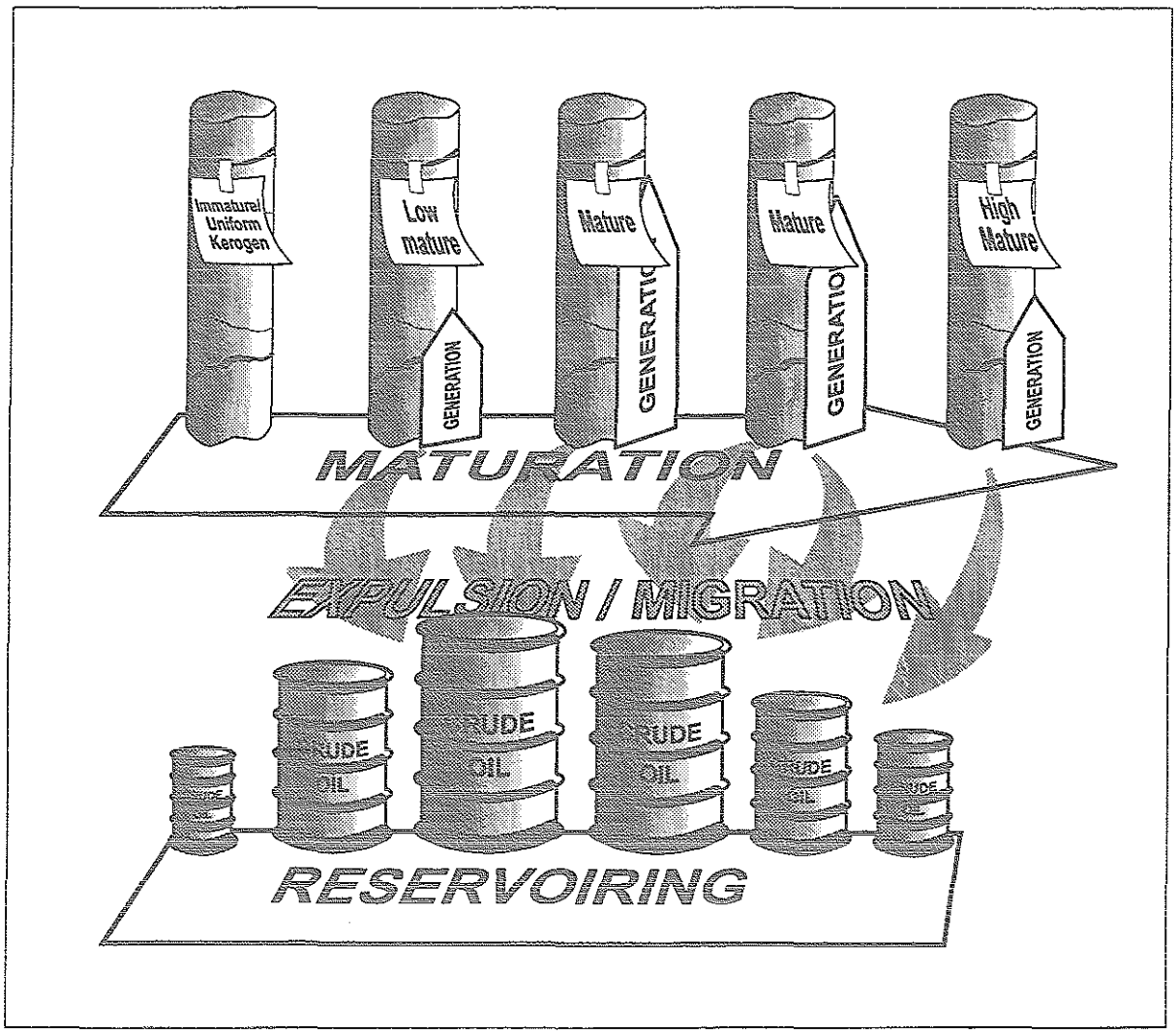

Fig. 1: Schematic display of the attributes of an integrated petroleum system as required for studying petroleum generation, migration and reservoiring as a function of maturity.

1.1 Approach

The Bakken petroleum system of the Williston Basin (U.S.A./Canada) appears to combine certain attributes which are a prerequisite for addressing the above aspects:

- Uniformity of organofacies

  Depositional conditions (input of organic matter) are believed to have been uniform during sedimentation of the Bakken Shale. Hence, the organofacies (kerogen type II) can be considered to be uniform on a basinwide scale (Meissner, 1978; Webster, 1984; Martiniuk, 1988). This simplicity is advantageous as the influence of lateral or vertical facies variations on petroleum generation in the course of maturation can be neglected. In addition, the artificial maturation sequence as derived from heating of immature Bakken Shale equivalents is directly compatible to nature.
- Broad maturity spectrum

  The broad spectrum of maturity of the Bakken source rock ensures that all phases of petroleum generation are "captured" from onset to deadline of oil formation (Webster, 1984; Price et al., 1984). Therefore, the progressive and successive effects of hydrocarbon generation and expulsion have been imparted on recoverable samples.
- Inferred closed system

  Entrapment of Bakken oil is considered to take place within the source rock itself ostensibly with fractures as the reservoir medium. This oil therefore may not have undergone secondary migration. On the basis of high resistivity readings derived from well logging, it was concluded that the pore network of mature Bakken Shales is saturated with in-situ generated hydrocarbons leading to overpressuring (Murray, 1968; Finch, 1969; Meissner, 1978). However, the questions how overpressuring is created and whether the in-situ reservoir model can be extrapolated on a basinwide scale are still controversely discussed. The close association of source rock and reservoir enables to trace the crude oil directly back to its origin as regards compositional nature. Furthermore, mixing effects due to an oil from a source different than the Bakken Shale can be neglected because the unique signatures of these oils are readily recognisable (Fowler et al., 1986; Hoffmann et al., 1987).
- Comprehensive literature data base

  Various aspects of Bakken petroleum geology have been the subject of intense research in the course of the last decades. All these studies have contributed to the very good knowledge of the nature of the Bakken Shale as a classical marine, organic rich, oil-prone source rock.

The combination of the attributes above make the Bakken Shale an ideal candidate for studying source rock as well as reservoir processes. Due to certain features which constrain the broad scope of potential influences, the Bakken petroleum system can be considered a "natural laboratory".

1.2 Objectives

The objectives of the present study are as follows:

- To establish the nature and occurrence of petroleum as a function of maturation and expulsion/primary migration in a constrained natural system.

- To investigate the extent of contribution of different mechanisms to the process of primary migration.
- To unravel the cause and regional dimension of high reservoir pressures in the Bakken Formation.
- To differentiate the types and magnitudes of generation-induced from migration-induced effects.
- To evaluate the natural maturity series with simulation experiments in order to test how such pyrolysis data can contribute to the understanding of the fate of naturally formed petroleum in a closed system.

2 Geology of the Bakken Petroleum System

The Bakken petroleum system is one of several hydrocarbon systems in the Williston Basin. The latter represents one of the largest sedimentary basins in North America. It is an intracratonic basin (Carlson & Anderson, 1965) embedded in the crystalline basement of the North American craton. The roughly elliptical shape of the basin is bounded by the following structures: The Canadian Shield in the northeast, the Big Snowy Uplift in the west, the Black Hills in the southwest and the Sioux Uplift in the southeast (Landes, 1970). The deposits of the basin cover the states of Montana, North and South Dakota on the US side, and Saskatchewan and Manitoba on the Canadian side. The Nesson Anticline and the Billings Anticline are the two principal structural features in the North Dakota portion of the basin. Both anticlines, which are topographically not visible due to concealment by thick glacial deposits strike approximately north-south and play an important role for petroleum geology in the Williston Basin, as most fields are associated with these two structures. The North Dakota portion of the basin, the study area of the present investigation, covers approximately 65% of the area of North Dakota.

2.1 Evolution and Stratigraphy of the Williston Basin

The sedimentary record of the Williston Basin exhibits a maximum thickness of more than 4500m with the depocentre located near Williston, North Dakota (Carlson & Anderson, 1965). It contains deposits from Cambrian to Quaternary age with strata from all Phanerozoic periods. Nonetheless, the burial history of the basin is characterized by several sedimentary hiatus (Bluemle et al., 1986). Although the burial history of the Williston Basin is considered to be rather simple compared to other hydrocarbon bearing sedimentary basins of the world (Sweeney et al., 1992) the mechanism of subsidence of the basin is still a subject of controversy. Several models have been suggested for its evolution (reviewed by Morel-à-l'Huissier et al., 1990): Ahern & Mrkvicka (1984) developed a thermal model which is based on the cooling of an initially hot subcrustal region leading to contraction of the lithosphere. Fowler & Nisbet (1985) discussed the sagging of the basin as a consequence of the phase transformation of a mafic igneous intrusion into an eclogite. Furthermore, they related the incomplete sedimentary record to eustatic changes in sea level. A hypothesis based solely on tectonic considerations is provided by Gerhard et al. (1982). Due to the lack of indication of abnormally high heat flow that would account for a heat source beneath the basin they proposed a 'pull-apart' basin model which is the result of regional left-lateral shearing along the Colorado-Wyoming and Fromberg zones. However, as Morel-à-l'Huissier et al. (1990) have pointed out, the principal regional stress regime of the basin formation process is difficult to determine. Finally, Sears & Alt (1990) provided some evidence for an extraterrestrial impact event. The regular, rather simple geometry of the Williston Basin is displayed in Fig. 2.

Webster (1984) reconstructed the burial history of the Williston Basin and incorporated the unconformities of the section as erosional events (Bluemle et al., 1986). According to this scheme, there are four major periods of possible erosion in the basin, namely early Pennsylvanian, middle Triassic to early Jurassic, late Jurassic to early Cretaceous and Tertiary to Quaternary.

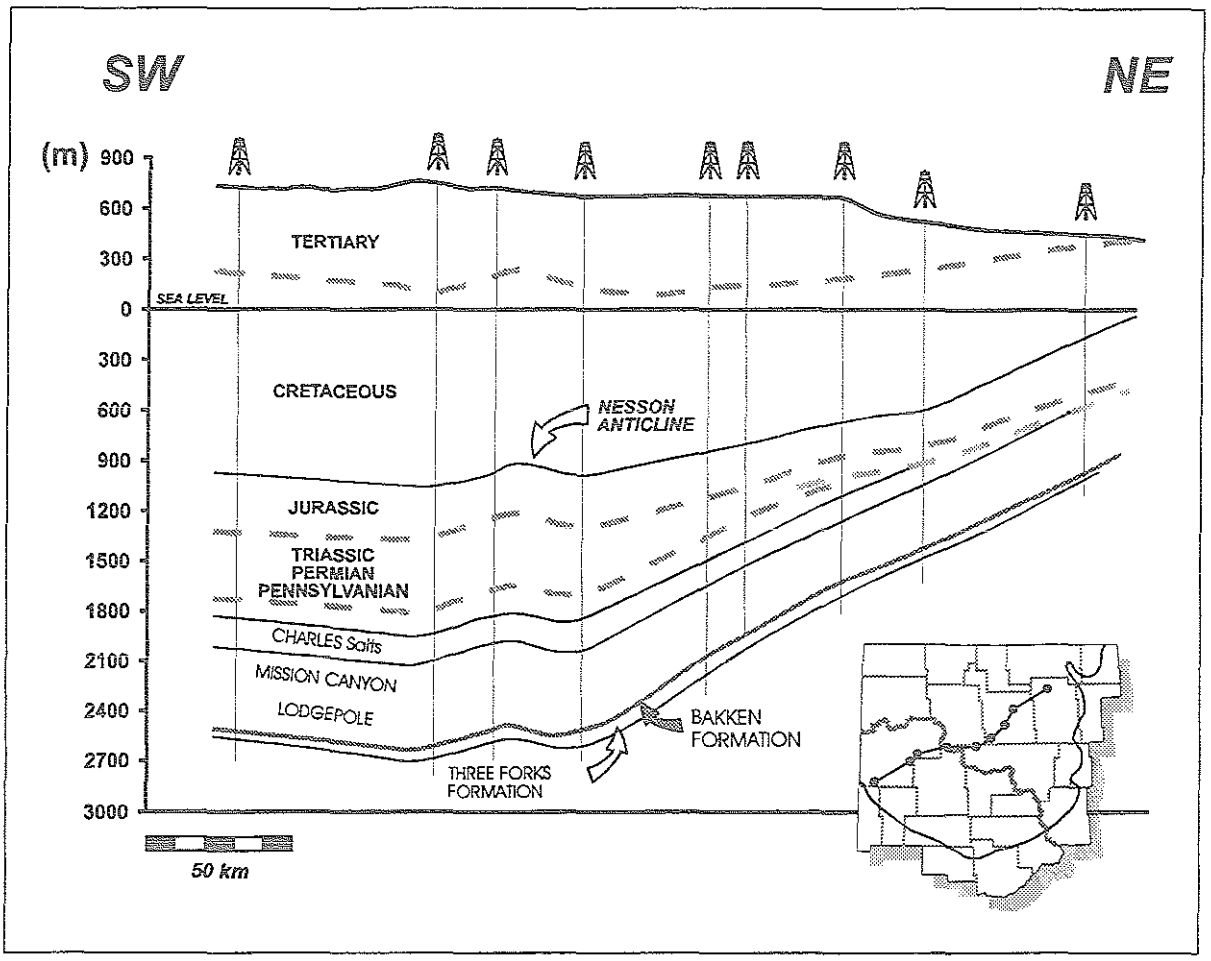

Fig. 2: Generalized cross section of the study area modified from Webster (1984). Strata older than the Three Forks Formation (Devonian) are not included. Dashed grey lines designate major unconformities according to the sequence subdivision scheme by Sloss (1963). Thickness of Bakken Formation is not to scale.

Although Webster (1984) pointed out that the duration of these erosional phases and accordingly the sediment loss are hard to quantify, he estimated them to be less than 100m. This estimate might be questioned in the light of the work by Neuzil (1993) on the Cretaceous Pierre Shale in South Dakota. Based on geologic evidence, he inferred an erosion of 360-400m of overburden in the last 4.5Ma.

Sweeney et al. (1992) calculated the time-temperature history for the Williston Basin exemplified by an Antelope field well (Fig. 3). These calculations were based on present-day thermal conductivity values determined by Gosnold (1991) using results from core sample analysis and measured temperature-depth curve interpretations. From this diagram it becomes apparent that the maximum burial depth for the Bakken Shale was reached at late Cretaceous.

The question whether the Bakken source rock is still actively generating hydrocarbons at present or whether it is in an equilibrated state, is of particular importance for expulsion processes (ch. 5.2). The burial history based on stratigraphic considerations implies that the Williston Basin is a slowly subsiding basin with moderate sedimentation rates and minor erosion events (Webster, 1984; Bluemle et al., 1986). More recent reconstructions of the burial history and, most importantly, the temperature history of the basin using kinetic modeling (Sweeney et al., 1992)

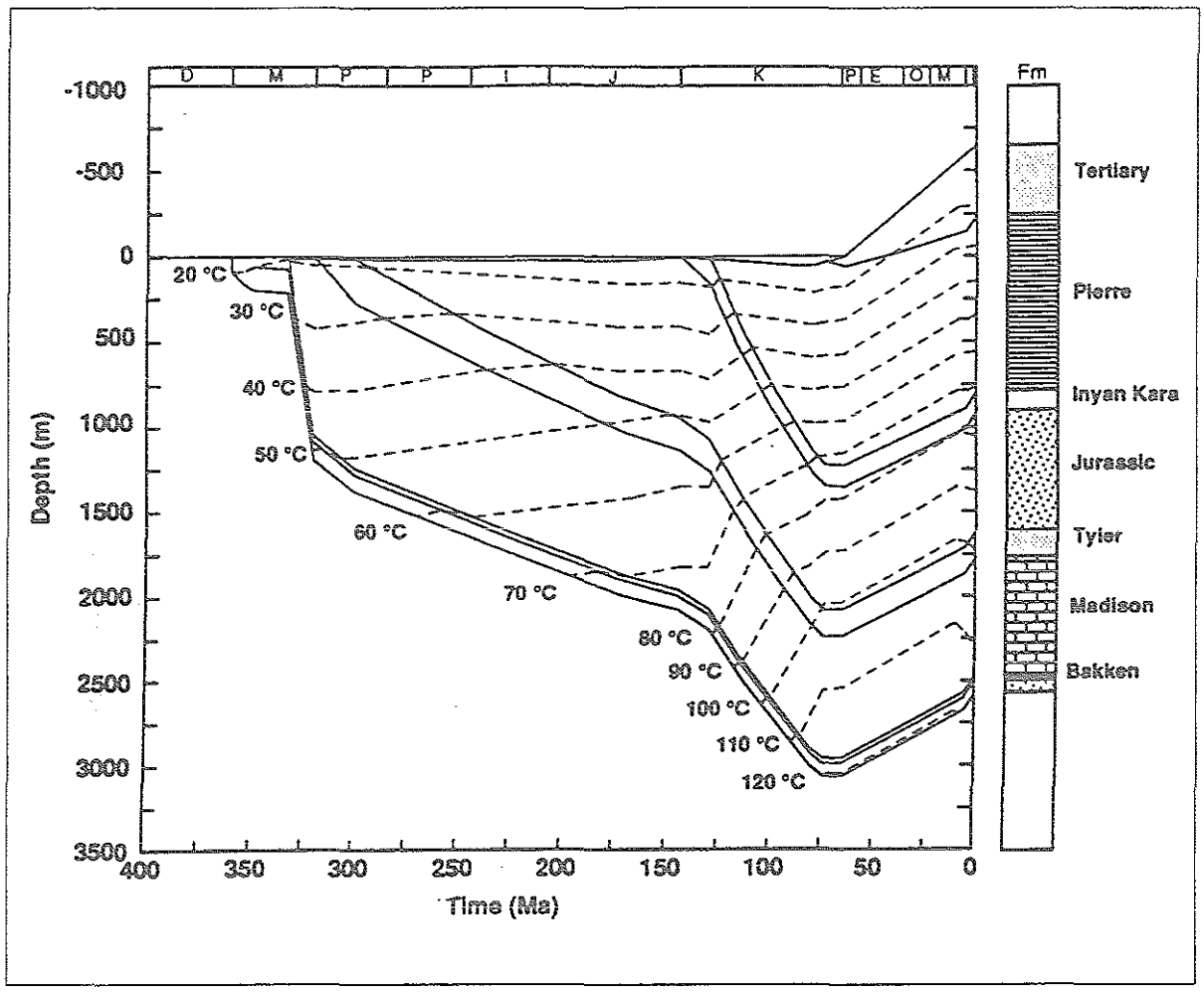

Fig. 3: Thermal history for an Antelope Field well from Sweeney et al. (1992) for strata younger than the Devonian Three Forks Formation (incl. "Sanish Sand").

and numerical modeling tools (Burrus et al., 1994a) revealed that the heat flow can be considered constant throughout the entire evolution of the Williston Basin. The latter authors inferred an area of higher heat flow along the Nesson Anticline, but this regionally higher heat flow is believed to be constant through time as well. With the prerequisite that the sedimentary sequence of the Williston Basin has not experienced any major erosional events especially in recent times, the rather simple and temporally constant temperature history may indicate that the Bakken petroleum system indeed is "live" at present time and actively generating petroleum where the Bakken Shale is in the respective generation zone.

The stratigraphy of the Williston Basin (Fig. 4) is described in detail in Carlson & Anderson (1965) and Gerhard et al. (1982). The stratigraphic record is divided into subdivisions according to Sloss (1963). They are labelled the Sauk Sequence (Cambrian-Lower Ordovician), the Tippecanoe Sequence (Ordovician-Silurian), the Kaskaskia Sequence (Devonian-Mississippian), the Absaroka Sequence (Pennsylvanian-Triassic), the Zuni Sequence (Jurassic-Tertiary) and the Tejas Sequence (Tertiary-Quaternary). In the following, the Kaskaskia Sequence will be focussed on, as the Bakken petroleum system is part of this sequence: Its sedimentary fill adds up to 1370m of preserved strata (Bluemle et al., 1986). The dominant lithologies are limestone and evaporites, indicative of a predominantly marine depositional environment. Sedimentation on an

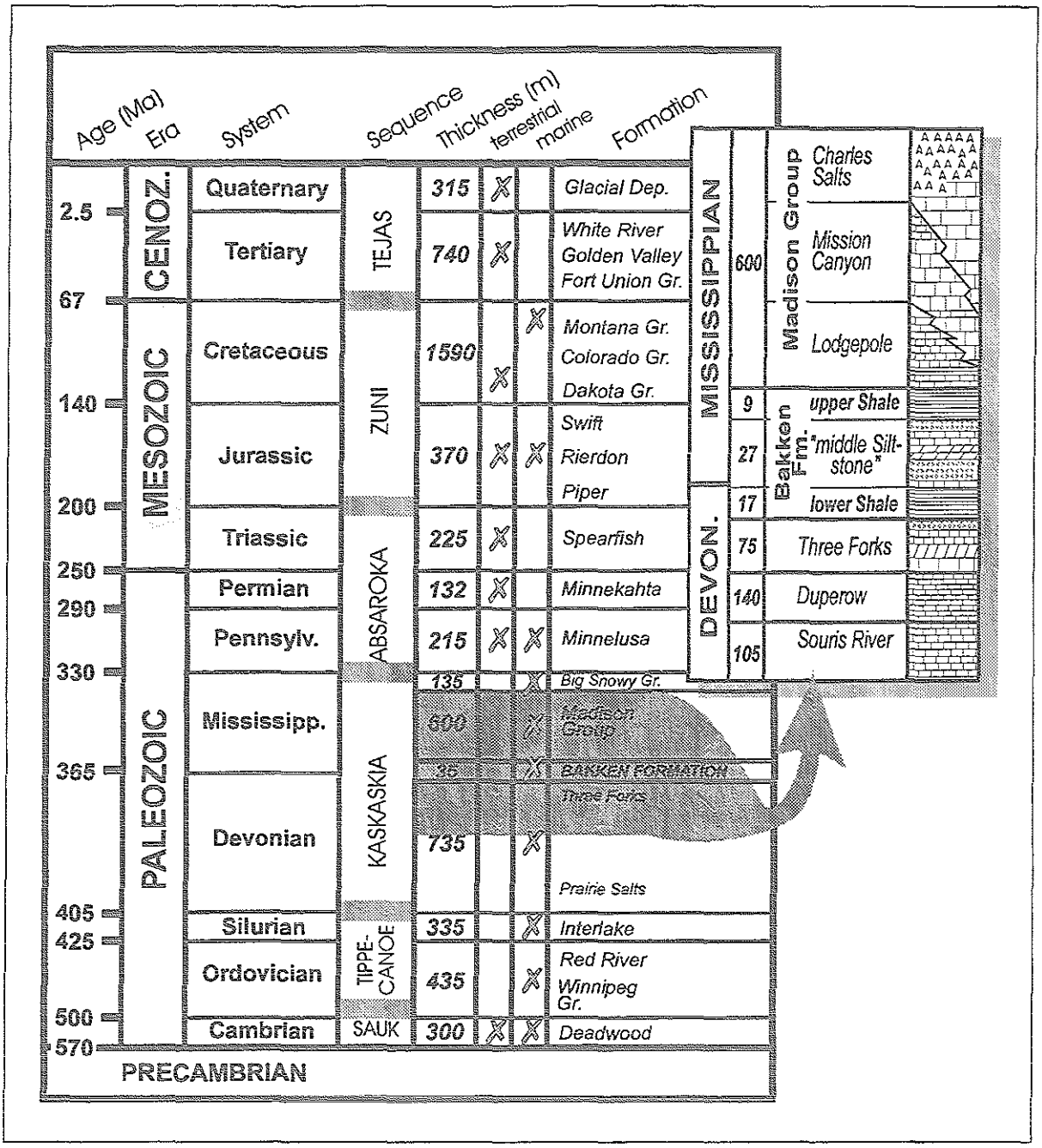

Fig. 4: Generalized stratigraphy of the Williston Basin compiled after Bluemle et al. (1986), Carlson & Anderson (1965) and Gerhard et al. (1982). The sequence subdivisions are according to Sloss (1963). The age and thickness of the formations are not to scale. A simplified characterisation of the depositional environment ("terrestrial" and/or "marine") of the formations and systems, respectively is indicated by crosses. The enlarged section on the right hand side shows generalized lithologies and thicknesses of formations which are relevant for the present study.

eroded surface of earlier Palaeozoic rocks started with the deposition of Winnipegosis carbonates. These limestones were rich in stromatoporoids and reef structures. Such depositional conditions prevailed during most of the Devonian (including late Devonian Duperow and Birdbear Formation), interrupted only by the early Devonian Prairie salts and a temporary influx of clastics

(Gerhard et al., 1982) in the Dawson Bay unit (middle Devonian). The sediments of the Three Forks Formation (shales, anhydrites, siltstones and dolomites) formed the base for the transgressive deposits of the Bakken Formation (Upper Devonian to Lower Mississippian). Locally, the top of the Three Forks Formation is represented by a well-cemented quartz sandstone referred to as the "Sanish Sand" (Webster, 1984). As this stratum exhibits relatively high porosities (5.5%) and permeabilities (>1.0mD) (Murray, 1968), it acts as an important reservoir. Isopach maps of the Three Forks Formation might indicate erosion on the flanks of the basin (Carlson & Anderson, 1965) prior to sedimentation of the Bakken Formation. The organic richness of the Bakken Shales (upper and lower Shale, interrupted by a middle member of highly variable lithology) reflect an anoxic sedimentary environment. The 600m thick Madison Group above the Bakken Formation consists of three members (Lodgepole limestones, Mission Canyon limestones and Charles salts) and represents a cyclical carbonate and evaporite deposition (Carlson & Anderson, 1965). The limestones of the Madison Group act as important hydrocarbon reservoirs. For the sake of convenience, the Madison Group is often subdivided in intervals based on widespread evaporite beds associated with fine-grained clastics. These marker-type horizons (Bottineau, Tilston, Frobisher-Alida, Ratcliffe and Poplar) are easily detected on appropriate well logs (Carlson & Anderson, 1965). The Kaskaskia Sequence is concluded by clastics and carbonates of the late Mississippian Big Snowy Group deposited in alternating restricted and normal marine environments.

2.2 The Bakken Petroleum System

2.2.1 Stratigraphy and Lithology

Webster (1984) gave a good overview of the stratigraphy and lithology of the Bakken Formation while LeFever et al. (1991) provided a comprehensive update with many details on this issue. The three informal members of the formation (Fig. 4) are easily recognized on wireline logs, as the upper and lower shales have usually very high gamma-ray readings (>200 API; LeFever et al., 1991). In the study area, the entire Bakken Formation ranges in thickness from a maximum of 53m to a depositional pinch out at the edges. Both shale units are relatively thin (17m and 9m as a maximum for lower and upper shale, respectively) while the middle member reaches a maximum thickness of 27m (LeFever et al., 1991). The three members exhibit an onlapping relationship and show no surface outcrop. The boundary between lower Bakken Shale and the middle member has been suggested to be the boundary between Devonian and Mississippian based on conodont fauna from the shales (Hayes & Holland, 1983). However, Thrasher (1985) assigned the systematic boundary into the middle member.

Lithologically, both shale members are referred to as being very similar and uniform on a basin-wide scale (Meissner, 1978; Webster, 1984; Martiniuk, 1988; LeFever et al., 1991): They are dark coloured, noncalcareous, fissile and mostly display a massive, isotropic texture. A fine lamination can be encountered in selected samples. Pyrite is ubiquitous in the form of laminae, lenses or finely disseminated throughout the rock. Based on results derived from thin section (Webster, 1984) and XRD analysis (Webster, 1984; Cramer, 1991), quartz appeared to be the dominant mineral while the clay content, atypical for a shale, was rather low. Further accessory

minerals are potassium-feldspar, calcite, dolomite and anhydrite. Both shales are characterized by very high contents of organic matter (average of 11.3wt.-% organic carbon; Webster, 1984). On the basis of an average TOC content of 15wt.-%, Price & Clayton (1992) calculated that 39% of the rock volume would consist of organic matter. Mostly, the organic matter is uniformly distributed throughout the rock matrix. Alginites, sporinites and small amounts of vitrinites are the principal macerals (Webster, 1984).
The fossil content is made up of conodonts, fish remains and various invertebrates.
The lithology of the middle member is strikingly different to both shale units and is also highly variable (Webster, 1984; LeFever et al., 1991): It consists of siltstones and sandstones, but lesser amounts of shales, dolostones and limestones (oolites) are also present, indicating lateral and vertical changes in depositional environment. A detailed core analysis enabled the subdivision of seven lithofacies units (LeFever et al., 1991). However, as siltstone is the predominant lithology of the middle member, in the literature this stratum is conveniently referred to as the middle Siltstone Member.

2.2.2 Petroleum Geology

A Brief History of Bakken Exploration and Production

The history of petroleum production from the Bakken Formation in the Williston Basin began in 1953, when the #1 Woodrow Starr was completed as the discovery well for the Antelope field (McKenzie Co.) (LeFever, 1991). From that date on, the Nesson Anticline and particularly the Antelope Anticline area were the prime target for exploration and production in the North Dakota portion of the basin. After a period of reduced activities in the Bakken play, the area of interest was shifted from the centre of the basin to the southwest depositional pinch out zone of the Bakken Formation, due to the discovery of the Elkhorn Ranch field in the Billings Anticline area (1961). The discovery well, initially aimed for the Ordovician Red River formation recovered oil in a drill stem test from the Bakken Formation. Drilling activities in North Dakota have considerably changed since the introduction of horizontal drilling techniques especially in the Billings Anticline area. In 1987, the first horizontal well was completed in North Dakota, quickening the Bakken Formation as an important economic reservoir. Based on 1989 production figures, fields in the Billings Anticline area which are producing from horizontal wells (e.g. Elkhorn Ranch, Bicentennial, Roosevelt) have exceeded production from Nesson and Antelope Anticline wells.
Production data and results from a number of studies (Williams, 1974; Osadetz et al., 1991; Price & LeFever, 1992) characterize Bakken crude oil as high-quality petroleum. API gravtities are relatively high (40-45°) and sulfur content is normally rather low (< 0.2wt.-%). Data from horizontal wells reveal production gas-oil ratios of 0.16-0.4kgkg^{-1}.

Oil-Source Rock Correlation

Oil-source rock correlations and the discrimination of petroleum systems in the Williston Basin were first carried out by Williams (1974) and Dow (1974), respectively. According to their

studies, three different petroleum systems existed bearing three different types of oil. The first comprised of the Ordovician-Silurian Winnipeg-Red River system, the second was the Bakken-Madison system (Devonian-Mississippian) and the third was assigned to the Permian-Triassic Tyler Formation. A positive correlation of Madison oils with the Bakken Shale source was established using light hydrocarbons (C^4-C^7), C^{15+}-n-alkanes and carbon isotope ratio ($\delta^{13}C$) (Williams, 1974). Based on the studies of the latter, Dow (1974) inferred a migration of Bakken sourced oil along fractures and faults into the Madison limestone reservoirs. He attributed such a vertically oriented migration direction to the Nesson Anticline area, where the petroleum liquid was focussed by the anticlinal structure. Charles salts of the upper Madison Group (Fig. 2) acted as efficient seals. Additional to the vertical migration scheme, Dow (1974) also postulated updip migration within the Mississippian along appropriate continuous porosity zones. The hydrocarbons were then trapped by porosity pinch out at the Madison-Jurassic unconformity at the marginal regions of the basin. However, in order to explain the mismatch between the amount of generated (based on estimations) and discovered oil, he concluded that expulsion of Bakken oil was locally inhibited by the absence of fractures.

The general validity of oil-source rock correlations as exemplified above was questioned in a study on sequential extracts derived from whole rock Bakken Shale samples (Price & Clayton, 1992): Here it was shown that the molecular composition of the bitumen is not uniformly distributed in the rock but varies significantly. Clearly, this bears serious consequences on oil-source rock correlations, as these are normally established using whole extracts from powdered rock samples. Price & Clayton (1992) inferred that the bitumen which is most accessible to solvents in the lab (first extraction step), represents the hydrocarbon phase that is most readily expelled in the natural system.

The positive correlation between the Bakken Shale source and the Madison reservoir which later was supported by a study by Leenheer (1984), was considered valid for a long time. However, more recently, Canadian investigators provided evidence that this positive correlation was erroneous. Brooks et al. (1987) discriminated three compositionally different oil families (A, B, C) in the Canadian portion of the Williston Basin and questioned the Bakken-Madison correlation. The essence of the studies by Osadetz et al. (1990, 1991 and 1992) was the definition of four distinct oil families derived from compositional (isoprenoid hydrocarbon ratios, biomarker ratios) as well as stratigraphic inferences. As regards the Bakken petroleum system, these authors concluded that Bakken sourced oils (family B) are restricted to the Bakken Formation and are absent in the Madison Group. In contrast, the Madison oils, attributed to family C, are not associated with Bakken reservoirs except for one field (Osadetz et al., 1992). The source for the family C-Madison oils are believed to be organic rich, bituminous carbonate rock bodies in the Mississippian Lodgepole Formation (Osadetz et al., 1991; Osadetz et al., 1992). This novel and refined model of oil-source rock correlations for Devonian-Mississippian petroleum systems on the Canadian side of the Williston Basin was extended to the US side by Price & LeFever (1994). Accordingly, these authors also inferred the existence of an efficient source rock within the Lodgepole Formation although they had no direct evidence for identifying and locating this source rock.

An important inference deduced from the studies above is the particular closed-system nature of the Bakken Formation in terms of petroleum mobility. Hence, such a restrictive system implies that Bakken sourced oils can be considered untouched by long-distance migration.

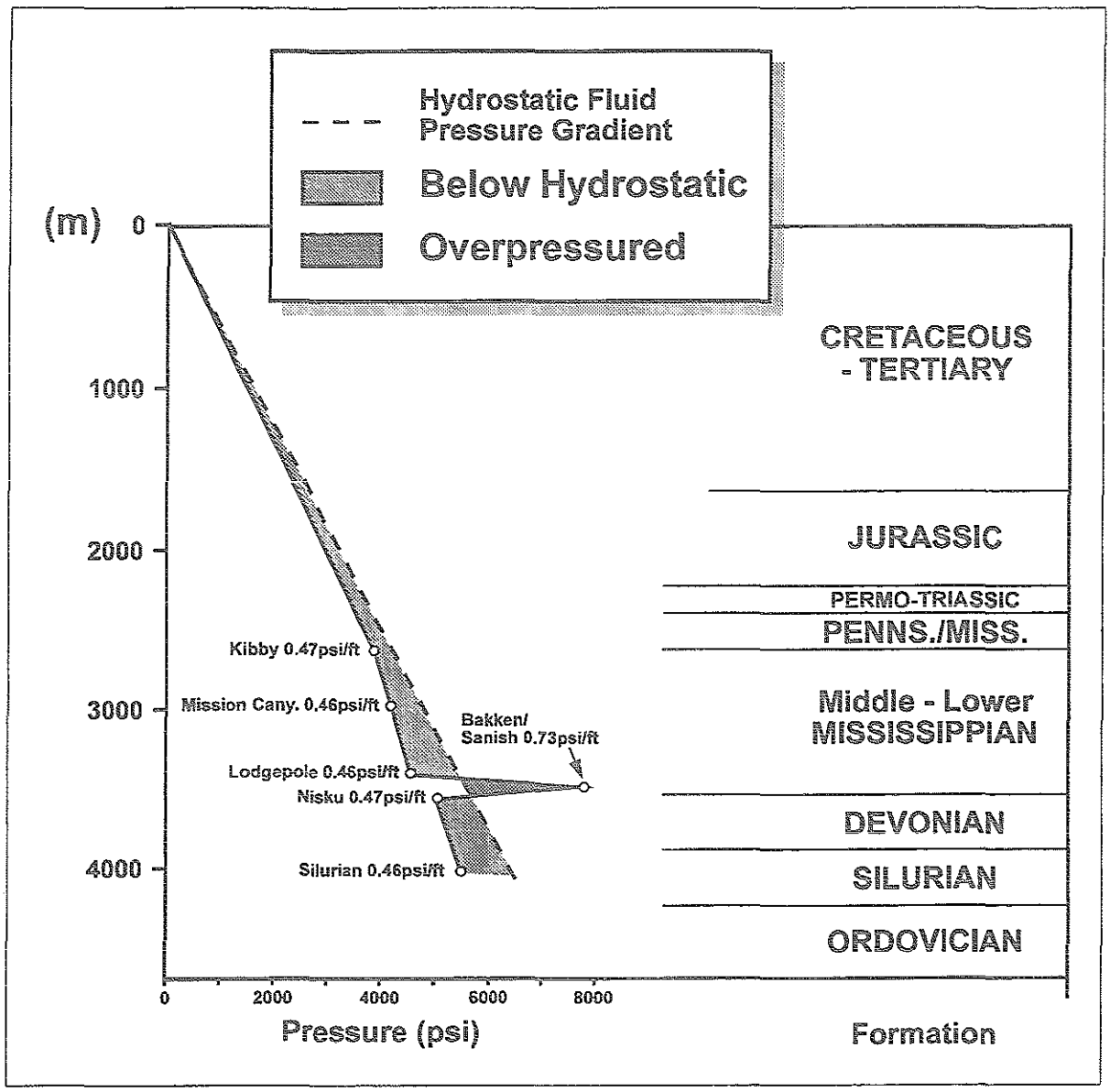

Fig. 5: Reservoir pressure/depth profile for an Antelope Field well showing abnormally high pressure gradients for the Bakken Formation. Reproduced from Meissner (1978).

Reservoir Properties

As stated before, most of the reservoirs in the North Dakota portion of the Williston Basin are linked to the two principal structures of the basin, the Nesson and Billings Anticline. The evolution of the Nesson Anticline was initiated in the Precambrian as a result of faulting of the crystalline basement blocks (Anderson et al., 1983). Many wells in the Nesson Anticline area produce from the Sanish Sand of the upper Three Forks Formation. The Antelope Anticline, which is a smaller structure offset from the north-south trending Nesson Anticline is believed to be a classic "drape fold" (Stearns, 1971) which is created by vertical movements of basement blocks where the steep flank overlies the downthrown block while the other flank is more gentle. Such tectonic stress (bending) resulted in the formation of open tensile fractures (Meissner, 1978), thus improving reservoir quality. The steep, northeast limb of the anticline seems to have a

higher degree of fracturing as more producing wells have been drilled on that side (LeFever, 1991).

Fields in the Billings Anticline area are normally associated with structural features such as faults, folds or both. However, the Bakken Formation is not the only producing stratum in this area. As of 1991, only two of 26 fields provided petroleum directly from the Bakken. A notable feature of oil production from pools in that area was that only trace amounts of water were produced (LeFever, 1991). The term "Bakken fairway" was established as a northwest-southeast oriented band paralleling the depositional pinch out of the Bakken in North Dakota and Montana (Hansen & Long, 1991a). It is used to describe an area with high potential for successful exploration and production. However, as Hansen & Long (1991b) have shown, there are only certain spots within the fairway which reveal good reservoir properties.

The overpressured nature (Fig. 5) of the Bakken petroleum system was recognized by Murray (1968) and Finch (1969). Murray (1968) reported an initial reservoir pressure of 7670psi (53mpa) at 2545m (8400ft) depth in the Sanish Sand of the upper Three Forks Formation. In that context, however, it must be pointed out that in these pioneering publications on reservoir pressure in the Bakken petroleum system, the abnormally high reservoir pressures were not exclusively tied to either of the two Bakken Shale members. Meissner (1978) came to the conclusion that the overpressuring is a direct result of the generation of hydrocarbons which are not expelled but remain in the source rock. In that more comprehensive study on the pressure issue, evidence was provided that the two shale units indeed may be overpressured, but again, an overpressured status might be extended to the entire Bakken Formation including the uBK, mBK and lBK as well as the Sanish Sandstone of the DTF. The question, whether abnormally high pressures occur in more than one member of the Bakken petroleum system and if so, in which members, is evaluated in ch. 5.3.

High fluid pressures were called upon to create vertical fractures in the Bakken petroleum system which may act as the reservoir medium, as the reservoir properties (porosity and permeability) of the Bakken Shale matrix are considered to be very poor (Meissner, 1978). The direct link of abnormally high reservoir pressures to extensive hydrocarbon generation was confirmed by results derived from 2d numerical simulations, but the degree of overpressuring was believed to be insufficient to reach hydraulic fracturing thresholds (Burrus et al., 1994a). However, the existence and principal formation mechanism (either tectonic and/or hydrostatic) of a fracture network that is capable of holding such large quantities of petroleum discovered so far in the Bakken is still a subject of controversy in the literature. Finch (1969) attributed the fractures to tectonic forces due to vertical movements of the Precambrian basement blocks. Subsequently, these fractures were said to be filled with water and then with hydrocarbons. In the final tectonic phase, the fluid-filled zone was compacted which led to an increase of pressure. Carlisle (1991) supported the theory of a combination of both principal mechanisms. Analysis of production data enabled Sperr (1990) to derive four different types of fractured reservoirs: The first type is associated with the thinning of the beds and the increase in fracture density at the depositional edge of the upper Bakken Shale in the Billings Anticline area. The second type of fracturing is of structural nature and occurs where the Bakken is draped over underlying structures such as Antelope Anticline. Hot spots with a higher heat flow initiating enhanced hydrocarbon generation form the third category. In the latter case, the fracturing is directly caused by overpressuring.

Fracturing along regional lineaments representing the edges of basement blocks characterize the fourth type of fracturing.

3 Methodology

3.1 Sampling and Sample Documentation

The sample set for the present study consisted of whole rock core samples (Bakken Shales) and crude oils. 29 wells were sampled for whole rock samples and provided a total of 182 samples. The majority was collected from the upper Bakken Shale (133), whereas 49 stem from the lower shale interval. The sample set was completed with 5 crude oils from Bakken reservoirs. The location of the sampled wells, all of which were drilled in the North Dakota portion of the Williston Basin, is shown in Fig. 6. Background information on the wells is tabulated in the appendix. During sampling, unusual macroscopical characteristics of the entire Bakken interval core were monitored in order to discriminate core sections and/or samples which exhibited local features unrepresentative for the Bakken Shale, such as silt lenses, macrofossils etc.

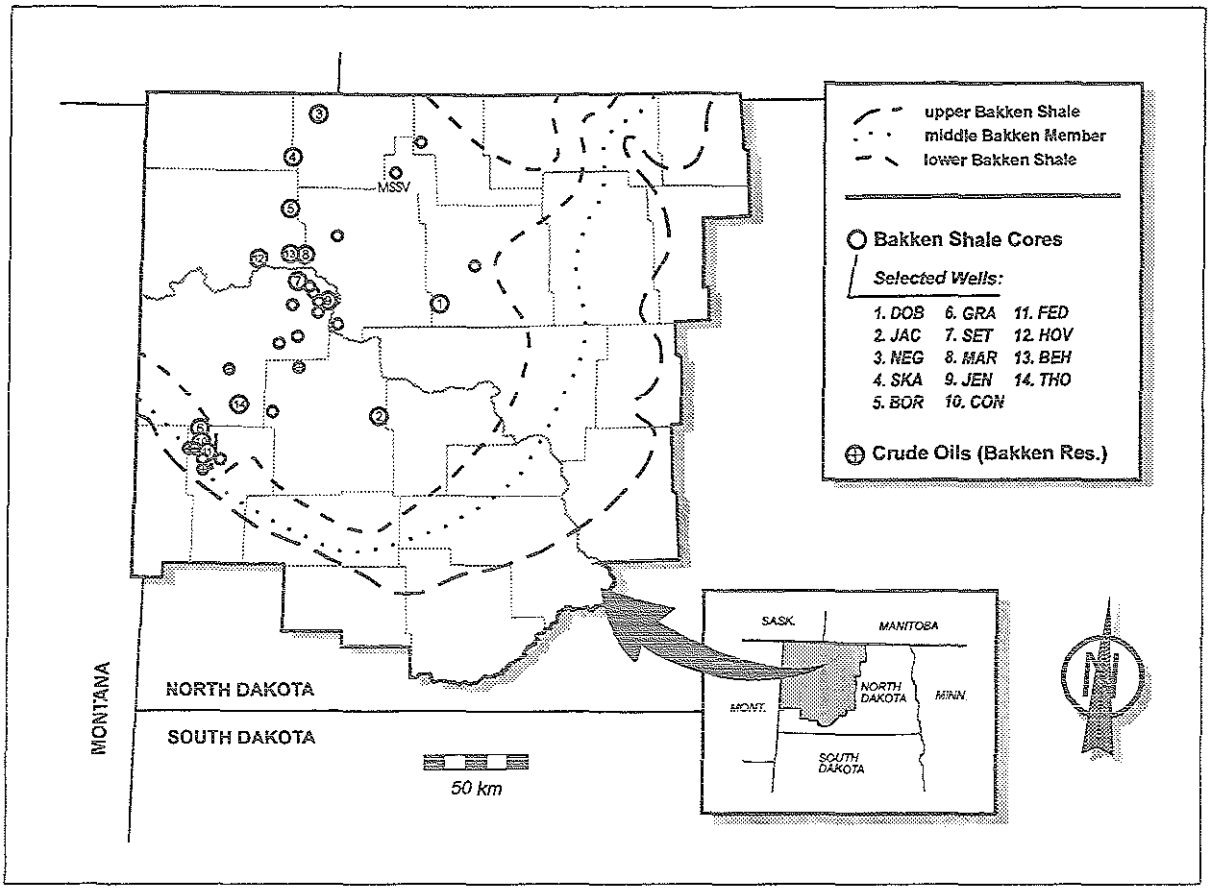

Fig. 6: Study area showing location of wells. Wells 1-14 (numbered in the order of increasing vitrinite reflectance) were considered representative for the entire basin and provided the cores for the selected set of samples (see methodology). One sample from well labelled 'MSSV' was employed for artificial maturation experiments using the MSSV technique.

In most cases it was not possible to sample the upper Bakken Shale (uBK) as well as the lower (lBK) of the same well because of the core quality. However, two cores, the Marathon Oil Dobrinski (DOB) and the horizontal Shell Connell #24-27 (CON) were sampled in close intervals over the entire range of the Bakken section in order to assess vertical and small-scale lateral facies variations.
Additionally, samples from 3 other type-II source rocks, namely the Posidonia Shale (Lower Toarcian, Hils Syncline, Germany), the Woodford Shale (Devon.-Miss., Anadarko Basin, U.S.A.) and the Chattanooga Shale (Upper Devonian, Appalachian Basin, U.S.A.) were analysed where indicated (thermovaporisation-gas chromatography) in order to compare Bakken Shale data with other source rock systems. Background information on the organic geochemistry and petroleum geology of these source rocks is provided by Rullkötter et al. (1988) and Muscio et al. (1991) for the Posidonia Shale, Cardott & Lambert (1985) for the Woodford Shale and North (1985) for the Chattanooga Shale.

3.2 Screening Analyses

Well-established screening analyses (pyrolysis, IATROSCAN, organic petrology) were performed in order to assess the type and nature of the solid as well as liquid organic matter of the Bakken Shale. This analytical database was used to reduce the number of samples for further more detailed analyses. Additionally, the following aspects were taken into account to ensure an optimum of representativity of the selected sample set for the Bakken in-source reservoir system:

- ⇨ cover of broad maturity range
- ⇨ cover of broad geographical area
- ⇨ sample availability of individual wells
- ⇨ selection of wells of as many types of status (dry, producing, overpressured etc. as deduced from production data, drilling reports etc.) as possible

3.2.1 Pyrolysis

All rock samples were analysed for total organic carbon (using a LECO IR-112 analyser) and by the Rock-Eval pyrolysis method (Espitalié et al., 1985) following established procedures.

3.2.2 IATROSCAN Analysis of Solvent Extracts

In order to rapidly obtain a comprehensive characterisation of the Bakken Shale bitumen, 108 crushed whole rock samples from 28 wells were solvent extracted using the ultrasonic method (5 minutes per sample in dichloromethane). Subsequently, the extracts were submitted to IATROSCAN analysis (Ray et al., 1982).
The three stage development of the saturate, aromatic and polar fraction was performed using n-hexane, toluene and dichloromethane, respectively as solvents (Ray et al., 1982). The bulk

compositional variabilities of Bakken extracts in one well were monitored based on fingerprinting of the IATROSCAN FID traces.

3.2.3 Organic Petrology

For petrological analysis (facies and maturity), 55 selected whole rock pieces representing all wells were orientated perpendicular to the bedding plane and mounted in a mixture of epoxi-resin (Scandiplex A) and hardener (Scandiplex B). Due to the ubiquitous high content of pyrite, the final polishing was carried out applying a special polishing emulsion designed originally for metallic surfaces (STRUERS OP-S Suspension) in order to obtain a surface quality good enough for the determination of vitrinite reflectance.
All samples were examined in plane polarized reflected white light and under blue light excitation (450-490nm). Selected sections were photographed.
Vitrinite reflectance measurements were made with a Zeiss Photomicroscope III in oil immersion at a wavelenght of 546nm using a measuring blind of 8µm diameter. Data were processed by HP 9816S hardware combined with Zeiss Coflex software.
Macerals were classified according to the nomenclature of Stach et al. (1982) and Hutton et al. (1980).

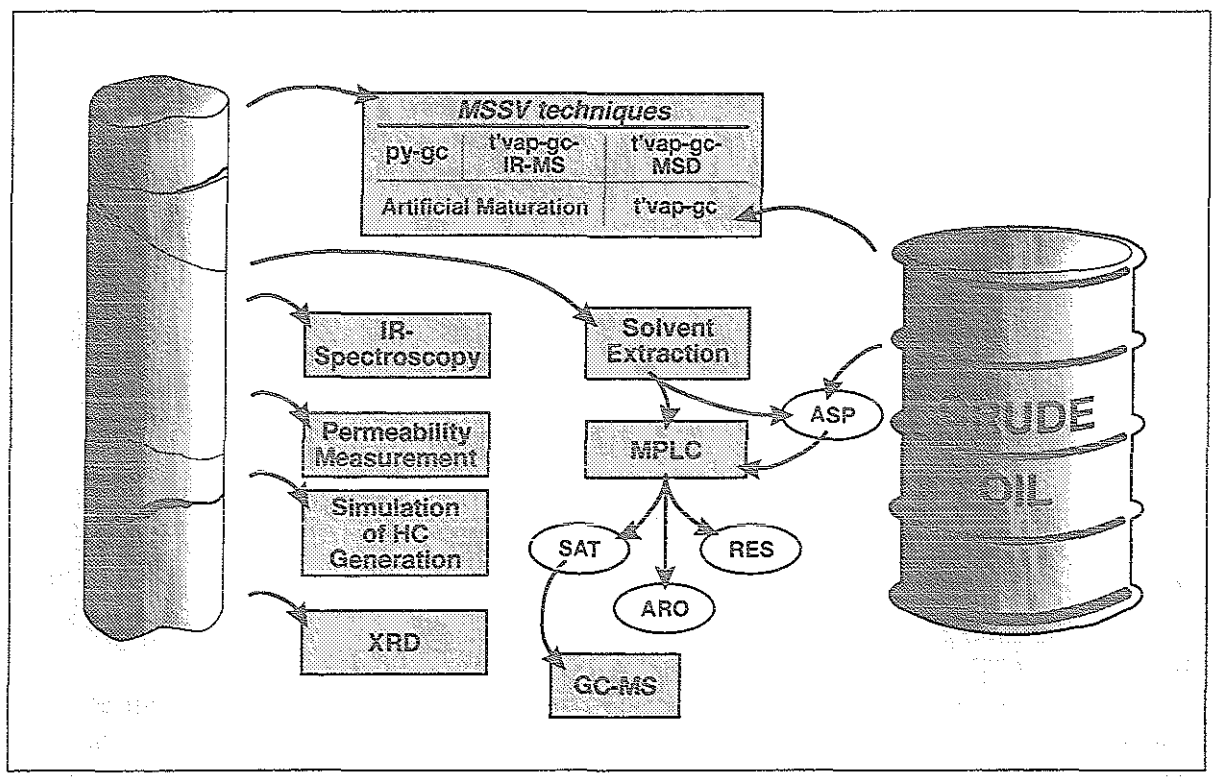

Fig. 7: Flow chart displaying analyses performed on selected set of samples.

3.3 Methodology of Selected Sample Set

The following analyses were applied to samples which were selected based on results of the prevailing analyses. The flow chart for this methodology is depicted in Fig. 7.

3.3.1 Organic Geochemical Analyses

Analyses Based on MSSV Technique

The following analyses are all based on the same basic experimental configuration, as described in Horsfield et al. (1989) and displayed in Fig. 8. This consists of a Quantum MSSV-1 Thermal Analysis Unit (sample holder with a programmable pyrolysis furnace and cryogenic trap) and a gas chromatograph. Identification of prominent peaks of the GC trace was carried out via retention time, correlation with literature data (Horsfield & Düppenbecker, 1991; Requejo et al., 1992) and/or mass spectra.

41 Bakken Shale whole rock samples from 14 wells covering the entire maturity range were submitted to open-system ***pyrolysis-gas chromatography*** (py-gc) analysis.
It has been shown that yield and composition of pyrolysates are affected by organic richness and the mineral matrix of the rock (Espitalié et al., 1980, Horsfield & Douglas, 1980). Experiments using mixtures of kerogens and minerals documented that especially clay minerals may retain heavy hydrocarbon products on the mineral surface (Espitalié et al., 1980). The high average organic richness and low clay content of Bakken Shale *whole rock* samples (ch. 2.2.1) therefore was advantageous in that laborious kerogen isolation treatments were not necessary.
The sample was placed into the central part of a glass tube (26mm long; inner sleeve diameter 3mm). The remaining volume was filled with cleaned quartz wool (630°C in air, 1 hour). After flushing the sample at 300°C (5min.) to remove volatile material, it is pyrolysed using programmed heating from 300°C (50°C/min.) to 600°C (3min. isothermal). The products were cryogenically trapped and separated by on-line gas chromatography. An HP-1 column (1.65µm film thickness, 26.5m x 0.31mm) connected to a FID and a sulfur compound sensitive Hall detector was used with He as carrier gas. Programmed heating started at -10°C (2min. isothermal) with a subsequent rate of 8°C/min. up to 320°C. Quantification was performed using n-butane as an external standard.
The thermally releasable organic matter (<300°C) of 47 Bakken Shale samples from 18 wells covering the entire spectrum of maturity was analysed by ***thermovaporisation-gas chromatography*** (t'vap-gc). In order to compare yield and composition of Bakken Shale thermal extracts with other source rock systems, a set of 8 samples from 3 different type-II kerogens (Posidonia Shale, Woodford Shale and Chattanooga Shale) were investigated under identical conditions. Preliminary experiments had revealed that even finely ground samples (disk mill) yielded relatively high amounts of highly volatile light hydrocarbons. Therefore, to minimize the loss of gaseous compounds during sample preparation, the coarsely ground sample (agate

mortar) was placed into a glass tube (30mm long; inner sleeve diameter 1.5mm; ca. 50µl internal volume) which was sealed directly after loading and placed into the sample holder of the pyrolysis furnace (300°C). Each sample was cracked open by piston action. The products were cryogenically trapped and analysed by gas-chromatography. The temperature program and GC configuration was the same as that used for py-gc analyses.

The same experimental set-up was employed for the whole oil gas chromatography analysis of 5 crude oils from Bakken reservoirs. For this type of sample, the glass tube was filled with purified quartz wool on which an appropriate amount of crude oil was injected using a syringe. Subsequent analytical steps were according to the descriptions above.

In order to confirm peak identification (cycloalkanes, alkylbenzenes) of the thermovaporisation compounds, two samples from different levels of maturation were analysed by ***thermovaporisation-gas chromatography-MSD*** (t'vap-gc-MSD). Sample preparation and treatment was the same as for t'vap-gc. Analyses were run on a 50m x 0.31mm HP-1 fused silica column. Heating went from 40°C (6min. isothermal) at a rate of 5°C/min. up to 300°C (22min. isothermal). GC-MS analyses were performed on a Fisons Instruments MD 800 (ionizing voltage: 70eV; source temperature: 220°C) using He as carrier gas.

In order to determine isotopic compositions ($\delta^{13}C$) of individual thermovaporised products, selected samples were submitted to ***thermovaporisation-gas chromatography-isotope ratio-mass spectrometry*** (t'vap-gc-IR-MS). Preparative sample treatment was as described above for t'vap-gc analyses. Data are reported as $\delta^{13}C$ relative to the PDB standard and corrected for ^{17}O contribution. Aliquots of the same sample set were analysed utilizing two mass spectrometers with two different GC columns (fused silica HP-1column and Poraplot column). The first set-up comprised of an OPTIMA Isochrom-based GC-IR-MS system (Hall et al., 1993).The HP-1 column (0.3µm film thickness, 50m x 0.32mm) was coated with OV-1 stationary phase. He was used as carrier gas. Programmed heating started from 20°C (2min. isothermal) to 300°C (15min. isothermal) at 4°C/min. The second configuration (GC: Varian 3400; MS: MAT 252) was equipped with a Poraplot column (10µm film thickness, 25m x 0.32mm). Here, the GC heating program was from 30°C (4min. isothermal) to 250°C (10min. isothermal) at 12°C/min..

Artificial maturation was performed on aliquots of one immature Bakken Shale sample (0.49% R_o; Ropertz, 1994; well labelled "MSSV" in Fig. 6) in a convection oven at the following isothermal heating conditions: 300°C (2 and 5 days), 330°C (1, 2 and 5 days) and 350°C (1,2 and 5 days). In this case, purified glass beads (630°C in air, 1 hour) were used to fill the remaining volume of the glass tube. Both the artificially generated products as well as the residual kerogen of each artificial maturation level were analysed via gas chromatography and programmed heating py-gc, respectively.

Infrared Spectroscopy

Infrared spectroscopic analysis was applied to organic rich unextracted Bakken Shale samples (TOC > 12wt.-%) from 14 wells (R_o: 0.31 to 1.57), one sample of each well. The experimental configuration and parameters were as outlined in Schenk et al. (1986): The samples were dried under vacuum for 24 hours and mixed with 200mg of KBr. Thorough mixing was ensured by using a mill (3 min.). The mixture was pressed into pellets in an evacuated 13mm die under a pressure of 8tons/cm^2. The analytical set-up comprised of a Perkin-Elmer 783 dispersive

spectrophotometer coupled to a Perkin-Elmer 3600 data station equipped with PE 780 software for calculation of band areas. Aliphatic band areas were determined for the wave number range between 3010 - 2730cm^{-1}.

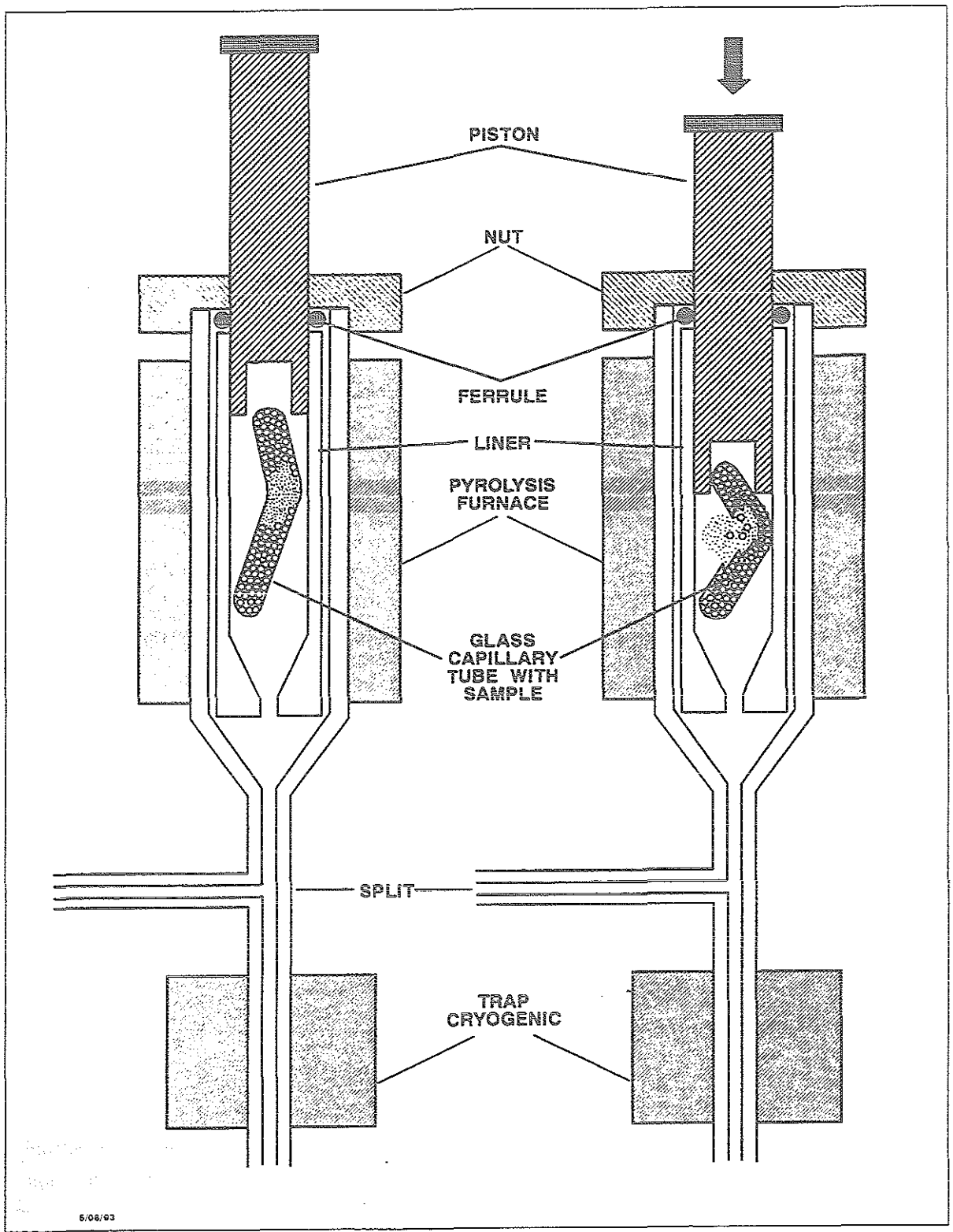

Fig. 8: Schematic set-up (cross section) of a Quantum MSSV-1 Thermal Analysis Unit. This basic experimental configuration was used for all analyses based on the MSSV technique (reproduced from Mycke et al., 1994).

Solvent extraction was carried out on finely ground Bakken Shale samples (29 samples from 14 wells encompassing the entire maturity range) using an azeotropic mixture (23.4wt.-% methanol, 29.9wt.-% acetone and 46.7wt.-% chloroform) and applying the flow-blending method as described by Radke et al. (1978). Known amounts of internal standards were added prior to extraction for the quantification of saturated hydrocarbons (androstane) and aromatic hydrocarbons (1-phenylhexane, 1-phenylheptane, 1,8-dimethylnaphthalene, 1-phenylnaphthalene, 1-ethylpyrene, 1-butylpyrene). The extraction was carried out in a 1litre stainless steel centrifuge beaker into which the blending device was inserted. Copper powder was added to each sample in order to remove elemental sulphur. After extraction was completed the excess solvent was evaporated at room temperature under reduced pressure (250mbar) and extract yield was determined.

The ***asphaltene fraction*** was obtained from 29 flow-blending extracts and 5 crude oils using a method adapted from the one of Speight et al. (1983): Aliquots of whole extracts and crude oils were mixed with small amounts of redistilled, purified n-hexane and subsequently immersed into the ultrasonic bath in order to achieve thorough mixing of the reagents. Thereafter ca. 250ml n-hexane was added and the liquid was set to react for 24 hours at ambient temperature. Care was taken that the ratio of extract and crude oil, respectively to n-hexane was equal for all samples.

The precipitates (asphaltenes) were removed by filtering and stored in solution (dichloromethane).

Deasphaltened extracts (29) and crude oils (5) were submitted to ***medium pressure liquid chromatography*** (MPLC) (Radke et al., 1980a). The saturate, aromatic and polar fraction were obtained using silica gel as the stationary and n-hexane as the mobile phase.

The saturated and aromatic hydrocarbon fractions were analysed by ***gas chromatography*** (GC). The first of these were analysed using a HP 5890 gas chromatograph equipped with an 'Ultra 1' column (50m x 0.2mm) coated with cross-linked methyl silicone gum phase (0.33µm film thickness). The oven temperature was programmed from 90°C (4min. isothermal) to 310°C at 3°C/min. H_2 was used as the carrier gas. Sample introduction was performed by an on-column injection system. The experimental conditions for aromatic fraction analysis were the same as for the saturate fraction except for the following parameters: An 'Ultra 2' column was used coated with cross-linked 5% phenylmethyl silicone gum phase and He as the carrier gas. The oven temperature was programmed from 90°C (4min. isothermal) to 120°C (50°C/min.) followed by 3°C/min. up to 310°C. Identification of prominent peaks was carried out via retention time. Corrections for evaporation losses were applied (aromatic fraction).

16 samples from the saturate fraction from extracts and crude oils were selected for ***gas chromatography-mass spectrometry*** (GC-MS) analysis. The low abundance of biomarker molecules (steranes and hopanes) in the GC trace required a molecular sieve treatment of the samples in order to remove the normal alkanes. A 5Å molecular sieve was activated using iso-octane (3 hours at 350°C, 1Torr vacuum). The saturated fraction was set to react with the molecular sieve for 24 hours at 90°C.

For GC-MS analysis a VG 7070E mass spectrometer coupled to a Carlo Erba Fractovap model 4160 gas chromatograph was used (ionisation voltage: 70eV; source temperature: 220°C). Samples were introduced via a cold trap injection system (KAS 2, Gerstel) onto an 'Ultra 2' column (50m x o.32mm, film thickness 0.25µm). He was used as the carrier gas and the oven

was programmed from 110°C to 300°C (30min. isothermal) at 3°C/min. The metastable method was applied.

3.3.2 Petrophysical Analyses

Determination of Permeability

The sample preparation for measuring permeability of the Bakken Shale required the cutting of accurately sized cylinders of 28.5mm diameter and max. 30mm thickness. The brittle and sometimes laminated appearance of the Bakken samples created many problems during the preparation of the samples in that many plugs crumbled in the course of drilling and cutting. Unfortunately, these difficulties together with the minor availability of large pieces of cores consequently led to only a small number of samples (8) which were finally suitable for the permeability measurements.
The experimental set-up for measuring permeability (Hanebeck et al., 1994) is depicted in Fig. 9 and consists of a flow cell in which the cylindrical rock sample is sandwiched between two porous stainless steel plates which again are placed between two pistons. The cylinder walls of the sample as well as the frits and pistons are covered with a two-layered sleeve consisting of a teflon shrink tube and a thin-walled aluminium tube to which a confining pressure is applied. The sample holders are equipped with two 1/16" stainless steel tubes for introduction and removal of fluids.
Permeability was determined using water as the flow-through medium by applying a pressure gradient to the corresponding liquid on one side of the sample and monitoring the amount of liquid that reaches the other side as a function of elapsed time. In some experiments, increasing confining pressures were applied in order to investigate how permeability changes as function of lithostatic pressure.
Spreadsheets including background data on the rock plugs and analytical parameters of the experiments are given in the appendix.

Experimental Simulation of Petroleum Generation under Subsurface Conditions

Following the experimental conditions as laid out by Hanebeck et al. (1994) the behaviour of a Bakken Shale sample (0.68% R_o) under simulated subsurface conditions (overburden load, elevated temperature and pressure) was examined using the same experimental set-up as for permeability measurements (Fig. 9). In order to monitor how organic geochemical properties (organic richness, hydrocarbon generation potential, maturity and composition of generated material) as well as petrographic properties (fabric, distribution of organic matter etc.) are affected during the experiment, the sample was analysed at the end of the experiment (TOC content, pyrolysis, measurement of vitrinite reflectance) and the values compared to a reference sample which represented pre-experiment conditions.

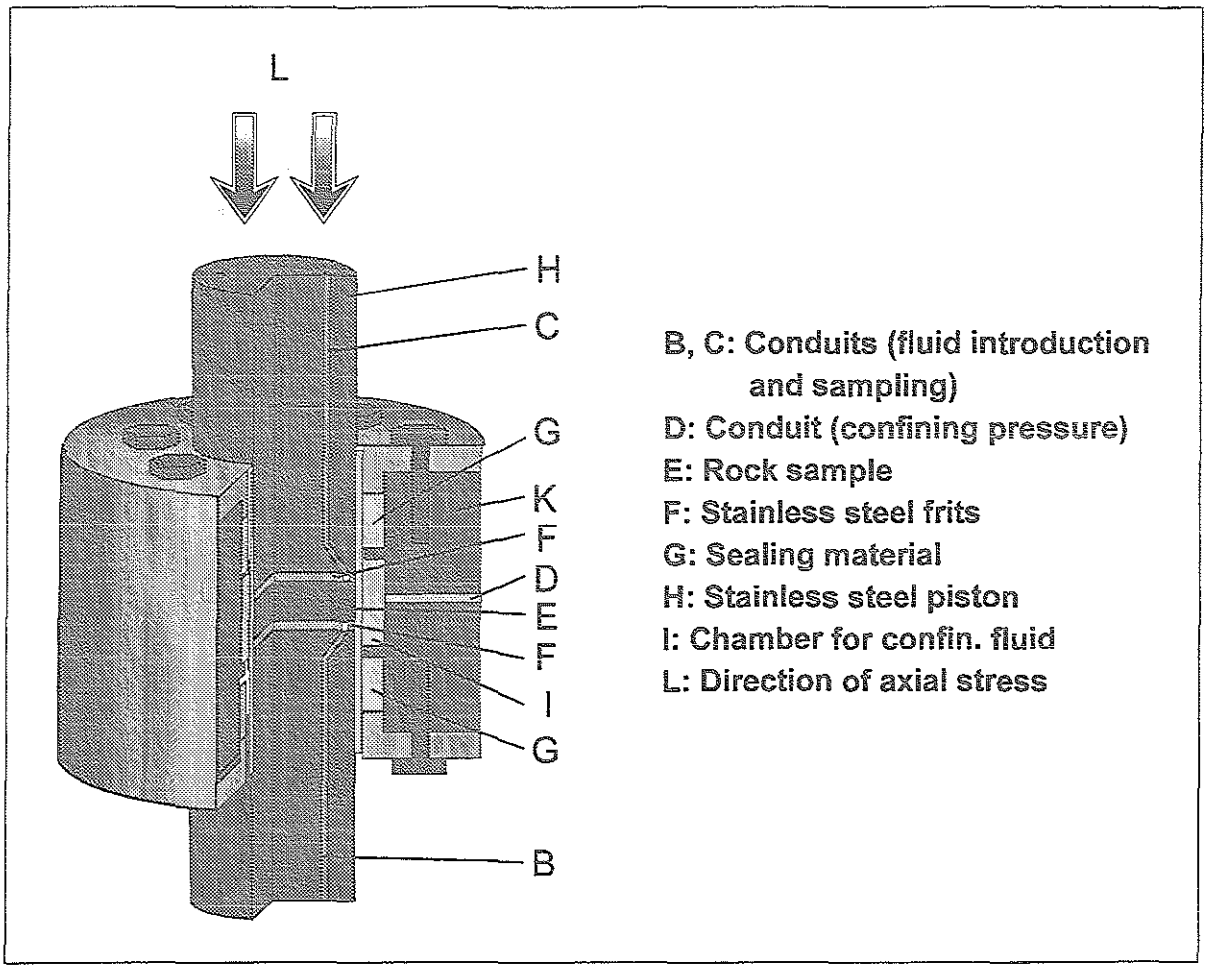

Fig. 9: Cross section of high temperature-high pressure triaxial flow cell which was used for determination of permeability and experimental simulation of petroleum generation under subsurface conditions. Reproduced from Hanebeck et al. (1994).

3.3.3 Mineralogical Analysis

Three Bakken Shale samples from three different levels of thermal evolution were investigated using *X-ray diffraction* (XRD) analysis in order to examine the mineral matrix of the rock. The solvent extracted powdered rock samples were treated with buffer (Na-acetate and acetic acid) and diluted H_2O_2 to remove carbonates and organic matter, respectively. The fine clay fraction (< 0.5µm) was collected using ultracentrifugation and saturated with Ca^{2+} ($CaCl_2$) to obtain a homoionic form with maximum expandability. Prior to XRD analysis fine clay samples were saturated with ethylene-glycol (vapor method).

4 Results

In the following, the results derived from screening techniques (organic petrology, organic carbon determination, Rock-Eval pyrolysis and IATROSCAN) are presented and discussed. They were used in order to assess maturity of the present sample set and to elucidate whether organic geochemical characteristics are exclusively associated with either of the two shale strata.

4.1 Bulk Characterisation of Solid Organic Matter

4.1.1 Kerogen Type and Abundance

Microscopic examination (reflected light) of Bakken Shale polished sections (lBK and uBK) revealed that large proportions of the fine-grained material is made up of dark, amorphous organic matter. Predominantly, the organic matter is finely disseminated throughout the rock without being locally concentrated. The finely dispersed, streaky appearance argues for bituminite which has been purported to be a decomposition product of algae, animal plankton, bacterial lipids and similar precursors (Stach et al., 1982). Furthermore, alginite, the maceral which is typical for oil shales (Stach et al., 1982) and oil-prone source rocks, can be encountered most often and can be easily detected under fluorescent light. Estimated proportions of the two predominant macerals are 25-30% bituminite and 10-15% alginite. These macerals were found for both shale units and from all depths and locations in the basin. However, as regards microscopic appearance of the kerogen and occurrence of macerals, depth-related properties can be observed: The fabric of relatively shallow samples (2000-ca. 2900m below surface) is characterised by larger components such as grains of pyrite, dolomite- and calcite-crystals, macerals and fossil fragments randomly incorporated into the rock matrix. Very few samples display a distinct lamination of light and dark components. A frequently observed feature of the shallow sample set is a 2-dimensional kerogen network in which some grey organic fragments are incorporated. The latter may be vitrinite particles. The alginite-submacerals still possess their original tube-like shape. Alginite A (Hutton et al., 1980), derived from the Chlorophyta *Tasmanites* was found to be most abundant together with minor amounts of alginite B (Hutton et al., 1980). These flat, elongated components emphasise the laminated fabric of the sediment in shallow samples.

Although it was not possible to define a clear boundary, it is evident that sections from greater depths (> ca. 2900m below surface) display different features: Here the sediment consists of a fine-grained, homogeneous matrix, in which a distinctive preferred orientation (lamination) of the organic matter is hardly discernable. Larger light-coloured components are very scarce to almost absent. At this level of burial, the only clearly identifiable particle types are either fragmentary or idiomorphic carbonate crystals. Well-defined macerals such as distinctly shaped alginite, a common feature of samples from shallow depths, are absent in samples of greater depths.

The slight variations in sedimentologic features (e.g. lamination) and the more distinctive change in the appearance of the kerogen could be related to differences in the depositional environment. This phenomenon would infer that the Bakken Shales of the depocentre and Billings Anticline

area (Fig. 6) were deposited under conditions different to the rest of the study area. This conclusion is contrary to what other studies (Meissner, 1978; Hayes & Holland, 1983; Webster, 1984) have shown. On the basis of visual (macroscopic and microscopic) sample examination these authors described the Bakken Shale as a sediment with a basinwide uniform organofacies.

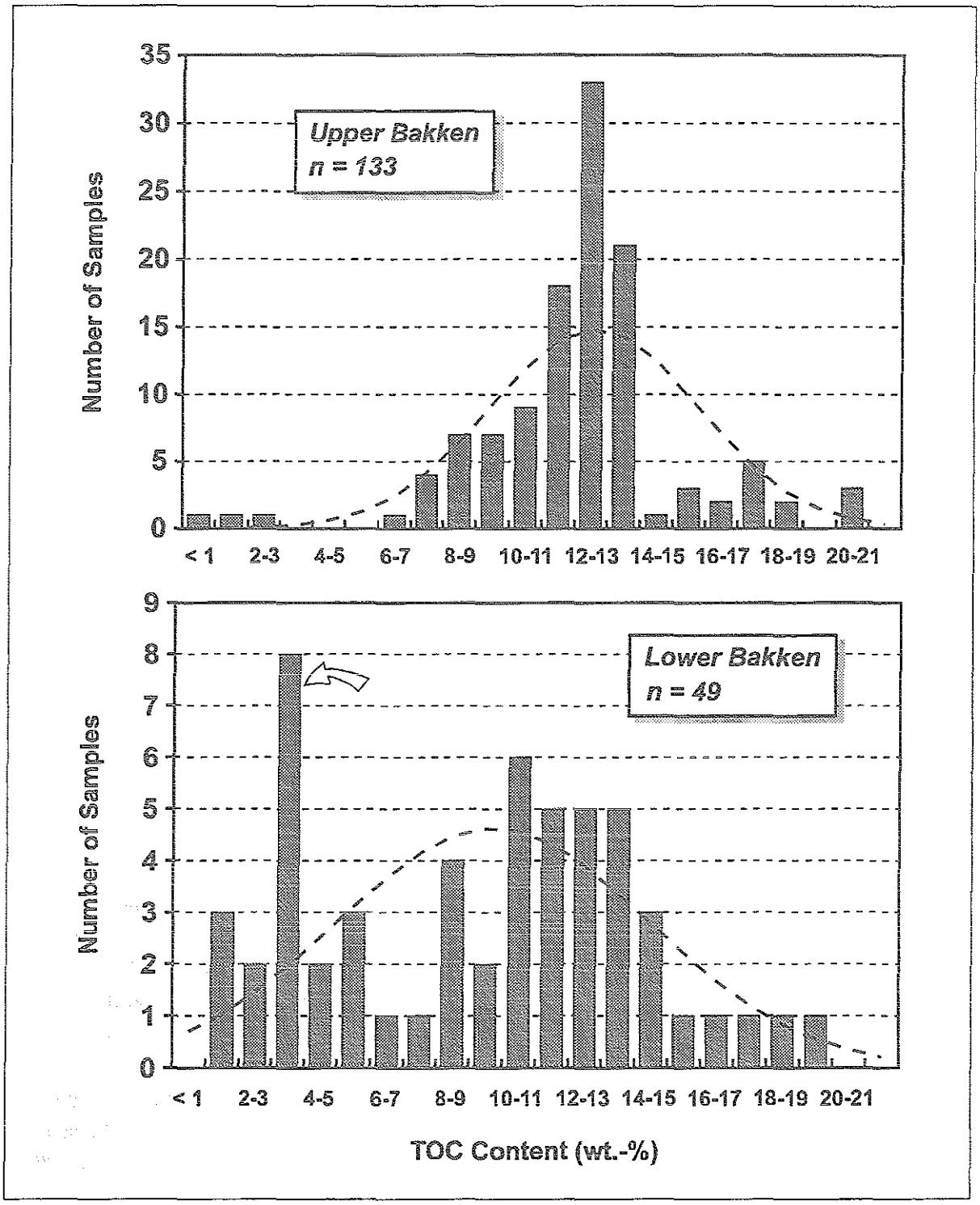

Fig. 10: Histogram distribution of TOC content for uBK and lBK. Arrow designates data which are derived from wells (lBK) located in a near-shore environment unfavorable for organic matter preservation.

An alternate explanation would be that the observed changes are a result of maturation. For instance, maturity related changes in organic matter habit have also been reported for the Toarcian Posidonia Shale in NW Germany (Littke et al., 1988): In this case, corresponding observations were made at a maturity level where $R_o = 0.9\%$.
Bakken samples from the *lower* shale unit from three wells (WAS, PIE and DOB) all of which were drilled close to the depositional pinch out of the lower Bakken Shale exhibit a kerogen of strikingly different nature: The macerals were fluorescing in orange colours and were structured like sporinite. Additionally, the overall lighter colour of the rock argues for lesser amounts of organic matter. This finding argues that the depositional environment at the rim of the Williston Basin has undergone more terrigenous sedimentation with less reducing conditions (impeded preservation of organic matter) than areas which were located in the center.

The results derived from TOC measurement and Rock-Eval pyrolysis (Tab. B, Appendix) confirm the high organic richness and the good source rock quality of the Bakken Shale as a whole. Fig. 10 displays the distribution of organic carbon as a histogram for the lower and upper shale unit. The upper shale unit exhibits a relatively narrow distribution curve with an average value between 12-13wt.-% TOC. Individual low TOC values are due to local layers of silty siliceous material in the usually fine-grained matrix, as macroscopic examination of the corresponding hand specimen reveals. This phenomenon leads to a dilution of the TOC content and a reduction of the value. The pattern for the lower shale appears to be broader indicating higher variability of organic richness. High frequencies in the group of 3-4wt.-% TOC are for those wells which are located close to the depositional edge of the basin (e.g. well PIE and the lower shale of well DOB). As already deduced from organic petrology, this feature is inherited from a near-shore environment of sedimentation where the input of organic matter was reduced and/or conditions were less favourable for its preservation. However, these wells are not representative for the entire Bakken system. If they are discarded, the averaged values for both shale strata are almost identical.
Van Krevelen-type diagrams, where the Rock-Eval parameters Hydrogen-Index (HI) and Oxygen-Index (OI) are plotted against each other, are commonly used for kerogen typing (Espitalié et al., 1977). Fig. 11 shows such a diagram in which the datapoints for uBK and lBK are discriminated. The upper Bakken Shale consists almost entirely of type II kerogen. The organic content of the lBK is also characterized by predominantly type II kerogen. Although the kerogen of two wells (JEN and JOH, Tab. B, Appendix) reveals HI/OI relationships which indicate a slight bias to a more terrigenous material, it is apparent that the kerogen-type for both shale units can be designated as type II. It must be noted that this way of plotting kerogen-type relevant parameters is not suitable for detecting variations in source rock quality in the shallow wells PIE and DOB (lower shale unit). Below, this point is discussed by examining samples from two individual wells.
Fig. 12 provides some insight into vertical small-scale variations in kerogen quality in addition to shale unit-specific features, as exemplified by the TOC content and HI of two wells, the shallow DOB (uBK and lBK) and the deeper JEN (uBK and lBK). These cores are labelled #1 and #9 in Fig. 6, respectively. In the immature core DOB the distribution of organic carbon content and HI between upper and lower Shale is rather heterogeneous. The upper Shale is generally organic rich and shows a relatively high genetic potential for hydrocarbons (HI), the lower, in contrast, can be considered a low-quality source rock. Such low results could be brought about by a local

depletion in organic carbon. As already laid out in section 4.1.1, the lower Shale interval of this core was located near the shore line of the depositional basin where oxic conditions have prevailed. Accordingly, TOC content is reduced. These conditions are also manifested in the samples of well PIE, which show similar results (Tab. B, Appendix).

The distribution of TOC and HI in the mature well JEN where the Bakken Shales are at a depth of ca. 3050 to 3130m below surface in the central part of the basin (Fig. 6) illustrates that organofacies is rather homogeneous and that there are no significant shale unit-specific differences: TOC as well as HI exhibit only a small range of variability for both shale units (between 9 and 14wt.-% and between 130 and 180, respectively). Hence, there is compelling evidence that the samples from wells located distant to the depositional edge of the respective shale unit can be considered uniform with respect to source rock quality.

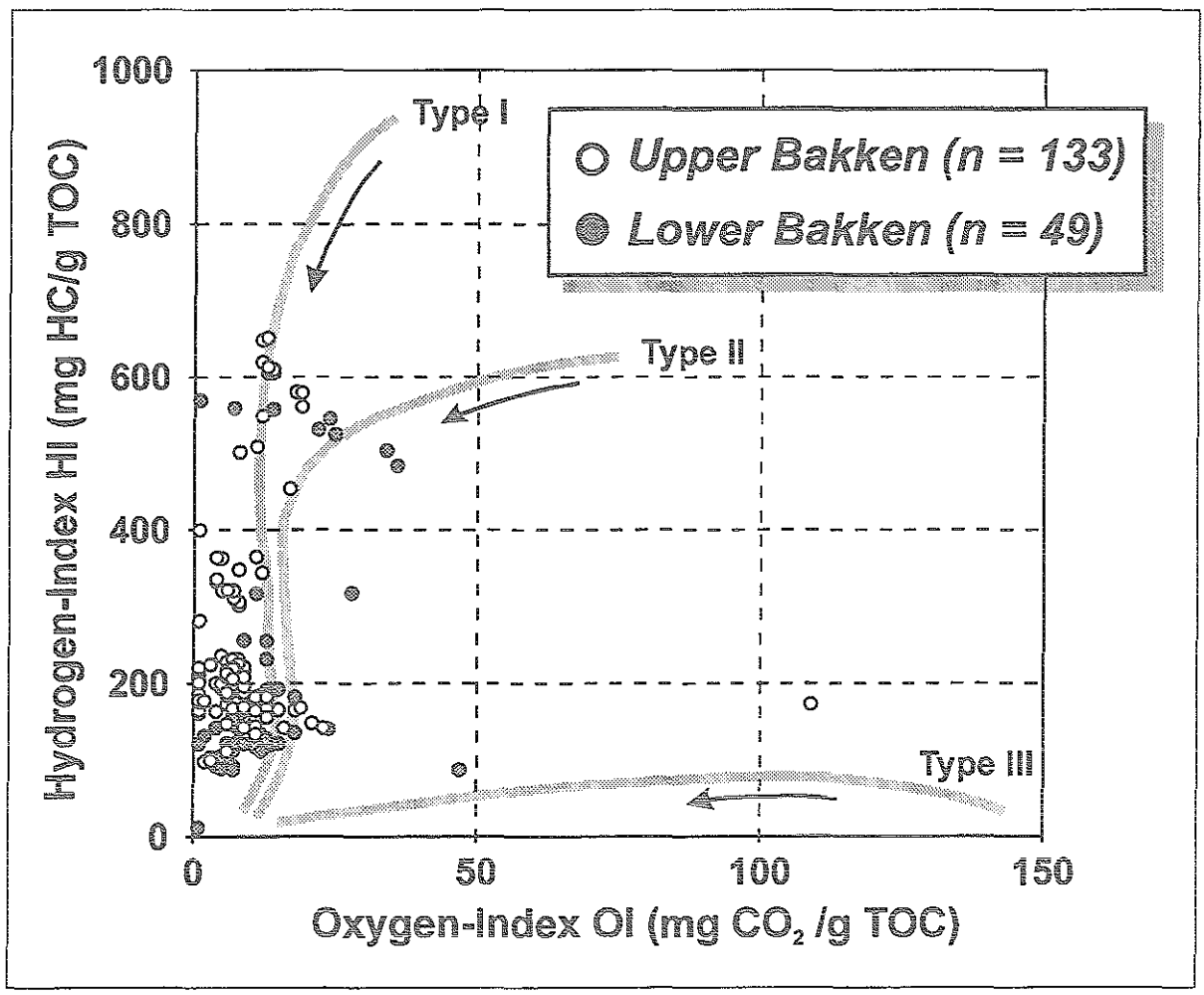

Fig. 11: Van Krevelen-type diagram (HI vs. OI) derived from Rock-Eval analysis of the entire Bakken Shale sample set. Maturation pathways and boundaries for different kerogen types are adopted from Espitalié et al (1977).

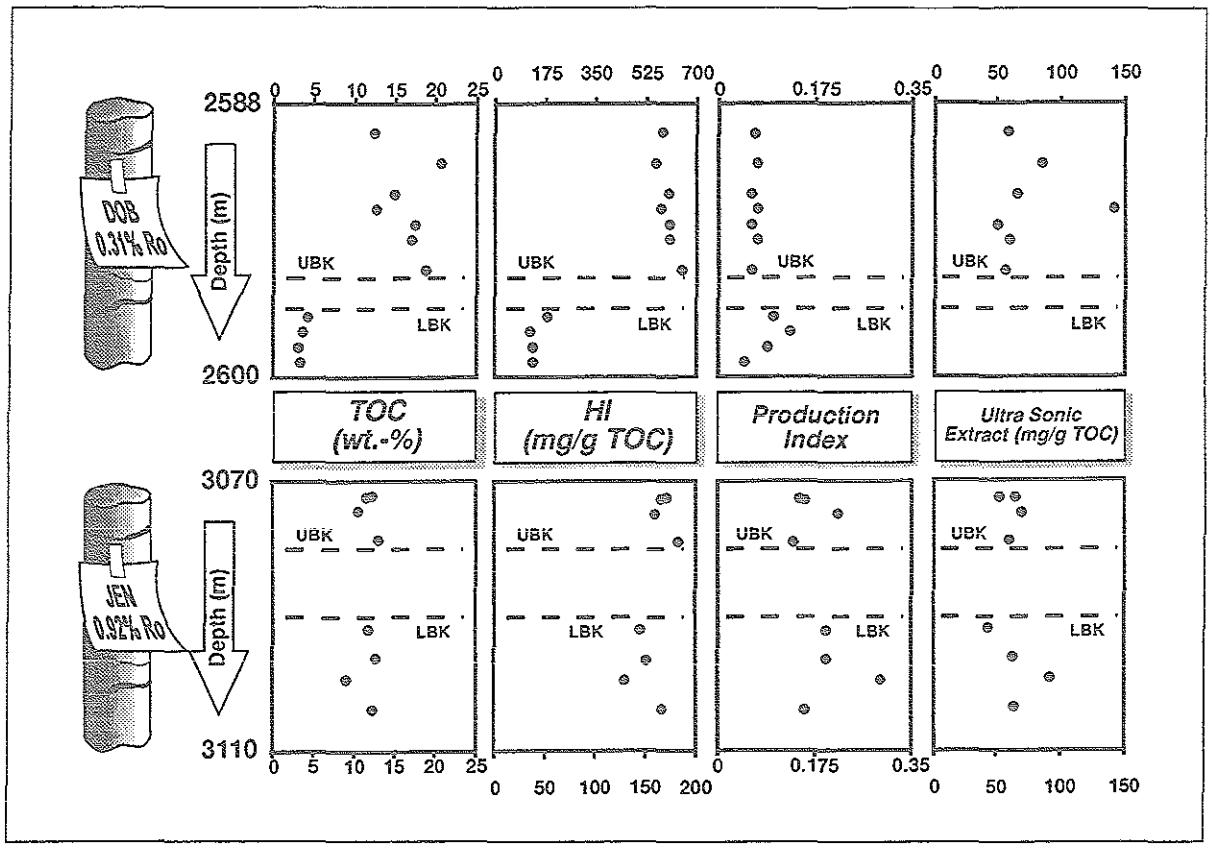

Fig. 12: Comparison of TOC, Rock-Eval parameters and yield of solvent extract (ultra sonic method) of lower (lBK) and upper (uBK) Bakken Shale samples taken from a shallow, immature well (DOB, 0.31% R_o) and a relatively deep, mature well (JEN, 0.92% R_o). Note the difference in scale for the two wells with respect to Hydrogen Index.

4.1.2 Maturity

With respect to the low thickness of the Bakken Formation (max. ca. 50m; ch. 2.2.1), the measurement of vitrinite reflectance on one polished section per borehole (either shale unit) was considered adequate for a representative determination of maturity. Despite the confirmed marine nature of the Bakken Shale (Webster, 1984; Price et al., 1984), terrigenous macerals of the vitrinite group typically make up 5vol.-% of the total of organoclasts (liptinites, vitrinites and inertinites) (Ropertz, 1994). In order to substantiate the measurements of reflectance, arguments like regional distribution of wells in the basin and correlation with depth as well as literature data had to be considered in evaluation of the results.

Tab. 1 displays the results of R_o determination. Although the measured values cover a broad range from 0.24% (WAS) to 1.57% (THO), the majority of the values lie between 0.9 and 1.2%. According to the general relationship of maturity zonation and vitrinite reflectance (Tissot & Welte, 1984), this feature indicates that most of the sampled wells are in the mature zone of the oil-window.

Table 1: Vitrinite reflectance as determined for the entire set of wells (total of 28). Well # refers to location of wells in study area (Fig. 6). Wells marked * were only used for screening analyses (ch. 3.2)

Well #	Well name	R_o (%)	Well #	Well name	R_o (%)
*	WAS	0.24	8	MAR	0.90
*	PIE	0.27	9	JEN	0.92
1	DOB	0.31	10	CON	0.94
2	JAC	0.55	*	MIN	0.95
3	NEG	0.57	*	WEB	0.95
*	TEX	0.66	*	GIL	0.98
4	SKA	0.68	11	FED	0.99
5	BOR	0.72	*	REE	1.05
*	FOR	0.72	*	UST	1.05
*	JOH	0.74	*	MOI	1.08
*	ASW	0.81	12	HOV	1.11
7	SET	0.83	*	HHS	1.11
6	GRA	0.83	13	BEH	1.26
*	XYZ	0.89	14	THO	1.57

The determination of vitrinite reflectance as a tool to establish the level of maturity of kerogen has been used for several decades (e.g. Vassoevich et al., 1970). In contrast to chemical methods, where normally the kerogen as a whole is analysed, the measurement of R_o has been considered to be unaffected by variations in kerogen composition (Tissot & Welte, 1984) and it also enables the investigator to discriminate indigenous vitrinite, which reflects the thermal evolution of the in-situ organic matter, from potentially reworked particles. While other maturity parameters are only sensitive in certain intervals of thermal alteration, vitrinite reflectance can be used over the entire range of organic matter maturation and is therefore considered to be the most reliable and most often used maturity indicator (Dow, 1977). Furthermore and most importantly, vitrinite reflectance is commonly used to define principal zones which are associated with enhanced oil and gas (wet gas and dry gas) generation (Vassoevich et al., 1970; Tissot & Welte, 1984).

In the present study, this parameter also provides the framework for most considerations related to increasing maturation. Hence, the maturity spectrum as derived from R_o measurement appears to be rather broad (0.24 to 1.57% R_o) implying that the sample set incorporates equivalents from immature, mature and overmature stages of hydrocarbon generation. With respect to the absolute values, however, Webster (1984) attributed the maximum R_o value for the Bakken Shale in the North Dakota portion of the Williston Basin to be considerably lower (ca. 1.0%).

The cross-plot of T_{max} (values combined from both shale units) with R_o (Fig. 13) shows a very good fit. Up to ca. 1.0% R_o, the trend is fairly consistent with data from the type II Posidonia Shale kerogen (Rullkötter et al., 1988) and marine shales from the Cretaceous of British Columbia (Leckie et al., 1988). However, it is evident that the rather well-defined relationship between both maturity parameters is less pronounced for the *mature* zone and that the highest value for R_o (1.57%) is not related to the highest T_{max} (453°C). Furthermore, while the spectrum for vitrinite reflectance for the mature samples is relatively broad (0.7% to almost 1.6%), the

range for T_{max} is rather narrow (439 to 453°C). This feature might indicate that the range of thermal evolution for the mature sample set as established by vitrinite reflectance is too wide. Hence, it cannot be excluded that the highest R_o values (BEH: 1.26% R_o; THO: 1.57% R_o) might have been derived from inertinite particles. Alternatively, the ubiquitous presence of pyrite grains close to vitrinite macerals might have interferred with the measurement of reflectance of a given vitrinite. Considerations with respect to well location also corroborate that the level of maturity for wells BEH and THO as deduced from R_o is too high: The location of well BEH is directly adjacent (same section; distance ≤ 1.6km) to well MAR (0.9% R_o). R_o values measured for other wells in this area covered a range between 0.8% and 1.0% R_o, thus outlining a regional R_o trend similar to the one established by Webster (1984). In the case of well THO there is a similar pattern: Except for THO (1.57% R_o), all other wells in the Billings Anticline area exhibit much lower R_o values (0.9% to 1.1%).

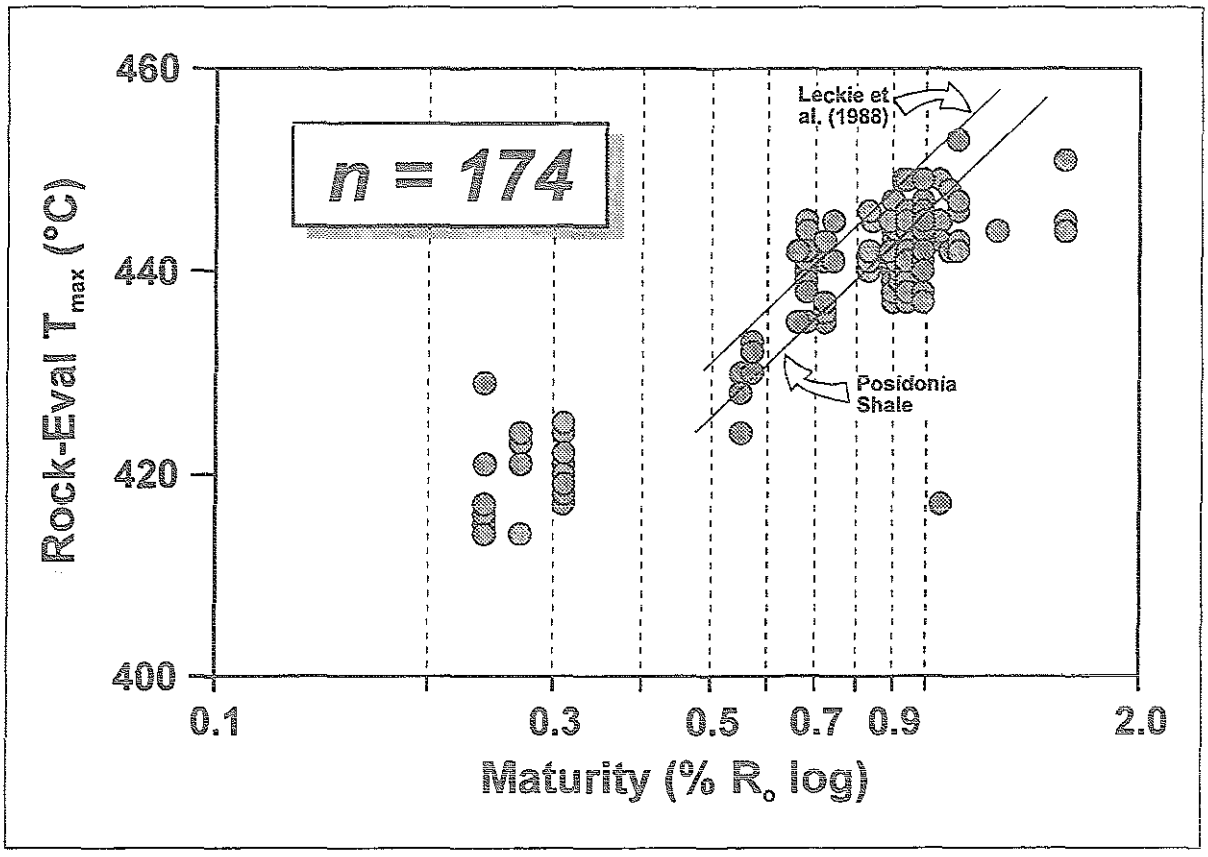

Fig. 13: Relationship of maturity parameters (T_{max} vs. R_o) for 174 samples from both shale units including superimposed data from other type II kerogens. Posidonia Shale values are taken from Rullkötter et al. (1988).

As the reflectance of vitrinite is a direct and irreversible measure for the thermal history of the associated organic matter, local anomalies in R_o values might be an expression of a higher heat flow in that particular area. As regards well BEH, however, it appears to be very unlikely that such an inferred "hot spot" does not affect the kerogen of the adjacent well MAR. Furthermore, such an enhanced heat flow should also have some bearing on the kerogen in terms of reduced hydrocarbon generation potential. However, neither bulk (Rock-Eval HI) nor compostional parameters (py-gc) provide any evidence for such a conclusion. Based on Rock-Eval analyses,

Price et al. (1984) provided some evidence that there are two different paleo heat flow zones in the Williston Basin. However, all samples of the present study above 0.57% R_o fall within one of these two paleo heat flow zones. Thus, there is apparently no evidence from geology or basin analysis which would support the existence of locally raised heat flows.

Alternatively, both samples from wells BEH and THO on which R_o was measured may contain at least two different populations of vitrinites. Indeed, in the light of the very low abundance and the small size of the vitrinite particles, it may have been difficult to discriminate between indigenous vitrinite and potentially reworked macerals of the same group exhibiting an enhanced degree of reflectance. Additionally, different vitrinite populations can occur in oil shales (Hutton & Cook, 1980; Kalkreuth & Macauley, 1984) and coals, namely vitrinite 1 (hydrogen-poor, high reflectance, non-fluorescing) and vitrinite 2 (hydrogen-rich, low reflectance, weak fluorescence) (Buiskool Toxopeus, 1983).

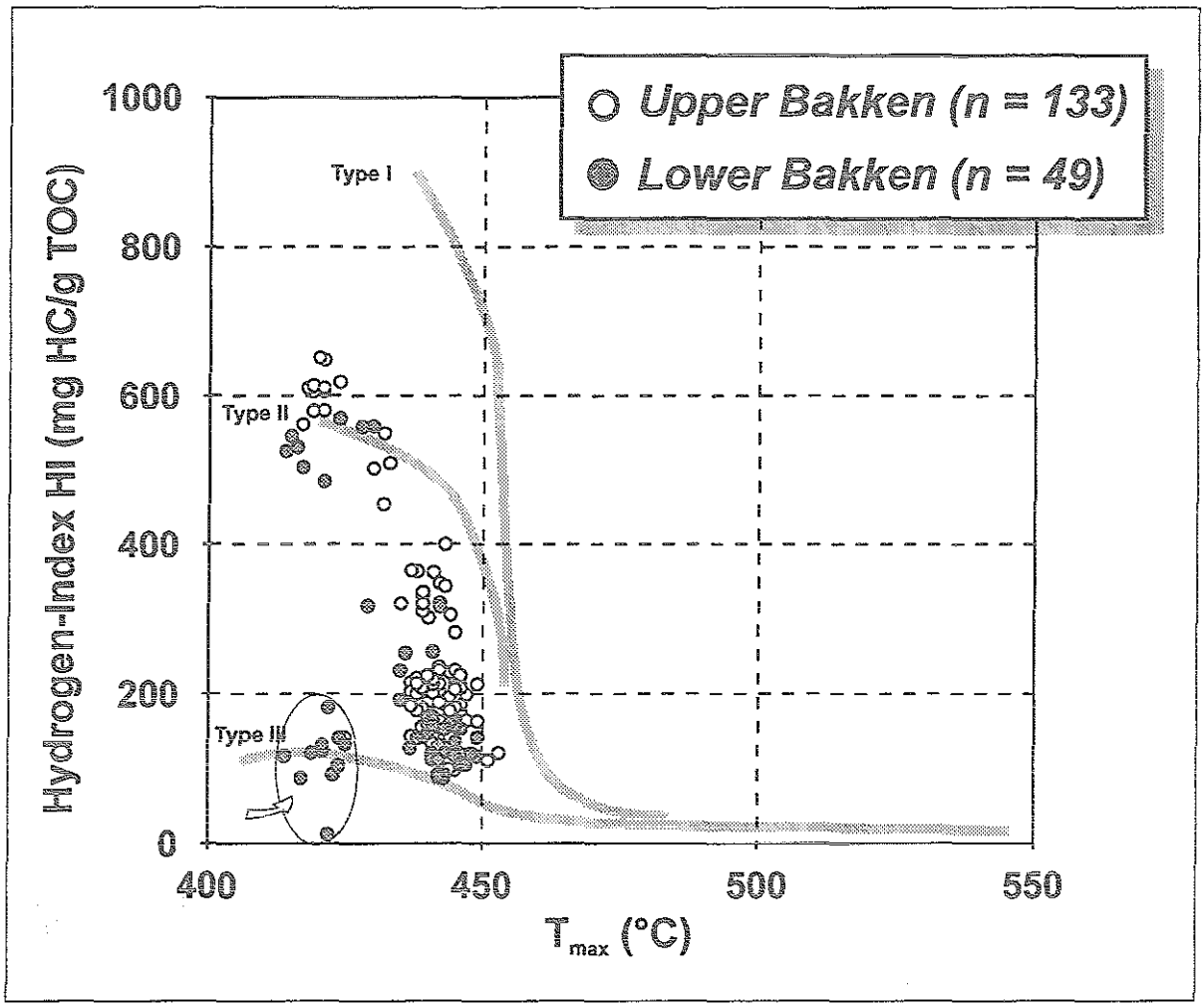

Fig. 14: Cross-plot of genetic potential (HI) and maturity (T_{max}) elucidates that the majority of the samples stems from the mature zone (430 to 450°C T_{max}). Datapoints surrounded by solid line and marked by arrow are from immature (< 0.4% R_o) well PIE (6), well WAS (2) and from the IBK of well DOB (4) and illustrate that the corresponding kerogen is of type III.

Fig. 14 displays the relationship between HI and T_{max}. A maturation pathway is described indicating a successive generation of hydrocarbons (decrease in HI) paralleled by a continuous

increase in T_{max}. It becomes also evident that the majority of the samples fall into the mature zone, where the hydrocarbon generation potential (HI) of the residual kerogen is already diminished to values between 300 and 100. The diagram also might provide some evidence that kerogens from the upper shale unit show a higher generative capacity for petroleum than their lower equivalent of the same maturity (zone of 435° to 450°C T_{max}). This is most pronounced for the shallow wells, as Fig. 12 has revealed, but may also be applicable to higher depths (Fig. 14). However, this phenomenon might also be due to the normal scatter of the datapoints.

Based on the careful evaluation of the vitrinite reflectance measurements and Rock-Eval maturity parameters as well as regional trends it has to be pointed out that the actual maturity range as covered by the samples of the present study only goes up to ca. 1.1% R_o (well HOV). This feature is indicated by a line ("stop" sign) intersecting the R_o axis at 1.1% in diagrams in which data are plotted versus a R_o scale (ch. 5 "discussion and interpretation").

Strong evidence that well HOV (1.11% R_o) may represent the most mature member of the present study is also provided by aromatic maturity parameters (ch. 4.5).

Comparison of the natural maturity sequence with equivalent data from simulated maturation is discussed in ch. 5.2.2 and serves as a further indicator for maturity assessment. Fig. 77 illustrates that the natural pyrolysates from well HOV displayed the lowest values for total yield as well as for the three subfractions (C_{1-5}, C_{6-14}, C_{15+}) of the entire maturity spectrum. With the prerequisite that major facies shifts can be excluded, this implies that this well has suffered from the most comprehensive organic matter conversion (loss of hydrocarbon generation potential) of all wells. Additionally, these values are almost identical with the lowest corresponding values as derived from the most severe level of artificial maturation (350°C/5 days). With respect to the evaluation of maturity assessment, this feature might serve as a complimentary indication that well HOV indeed represents the most mature well of the present sample set.

4.2 Bulk Characterisation of Mobile Organic Matter

This section focusses on yield and composition of the volatilizable organic matter from screening analyses (Rock-Eval S1, solvent extract and subsequent IATROSCAN analysis) of the two shale units. Emphasis was laid on detecting potential dissimilarities of the upper vs. lower Bakken Shale.

4.2.1 Yield as a Function of Maturity

The yield of the volatilisable organic matter in the Bakken was determined using thermal (Rock-Eval pyrolysis) and solvent extraction (ultrasonic) methods. Results are listed in Tab. 2.

Table 2: Extract yield as derived from ultra sonic extraction (dichloromethane) of 108 Bakken Shale samples from the entire set of wells. Additional background data (S1) from Rock-Eval pyrolysis. Well # refers to location of wells in study area (Fig. 6). Wells marked * were only used for screening analyses (ch. 3.2)

Sample ID	Well name (#)	R_o (%)	Extract (mg/g rock)	Extract (mg/g TOC)	S1 (mg/g rock)	S1 (mg/g TOC)
E34291	WAS*	0.24	5.93	58.73	2.28	22.57
E34292			1.40	40.21	0.59	17.00
E34293			6.02	44.91	3.92	29.25
E34295			6.09	46.12	3.84	29.09
E34257	PIE*	0.27	1.11	96.31	0.44	38.26
E34267	DOB	0.31	1.35	45.35	0.56	18.79
E34270	(1)		7.38	59.02	5.25	42.00
E34272			17.92	86.14	8.20	39.42
E34275			9.95	66.32	5.60	37.33
E34276			18.00	141.73	5.19	40.87
E34277			8.88	50.47	6.76	38.41
E34278			10.33	60.43	7.77	45.44
E34280			10.70	56.61	8.39	44.39
E34263	JAC	0.55	12.63	74.29	7.78	45.76
E34264	(2)		9.82	50.60	9.08	46.80
E34287	NEG	0.57	24.00	150.94	5.35	33.65
E34288	(3)		21.70	106.90	8.23	40.54
E34435	SKA	0.68	5.56	56.37	2.10	21.28
E34436	(4)		7.15	64.37	2.64	23.78
E34437			7.58	71.55	2.31	21.79
E34438			9.60	61.96	4.10	26.45
E34440			9.18	77.12	3.25	27.31
E34441			10.65	82.54	3.83	29.69
E34443			10.96	68.10	5.13	31.86
E34444			8.23	66.88	3.38	27.48
E34299	FOR*	0.72	6.57	56.60	4.06	35.00
E34300			6.25	58.96	3.27	30.85
E34306	BOR	0.72	9.53	72.76	2.38	18.17
E34307	(5)		8.28	65.21	2.89	22.76
E34308			10.81	81.91	3.40	25.76
E34317	JOH*	0.74	6.84	53.40	3.83	29.92
E34318			9.33	74.05	6.25	49.60
E34334	ASW*	0.81	9.17	82.61	5.06	45.59
E34336			8.77	79.00	4.78	43.06
E34342	SET	0.83	9.89	110.22	4.92	54.85
E34343	(7)		8.87	69.28	5.39	42.11
E34344			8.12	59.30	5.79	42.26
E34345			6.61	59.05	3.71	33.13
E34364	GRA	0.83	6.68	72.25	3.55	38.38
E34366	(6)		6.31	61.29	3.12	30.29
E34368			6.61	65.43	2.93	29.01
E34355	XYZ*	0.89	6.74	61.85	3.23	29.63
E34356			6.79	67.88	3.51	35.10
E34320	MAR	0.9	6.29	69.39	2.43	26.82
E34321	(8)		7.83	76.07	3.80	36.89
E34322			7.44	55.96	4.39	33.01
E34323			7.36	70.78	3.22	30.96
E34324			8.05	71.89	3.56	31.79
E34325			6.93	79.34	3.24	37.07
E34326			8.34	69.53	3.64	30.33
E34328			6.28	76.25	4.44	53.88

Sample ID	Well name (#)	R_o (%)	Extract (mg/g rock)	Extract (mg/g TOC)	S1 (mg/g rock)	S1 (mg/g TOC)
E34310	JEN	0.92	6.37	52.19	3.66	30.00
E34311	(9)		7.33	64.30	3.71	32.54
E34312			7.78	59.81	3.75	28.85
E34313			5.00	42.37	4.39	37.20
E34316			7.81	64.04	4.01	32.87
E34449			7.20	69.23	4.63	44.52
E34454			7.89	62.59	4.80	38.10
E34455			8.21	92.52	4.88	55.02
E34376	CON	0.94	0.86	7.50	4.04	35.13
E34378	(10)		8.50	100.59	3.85	45.56
E34379			7.39	67.79	3.72	34.13
E34381			7.67	60.42	4.19	32.99
E34382			7.08	63.78	3.89	35.05
E34383			6.40	62.75	4.22	41.37
E34412			6.64	79.86	3.12	37.55
E34386			5.54	45.37	3.98	32.62
E34389			7.93	61.97	5.29	41.33
E34390			6.79	54.32	3.80	30.40
E34394			6.77	63.28	4.12	38.50
E34396			7.97	62.73	4.12	32.44
E34398			7.12	54.79	4.22	32.46
E34400			8.36	62.41	3.75	27.99
E34402			7.15	52.94	3.52	26.07
E34403			7.14	52.51	4.58	33.68
E34405			7.59	60.25	3.86	30.63
E34409			7.93	61.47	3.82	29.61
E34412			6.64	51.47	3.46	26.82
E34414			8.16	62.77	3.64	28.00
E34416			7.79	59.50	3.68	28.09
E34419			7.05	55.09	3.24	25.31
E34337	MIN*	0.95	7.42	51.88	4.74	33.15
E34338			7.40	62.18	4.42	37.14
E34353	WEB*	0.95	9.51	112.15	4.25	50.12
E34354			8.26	73.71	6.10	54.46
E34302	GIL*	0.98	5.60	37.61	3.99	26.78
E34303			4.40	33.56	4.31	32.90
E34422	FED	0.99	7.05	56.86	3.57	28.79
E34425	(11)		7.50	59.97	3.88	31.04
E34426			7.29	66.29	4.36	39.64
E34428			7.82	97.85	3.47	43.43
E34430			7.52	73.76	3.87	37.94
E34432			6.80	50.33	3.69	27.33
E34434			6.39	46.00	4.85	34.89
E34305	REE*	1.05	8.50	59.47	4.40	30.77
E34357	MOI*	1.08	6.37	66.79	3.66	38.36
E34358			6.41	67.14	3.70	38.78
E34304	HHS*	1.11	7.27	55.92	3.78	29.08
E34347	HOV	1.11	6.99	68.55	4.53	44.41
E34349	(12)		7.98	73.84	4.88	45.19
E34350			6.87	56.75	4.25	35.12
E34351			5.58	55.79	4.03	40.30
E34331	BEH*	1.26	7.73	64.95	4.03	33.87
E34360	THO	1.57	6.68	56.57	5.38	45.59
E34361	(14)		7.22	80.66	3.96	44.25
E34362			6.41	53.89	5.19	43.61

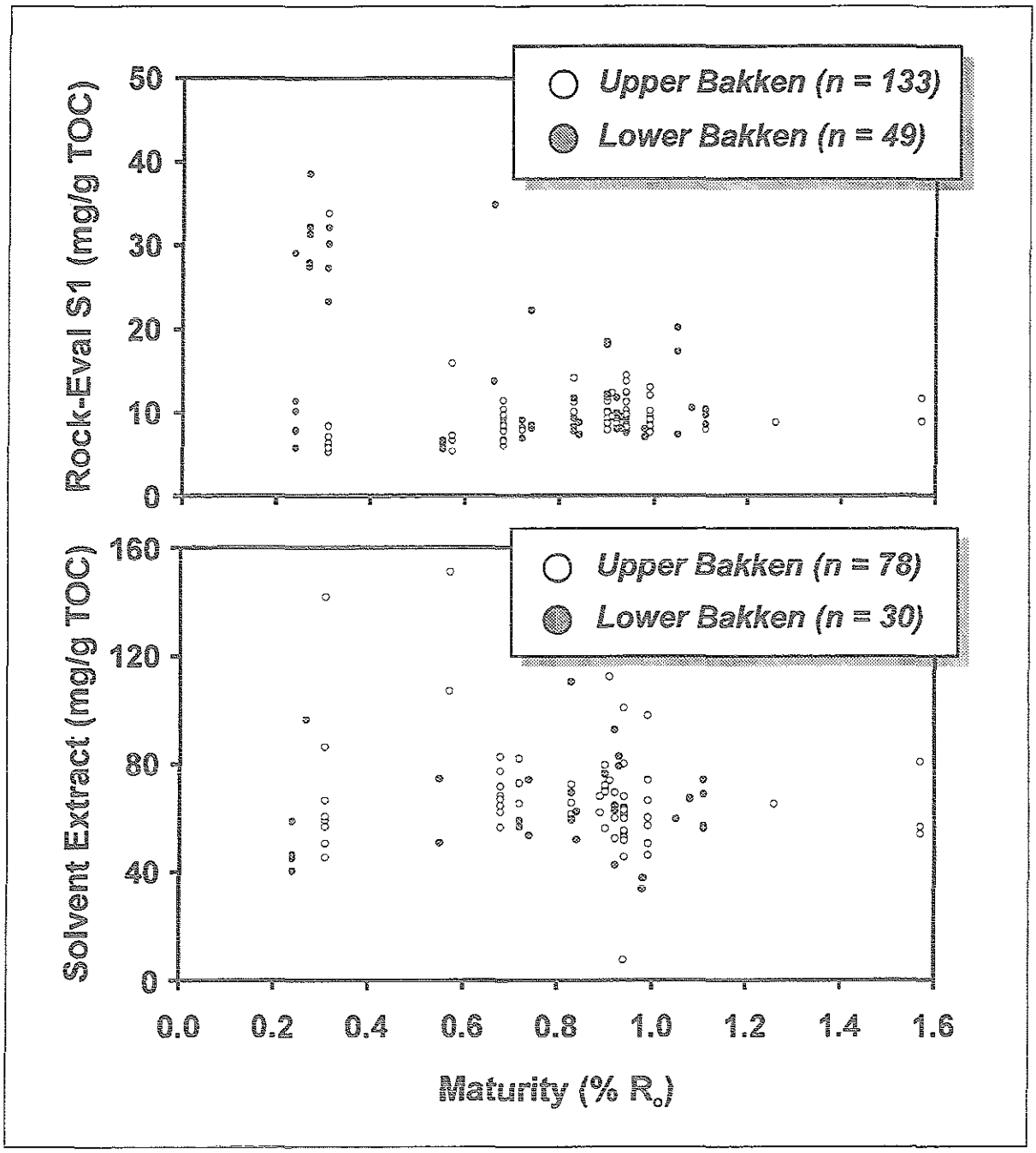

Fig. 15: The thermally releasable organic matter (S1) as well as the solvent extract (ultra sonic) of the both Bakken Shale units show maximum yield as well as variability at low levels of thermal evolution (< 0.7% R_o).

The yield of mobile organic phase of the Bakken Shale, expressed as S1 normalized to TOC, falls in a step-like pattern if plotted against maturity (Fig. 15): In the low mature zone (< 0.7% R_o), the yield as well as the scatter of the datapoints are relatively high for S1 material. This phenomenon of high variability in samples from shallow depths has also been encountered with respect to TOC content and Rock-Eval HI (ch. 4.1.1). The organically lean samples from wells close to the depositional edge (PIE at 0.27% and the IBK of DOB at 0.31% R_o), however, show extremely low values for S1, which also corroborates that samples from this region are not representative for the Bakken system, as has been shown before (ch. 4.1). Between 0.6 and 0.7% R_o, the yield

of thermally releasable organic matter drops and at the same time, the variability of the data is reduced. From that level of maturation on, averaged values for S1 remain fairly constant.
The values for the solvent extractable bitumen, depicted in Fig. 15, also outline a maturity zonation similar to the S1 data, but not as pronounced: Samples less mature than 0.6% R_o, especially well NEG at 0.57% R_o (107 to 151mg/g TOC), contain relatively high amounts of bitumen. Again, from 0.65% R_o on, extract yield remains in the range of 30 to 100mg/g TOC. Bitumen yields in this range have also been reported for other marine type-II kerogens (Louis & Tissot, 1967; Tissot et al., 1971; Powell & McKirdy, 1975; Rullkötter et al., 1988).

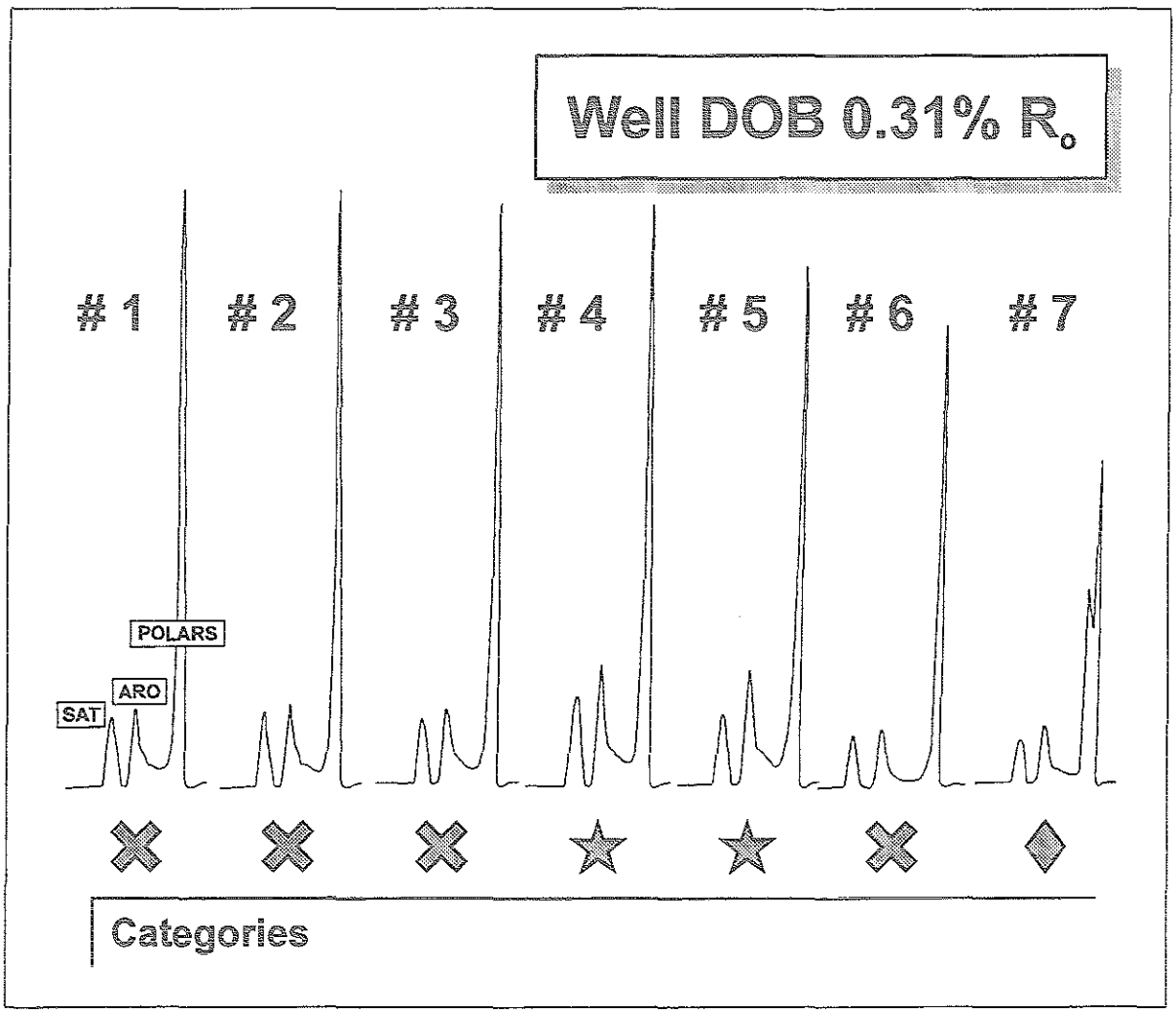

Fig. 16: Suite of IATROSCAN traces for solvent extracts exemplified for well DOB. Traces were categorized based on their fingerprint using various criteria as explained in text. Extracts belonging to the same category are marked with the same symbol.

4.2.2 Composition of Extracts

The FID traces derived from IATROSCAN analysis of 108 ultrasonic extracts were used to monitor bulk compositional differences (relative amount of saturate, aromatic and resin fraction) of the extracts within one well based on the fingerprint of the IATROSCAN trace. Although multiple quantitative analysis of a standard extract revealed that the reproduciblity of the IATROSCAN device was too poor to enable an accurate quantification of the three fractions the

fingerprint of each IATROSCAN trace could be used to evaluate potential compositional heterogeneities as regards the bulk composition of bitumen within one well. Criteria such as the shape of the individual peaks (e.g splitting of polar compound peak), the predominance of fractions over each other within a given sample (e.g. SAT vs. ARO), separation of aromatic fraction from polar compound peak were used to categorize extracts. Samples which displayed similar fingerprints were combined in one category. Fig. 16 shows a suite of IATROSCAN traces from the immature well DOB including categorization. Tab. 3 shows the number of extract categories for each well. The results from IATROSCAN were used in order to reduce the number of samples for further extraction and GC analysis.

Table 3: Evaluation of ultra sonic extract composition based on IATROSCAN analysis (fingerprinting) and categorisation deduced thereof. Wells of which less than three extracts were analysed were not categorised. Well # refers to location of wells in study area (Fig. 6). Wells marked * were only used for screening analyses (ch. 3.2)

Well #	Well name	R_o (%)	A	B	Number of categories	Remarks (composition)
*	WAS	0.24	2.10	4	4	extremely heterogeneous
*	PIE	0.27		1		
1	DOB	0.31	2.40	8	3	rather homogeneous
2	JAC	0.55		2		
3	NEG	0.57		2		
4	SKA	0.68	11.20	8	2	poor separation of aromatic/NSO fraction
*	FOR	0.72		2		
5	BOR	0.72	0.60	3	2	heterogeneous aromatic fraction
*	JOH	0.74		2		
*	ASW	0.81		2		
6	GRA	0.83	3.30	4	1	very homogeneous
7	SET	0.83	2.70	4	2	rather homogeneous
*	XYZ	0.89		2		
8	MAR	0.90	)[x]	8	3	
9	JEN	0.92	)[x]	8	3	rel. high SAT/ARO ratio (>>1.0)
10	CON	0.94	)[xx]	22	2	
*	MIN	0.95		2		
*	WEB	0.95		2		
*	GIL	0.98		2		
11	FED	0.99	2.00	7	2	high NSO content!
*	REE	1.05		1		
*	MOI	1.08		2		
12	HOV	1.11	3.40	4	2	rel. high SAT/ARO ratio (>>1.0)
*	HHS	1.11		1		
13	BEH	1.26		1		
14	THO	1.57	1.20	3	1	

A: Approximate depth range of extracted samples (m)
B: Number of analysed extracts (shales only)
)[x]: samples from lBK and uBK
)[xx]: horizontal well

4.3 Representativity and Quality of the Sample Set - Summary

The goals and philosophy of the present research project required certain attributes of the sample set. Based on the results and data that have been obtained from organic petrology, Rock-Eval pyrolysis, ultrasonic extraction and IATROSCAN analysis, it was possible to single out certain samples and/or cores which appear to be unrepresentative for the Bakken petroleum system. Accordingly, samples and/or cores were eliminated which contained terrigenous kerogen (organic petrology, Rock-Eval) and which had very low contents of organic matter (TOC < 5wt.-%). Moreover, the number of samples for further studies could be reduced. Furthermore and importantly, the results from screening analyses confirm that the two shale units of relatively deep buried Bakken Formation (> 2900m) do not exhibit *bulk* properties that are preferably associated with either of the two strata. Hence, shale samples from either stratum appear to be representative for the entire Bakken system.
Tab. 4 displays the selected set of wells with the maximum number of samples available for further analyses (t'vap-gc, py-gc, IR spectroscopy, analysis of solvent extracable organic matter).

Table 4: Selected set of wells (total of 14) covering the entire maturity spectrum. Samples from this set of wells were chosen for further methodology (see "methodology of selected sample set"). Number of samples give the maximum number of samples available for analyses. Well # refers to location of wells in study area (Fig. 6).

Well #	Well name	R_o (%)	Number of samples uBK	lBK	Well #	Well name	R_o (%)	Number of samples uBK	lBK
1	DOB	0.31	13		8	MAR	0.90	9	
2	JAC	0.55		3	9	JEN	0.92	4	2
3	NEG	0.57	3		10	CON	0.94	51	
4	SKA	0.68	11		11	FED	0.99	13	
5	BOR	0.72	3		12	HOV	1.11		5
6	GRA	0.83	4		13	BEH	1.26	1	
7	SET	0.83		4	14	THO	1.57	3	

In the subsequent sections the analytical results of more detailed and refined methods performed on the selected set of samples/wells are laid out. They were used to assess the molecular composition of Bakken Shale organic matter (both naturally and artificially matured residual kerogen and natural products). Finally, the reservoir quality (permeability) and the composition of mineral matrix of the Bakken Shale are presented.

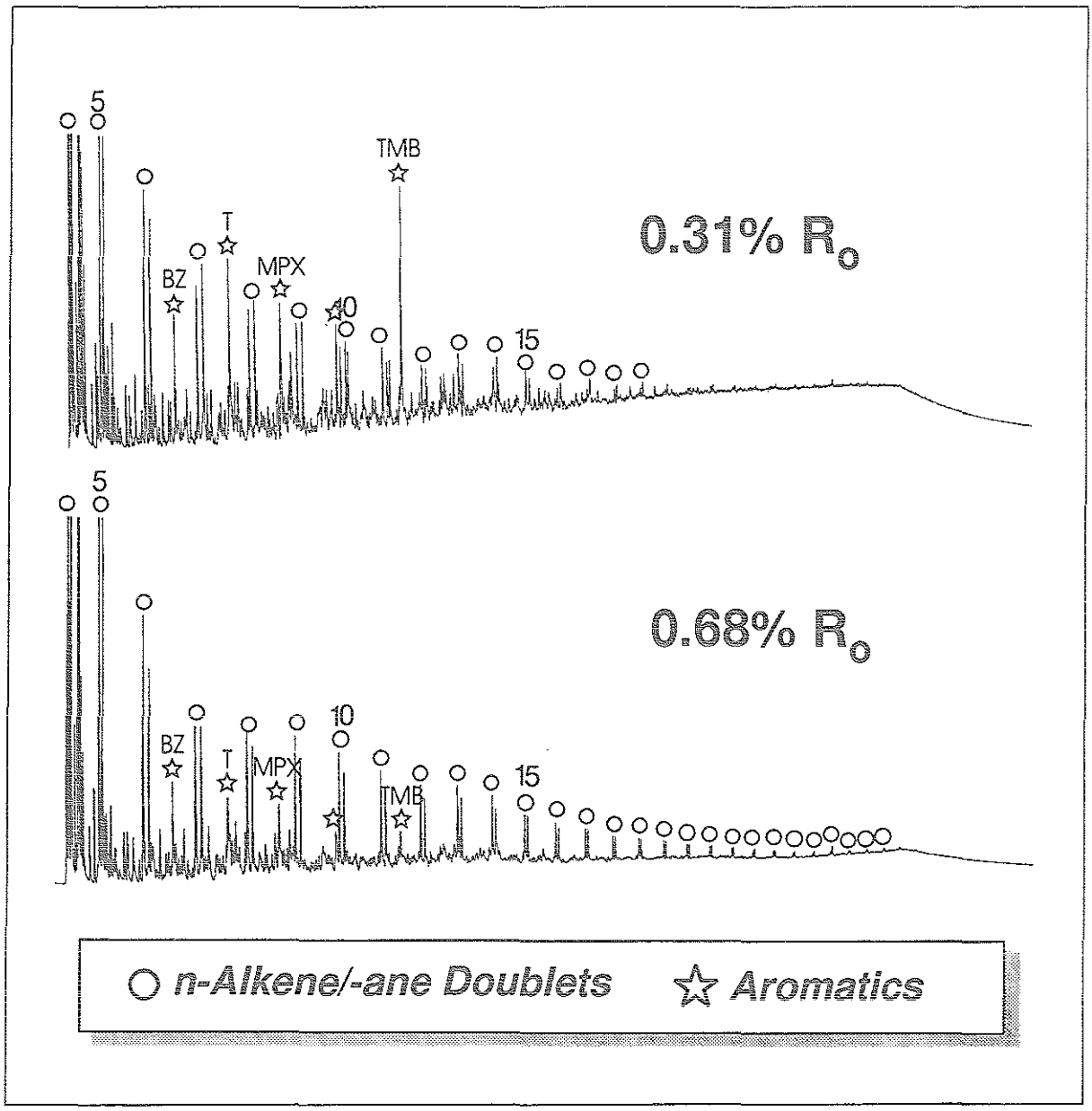

Fig. 17: Fingerprints as derived from open-system py-gc of two whole rock Bakken Shale samples as representative for low-mature and high-mature stages of thermal alteration. Numbers indicate total numbers of carbon atoms. BZ, T, MPX and TMB refers to benzene, toluene, meta-/paraxylene and 1,2,3,4-tetramethylbenzene, respectively.

4.4 Detailed Composition of Kerogen

The fingerprints derived from open-system py-gc (Fig. 17) exhibit an overall predominance of short-chain n-alkane/n-alkene-doublets, the abundance of which decreases with increasing chain length. This signature is typical for marine type-II kerogens. Distinct sulfur-aromatic peaks as derived from pyrolysis using a Hall detector are quantitatively irrelevant and exist only in samples below 0.6% R_o (wells DOB, JAC and NEG).

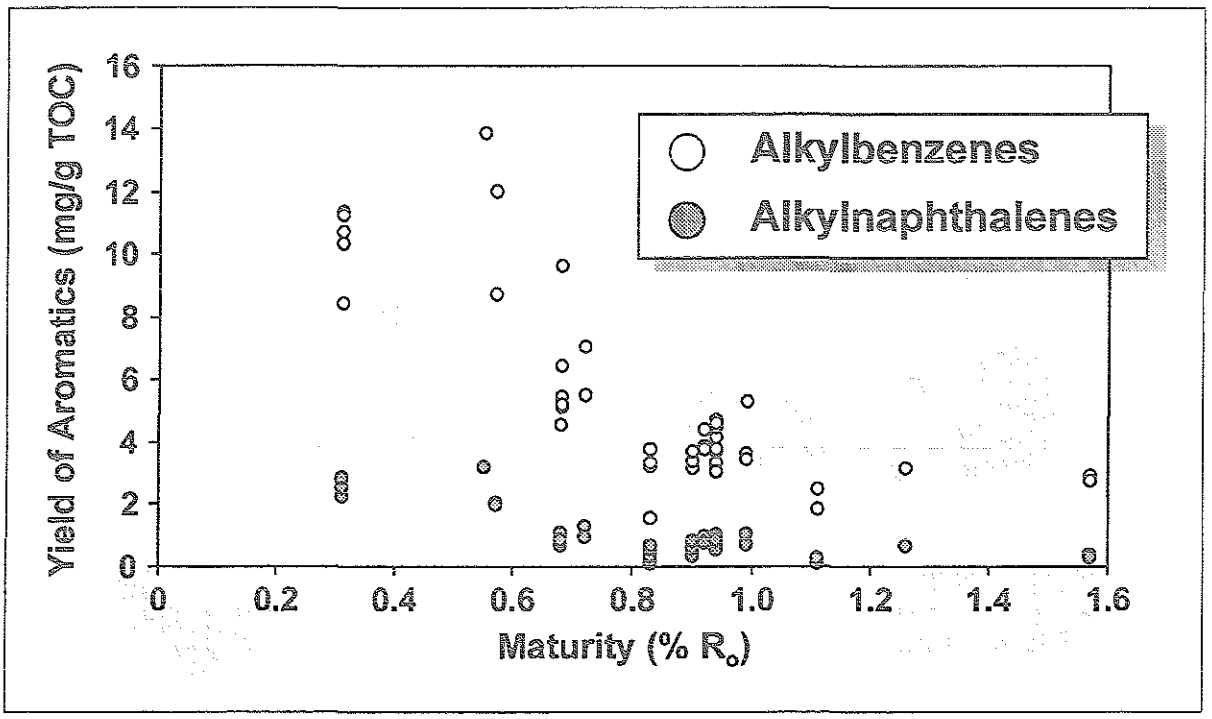

Fig. 18: Absolute yield of monoaromatic (alkylbenzenes) and diaromatic (alkylnaphthalenes) pyrolysates in the Bakken Shale kerogen as a function of maturity. The term 'alkylbenzenes' incorporates the sum of benzene, toluene, ethylbenzene, meta-/paraxylene, orthoxylene, C_3-benzene and 1,2,3,4-tetramethylbenzene. 'Alkylnaphthalenes' includes 2-methylnaphthalene, 1- methylnaphthalene, all dimethylnaphthalenes and trimethylnaphthalenes.

Individual samples of a given well show a pronounced uniformity as regards bulk composition. Additional to the n-alkenes and n-alkanes, a series of alkylbenzenes (benzene, toluene, ethylbenzene, meta-/paraxylene, orthoxylene) represents the second most abundant compound group. The presence of these alkylbenzenes in pyrolysates is quite common (Larter & Douglas, 1980; van Graas et al., 1981; Solli & Leplat, 1986). However, immature Bakken kerogens (up to 0.6% R_o) yielded quantitatively more aromatics on pyrolysis than mature ones. This feature is illustrated in Fig. 18. for both mono- (alkylbenzenes) and diaromatic (alkylnaphthalenes) hydrocarbons. While the maturity-related trend is similar for both compound groups - namely a sharp decrease in yield between 0.57% and 0.68% R_o - higher absolute values can be assigned to the alkylbenzene series (roughly 4-fold).

1,2,3,4-tetramethylbenzene is one of the most prominent peaks in the pyrolysis-gas chromatograms, especially at low levels of maturity (Fig. 19). This particular compound has been

postulated to be derived from moieties arising from diaromatic carotenoid structures in green photosynthetic sulfur bacteria (Chlorobiaceae). These structures are incorporated into the kerogen macromolecule during diagenesis of the organic matter and, on pyrolysis, yield 1,2,3,4-tetramethylbenzene via β-cleavage (Requejo et al., 1992). Its occurrence indicates that bacterial photosynthesis took place in an anaerobic environment (Abella et al., 1980). The presence of this particular compound has also been reported for kerogen pyrolysates, bitumens and crude oils derived from the Duvernay Formation (chronostratigraphic equivalent of the Bakken Formation in the Western Canada Basin) as well as Bakken kerogens, hence qualifying it as a biomarker compound for oil-source rock correlations (Requejo et al., 1992). The significance of the aromatic pyrolysate in general (aromaticity) and the occurrence of 1,2,3,4-tetramethylbenzene in particular will be discussed in ch. 5.1.3 with respect to the gas generative potential of the Bakken Shale.

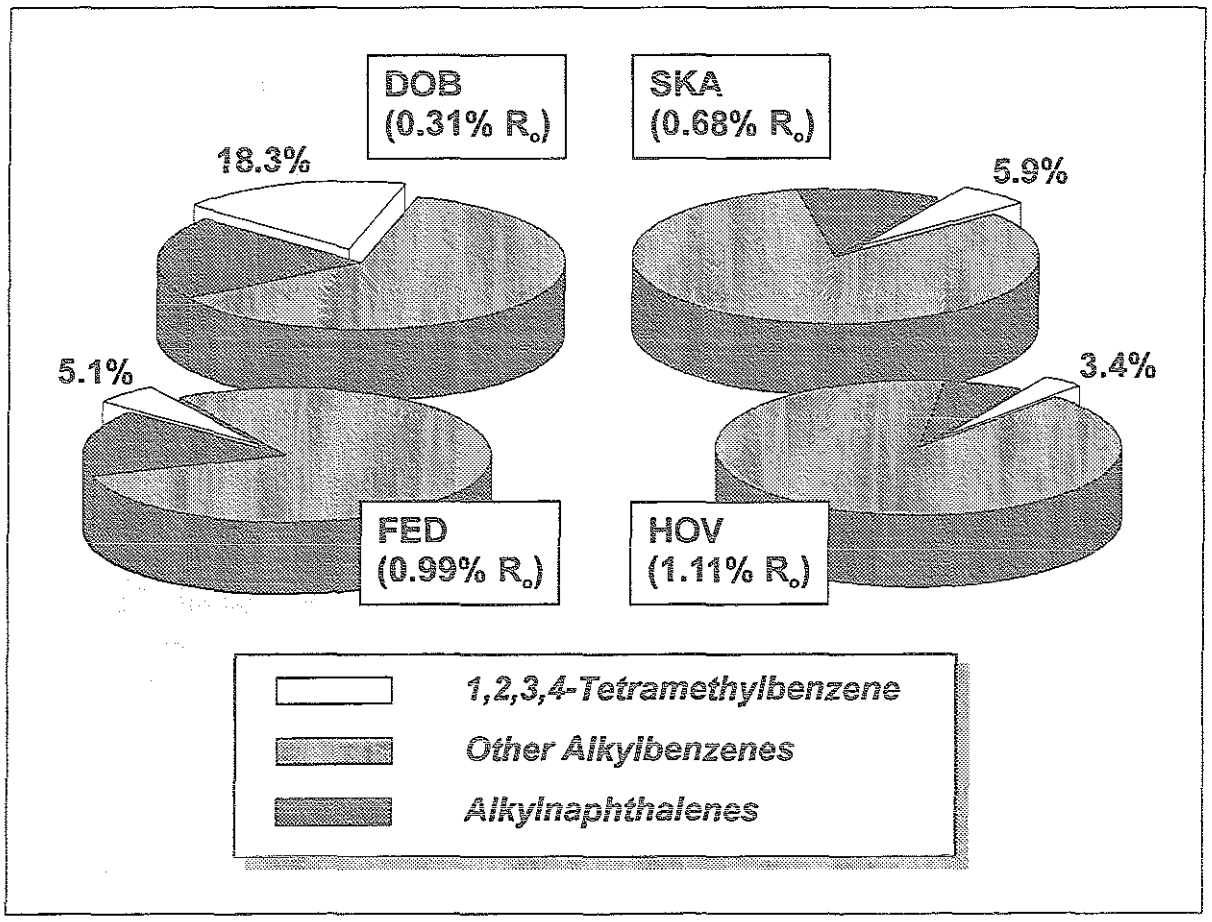

Fig. 19: Evolution of 1,2,3,4-tetramethylbenzene content in Bakken Shale pyrolysates relative to other aromatic hydrocarbons for four different stages of maturity. The term 'alkylbenzenes' incorporates the sum of benzene, toluene, ethylbenzene, meta-/paraxylene, orthoxylene and C_3-benzene. 'Alkylnaphthalenes' includes 2-methylnaphthalene, 1- methylnaphthalene, all dimethylnaphthalenes and trimethylnaphthalenes.

The chain length distribution of n-alkyl pyrolysates provides evidence for classifying kerogens in terms of bulk composition (Horsfield, 1989). Fig. 20 elucidates that the relative composition of the n-alkyl-yielding moieties in the Bakken kerogen macromolecule remains uniform throughout natural maturation. This has been observed before for the Toarcian Posidonia Shale

(Düppenbecker & Horsfield, 1990; Muscio et al., 1991) and the La Luna Formation (Ropertz, 1994). Gross compositional heterogeneities as a result of facies variations during sedimentation of the Bakken Shale appear to be absent. Accordingly, the results deduced from open-system pyrolysis corroborate that the pyrolysable portion of the kerogen in part consists of a rather limited number of n-alkyl precursors and that on this criterion the Bakken Shale bears a uniform kerogen type. Variations in organofacies as reported by Webster (1984) and Price et al. (1984), namely low organic carbon content and influx of terrigenous organic matter, apparently are applicable only to the shallow parts of the depositional area, as already laid out in chapter 4.1.1.

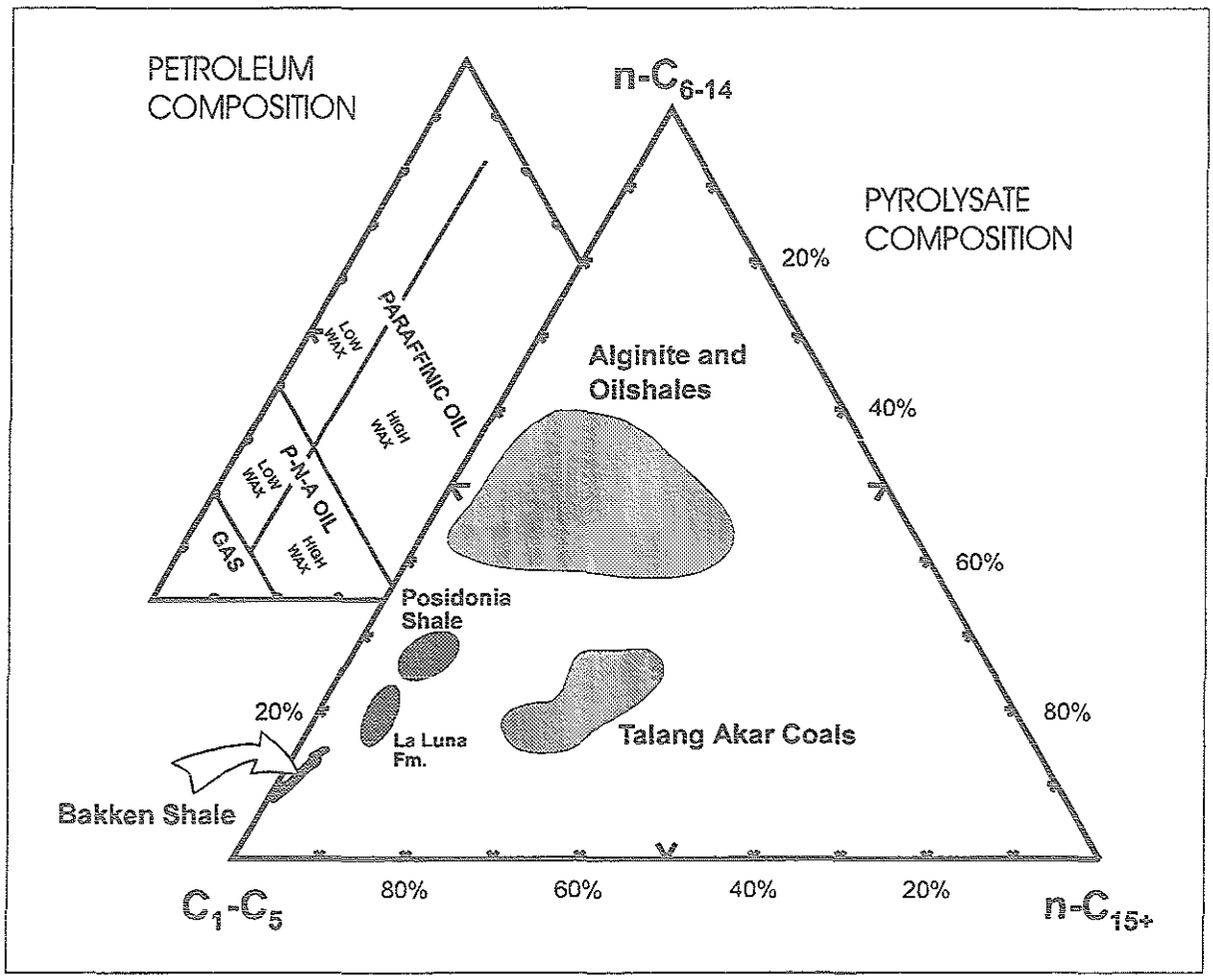

Fig. 20: Ternary diagram as derived from open-system py-gc displaying the relative composition of short- (C_1-C_5), medium- (C_{6-14}) and long-chain (C_{15+}) n-alkyl-pyrolysates (chain length distribution) of the Bakken Shale covering a maturity spectrum from 0.31% R_o to 1.57% R_o. Data from various organic rich sediments and inferred petroleum composition superimposed from Horsfield (1989) and Muscio et al. (1991).

The uniformity in organic matter quality, as indicated by py-gc, is corroborated by the similarity of the spectral fingerprints derived from IR spectroscopy. The most significant change with increasing catagenesis is the increase of the ratio of methyl to methylene (CH_3/CH_2). This phenomenon can be interpreted as a change in chain length of alkyl substituents with increasing maturity. This feature, however, is not consistent with py-gc results, which indicate maturity

independent uniformity. Changes in chain length of alkyl substituents coincide with an overall reduction of absorbance elucidating progressive thermal decomposition of the organic matter.

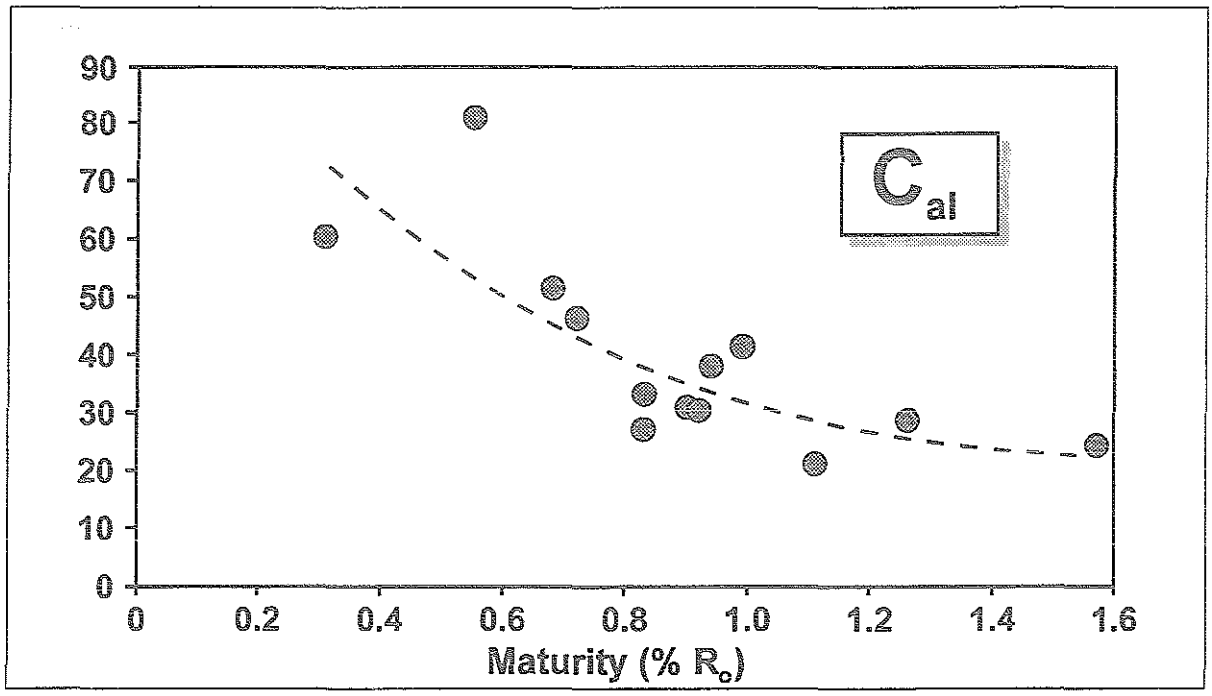

Fig. 21: Correlation of maturity parameters derived from optical analysis methods (IR spectroscopy (C_{al}) vs. vitrinite reflectance) reveals a good fit up to 1.0% R_o. The uniformity of C_{al} values between 1.0% and 1.6% R_o might indicate that the maturity spectrum established by R_o measurement is less broad.

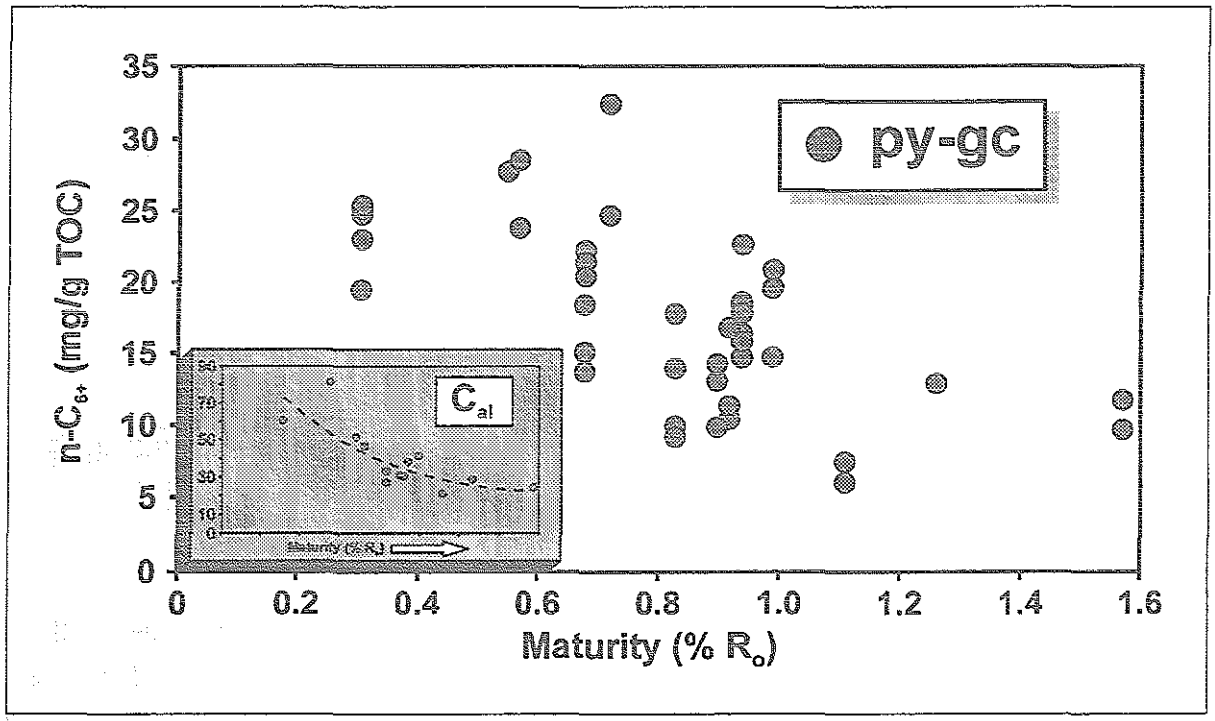

Fig. 22: Absolute yield of C_{6+}-n-alkyls in in Bakken Shale pyrolysate as a function of maturity. Evolutionary trend of IR parameter (C_{al}) has been inserted for reasons of comparison.

Fig. 21 shows the amount of aliphatic carbon (normalized to weight of rock) as derived from IR spectroscopy (C_{al}) as a function of vitrinite reflectance. A broad negative trend with proceeding maturation is clearly discernable and can be interpreted as progressive removal of aliphatic substituents by thermal degradation and/or transformation of aliphatic carbon into fixed aromatic carbon (Schenk et al., 1986). The evolution of C_{6+} n-alkyls in the pyrolysate of the Bakken Shale maturity suite, as depicted in Fig. 22, also shows a rather broad decrease with increasing maturity, i.e. the absolute amount of moieties in the residual kerogen yielding long-chain pyrolysates declines as catagenesis proceeds.
Although maturity trends could be established using IR spectroscopic data, the routinely applied method is not suitable to make statements on the bulk composition (aliphaticity/aromaticity) of the Bakken organofacies based on whole rock material, because the signals deduced from the mineral matrix mask most of the organic absorptions below wavenumber 1500 cm^{-1} (Schenk et al., 1990). For such intentions, therefore, an effective and thorough kerogen isolation procedure is required. This analytical step, however, was not applied in the present study.

Although the results deduced from kerogen analysis (py-gc of n-alkyl kerogen part) provide strong arguments for a constant kerogen type on a basinwide scale with compositional modifications solely related to the imprints of maturity, it cannot be ruled out unequivocally that variations in kerogen type occurred during deposition of the Bakken Shale. The relatively sharp decrease of alkylbenzenes between 0.57% and 0.68% R_o might argue against a constant kerogen type and for the presence of at least two types of kerogen. However, such a twofold separation is not congruent with the two sample sets as revealed by organic petrology and screening analyses (ch. 4.1).

4.5 Bitumen and Crude Oils

This section includes data derived from solvent extract and crude oil analysis (MPLC, GC analysis of fractions, GC-MS of saturated biomarker compounds), i.e. results pertain to the boiling range which in the literature is conveniently referred to as C_{15+} material.

4.5.1 Bulk Characterisation

Fig. 23 displays the yield of bitumen as a function of maturity (flow blending extraction).
Regarding the *maximum* values for each well, the diagram can be separated into two zones: First, it clearly shows a slight decrease of extract yield at low levels of maturity (0.3 to 0.7% R_o) from 157mg/g TOC to 73mg/g TOC. A sudden change marks the beginning of the second zone at 0.8% R_o: Within a relatively narrow range of maturation (from 0.8% to 1.1% R_o), extract yields rise from 100 to max. 358mg/g TOC. Beyond 1.1% R_o, the content of bitumen slightly decreases to relatively low values (81mg/g TOC for 1.57% R_o). These relatively low values for the three most mature wells (HOV, BEH and THO), however, ought to be viewed in the light of the number of samples submitted to solvent extraction (2, 1 and 1, respectively). Hence, representativity of these values has to be considered carefully. Interestingly, the minimum extract yield zone at 0.6/0.7% R_o has been reported for bituminous coals (Ottenjann et al., 1982). It is

considered to be indicative for the presence of two populations of extractable organic matter in vitrinite (< 0.6% R_o and > 0.6% R_o, respectively) in bituminous coals (Wolf, 1993; written communication).

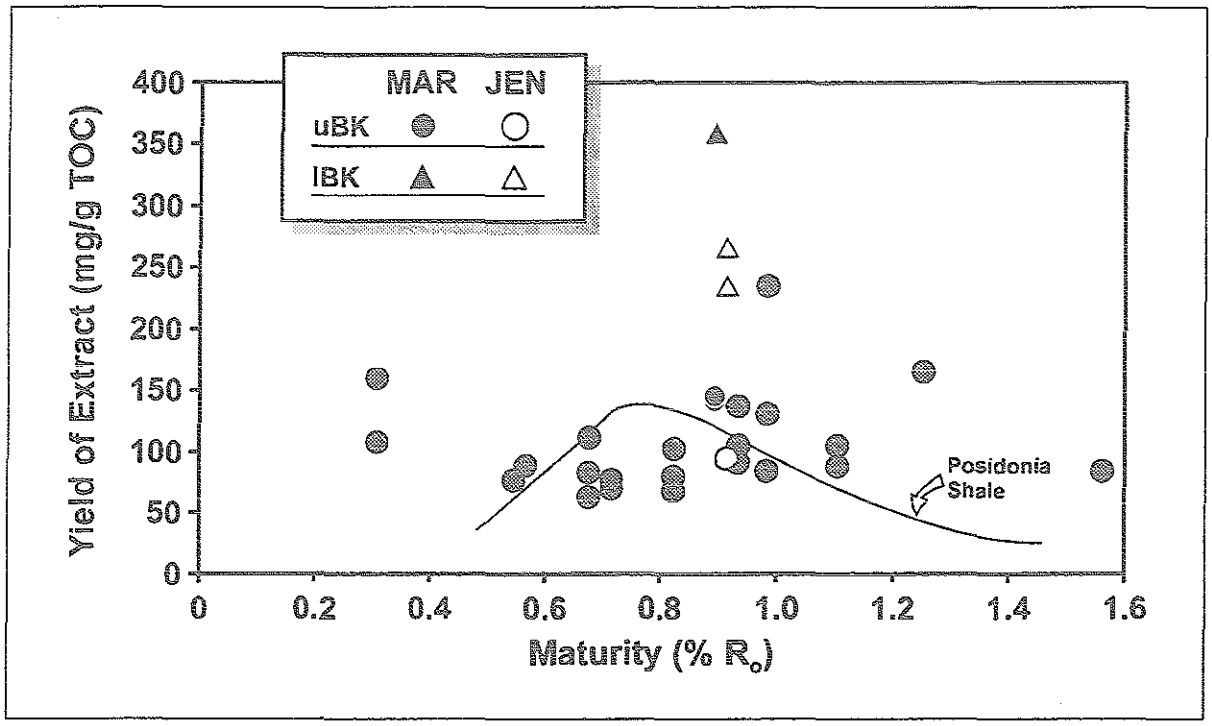

Fig. 23: Whole extract yield (flow blending method, azeotropic solvent mixture) related to level of maturity for Bakken Shale samples. Where extract yield was determined for samples from both shale units of the same well, triangles designate datapoints from the Lower and circles from the Upper Bakken Shale (at 0.9% (MAR) and 0.92% R_o (JEN)). Trend for Posidonia Shale has been superimposed using data from Rullkötter et al. (1988).

It should be pointed out that for those wells of the mature zone (>0.8% R_o) where samples from both shale strata of the same well were available, the lower always contains roughly twice as much bitumen as the upper (wells MAR and JEN). Such significant, shale unit-specific differences were not encountered in the results from ultra sonic extraction (ch. 4.2). This phenomenon is surprising considering that kerogen type and hydrocarbon generation potential do not vary significantly in both shale units of a given well in the basin center, as established by screening parameters (Rock-Eval, ch. 4.1.1) and exemplified for well JEN in Fig. 12. In ch. 5.2.2, these heterogeneities are discussed with respect to expulsion/migration.

The extract data of the present study (absolute extract yield as well as distribution pattern as a function of maturity) do not reflect the corresponding results which Price et al. (1984) obtained using dichloromethane as solvent. In the latter contribution, absolute extract yields varied between 20 and 60mg/g TOC (except for one sample: ca. 120mg/g TOC) and significant differences in extract yield between both shale units of the same well (for instance well JEN of the present study) were not reported. Moreover, a sharp increase in bitumen yield for mature samples, as observed in the present study, appears to be absent in Price et al. (1984). The latter authors attributed the phenomenon of a lack of buildup of bitumen to efficient primary migration processes. The overall higher absolute yields of the present study may be a consequence of the

azeotropic solvent mixture (ch. 3.3.1), as reflected by the bulk composition of the extracts. For other marine source rocks containing type II kerogens (e.g. Lower Toarcian of the Paris Basin), Louis & Tissot (1967) acquired absolute extract amounts similar to the ones of the present Bakken study using the same type of solvent.

Fig. 24 illustrates the bulk composition (normalized percentage) of the *deasphaltened* extract. The average composition with reference to compound groups (ca. 10-30% saturates, 10-20% aromatics, 50-80% resins) does not change significantly with increasing maturation. Normally, the relative amount of polar non-hydrocarbons (resins) is believed to decrease as maturation proceeds (Tissot et al., 1971; Albrecht et al., 1976).

The bulk composition of Bakken Shale derived crude oils (Fig. 24) shows a very uniform pattern with low compositional variations between samples from different oil fields. The relative composition of the crude oils reflects its light oil character (40°-45° API; Price & LeFever, 1994), with high quantities of saturates, rather low amounts of aromatics and very low yields of heterocompounds. This distribution is in sharp contrast to the relative composition of the solvent extracts which is dominated by high concentrations of polar material.

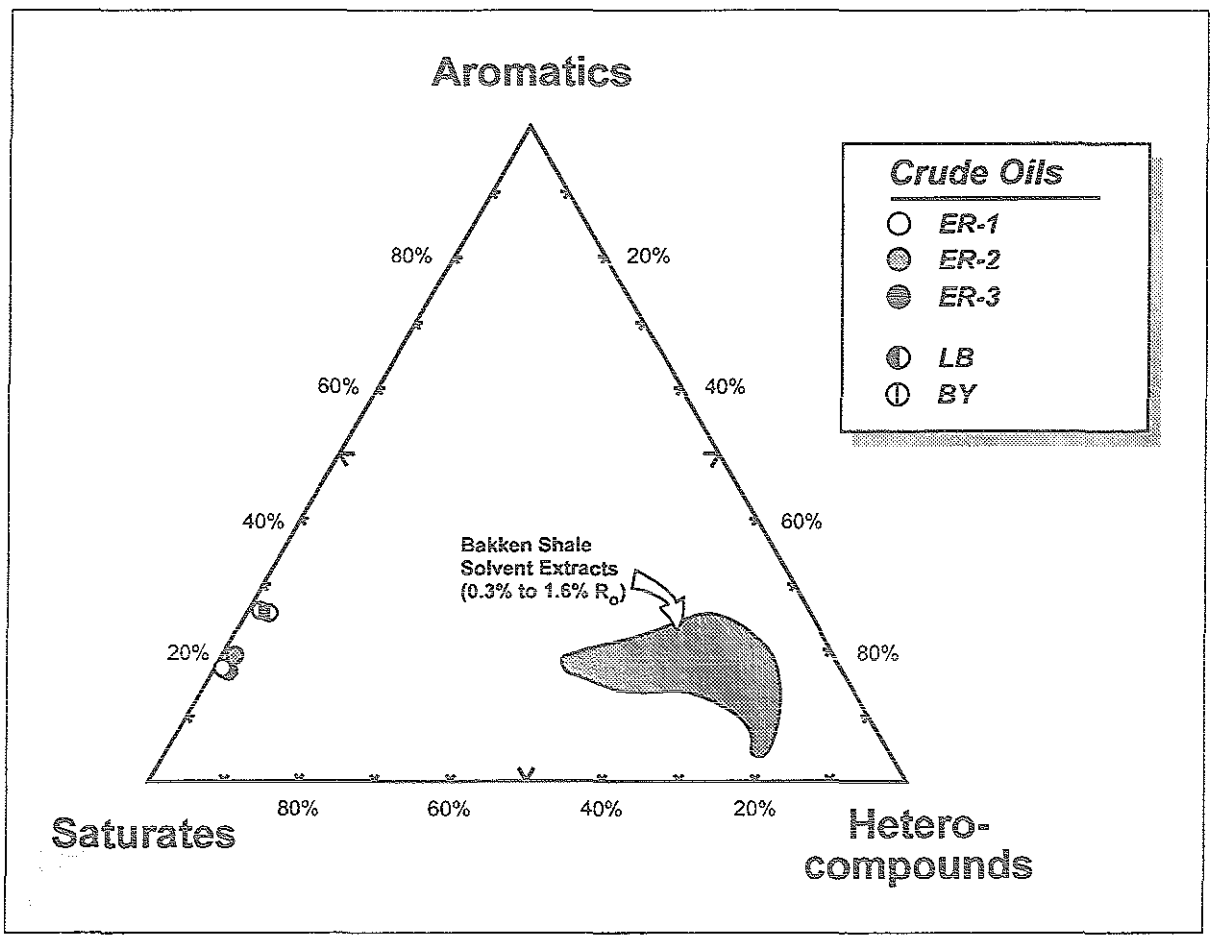

Fig. 24: Relative composition of deasphaltened Bakken Shale solvent extracts (flow blending method, azeotropic solvent mixture) and deasphaltened crude oils produced from Bakken reservoirs with respect to MPLC fractions.

4.5.2 Yield of Compound Groups

The *asphaltene* contents of Bakken Shale extracts of the present study, as listed in Tab. 5, are plotted vs. R_o in Fig. 25. Low mature extracts contain more n-hexane insoluble precipitates than high mature ones, thus outlining a broad decrease of asphaltene yield with increasing maturation. Finally, the high mature stage (>1.0% R_o) is characterised by uniformly low contents of asphaltenes. Differences in yield of solvent extractable organic matter (Fig. 23) and MPLC fractions (see below) between both shale units cannot be assigned to the asphaltene fraction. Indeed, asphaltene concentration exhibits no shale unit specific pattern as observed for whole extract and the saturated, aromatic and resin fraction (see below). This phenomenon will be evaluated and discussed with respect to expulsion/migration processes (ch. 5.2.2). The Bakken crude oils yielded only in one case (ER-3) n-hexane-insoluble precipitates (52mg/g oil). For all other oil samples, addition of excess n-hexane had no effect, thus confirming the nature of Bakken petroleums as being overall very light oils (40°-45° API; Price & LeFever, 1994).

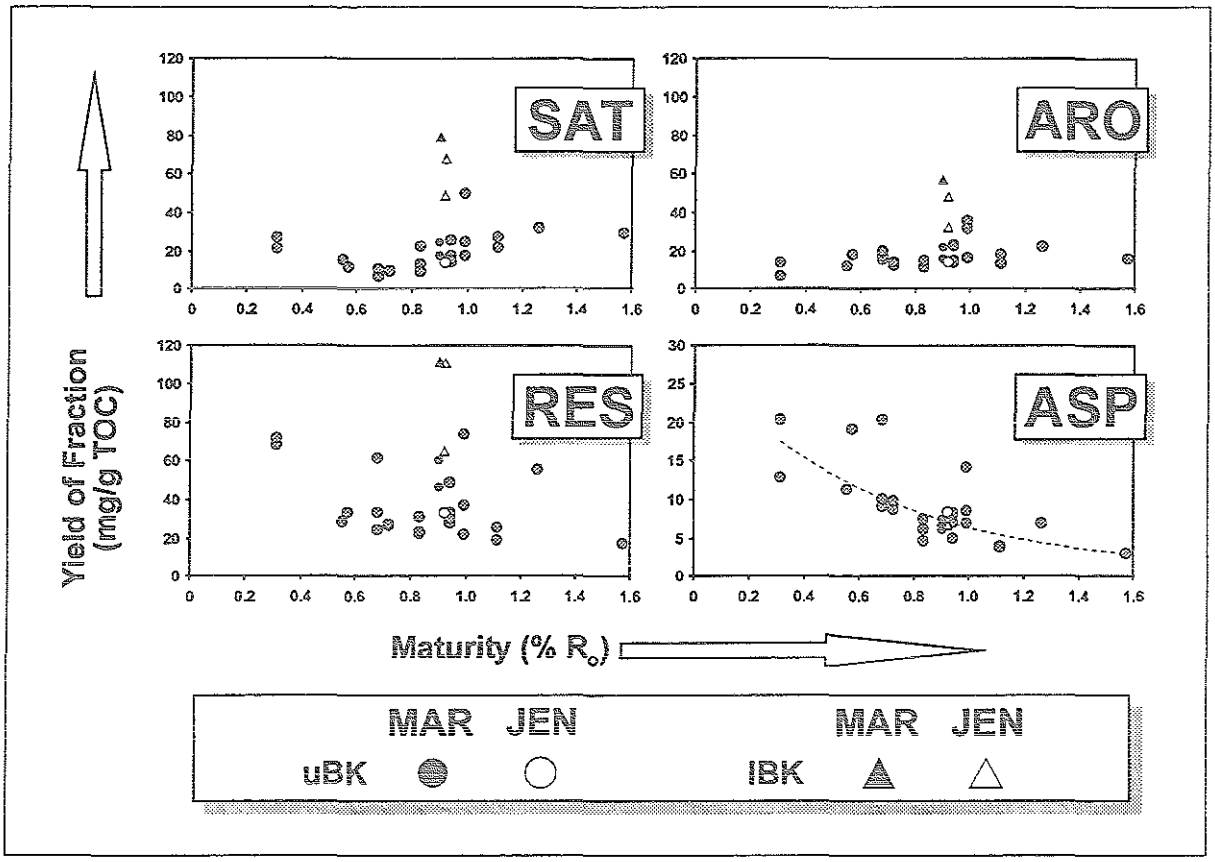

Fig. 25: Evolution of compound group yield (MPLC fractions and n-hexane-insoluble asphaltenes) as a function of maturity. Data is normalized to yield of whole extract (Fig. 22). Analogous to Fig. 22, triangles and circles refer to the lower and upper shale unit of the same well, respectively. Note that the scale for the vertical axis for all diagrams is up to 120mg/g TOC except for the asphaltene plot (up to 30mg/g TOC). Trend line for asphaltene diagram was determined by regression analysis.

In the present study the absolute yields of asphaltenes (normalized to TOC) derived from extracts are generally similar compared to other studies on the Bakken Shale (Price et al., 1984). For the Toarcian of the Paris Basin, the hexane-insoluble asphaltene yields covered a range of ca. 10 to 25mg/g TOC (Louis & Tissot, 1967).

Table 5: Yield of saturate (SAT), aromatic (ARO) and resin (RES) fraction as derived from MPLC of extracts and crude oils, respectively. Extract values are normalized to total extract yield. Asphaltenes (ASP) were precipitated using n-hexane. Well numbers refer to location of sampled wells in Fig. 6.

Sample ID	Well name (#)	R_o (%)	SAT	ARO	RES	ASP	SAT	ARO	RES	ASP
	Extracts		(mg/g extract)				(mg/g TOC)			
E34270	DOB (1)	0.31	196.5	127.4	550.6	122.5	20.69	13.42	71.21	12.90
E34276			167.3	40.0	429.6	130.1	26.36	6.30	67.72	20.51
E34263	JAC (2)	0.55	202.1	157.3	382.2	154.5	14.87	11.58	28.12	11.36
E34288	NEG (3)	0.57	129.9	204.6	382.8	224.5	11.16	17.58	32.89	19.29
E34437	SKA (4)	0.68	97.3	179.0	530.7	187.9	10.62	19.54	61.01	20.50
E34440			128.7	212.9	411.6	114.5	10.26	16.97	32.80	9.13
E34443			102.5	253.3	400.1	170.5	6.10	15.07	23.81	10.14
E34306	BOR (5)	0.72	133.5	182.1	403.8	148.9	8.87	12.11	26.85	9.90
E34308			123.7	183.7	354.4	118.4	9.15	13.58	26.21	8.76
E34366	GRA (6)	0.83	192.8	174.6	337.3	114.3	12.51	11.33	21.89	7.42
E34343	SET (7)	0.83	284.6	143.7	294.7	59.7	21.86	11.04	22.63	4.59
E34345			87.8	143.9	305.7	60.9	8.75	14.35	30.50	6.08
E34321	MAR	0.90	120.4	109.4	428.2	53.3	16.79	15.27	59.73	7.43
E34322	(8)		167.0	151.1	320.4	42.4	23.84	21.57	45.73	6.05
E34328			217.9	158.6	307.4	19.9	78.20	56.91	110.30	7.15
E34449	JEN (9)	0.92	145.0	149.6	352.7	91.0	13.31	13.73	32.36	8.35
E34454			180.6	180.6	413.9	25.0	47.90	47.90	109.77	6.62
E34455			285.7	136.9	273.7	30.6	66.93	32.06	64.12	7.16
E34376	CON	0.94	246.3	224.1	322.5	69.2	25.02	22.77	32.77	7.04
E34389	(10)		154.4	153.8	310.2	56.0	13.58	13.52	27.28	4.93
E34403			126.1	165.7	358.3	60.1	16.97	22.30	48.21	8.09
E34416			142.2	140.7	287.8	80.7	14.49	14.33	29.31	8.22
E34425	FED	0.99	187.5	244.4	285.3	66.9	24.03	31.32	36.57	8.57
E34430	(11)		210.5	151.7	312.9	60.9	49.22	35.48	73.18	14.25
E34434			210.5	197.1	265.4	86.0	17.02	15.94	21.45	6.96
E34347	HOV	1.11	313.4	151.4	217.5	45.8	26.62	12.86	18.47	3.89
E34351	(12)		208.9	174.6	245.1	36.7	21.25	17.75	24.92	3.73
E34331	BEH (13)	1.26	192.1	133.8	336.4	42.2	31.32	21.81	54.86	6.88
E34362	THO(14)	1.57	354.6	187.8	206.8	36.3	28.77	15.24	16.78	2.94
	Oils									
	Field	API	(mg/g oil)				(% of oil)			
	BY	38.4	460	170	40	0	70.56	25.95	3.49	0
	LB	45.4	340	120	40	0	68.00	24.80	7.20	0
	ER-1	47.1	380	80	20	0	79.16	17.26	3.58	0
	ER-2	43	450	110	20	0	76.63	19.16	4.21	0
	ER-3	43.4	280	60	30	52.2	66.32	14.21	7.11	12.36

The maturity related trend of the maltene subfractions (saturates, aromatics and resins) is strikingly different to the asphaltene pattern, especially as regards the relationship between lower and upper shale unit of a given well:

The yield of the ***saturated*** and ***aromatic hydrocarbon*** fractions, which quantitatively are the main constituents of crude oil (Tissot & Welte, 1984) was derived from MPLC of deasphaltened extracts and is given in Tab. 5.
The distribution pattern as a function of thermal evolution (Fig. 25) is strikingly different to the asphaltene plot (Fig. 25), but evidently bears similarities to the whole extract plot (Fig. 23): Both hydrocarbon compound groups have several properties in common: (1) After a uniform distribution of intermediate to minimum values (between 0.6% and 0.8% R_o), the higher stages of maturation (>0.8% R_o) are characterised by relatively high yields (especially between 0.8% and 1.0% R_o) with maxima for the wells MAR, (0.9% R_o), JEN (0.92% R_o) and FED (0.99% R_o). (2) The maturity interval 0.8% to 1.0% R_o exhibits a broad scatter in values. (3) Interestingly, samples from the lower shale of a given well always yielded higher quantities of each hydrocarbon fraction than the corresponding upper shale of the same well. This feature is analogous to whole extract yield (Fig. 23).

The ***resins***, designated as the MPLC fraction that remains on the column and which is eluted using ethanol (Radke et al., 1980a), reveal a distribution pattern which is grossly similar to the distribution of the hydrocarbon fractions (saturates and aromatics) of the solvent extracts. However, variability of data is more pronounced (Tab. 5; Fig. 25). They range between 17mg/g TOC for well THO (1.57% R_o) and 110mg/g TOC for well MAR (0.99% R_o). Well DOB (0.31% R_o) also provided very high amounts of resins (between 68 and 71mg/g TOC). Only the portion >0.8% R_o exhibits analogy to the yields of whole extract (Fig. 23) and aromatic hydrocarbons (Fig. 25): A distinct increase in values between 0.8% and 1.0% R_o followed by an equally pronounced decrease beyond 1.0% R_o. However, the datapoint for well BEH does not fit into this trend, as it exhibits rather high resin yields (55mg/g TOC) compared to the next higher and lower mature wells (HOV and THO, respectively).

4.5.3 Molecular Characterisation

The most striking feature derived from gas chromatographic analysis of the ***saturates*** fraction of the Bakken extracts is their uniformity in distribution pattern and their virtual maturity independence on a molecular level.
Fig. 26 shows the n-alkane distribution pattern at 6 different levels of maturity (0.31, 0.83, 0.92, 0.99, 1.11 and 1.57% R_o). The concentration of the low-molecular weight compounds (carbon number range C_{14} to C_{18}) is clearly high whereas heavier n-alkanes bearing more than 20 carbon atoms are low. Such a distribution pattern is typical for solvent extractable organic matter from marine sediments (e.g. Lower Toarcian, Tissot et al. (1971)) and marine crude oils (Tissot et al., 1977; Lijmbach, 1975). Hence, a unimodal distribution pattern which apparently is not affected by maturity related imprints is clearly visible. With the prerequisite that facies effects caused by different types of organic matter precursors (ch. 2.2.1) can be considered insignificant, the predominance of C_{14} to C_{18} n-alkanes might reflect that carbon-carbon bond cracking reactions of mobile long-chain components (waxes, resins) are occurring yielding short-chain low-molecular weight hydrocarbons (Connan et al., 1975). This feature might be related to enhanced thermal alteration of the in-situ soluble organic matter in the Bakken Shales. In ch. 5.3, this is discussed within the framework of generation and migration in the Bakken petroleum system. The

phenomenon that light (C_{9-11}) as well as heavy (C_{25-31}) hydrocarbons were missing in the saturate compound group of the Bakken Shale resulting in a relative increase of the range C_{12-24} was interpreted to be brought about by primary migration via gaseous solution (Price et al., 1984). Generally, processes leading to a shift in n-alkane distribution from heavy to light components are attributed to the final stage of catagenesis after the peak of hydrocarbon generation has already been passed (Tissot & Welte, 1984, p. 205). Mango (1991), however, has questioned this theory because he has found some evidence that generated hydrocarbons are more stable than their precursors in the kerogen when submitted to increasing thermal alteration. If the latter indeed is applicable to the Bakken Shale, then the predominance of light hydrocarbons might not be indicative of a high level of thermal alteration.

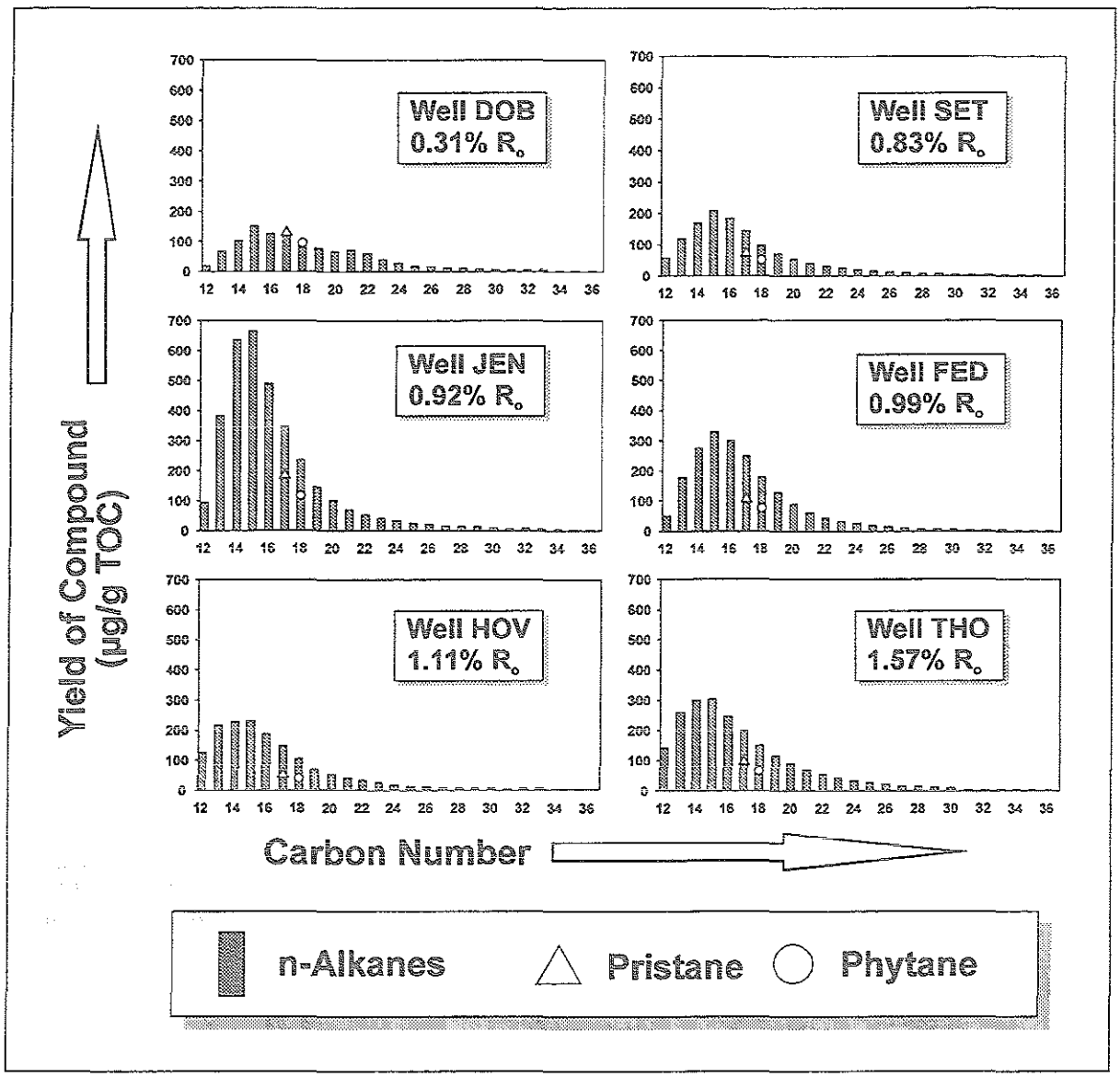

Fig. 26: Distribution pattern of saturated hydrocarbon fraction (MPLC) as derived from GC analysis of solvent extracts for six selected levels of maturity. White bars denote pristane and phytane. Numbers indicate carbon atoms.

Compositional uniformity is also reflected by parameters based on selected compounds, like odd- and even-numbered n-alkanes (CPI), isoprenoids (pristane/phytane ratio Pri/Phy) and

isoprenoid/n-alkane ratios (pristane/n-$C_{17:0}$). These indices are used to establish maturity trends. The values for these parameters are listed in Tab. 6. Fig. 27 illustrates the evolution of four selected ratios ($CPI_{23..25}$, LHCPI, Pri/Phy and Pri/n-$C_{17:0}$) as a function of vitrinite reflectance.
The carbon preference index (based on Bray & Evans, 1961) for the carbon atom range 23 to 25 remains more or less constant throughout maturation (range of values from 0.9 to 1.04). Additionally, a slight preference of even-numbered n-alkanes can be observed, indicated by an average CPI value slightly below 1.0 for all levels of thermal evolution. CPI values significantly >1 which are inherited from organic input of terrestrial origin and which are usually indicative of low levels of maturation (Louis & Tissot, 1967; Albrecht et al., 1976) are absent in the n-alkane fraction of samples from the present Bakken study.

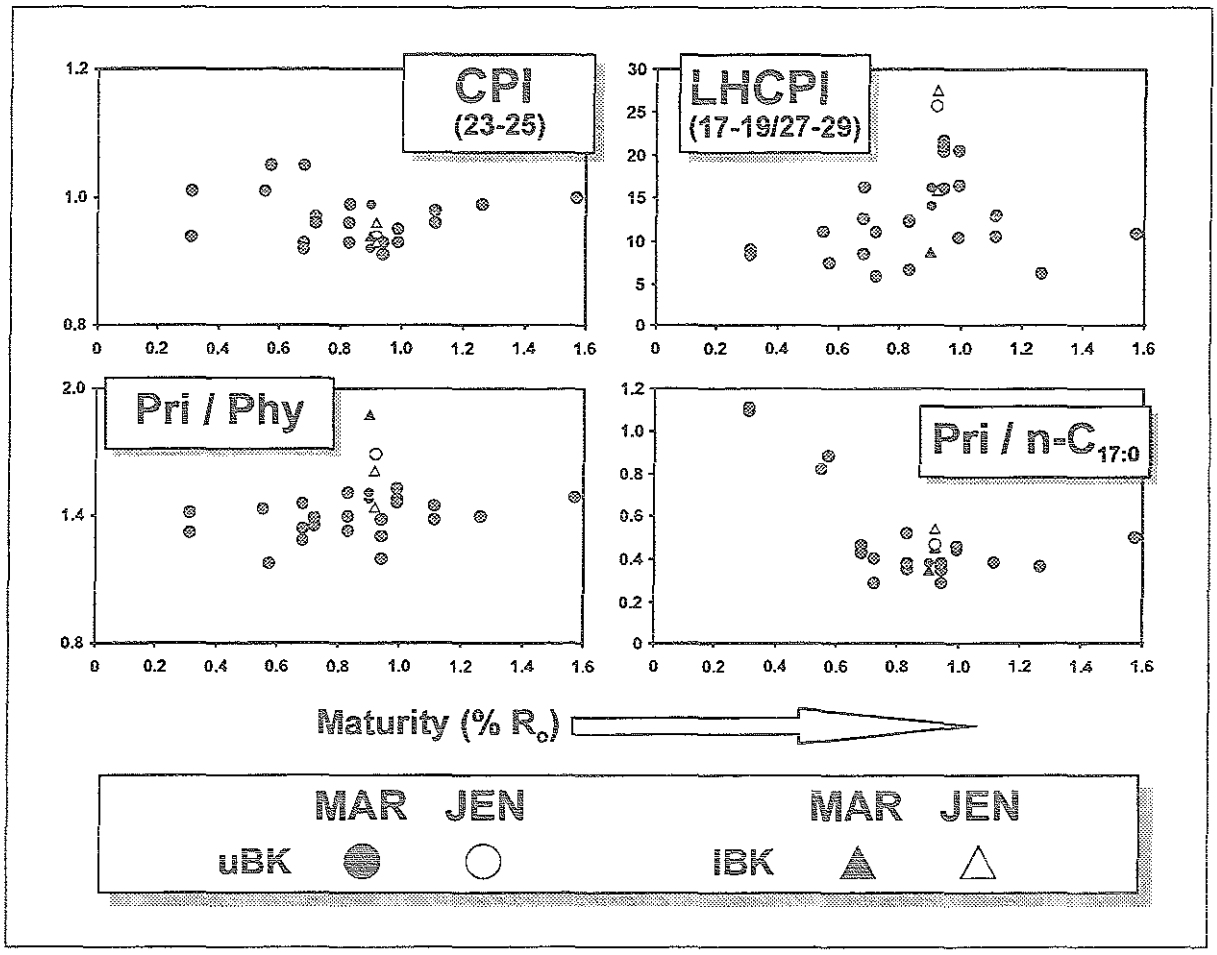

Fig. 27: Maturity related evolution of selected parameters (CPI, LHCPI, Pri/Phy and Pri/n-$C_{17:0}$) of Bakken Shale solvent extracts (saturates fraction). Equations for calculation of parameters are given in the appendix. Triangles and circles refer to the lower and upper shale unit of the same well, respectively.

Basically, there are three different hypotheses which may account for the observed predominance of low-molecular-weight material in the Bakken saturated fraction:

- *Generation* - The organic matter of the Bakken Shale consists of moieties which predominantly generate light products directly from the kerogen.
- *Migration* - Selective removal of high-molecular-weight waxes (>C_{27}) via migration may be a plausible process. For instance, Price et al. (1984) also recognized a reduction in heavy n-

alkanes (>C_{27}) in the maturity zone of intense hydrocarbon generation and suggested that this feature is related to primary migration by gaseous solution. In the Bakken Shale samples of the present study, the extent of these processes seems to be enlarged between 0.9% and 1.0% R_o.

- *Thermal alteration* - High concentrations of low molecular weight n-alkanes in the soluble organic matter could be interpreted as the result of cracking reactions at the expense of long-chain-hydrocarbons present in the mobile organic matter (Connan et al., 1975). This hypothesis of an overall high degree of thermal alteration of the saturates fraction, as suggested by their distribution patterns, might also be derived from Fig. 27 which depicts the ratio of light (C_{17-19}) to heavy n-alkanes (C_{27-29}). The values are generally very high (above 5) - leading to an unimodal distribution pattern (Fig. 26) - but they rise to maxima between 0.9% and 1.0% R_o (up to 28 at 0.92% R_o).

An apparent maturity independence is also reflected by the Pri/Phy ratio (Fig. 27). The datapoints range somewhere between 1.3 and 1.5. However, a slight increase at 0.92% R_o (well MAR) reveals a maximum of 1.87.
In contrast to the molecular maturity parameters as discussed above (CPI, Pri/Phy) with their obvious maturity independence, the pristane/n-$C_{17:0}$ ratio outlines distinct changes with increasing maturity (Fig. 27), especially at immature levels. However, between 0.57% and 0.68% R_o, a sharp decrease occurs, followed by a relative uniformity of values for the rest of maturation. A decrease of the pristane/n-$C_{17:0}$ ratio with advancing catagenesis (depth) has already been observed in a Lower Toarcian shale by Tissot et al. (1971) though, in that study, values below unity were reached only at relatively high stages of catagenesis. A relative enrichment of pristane due to preferential expulsion of the n-C_{17}-alkane and a consequent increase of the corresponding ratio as discussed by Leythaeuser & Schwarzkopf (1986) for immature (<0.7% R_o) type III kerogens, however, appears to be no feasible process in case of the Bakken Shale, as the values remain rather constant in the maturity interval >0.6% R_o, where hydrocarbon generation and expulsion generally is believed to take place (Vassoevich et al., 1970).

Fig. 28 depicts the n-alkane distribution pattern of the crude oil samples. It must be pointed out that, due to the intrinsic light oil character of the Bakken crude oil (Price & Le Fever , 1992), the molecular composition may have been affected by sample preparation: After precipitation of asphaltenes the crude oils were set to evaporate. Hence, especially the low-molecular-weight hydrocarbons of the samples may have been submitted to evaporation losses. Clearly, this circumstance has to be kept in mind while evaluating ratios like LHCPI (see below). The n-alkane fraction of the Bakken oils reveals a pattern with the emphasis laid on short-chain components. On a detailed examination, certain distinctive features can be observed: Samples LB and ER-1, which represent the lightest oils of the present sample set (45.4 and 47.1° API), are characterized by maximum values for the n-C_{10} to n-C_{12} range, while the other samples, analogous to the n-alkane pattern of the Bakken bitumen, contain maximum amounts within the interval of n-C_{14} to n-C_{18}. Sample ER-3 exhibits a second maximum in the carbon number range of 30 to 32. The heaviest oil (sample BY, 38.4° API) exhibits a rather narrow distribution pattern that levels off already at carbon number 30. This is in contrast to all other oils which have fair amounts of long wax n-alkanes (> C_{30}).

Table 6: Molecular maturity parameters for the saturate fraction of Bakken solvent extracts and crude oils. Equations for calculation of ratios are given in the appendix. Well numbers refer to location of sampled wells in Fig. 6.

Sample ID	Well name (#)	R_o (%)	CPI-1 (23..25)	LHCPI	Pri/Phy	Pr/n-$C_{17:0}$
	Extracts					
E34270	DOB (1)	0.31	1.00	8.96	1.34	1.10
E34276			0.93	8.35	1.43	1.12
E34263	JAC (2)	0.55	1.00	11.11	1.44	0.83
E34288	NEG (3)	0.57	1.04	7.38	1.20	0.89
E34437	SKA (4)	0.68	0.92	8.43	1.47	0.43
E34440			1.04	12.62	1.36	0.43
E34443			0.91	16.36	1.30	0.47
E34306	BOR (5)	0.72	0.96	11.06	1.37	0.29
E34308			0.95	5.77	1.41	0.40
E34366	GRA (6)	0.83	0.98	12.37	1.52	0.52
E34343	SET (7)	0.83	0.95	6.53	1.41	0.38
E34345			0.92	12.23	1.34	0.35
E34321	MAR (8)	0.90	0.98	16.23	1.49	0.38
E34322			0.91	14.08	1.52	0.38
E34328			0.93	8.64	1.87	0.35
E34449	JEN (9)	0.92	0.93	25.86	1.69	0.47
E34454			0.92	27.66	1.45	0.45
E34455			0.95	15.89	1.61	0.54
E34376	CON (10)	0.94	0.90	20.48	1.32	0.37
E34389			0.90	21.11	1.23	0.35
E34403			0.92	21.74	1.22	0.29
E34416			0.91	16.12	1.40	0.38
E34425	FED (11)	0.99	0.94	10.39	1.49	0.46
E34430			0.92	16.54	1.54	0.44
E34434			0.94	20.65	1.47	0.45
E34347	HOV (12)	1.11	0.95	10.48	1.40	0.39
E34351			0.97	12.99	1.46	0.39
E34331	BEH (13)	1.26	0.98	6.14	1.41	0.37
E34362	THO (14)	1.57	0.99	10.84	1.49	0.50
	Oils					
	Field	**API**				
	BY	38.4	0.97	31.30	1.11	0.51
	LB	45.4	0.99	14.07	1.24	0.45
	ER-1	47.1	1.00	11.33	1.36	0.55
	ER-2	43.0	1.00	9.38	1.38	0.57
	ER-3	43.4	0.99	6.36	1.35	0.55

The same molecular parameters as determined for the extracts (Fig. 27) have also been calculated for the crude oils (Fig. 29). The values for the ratio of light (n-C_{17-19}) to heavy (n-C_{27-29}) n-alkanes (LHCPI) covers a range similar to the one derived from the extract data: Samples LB and ER-1, -2 and -3 show relatively low ratios (7 to 13), similar to the bulk of the extract data. Sample BY, however, consists of a high proportion of light relative to heavy saturated hydrocarbons (ratio of 31). Such a compositional feature was also associated with extract samples of well JEN (Fig. 27).

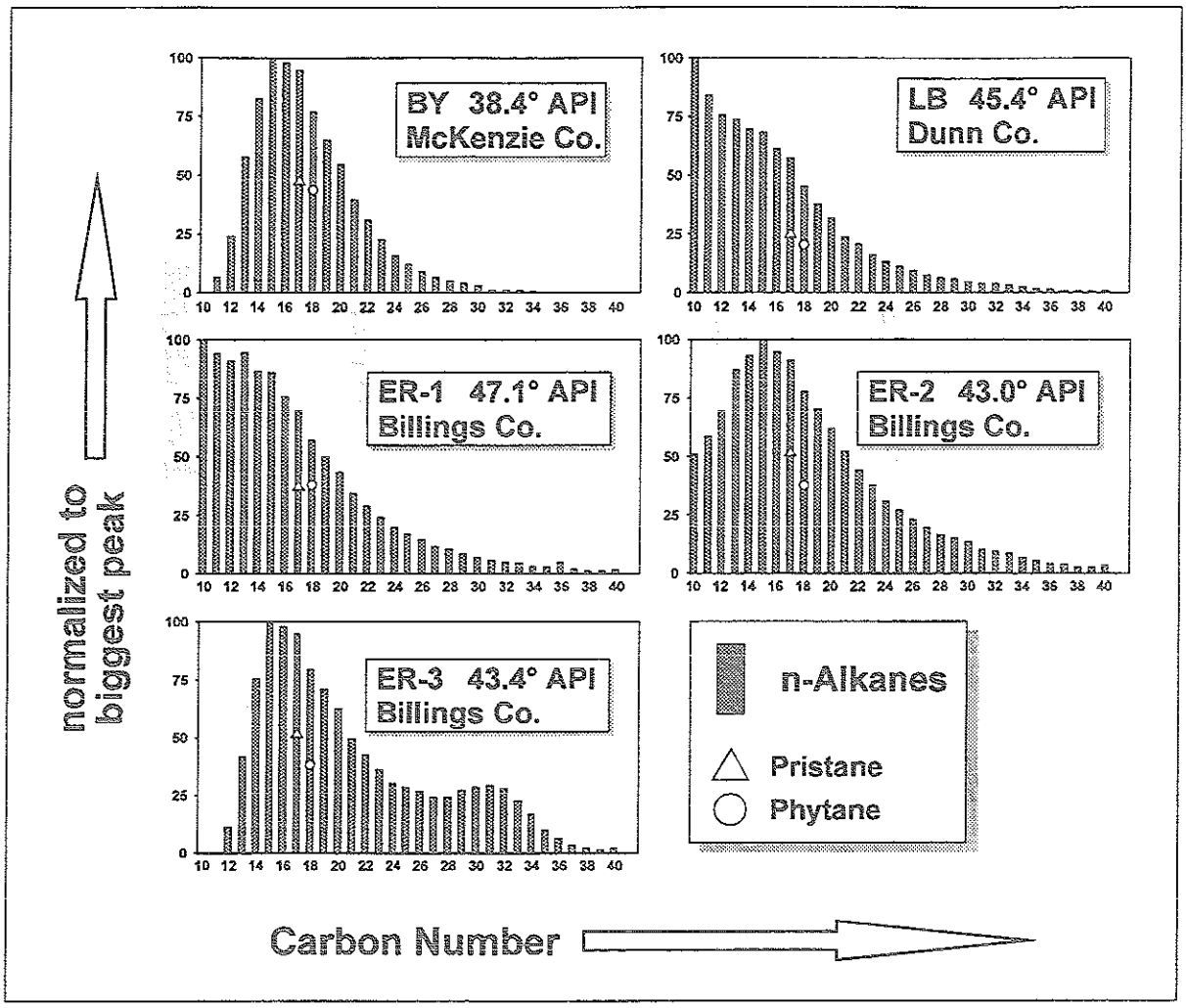

Fig. 28: Distribution pattern for n-alkanes and isoprenoids (pristane, phytane) of Bakken crude oils. Sample description includes oil gravity and location of well (county) from which the oil was produced.

The data for CPI-1, Pri/n-$C_{17:0}$ and Pri/Phy show only slight variations for all samples. The odd-even-predominance lies slightly below 1.0 and is identical for all oils. The results for Pri/n-$C_{17:0}$ vary from 0.4 to 0.5. In the case of the extracts, such a range of values was determined for samples of the mature zone (>0.6% R_o). The Pri/Phy ratio reveals a minor predominance of pristane (range of 1.1 to 1.3). The corresponding extract data were slightly higher (ca. 1.2 to 1.6).

Compositional variations of the ***aromatic*** hydrocarbon fraction in sedimentary organic matter, especially diaromatic (naphthalenes) and triaromatic (phenanthrenes) components as well as their alkylated homologs have been found to be controlled by among other things maturation (Radke et al., 1980b). Based on this concept, several maturity parameters, namely ratios of quantitatively prominent 2-ring and 3-ring aromatics were calculated (Radke et al., 1982; Radke & Welte, 1983) and applied to the aromatic hydrocarbon fraction of Bakken Shale extracts and crude oils in the present study.

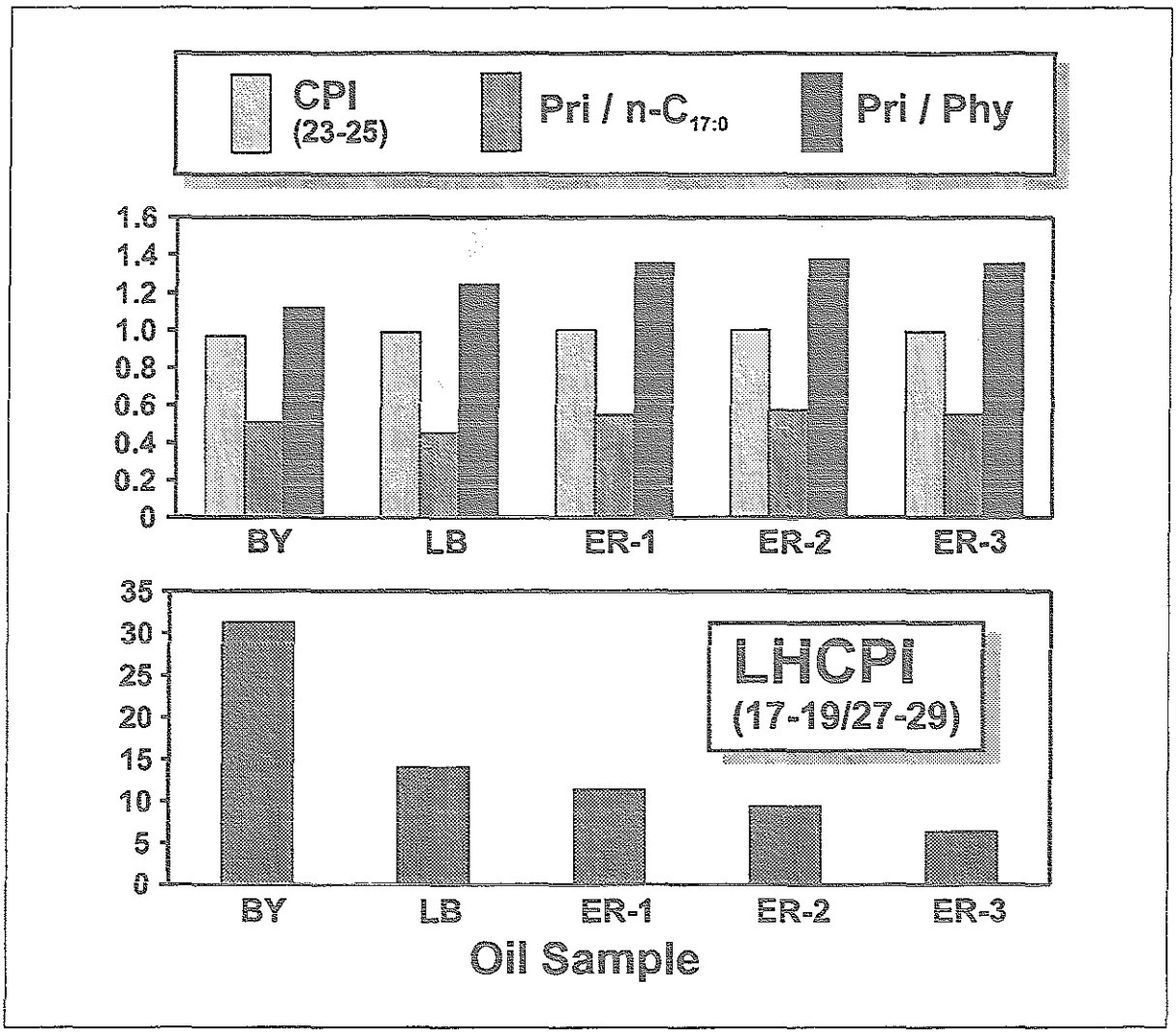

Fig. 29: Calculation of four selected parameters (analogous to Fig. 27) for Bakken crude oils.

A set of selected maturity parameters (Tab. 7; equations given in the appendix) based on the ratios of alkylnaphthalenes and alkylphenanthrenes are plotted versus vitrinite reflectance (Fig. 30). The diagrams clearly show that all parameters outline a broad increase as maturation proceeds. This is especially true for the main zone of catagenesis between 0.6% and 1.1% R_o.

The *alkylnaphthalene*-derived parameter TNR 2, which involves 4 of 5 trimethylnaphthalenes, outlines a positive linear trend throughout the entire maturity sequence (with exception of well BEH at 1.26% R_o), hence indicating that this ratio is useful for establishing maturity of the Bakken Shale organic matter. This is, however, true only in the maturity interval (0.7% to 1.1% R_o) typically associated with the main zone of hydrocarbon generation (Tissot & Welte, 1984). Therefore, it is useful for establishing the maturity level of crude oils.

The *alkylphenanthrene* ratio MPI-1 is known to show a good correlation with R_o for type III kerogens within the boundaries of the classical oil window (Radke & Welte, 1983) from 0.5% to 1.3% R_o. In Fig. 30, well HOV reveals the highest MPI-1 values of all wells and the second highest values for TNR-2 and MPR-3, thence corroborating its most mature status. Well THO (1.57% R_o) matches the values for the wells of maturity interval 0.8 to 1.0% R_o suggesting that the maturity level according to R_o may be too high.

Table 7: Molecular maturity parameters for the aromatic fraction of Bakken solvent extracts and crude oils. Equations for calculation of ratios are given in the appendix. Well numbers refer to location of sampled wells in Fig. 6.

Sample ID	Well name (#)	R_o (%)	TNR-2	MPI-1	MPR-3
	Extracts				
E34270	DOB (1)	0.31	0.65	1.18	0.69
E34276			0.82	1.18	0.70
E34263	JAC (2)	0.55	0.77	0.88	0.62
E34288	NEG (3)	0.57	0.70	0.75	0.61
E34437	SKA (4)	0.68	0.79	0.75	0.76
E34440			0.79	0.77	0.76
E34443			0.79	0.77	0.78
E34306	BOR (5)	0.72	0.75	0.68	0.63
E34308			0.75	0.70	0.67
E34366	GRA (6)	0.83	0.87	0.94	0.87
E34343	SET (7)	0.83	0.86	0.97	0.89
E34345			0.93	0.86	0.82
E34321	MAR (8)	0.90	0.84	0.87	0.84
E34322			0.83	0.88	0.87
E34328			0.82	0.95	0.94
E34449	JEN (9)	0.92	0.88	0.98	0.89
E34454			0.87	0.94	0.84
E34455			0.90	0.99	0.87
E34376	CON (10)	0.94	0.97	1.03	0.95
E34389			0.97	1.08	0.88
E34403			0.97	1.03	0.93
E34416			0.97	1.00	0.92
E34425	FED (11)	0.99	0.95	0.85	0.90
E34430			0.95	0.94	0.89
E34434			0.95	0.93	0.88
E34347	HOV (12)	1.11	0.94	1.21	0.96
E34351			0.94	1.21	0.99
E34331	BEH (13)	1.26	0.84	0.87	0.88
E34362	THO (14)	1.57	0.99	1.13	1.04
	Oils				
	Field	API			
	BY	38.4	0.89	1.21	0.92
	LB	45.4	0.91	1.01	1.15
	ER-1	47.1	1.01	1.01	1.12
	ER-2	43.0	1.01	1.03	1.22
	ER-3	43.4	0.97	0.99	1.15

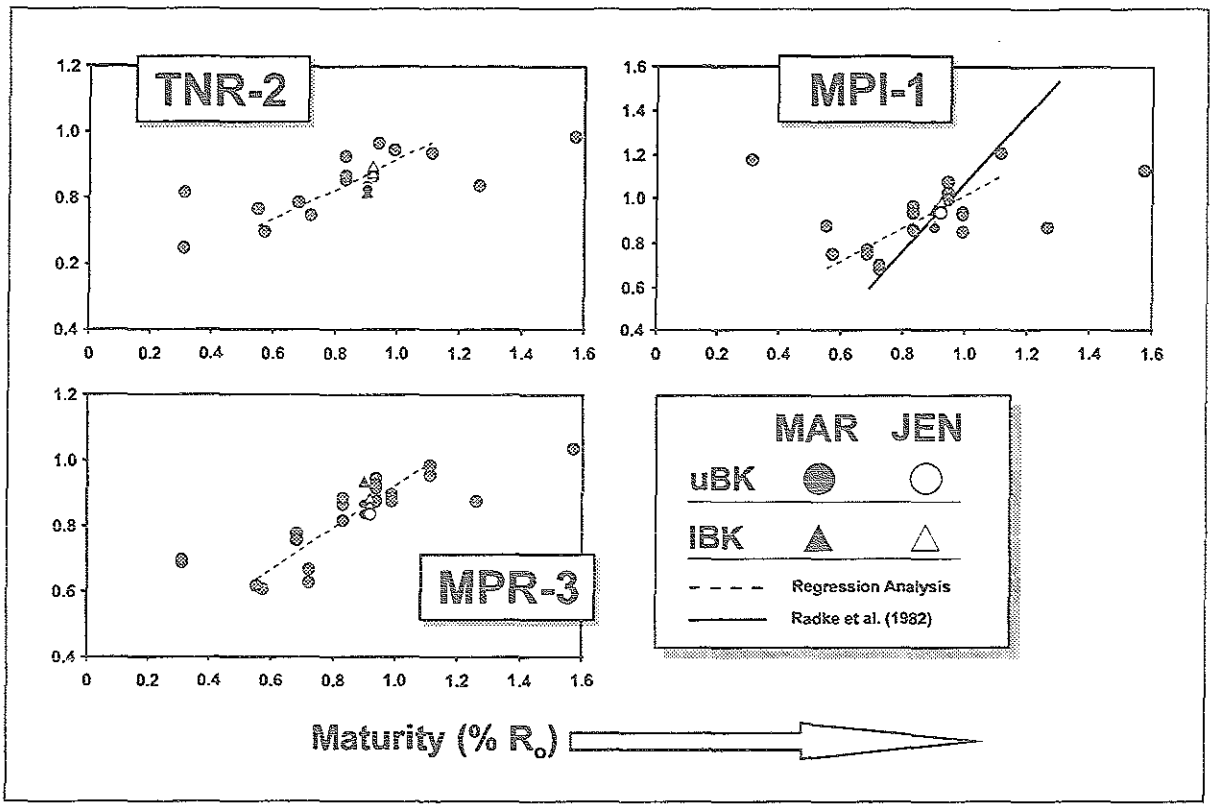

Fig. 30: Maturity related evolution of selected parameters (TNR-2, MPI-1 and MPR-3) of Bakken Shale solvent extracts (aromatic fraction). Parameters are based on the studies by Radke et al. (1982) and Radke et al. (1986). Equations are given in the appendix. Triangles and circles refer to the lower and upper shale unit of the same well, respectively. Trendlines were determined by regression analysis.

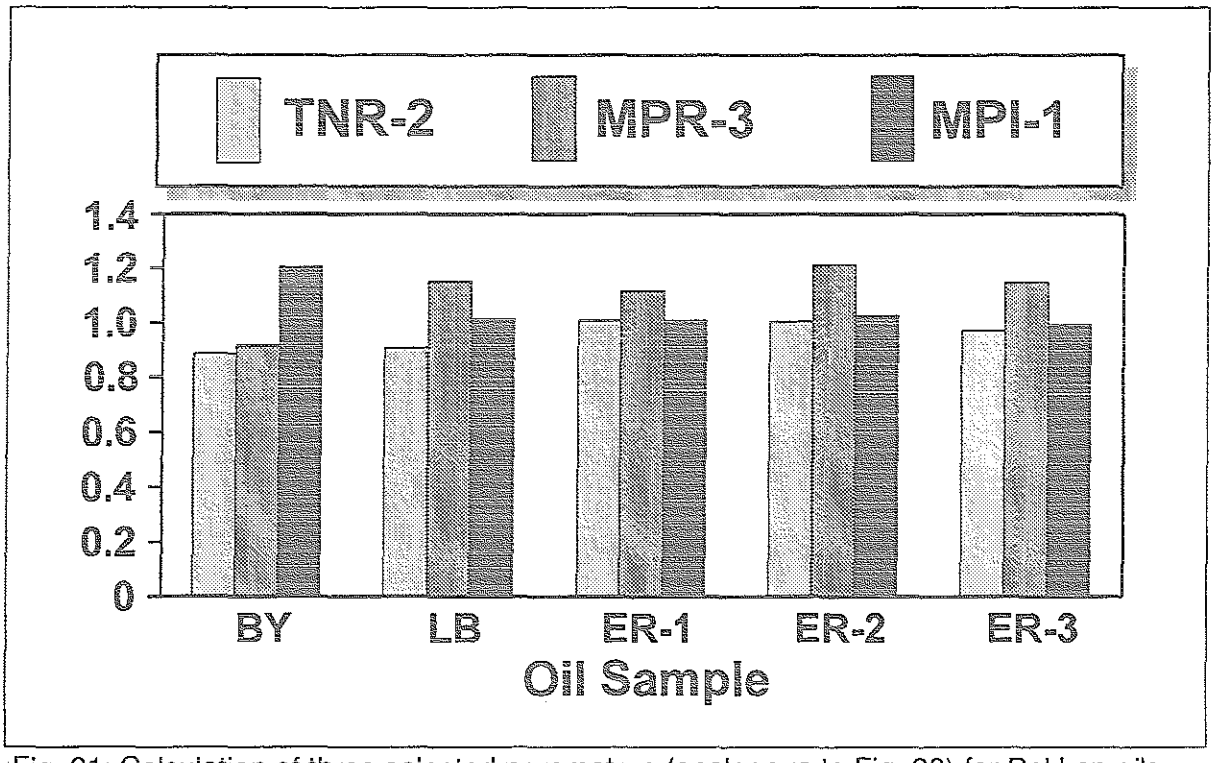

Fig. 31: Calculation of three selected parameters (analogous to Fig. 30) for Bakken oils.

In the light of relative maturity assessment it should be pointed out that for all parameters deduced from aromatic hydrocarbons mentioned above (TNR-2, MPI-1 and MPR-3) well BEH (1.26% R_o) always reveals ratios that are too low to fit into the observed maturation pathway outlined by the other values.

Fig. 31 gives maturity parameters as calculated for the Bakken crude oil samples. Analogous to the ratios based on the saturate fraction (e.g. LHCPI, Fig. 29), sample BY, which has the lowest density of all studied oil samples (38.4° API), yielded values distinctively different to the others: The alkylphenanthrene ratio MPI-1 namely, which is almost unity for all other samples, is 1.2 for sample BY. Additionally, parameter MPR-3 of sample BY is relatively low (0.9), while the values for the rest of the oil samples range between 1.1 and 1.2. Solely the alkylnaphthalene ratio TNR-2 indicates relative uniformity of all oils.

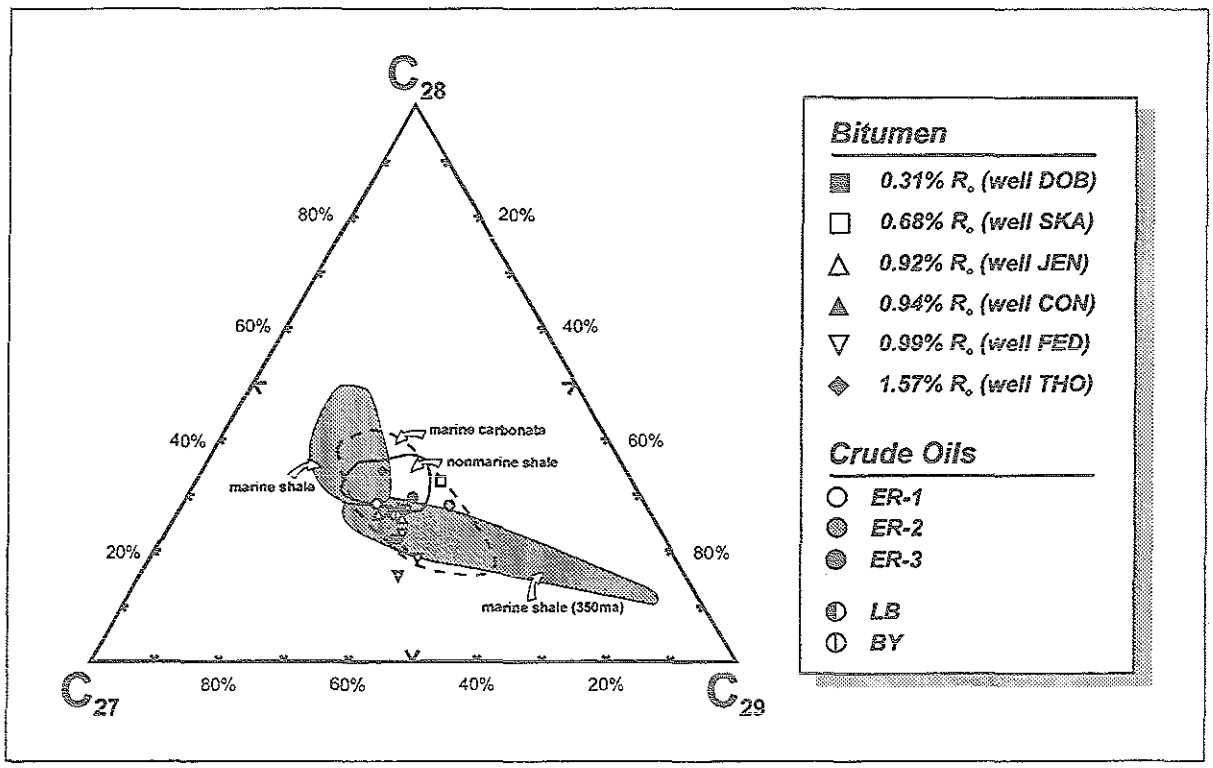

Fig. 32: Relative composition of C_{27}-, C_{28}- and C_{29}- ββ steranes ("regular" steranes) for Bakken solvent extracts and crude oils. Facies zonation superimposed after Moldowan et al. (1985).

4.5.4 Saturated Hydrocarbon Biomarkers

GC-MS analysis of the saturate hydrocarbon fraction of Bakken crude oils and selected extracts gave good quality results only for the most immature samples (DOB, 0.31% R_o and SKA, 0.68% R_o). The signal for the crude oil samples and the more mature extracts was very low (especially for the triterpanes) this being consistent with an overall high level of thermal evolution for the majority of the sample set, as already evidenced by molecular maturity parameters derived from

GC analysis (e.g. Pri/n-$C_{17:0}$; Pri/Phy; ch. 4.5.3). For certain samples, the quality of the mass spectrometric data was too poor to enable determination of some biomarker ratios. These restrictions should be kept in mind while interpreting the biomarker data.

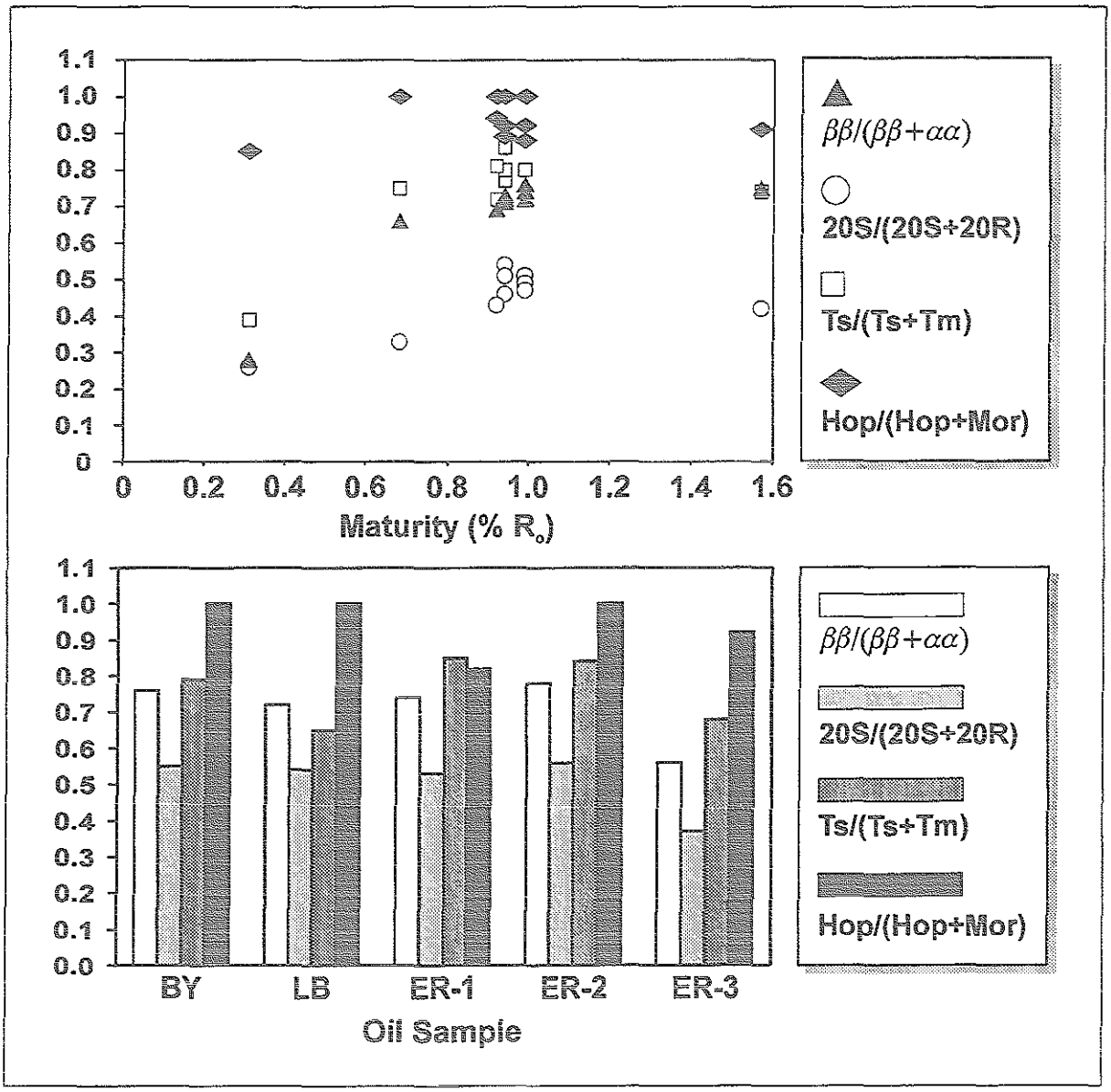

Fig. 33: Distribution of biomarker-derived maturity parameters for Bakken solvent extracts (top) and crude oils (bottom).

Fig. 32 shows the relative proportions of the regular steranes C_{27-29} for oils and extracts. The relative sterane composition is indicative for the original concentration of sterols in the depositional environment and therefore is related to depositional facies (Huang & Meinschein, 1979). In a later publication, however, this general postulate was questioned (Volkman, 1986). The diagram elucidates that the relative composition of the regular steranes for both sample sets (extracts and crude oils) remains uniform. Effects of increasing maturation don't seem to alter the sterane distribution of the extracts. Moreover, the majority of the datapoints falls into the zone for Paleozoic marine source rocks as defined by Moldowan et al. (1985). This is especially true for the crude oils, hence implying that the Bakken reservoired oils were not affected by mixing with a

petroleum phase from a source of a different depositional environment. Only three extract samples (SKA, FED and THO) yielded a distribution which lies outside the Paleozoic marine facies, suggesting a variation in organofacies. Other analyses which are considered suitable to investigate organofacies (organic petrology, py-gc), however, did not provide any evidence for distinctive facies variations in the Bakken Shale. Hence, the outliers in Fig. 32 might be due to the normal scatter of data.

Fig. 33 shows various commonly used biomarker derived maturity parameters (Waples & Machihara, 1991) plotted as a function of vitrinite reflectance. The ratio of two epimeric forms of the αα steranes (20S/(20S+20R) is considered the most reliable and useful biomarker maturity indicator (Rullkötter & Marzi, 1988). Indeed, for the extract samples, it shows a very good correlation with vitrinite reflectance up to 1.0% R_o. However, the most mature sample (well THO at 1.57% R_o) had approximately the same value (ca. 0.5) as the samples between 0.9% and 1.0% R_o. This in agreement with the conclusions by Mackenzie et al. (1980), who found that the equlibrium of this ratio is reached at ca. 1.1% R_o.

A similar pattern is described for two further parameters (ββ/(ββ+αα) and Ts/(Ts+Tm)): Each ratio shows a rather steady increase with increasing thermal alteration up to 1.0% R_o, before the curve levels off. The flat slope of the Hop/(Hop+Mor) parameter should be evaluated in the light of its pronounced sensitivity only for immature stages of maturation, as the equlibrium is reached very early (Mackenzie et al., 1980).

Assessment of maturity for the crude oils (Fig. 33) using the sterane ratios ββ/(ββ+αα) and 20S/(20S+20R) suggests that most of the oils have been formed at relatively high levels of maturity (corresponding to the zone of 0.8% to 1.0% R_o). The relatively low values for sample ER-3 (0.56 and 0.37, respectively) might argue for a slightly less mature generation level (ca. 0.6% to 0.8% R_o). However, this hypothesis is not corroborated by the triterpane data (Ts/(Ts+Tm) and Hop/(Hop+Mor)) which indicate the same maturity level for oil ER-3 as for the other oil samples.

4.6 Thermal Extract

In contrast to ch. 4.5 which dealt with composition and maturity related evolution of high molecular weight C_{15+} material, the following ch. 4.6 contains results derived from analysis of the thermally releasable organic matter. Hence, data is presented from thermal analysis (t'vap-gc) of rock samples and crude oils.

4.6.1 Characterisation of Thermally Releasable Organic Components

Thermovaporisation describes the thermally induced release of mobilisable organic matter which resides in the pore space of the host rock. Similar to a Rock-Eval type analysis, 300°C is considered to be the threshold, beyond which the realm of pyrolysis commences and generation of compounds is initiated. However, the boundary between thermovaporisation and pyrolysis is not fixed. Accordingly, a temperature range might exist where the two processes overlap. The

possibility of gaseous compounds being generated even at such low temperatures as 300°C was examined by heating a second aliquot of a given sample to 250°C. This modified experiment, however, provided qualitatively the same result which allows to conclude that the compounds resolved by chromatographic analysis are indigenous material in the rocks and released rather than generated. Quantitative data on compound groups and individual compounds are given in Tab. 8.

Table 8: Yield of gaseous (C_{1-5}), n-alkane (C_{6+}) products and individual compounds derived from t'vap-gc of Bakken Shale samples. MCP, DMCP, MCH and TMB refers to methylcyclopentane, dimethylcyclopentane, methylcyclohexane and 1,2,3,4-tetramethylbenzene, respectively. Well numbers refer to location of sampled wells in Fig. 6.

Sample ID	Well name (#)	R_o (%)	C_1-C_5 (mg/g TOC)	n-C_{6+}	MCP	DMCP	MCH	TMB
E34268	DOB (1)	0.31	6.90	4.19	1.13	1.34	0.76	0.22
E34270			5.56	5.64	1.22	1.43	0.81	0.25
E34273			6.02	4.78	1.13	1.50	0.77	0.22
E34278			5.07	4.68	1.05	1.36	0.70	0.19
E34280			4.96	3.91	0.98	1.22	0.68	0.18
E34263	JAC (2)	0.55	5.62	4.84	1.35	1.58	1.04	0.11
E34287	NEG (3)	0.57	5.24	2.52	1.17	1.20	0.73	0.16
E34290			2.02	5.03	1.00	1.49	0.93	0.32
E34438	SKA (4)	0.68	5.95	3.94	0.94	0.56	0.91	0.30
E34440			4.41	3.82	0.85	0.55	0.88	0.29
E34441			4.15	4.21	0.86	0.58	0.92	0.33
E34443			4.21	4.14	0.91	0.59	1.05	0.34
E34306	BOR (5)	0.72	1.98	6.78	0.66	0.53	0.78	0.22
E34307			2.45	3.30	0.74	0.60	0.89	0.24
E34365	GRA (6)	0.83	0.65	7.02	0.09	0.16	0.50	0.08
E34368			1.23	11.60	0.48	0.49	1.39	0.11
E34344	SET (7)	0.83	0.64	5.86	0.24	0.32	0.87	0.08
E34321	MAR (8)	0.90	0.65	10.31	0.18	0.27	0.66	0.15
E34322			1.62	9.50	0.49	0.45	1.10	0.11
E34325			0.58	5.79	0.07	0.13	0.36	0.12
E34325			0.73	5.11	0.21	0.28	0.69	0.12
E34310	JEN (9)	0.92	0.79	4.54	0.30	0.32	0.88	0.10
E34312			0.42	4.52	0.13	0.21	0.57	0.11
E34373	CON (10)	0.94	0.80	7.28	0.29	0.36	0.99	0.17
E34376			1.11	7.35	0.47	0.46	1.24	0.19
E34385			1.66	9.11	0.33	0.29	1.05	0.17
E34396			3.31	6.04	0.62	0.43	1.47	0.11
E34401			2.40	8.42	0.63	0.47	1.61	0.14
E34411			2.71	6.96	0.56	0.42	1.46	0.11
E34420			2.83	6.57	0.57	0.32	1.09	0.10
E34423	FED (11)	0.99	2.17	7.98	0.64	0.55	1.35	0.16
E34429			0.46	9.96	0.15	0.26	0.59	0.24
E34432			1.89	6.11	0.52	0.45	1.07	0.11
E34347	HOV (12)	1.11	0.63	6.44	0.09	0.02	0.13	0.18
E34350			0.47	5.24	0.08	0.03	0.20	0.16
E34331	BEH (13)	1.26	0.75	6.20	0.32	0.36	0.92	0.13
E34362	THO (14)	1.57	1.01	8.19	0.37	0.40	1.19	0.20

Fig. 34 illustrates the composition of the thermally released products in the Bakken Shale. Fingerprints of the two chromatograms (0.31% R_o and 0.94% R_o) are representative for immature (up to ca. 0.7% R_o) and mature (>0.7% R_o) levels of thermal evolution.

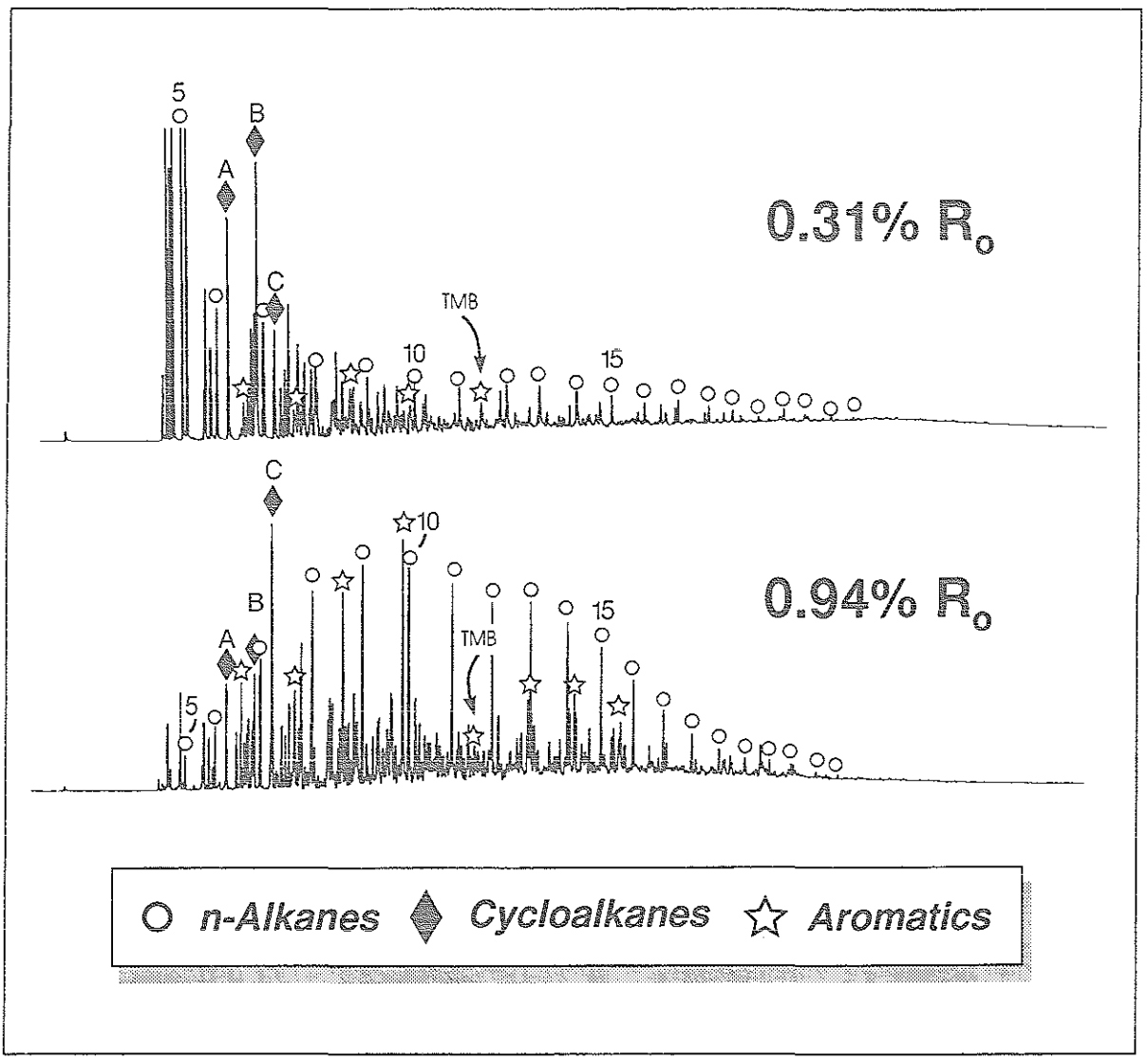

Fig. 34: Gas chromatograms as derived from t'vap-gc of two whole rock Bakken Shale samples as representative for low-mature and high-mature stages of thermal alteration. Numbers indicate total numbers of carbon atoms. Cycloalkanes are identified as methylcyclopentane (A), dimethylcyclopentane (B) and methylcyclohexane (C). TMB refers to 1,2,3,4-tetramethylbenzene.

As regards bulk composition, immature samples reveal high abundances of low-molecular-weight hydrocarbons (including methane) relative to C_{6+} compounds. Samples from higher levels of maturity, however, are generally characterized by a preponderance of medium-weight hydrocarbons (C_{7-20}) and relatively low yields of gaseous products.

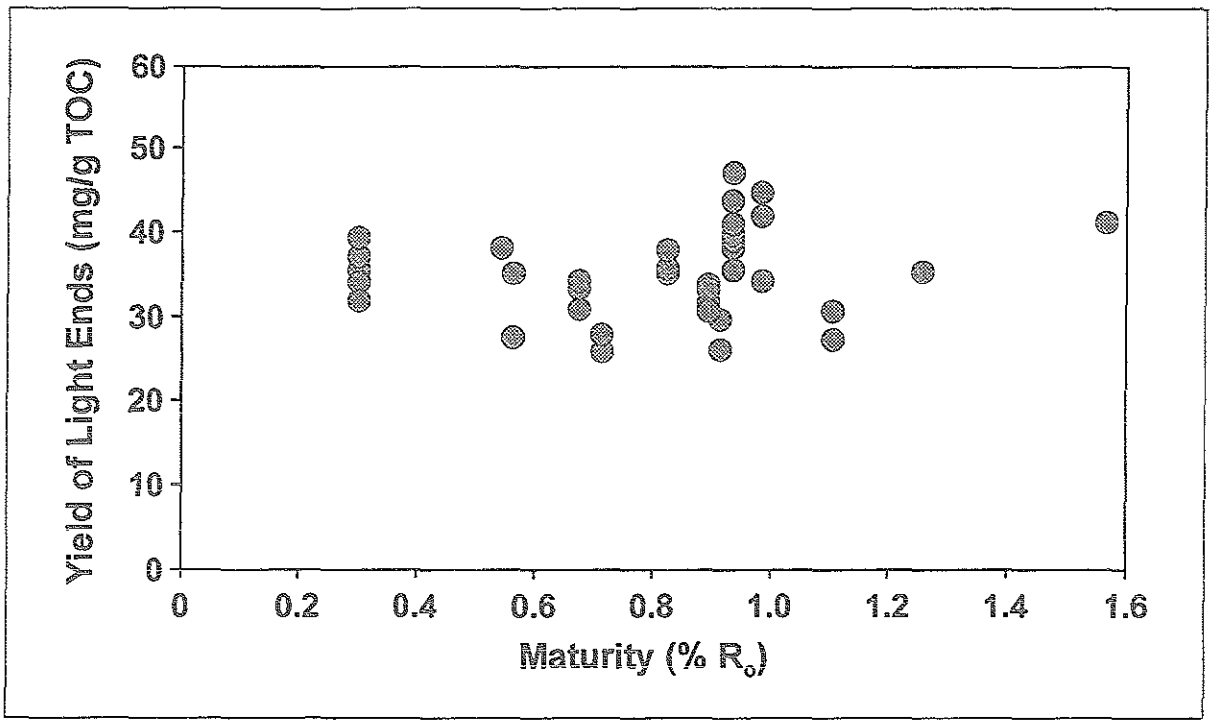

Fig. 35: Maturity related evolution of total yield of Bakken Shale thermovaporisation products (total response) as determined by t'vap-gc. All samples were taken from the Upper Bakken Shale.

Fig. 35 shows the total yield of thermally releasable compounds (< 300°C) as a function of maturity. It is evident that this distribution pattern is qualitatively similar to the one determined by solvent extraction (Fig. 23) and yield of saturate and aromatic fraction of the extracts (Fig. 25): Namely, while the low mature (< 0.8% R_o) and high mature (> 1.0% R_o) zones exhibit low to moderate values, the interval between these zones reveals maximum yields paralleled by considerable variability of the data. It must be pointed out, however, that due to lack of sample material the data derived from t'vap-gc cannot be used to differentiate between the upper and lower shale unit of a given well, as is the case for the solvent extract data. If the total response is separated into the gas portion (C_{1-5}) and the oil portion (C_{6+}), two different distribution patterns arise (Fig. 36): The relative amount of gas is considerably higher at immature maturity stages up to 0.7% R_o. The maturity interval 0.8% to 1.0% R_o is characterised by overall low values but again, a large scatter of datapoints is visible. Above 1.0% R_o, gas contents remain uniformly low. The distribution of oil-like compounds (Fig. 37), however, is close to the one of the total response: maximum yields (high variability) between 0.8% and 1.0% R_o, preceded and followed by moderate to low values.

On a molecular level, the Bakken Shale yields high amounts of cyclic compounds which visually dominate the thermovaporisation fingerprints. Light alkylcycloalkanes, such as methylcyclopentane, dimethylcyclopentane and methylcyclohexane are among the most prominent compounds throughout maturity. In addition to the alkylcycloalkanes, alkylbenzenes and, at higher stages of thermal evolution (> 0.6% R_o), alkylnaphthalenes become abundant. Apart from the alkylbenzenes like benzene, toluene and xylenes, which are common for most types of organic matter, the presence of one aromatic compound, namely 1,2,3,4-tetramethylbenzene is a peculiar feature of Bakken Shale derived organic matter. The presence and significance of this particular compound has also been referred to for the kerogen pyrolysates (ch. 4.4).

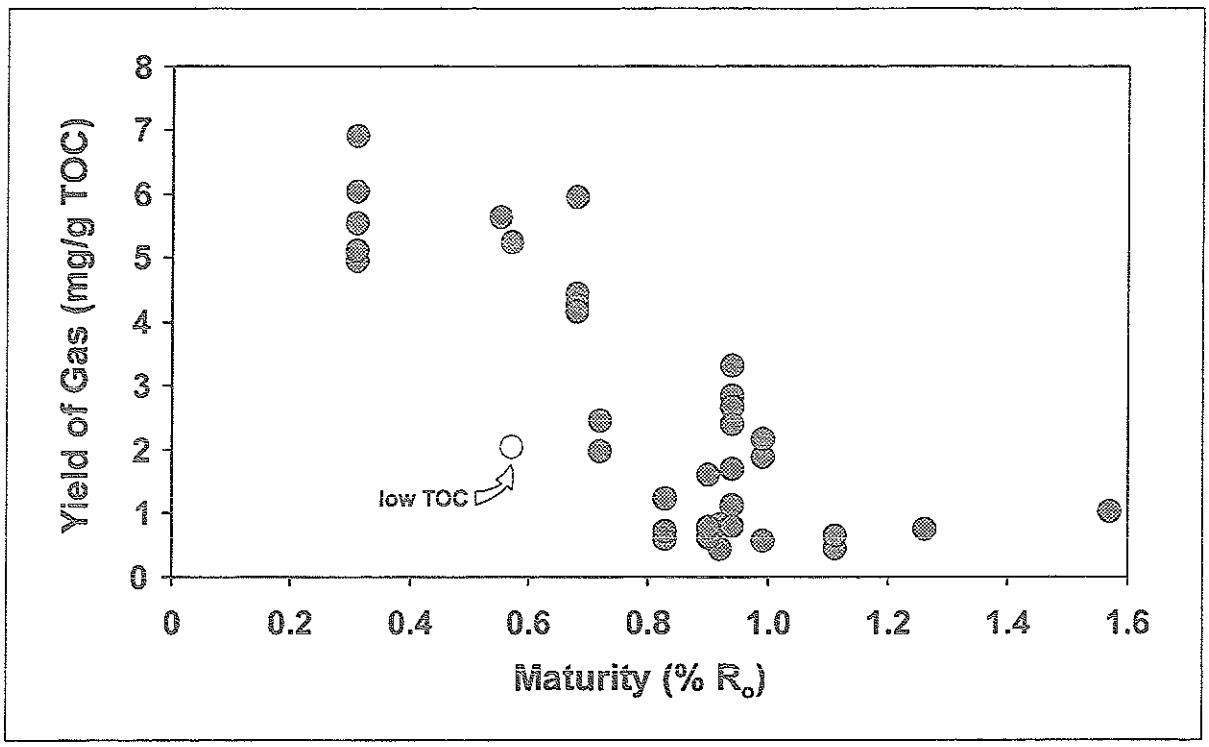

Fig. 36: Proportion of gaseous compounds (C_1-C_5) in the total yield of Bakken Shale thermovaporisation products as determined by t'vap-gc. Hollow circle refers to an individual sample with unrepresentatively low TOC content (6.4wt.-%).

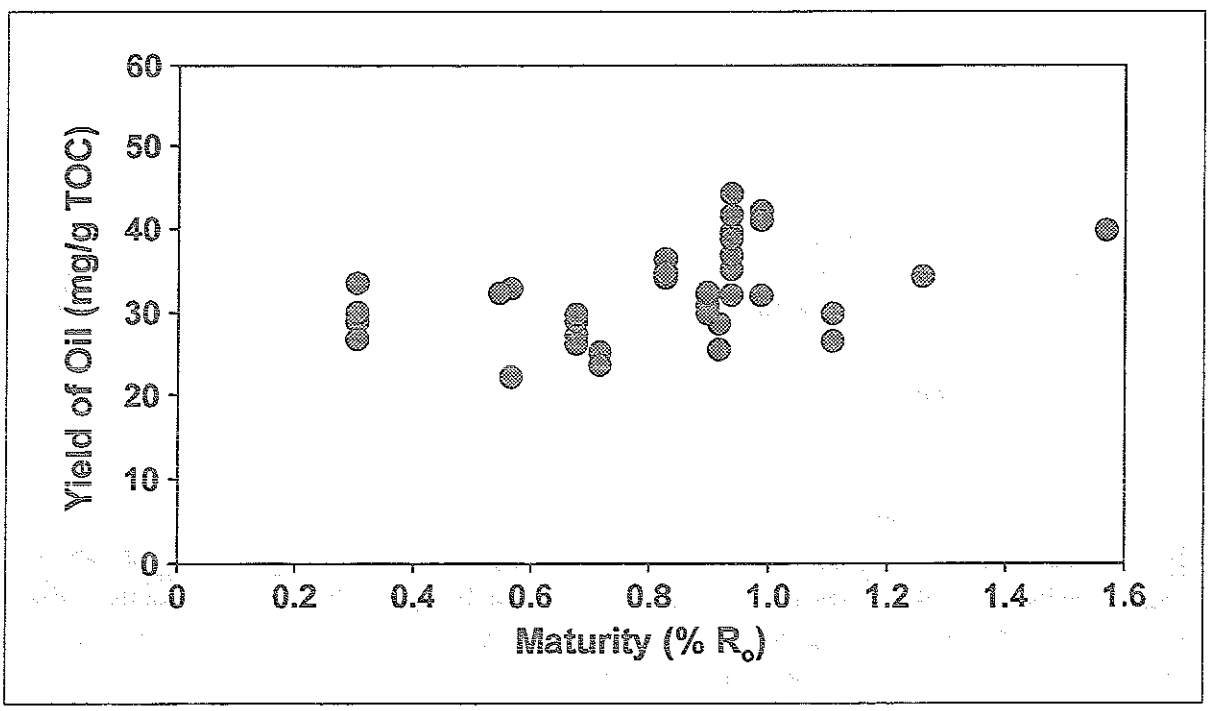

Fig. 37: Proportion of "oil" compounds (C_{6+}) in the total yield of Bakken Shale thermovaporisation products as determined by t'vap-gc.

The quantification of n-alkanes and selected aromatic hydrocarbons is displayed in Fig. 38. This diagram reflects the overall relative preponderance of n-alkanes at the beginning of maturation followed by a sharp drop at levels > 0.6% R_o. This is primarily due to the enhanced appearance of alkylated naphthalenes in the mobile organic matter.

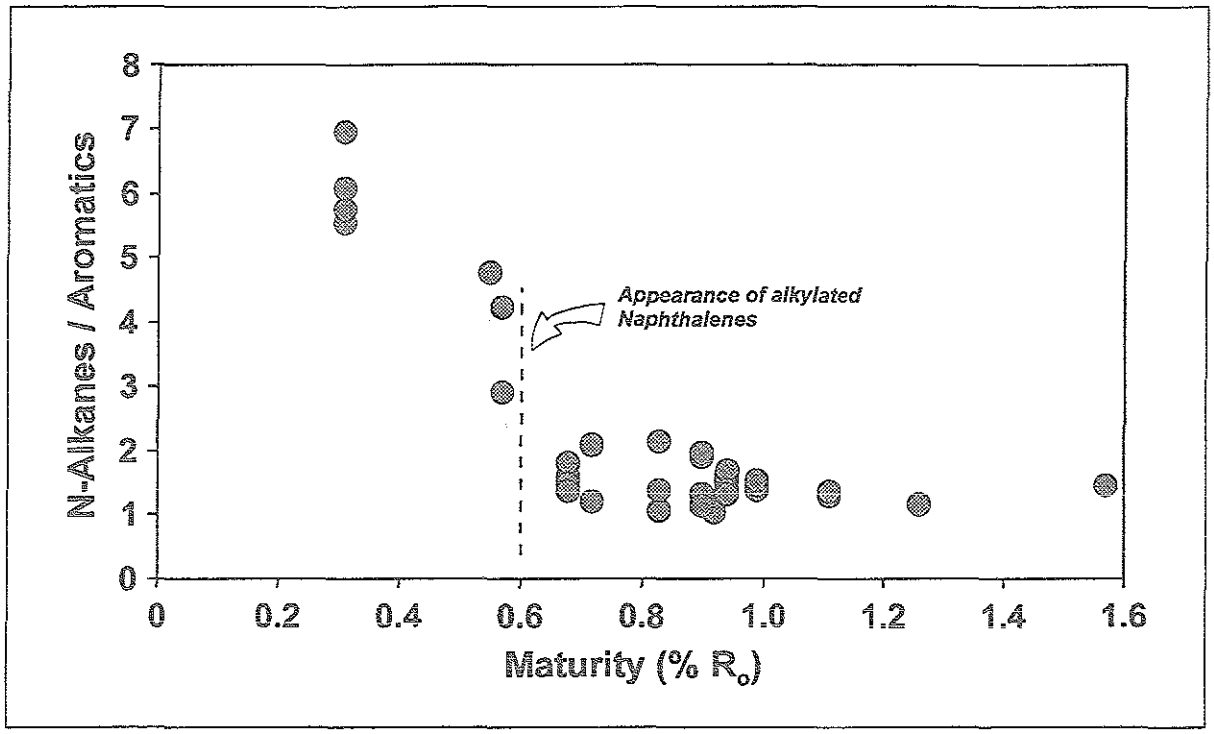

Fig. 38: Relationship of chain-like hydrocarbons (n-alkanes up to n-C_{26}) to mono- and bicyclic aromatics (benzene, toluene, ethylbenzene, meta-/paraxylene, ortho-xylene, C_3-benzene and alkylnaphthalenes) as a function of maturity (data based on t'vap-gc analysis).

4.6.2 Isotopic Composition of Thermally Releasable Organic Components

Stable carbon isotopic composition ($\delta^{13}C$) of the thermovaporisation products was determined utilizing two different GC column types, namely a BP-1 fused silica column and a poraplot column. The latter column is designed to rule out coelution effects due to CO_2 sourced from inorganic matter. Such coelution of isotopically heavy CO_2 with C_2 and C_3 would severely affect data quality of the latter two. Indeed, after analysis using standard column equipment (fused silica) the data on the gases was believed to be affected by coelution effects. Therefore, further analytical runs were carried out using the poraplot column.

Tabs. 9 and 10 give the mean values of triplicate measurements for each method.

Fig. 39 shows $\delta^{13}C$ for n-alkanes (up to n-C_{20}) using the standard experimental set-up. The values for the C_{6+} compounds outline a distribution pattern with only minor variations; lightest values being -35.1‰ for n-C_6 (0.31% R_o) and the heaviest -27.5‰ for n-C_{18} (0.9% R_o). The liquid (n-C_{6+}) hydrocarbons at the maturity level of 0.9% R_o are most enriched in ^{13}C as regards the average value (-28.3‰) whereas the C_{6+}-n-alkanes from the most immature samples (0.31% R_o) are isotopically lightest (average of -30.9‰).

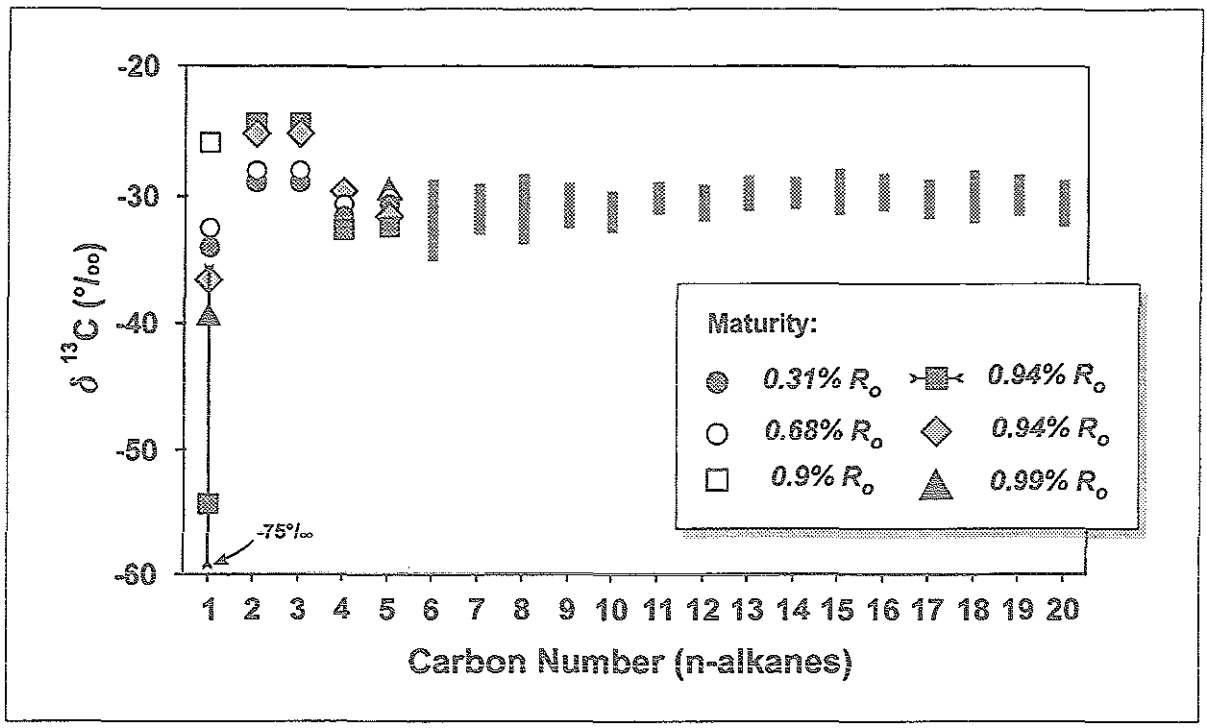

Fig. 39: Stable carbon isotopic composition of natural products as derived from on-line thermovaporisation-GC-IR-MS (triplicate measurements) using standard GC equipment (fused silica column). Selected samples cover a maturity spectrum from 0.31% to 0.99% R_o. Grey bars outline the range of values for n-C_{6+} alkanes. Isotope ratios are displayed as $\delta^{13}C$ relative to the PDB standard.

The values for n-hexane and n-octane cover the broadest range throughout maturity (from -35.1‰ to -28.7‰ and from -32.8‰ to -28.5‰, respectively). This variability of data is even more pronounced for the light hydrocarbons (C_1-C_5): The values for methane outline a very broad range from relatively heavy (-25.6‰ at 0.9% R_o) to light (-39.7‰ at 0.99% R_o) without any systematic relationship to level of thermal evolution. One sample shows an even higher value (-55‰), but threefold measurements for the latter were characterized by a very poor reproducibility. Ethane and n-propane are generally very enriched in ^{13}C (-28‰ to -25‰). $\delta^{13}C$ of both compounds reveals a stepwise increase with increasing maturity: While the values within the immature range (0.31 to 0.68% R_o) and for mature samples (0.94% R_o), respectively, are very similar, the difference between 0.68% and 0.94% R_o is relatively significant. N-butane and n-pentane exhibit isotope ratios which are similar to the values of the C_{6+}-n-alkanes, and their variability is relatively low (from -29.4‰ to -31.7‰ for n-butane and from -29.1‰ to -31.6‰ for n-pentane). With respect to maturity, it is noteworthy that the gases derived from the less mature samples (< 0.9% R_o) cover a spectrum of values that is much narrower than the range of the more mature Bakken gases (> 0.9% R_o).

Corresponding results (averaged values) using the refined experimental configuration specifically suited to gas analysis and resolution of CO_2 are depicted in Fig. 40. The reproducibility for individual compounds was very poor, as Tab. 10 reveals. For methane, the scatter of data is similar to that shown in Fig. 39: The values cover a broad range (from -42‰ at 0.94% R_o to -15‰ at 0.31% R_o). The variability of the values is reduced with increasing carbon number, while

the average value remains roughly constant. The sample at 0.94% R_o exhibited always the highest (heaviest) values for n-propane, n-butane and n-pentane. In contrast, the most immature sample (0.31% R_o) is isotopically lightest as regards n-C_3 and n-C_4; $\delta^{13}C$ for n-C_5 was not determined. The maturity level 0.68% R_o is characterised by rather constant values (between 33‰ and 36‰). The isotope ratio for CO_2 also remains constant (from 23‰ to 24‰).

Table 9: Stable carbon isotope ratios for individual n-alkanes (C_{1-20}; mean values of triplicate measurements) as derived from t'vap-gc-IR-MS using a standard fused silica column for five different stages of maturity. Values are calculated in $\delta^{13}C$ relative to PDB standard. Abbreviation n.d. refers to 'not determined'. Well numbers refer to location of sampled wells in Fig. 6.

Well name (#)	DOB (1)	SKA (4)	MAR (8)	CON (10)	CON (10)	FED (11)	FED (11)
R_o (%)	0.31	0.68	0.9	0.94	0.94	0.99	0.99
n-C_1	-33.7	-32.3	-25.6	-55.0	-36.6	-39.7	-26.4
n-C_2	-28.8	-27.9	n.d.	-25.3	-25.2	n.d.	n.d.
n-C_3	-28.8	-27.9	n.d.	-25.3	-25.2	n.d.	n.d.
n-C_4	-31.0	-30.2	n.d.	-31.7	-29.4	n.d.	-28.1
n-C_5	-29.9	-29.9	-29.1	-31.6	-29.5	-29.3	-29.3
n-C_6	-35.1	-31.3	-28.7	-32.2	-29.9	-29.1	-29.1
n-C_7	-32.1	-31.0	-28.7	-30.0	-29.8	-29.2	-29.1
n-C_8	-32.8	-31.9	-28.5	-29.8	-30.2	-31.2	-31.1
n-C_9	-31.6	-30.9	-28.7	-29.7	-30.6	-31.5	-30.3
n-C_{10}	-31.7	-31.1	-29.1	-30.1	-30.4	-30.8	-30.3
n-C_{11}	-30.6	-30.1	-28.5	-30.1	-30.1	-30.8	-31.7
n-C_{12}	-31.2	-31.0	-28.8	-30.1	-30.5	-30.6	-31.3
n-C_{13}	-30.5	-30.2	-27.9	-29.5	-30.3	-30.5	-31.8
n-C_{14}	-29.8	-29.9	-28.1	-28.9	-30.3	-30.5	-31.5
n-C_{15}	-28.7	-30.0	-27.8	-30.0	-30.5	-30.2	-31.5
n-C_{16}	-28.7	-29.6	-27.9	-30.0	-30.3	-30.3	-31.8
n-C_{17}	-29.7	-29.5	-28.0	-30.3	-29.9	-31.1	-31.9
n-C_{18}	-28.8	n.d.	-27.5	-30.2	n.d.	-31.2	-33.2
n-C_{19}	n.d.	n.d.	-27.7	-30.7	n.d.	n.d.	n.d.
n-C_{20}	n.d.	n.d.	-28.1	-32.2	n.d.	n.d.	n.d.

Table 10: Stable carbon isotope ratios for individual gaseous n-alkanes (C_{1-5}; mean values of duplicate measurements) and CO_2 as derived from t'vap-gc-IR-MS using a poraplot column for five different stages of maturity. Values are calculated in $\delta^{13}C$ relative to PDB standard. Abbreviation n.d. refers to 'not determined'. Well numbers refer to location of sampled wells in Fig. 6.

Well name (#)	DOB (1)	SKA (4)	CON (10)	HOV (12)
R_o (%)	0.31	0.68	0.94	1.11
n-C_1	-14.8	-35.5	-42.0	-33.6
n-C_2	n.d.	n.d.	n.d.	n.d.
n-C_3	-40.6	-33.4	-22.4	n.d.
n-C_4	-37.9	-32.7	-28.1	n.d.
n-C_5	37.3	-33.4	-30.4	n.d.
CO_2	-24.2	-24.2	-23.6	n.d.

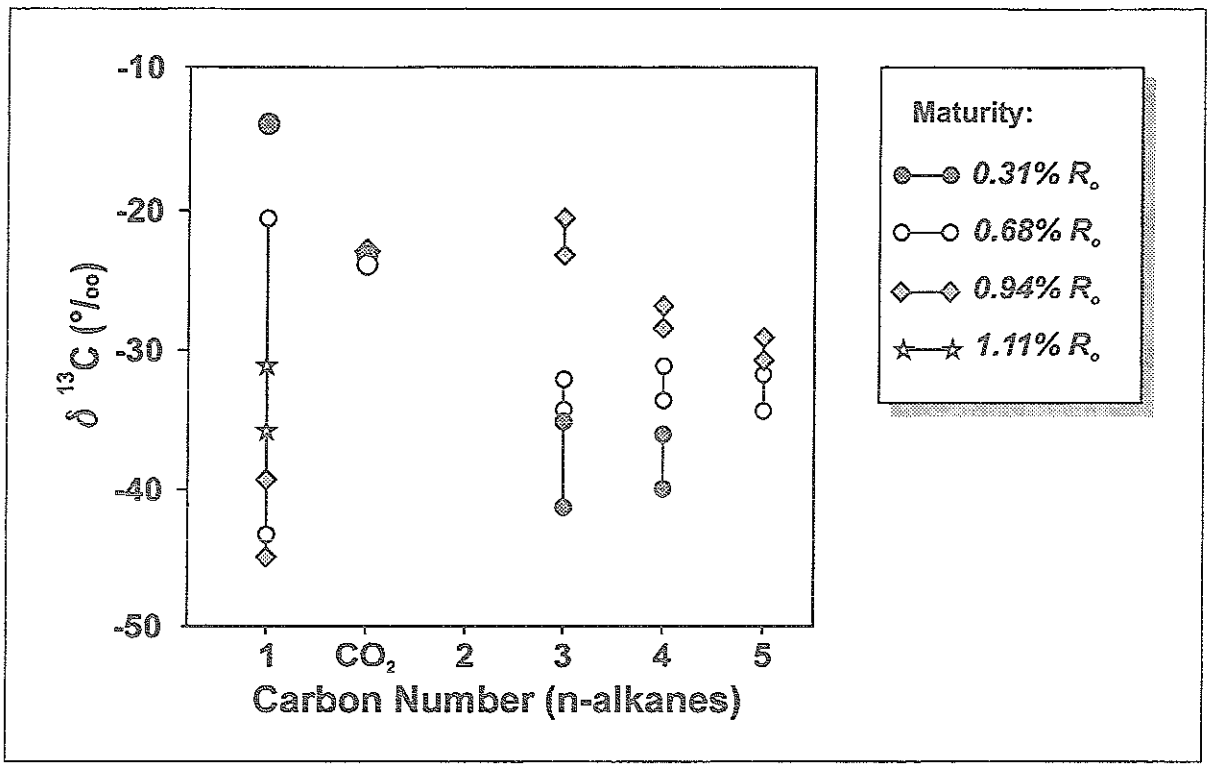

Fig. 40: Stable carbon isotopic composition of natural gaseous products (n-C_{1-5} including CO_2) as derived from on-line thermovaporisation-GC-IR-MS using a poraplot GC column. Datapoints are depicted with range of variability of triplicate measurements. For the sample at maturity 1.11% R_o (⋆), only methane was detected.

4.6.3 Crude Oils

The fingerprints derived from whole oil gas chromatography analysis (thermovaporisation technique) of Bakken crude oils (Fig. 41) elucidate that aliphatic hydrocarbons (normal alkanes, cycloalkanes and isoprenoids) are the dominating compound group. Samples ER-1, -2 and -3 reveal higher concentrations of long-chain n-alkanes clearly extending up to carbon number 28, while BY and LB are characterised by shorter chain length of the n-alkanes. BY is the only oil which shows a maximum of peak height at n-$C_{7:0}$/n-$C_{8:0}$. All other samples have a maximum at n-$C_{5:0}$.

Three low-molecular weight cycloalkanes methylcyclopentane, dimethylcyclopentane and methylcyclohexane, which were prominent peaks in the thermovaporisation products, are quantitatively also significant in the crude oils. Fig. 42 illustrates the relationship of normal alkanes to aromatics: The oil samples show conformably high values (range from 26 to 34). Interestingly, the ratios are several times higher than for the thermovaporisation products (Fig. 38).

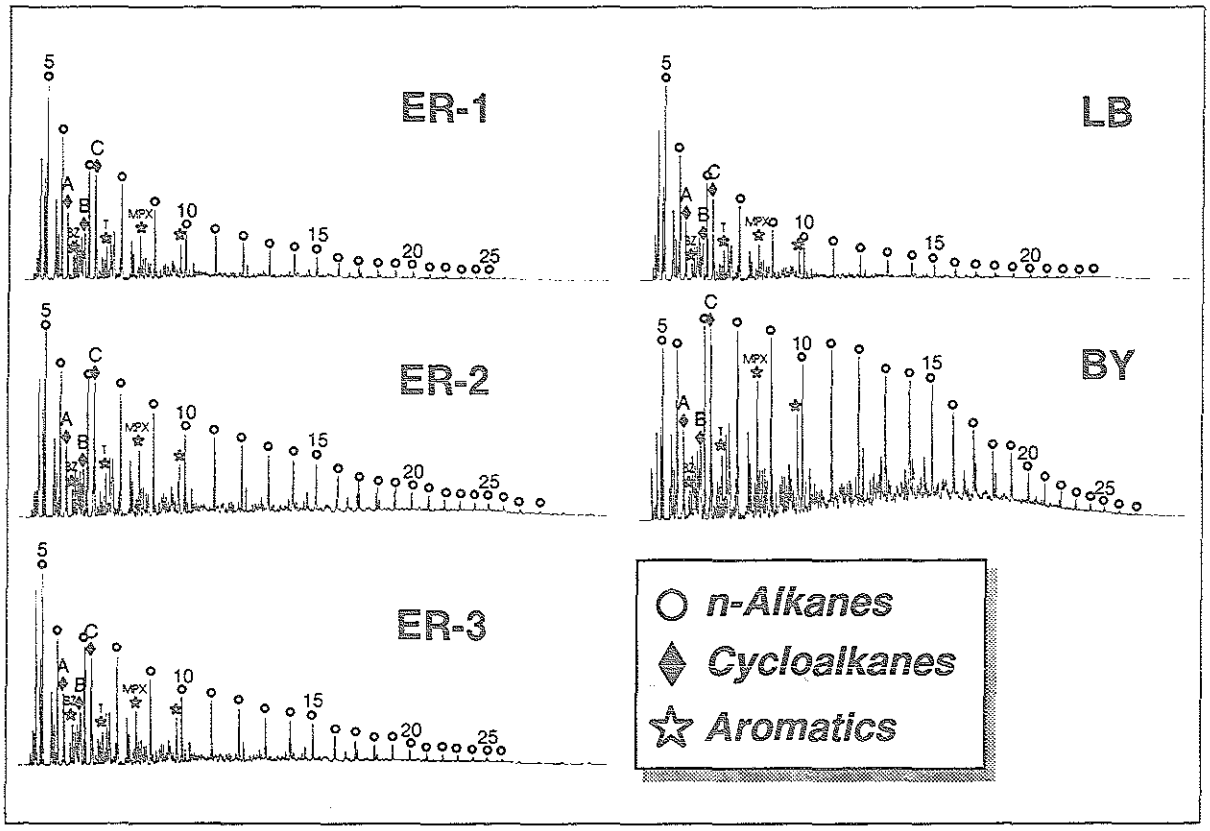

Fig. 41: Composition of Bakken crude oil light ends as deduced from whole oil t'vap-gc analysis. BZ, T, MPX and TMB refers to benzene, toluene, meta-/paraxylene and 1,2,3,4-tetramethylbenzene, respectively. Cycloalkanes are identified as methylcyclopentane (A), dimethylcyclopentane (B) and methylcyclohexane (C).

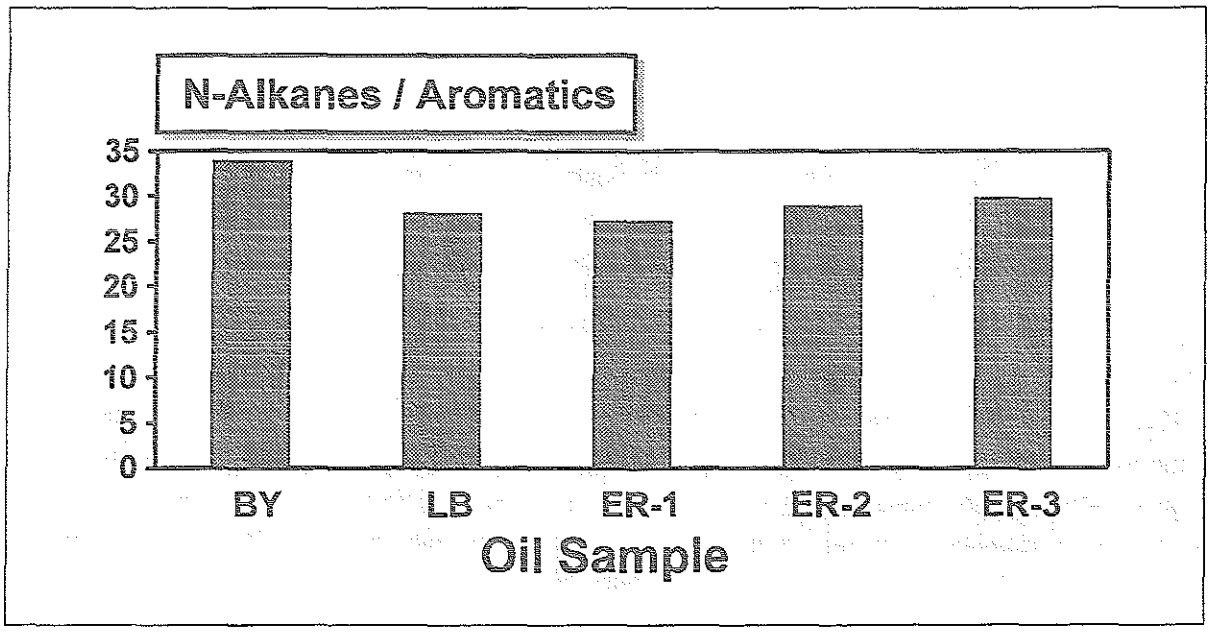

Fig. 42: Bulk composition of Bakken crude oil light ends based on the relationship of n-alkanes (C_{1+}) to aromatics (t'vap-gc analysis). 'Aromatics' include alkylbenzenes (benzene, toluene, ethylbenzene, meta-/paraxylene, orthoxylene and C_3-benzene).

1,2,3,4-tetramethylbenzene, which was a prominent peak in the residues (py-gc) as well as in the thermally releasable products (t'vap-gc) appears to be absent in the crude oils.

4.7 Artificial Maturation of Bakken Shale

Artificial maturation of Bakken Shale samples was performed using two different approaches/experimental configurations. In the MSSV approach (ch. 4.7.1), powdered rock samples were heated in a closed system under varying conditions (temperature, duration of heating). Both products and residual kerogen were analysed by t'vap-gc and py-gc, respectively and compositional changes monitored as a function of progressive artificial maturation.
In a second approach (ch. 4.7.2), an uncrushed whole core Bakken Shale sample was submitted to simulated lithostatic conditions (pressure and temperature) in order to investigate the effects of these parameters on bulk compositional properties of the whole rock.

Table 11: Bulk compositional data derived from closed-system artificial maturation (MSSV) of immature Bakken Shale equivalents (sample aliquots from well labeled 'MSSV' in Fig. 6). RT refers to unheated sample.

°C/days	C_{1+} total (mg/g TOC)	C_1-C_5	C_{6+} total	C_{6-14} total	C_{15+} total
Products					
RT	49.6	2.3	47.3	8.9	38.4
300/2	77.8	4.7	73.1	14.9	58.2
300/5	82.9	7.5	75.4	23.5	51.9
330/1	139.1	10.7	128.3	33.4	94.9
330/2	152.5	13.3	139.1	40.5	98.6
330/5	225.8	32.7	193.0	81.6	111.4
350/1	163.2	17.6	145.5	52.7	92.8
350/2	172.8	29.3	143.5	70.5	73.0
350/5	291.8	58.1	233.7	123.5	110.2
Residues					
RT	453.4	75.7	377.6	127.7	249.9
300/2	380.3	68.2	312.2	108.7	203.5
300/5	326.8	62.8	263.9	93.4	170.5
330/1	244.9	49.7	195.2	68.3	126.9
330/2	255.2	53.2	202.0	72.1	129.9
330/5	158.5	41.3	117.2	44.4	72.8
350/1	232.9	52.3	180.6	67.7	112.9
350/2	158.6	40.6	118.0	45.3	72.7
350/5	75.4	24.0	51.4	18.7	32.7

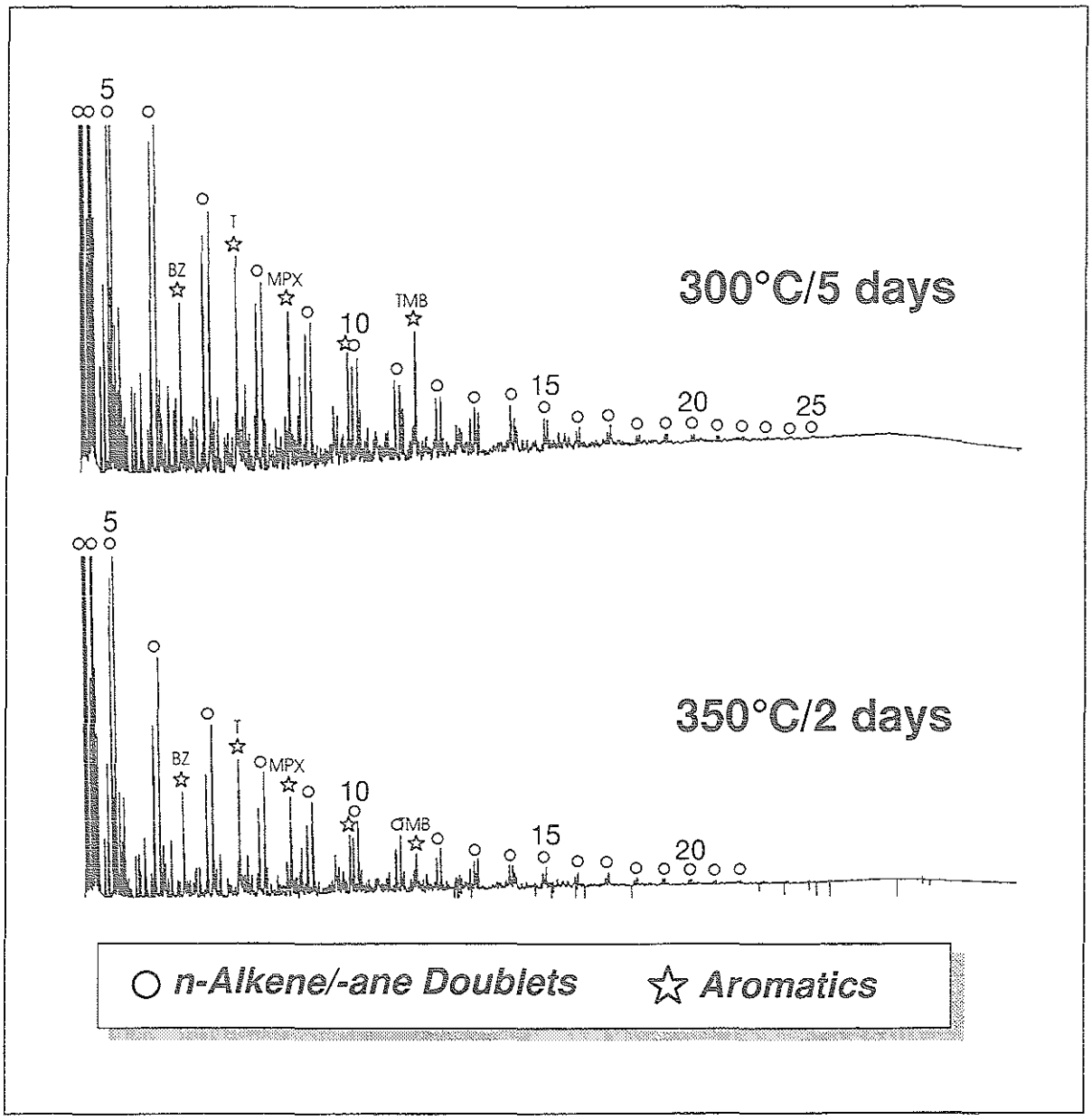

Fig. 43: Py-gc traces of *residues* derived from artificial maturation of (MSSV pyrolysis) of immature Bakken Shale equivalents (0.48% R_o; Ropertz, 1994) for mild (300°C/5 days) and severe (350°C/2 days) heating conditions. Numbers indicate total numbers of carbon atoms. BZ, T, MPX and TMB refers to benzene, toluene, meta-/paraxylene and 1,2,3,4-tetramethylbenzene, respectively.

4.7.1 Pyrolysis (MSSV Approach)

Evolution of Residual Kerogen

The fingerprints of the residue pyrolysates derived from artificial maturation (MSSV) of immature Bakken Shale equivalents, as displayed in Fig. 43, are compositionally very similar to

the pyrolysates of the natural sequence: N-alkene/n-alkane doublets of short to medium chain-length (up to max. 24 carbon atoms) dominate the GC-trace.

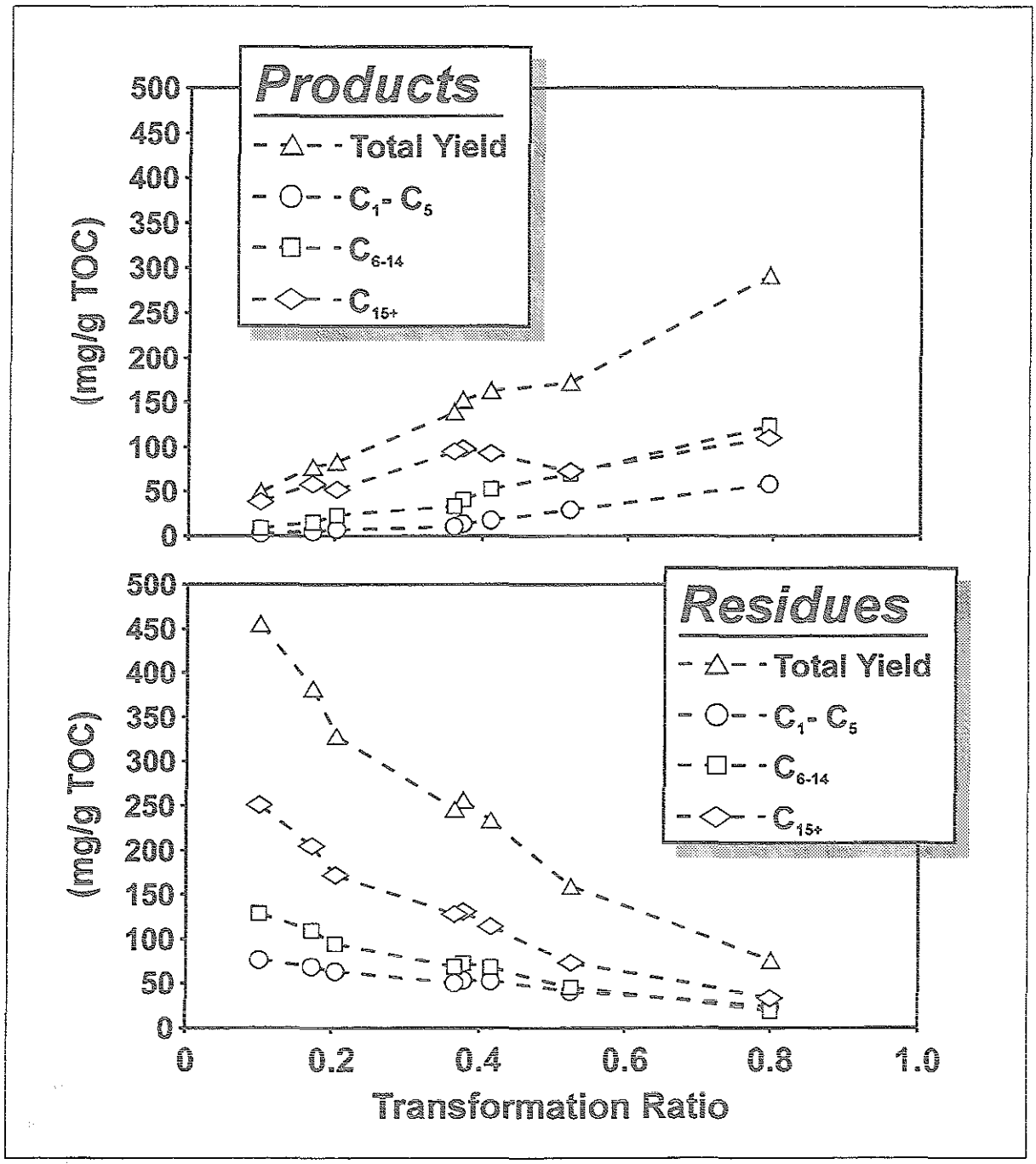

Fig. 44: Compositional evolution of the artificial maturity sequence (MSSV) for *products* (top) and *residues* (bottom) in bulk quantitative terms. The degree of conversion, expressed as tranformation ratio, is calculated by dividing the amount of products by the sum of products and residues.

Furthermore, a series of alkylbenzenes (benzene, toluene, ethylbenzene, meta-/paraxylene and orthoxylene) are very prominent, too. These compounds are also very abundant in the naturally matured Bakken kerogens (ch. 4.4) and have been reported for other kerogen pyrolysates as well (Larter & Douglas, 1980; van Graas et al., 1981; Solli & Leplat, 1986). The compound 1,2,3,4-

tetramethylbenzene represents one of the most abundant aromatic hydrocarbons in the pyrolysates. The origin and significance of this peculiar compound has already been referred to while laying out the results on composition of kerogens and thermally releasable light ends of Bakken organic matter (ch. 4.4 and 4.6).

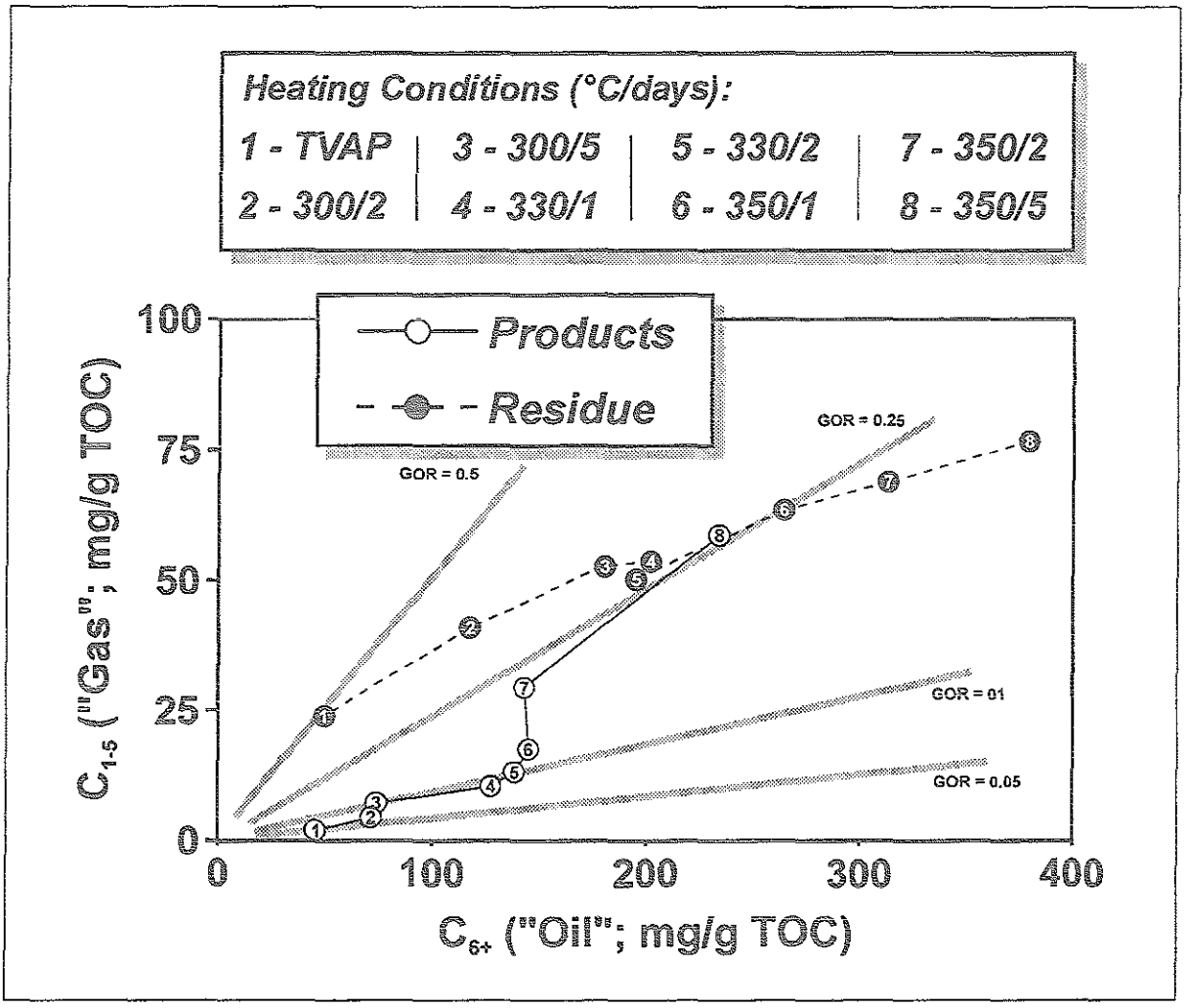

Fig. 45: Relationship of gaseous (C_{1-5}) to oil-like (C_{6+}) compounds of the artificial maturity sequence (MSSV) for *products* and *residues*.

Fig. 44 sheds some light on the compositional evolution of the artificial maturity sequence in quantitative terms. The corresponding data are listed in Tab. 11. The absolute yield of all detected products decreases with increasing maturation level, indicating that the reactive portion of the kerogen (Cooles et al., 1986) is relatively diminished, as thermal alteration proceeds. At the final stage (80% transformation) only ca 10% of the organic matter (normalized to TOC) is amenable to py-gc. Such evolutionary trends have also been reported for the artificially matured (MSSV) marine type II Posidonia Shale kerogen (Horsfield & Dueppenbecker, 1991). With respect to the boiling ranges (C_1-C_5, C_{6-14} and C_{15+}) it is apparent that their trends trace the pattern of the total yield, although the slope of the curve becomes flatter with decreasing molecular weight. Indeed, the yield for gaseous compounds (C_1-C_5) appears to remain roughly constant. Fig. 45 depicts the bulk composition of MSSV residues in terms of gas to oil ratio. This parameter, which is used to establish the composition of petroleum and its subsequent migration behaviour (phase behaviour)

as a function of pressure and temperature (England & Mackenzie, 1989), outlines an almost linear increase with proceeding conversion, indicating that the amount of gas yielding moieties in the kerogen becomes higher as artificial maturation continues. Such findings are consistent with observations from natural systems, where the gas-generative capacity of a residual kerogen is believed to increase (e.g. Lower Toarcian, Tissot & Welte, 1984). However, the slope of the curve and thence the absolute values for range of GOR of the Bakken system are overall higher than for similar kerogens, which were submitted to the same analytical approach (Düppenbecker & Horsfield, 1990): In that study, corresponding GOR values for the Lower Toarcian Posidonia Shale covered a range from ca. 0.1 to 0.25 (Bakken Shale: 0.2 to 0.45).

Evolution of Products

The two fingerprints (Fig. 46) of products derived from the artificial maturation display compositional features that can also be observed in the naturally generated organic matter (Fig. 34, ch. 4.6): The GC trace resulting from relatively mild heating conditions (300°C/5 days) is characterized by rather high concentrations of short-chain hydrocarbons (C_1-C_5) and high contents of 1,2,3,4-tetramethylbenzene relative to adjacent n-alkanes (C_{11}). The latter feature is interesting, as the thermovaporisation products showed considerably lower concentrations of 1,2,3,4-tetramethylbenzene. A further common feature between natural and artificial products is the presence of cycloalkanes in the latter. Such compounds, namely methylcyclopentane, dimethylcyclopentane and methylcyclohexane were among the most prominent peaks in the t'vap-gc fingerprints. In the MSSV products, they are also present in fair concentrations. The yield of other C_{6+} compounds in the artificially generated products like n-alkanes and alkyl substituted aromatic hydrocarbons is relatively low. The relatively large hump of unresolved components which has been encountered in the products of a similar kerogen (Lower Toarcian Posidonia Shale) at low levels of artificial maturation (Horsfield & Dueppenbecker, 1991) was not observed in the case of the Bakken. In contrast, more severe heating (350°C/2 days) resulted in a distribution pattern with short- and long-chain hydrocarbons and a lower ratio of 1,2,3,4-tetramethylbenzene to n-C_{11}. Also, such heating conditions yielded n-alkanes with distinctly higher carbon numbers (up to 28).

Fig. 44 illustrates that the total yield of products (as well as the individual compound groups) rises continuously to the level of maximum transformation (0.8). Interestingly, the high-molecular-weight fraction (C_{15+}) is characterised by a drop in yield at ca. 50% conversion. This might be interpreted as thermally induced cracking of high-molecular-weight compounds to low-molecular-weight material. Such phenomena have been observed in petroleum reservoirs (Connan et al., 1975). However, in the closed system conditions of the MSSV approach, the decrease in yield of C_{15+} material is not accompanied by an equivalent increase for $C_{1\text{-}5}$ and $C_{6\text{-}14}$ compounds (Fig. 44).

The evolution of the gas to oil relationship (Fig. 45) reveals a significant three-fold outline: At low and high levels of transformation, GOR steadily increases with the relatively flat slope indicating a bias to oil-like (C_{6+}) material. At intermediate stages of transformation, however, the yield of gaseous products drastically increases, while C_{6+} products remain relatively constant. Analogous to the decrease in heavy C_{15+} compounds shown in Fig. 44, this feature may also

illustrate that in this closed system gaseous hydrocarbons are being formed at the expense of high-molecular-weight products.

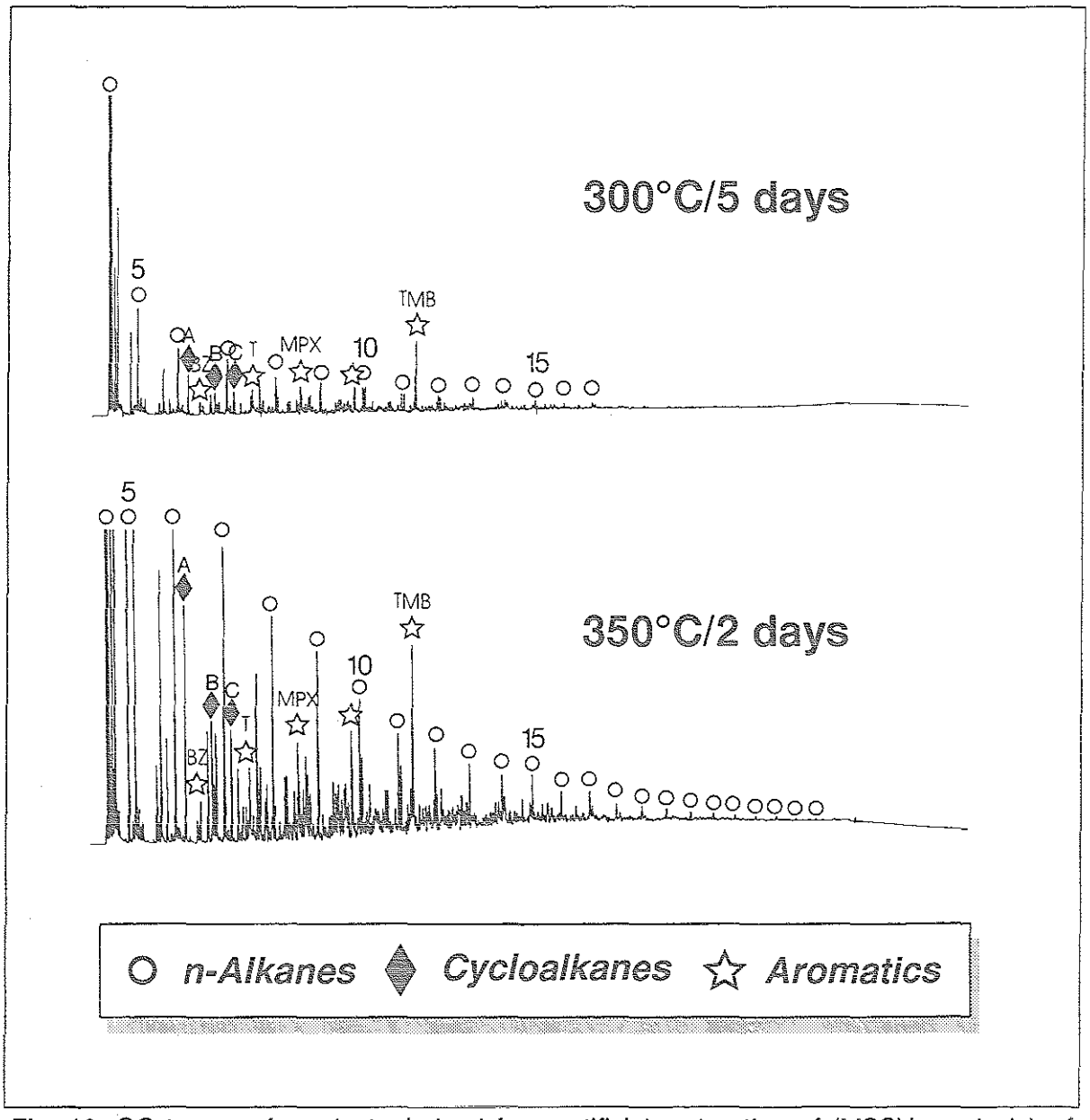

Fig. 46: GC traces of *products* derived from artificial maturation of (MSSV pyrolysis) of immature Bakken Shale equivalents (0.48% R_o; Ropertz, 1994) for mild (300°C/5 days) and severe (350°C/2 days) heating conditions. Numbers indicate total numbers of carbon atoms. BZ, T, MPX and TMB refers to benzene, toluene, meta-/paraxylene and 1,2,3,4-tetramethylbenzene, respectively. Cycloalkanes are identified as methylcyclopentane (A), dimethylcyclopentane (B) and methylcyclohexane (C).

4.7.2 Simulation of Lithostatic Conditions (Pressure and Temperature)

Evolution of Residual Kerogen

The evolution of a Bakken kerogen sample (well SKA, 0.68% R_o) which was submitted to simulated subsurface conditions (elevated temperature and overburden pressure) in terms of basic screening parameters (TOC content, Rock-Eval and vitrinite reflectance) is depicted in Fig. 47. The complete database is given in Tab. 12.
It must be pointed out that the compaction behaviour in terms of volumetric evolution of the rock sample as outlined by the compaction curve can only be assessed qualitatively, as in the course of the experiment parts of the rock sample were forced into the steel frits hence making accurate measurements of compaction based on thickness changes impossible. Nevertheless, the curve clearly shows that, after an initial stage of expansion of the plug due to thermal expansion, the sample reacted to an overburden load (equivalent to 25.5kN) and temperature of 316°C leading to a slow, but steady decrease in thickness relative to the original value.

Table 12: Bulk characterisation (maturity, hydrocarbon generation potential) of artificial maturity sequence deduced from experiments under simulated lithostatic conditions. SKA-AM denotes artificially matured sample (unextracted), while SKA-AM-extra refers to the solvent-extracted sample.

Sample	TOC (wt.-%)	S2 (mg/g rock)	T_{max} (°C)	HI (mg/g TOC)
SKA	13.3	42.02	443	322
SKA-AM	8.57	22.45	441	267
SKA-AM-extra	7.79	17.62	442	267

Changes in screening parameters from the preexperiment to the postexperiment stage (measured on solvent extracted samples) elucidate that the kerogen was altered: Organic richness decreased by ca 40% from 13.3 to 7.8wt.-%. The hydrocarbon generation potential (Hydrogen Index HI) was reduced from 322mg/g TOC to 226mg/g TOC. The latter value falls within the HI range for very mature Bakken Shale samples (0.9% to 1.0% R_o) of the natural maturity sequence (Tab. B, Appendix). Surprisingly, the value for T_{max} remained roughly constant. With respect to the relative distribution of T_{max} values for the entire sample set (Fig. 14, ch. 4.1) it becomes evident that only very immature samples are sensitive to T_{max}. From 0.7 R_o on, T_{max} remains virtually constant, although thermal alteration in terms of kerogen conversion (decrease in HI) still occurs. Hence, the invariance in T_{max} can be considered insignificant, especially, as R_o measurement clearly indicates a rise in maturity level from 0.69% to 1.18%. Accordingly, if these values are correlated with data on the natural Bakken system, the artificially matured sample seems to have entered the high mature stage (equivalent to maturity zone > 0.9% R_o).

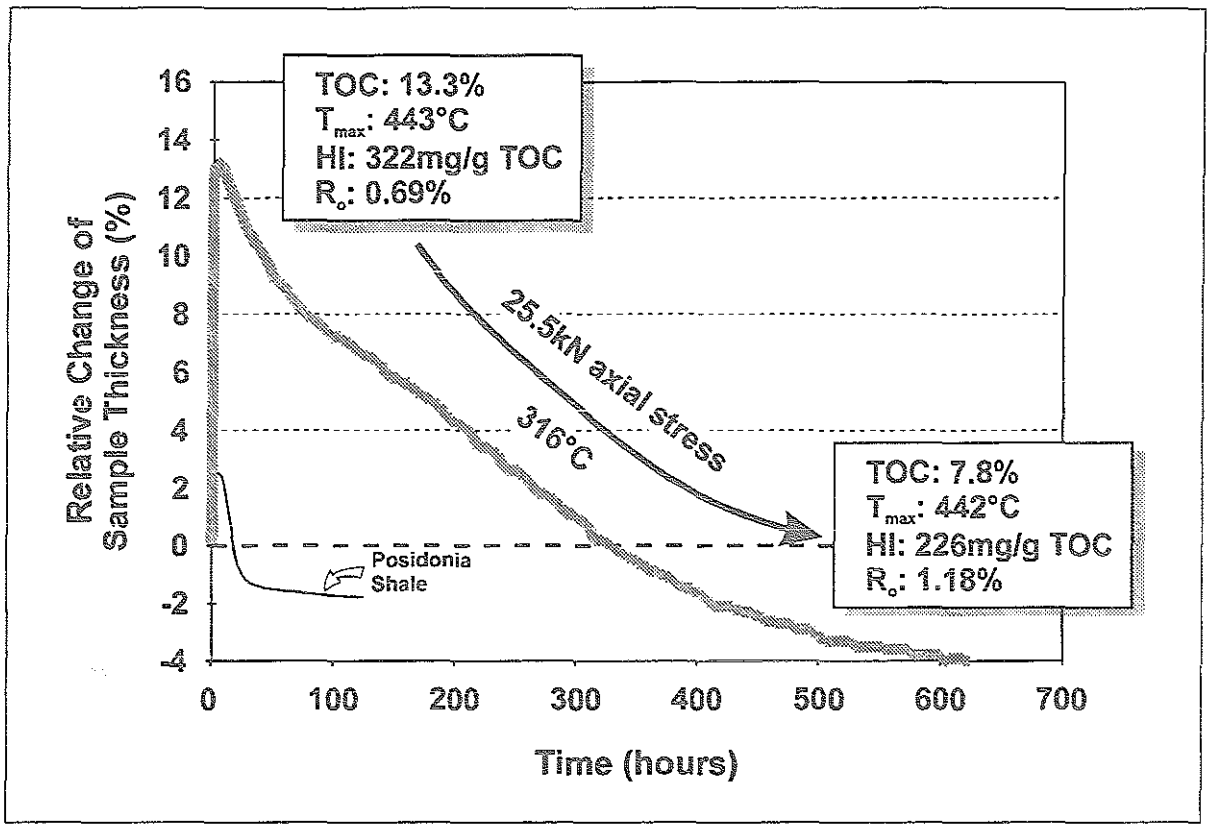

Fig. 47: Evolution of Bakken Shale kerogen during artificial maturation under constant lithostatic stress and temperature (experimental conditions according to Hanebeck et al. (1993)). The relative change in sample thickness as outlined by the curve should be evaluated in a semiquantitative manner (see text for explanation). Changes in organic richness, maturity and hydrocarbon generation potential during the experiment are monitored by measuring the corresponding parameters (TOC, T_{max}, R_o and HI) before and after completion of the experiment. Corresponding compaction curve for Posidonia Shale superimposed from Hanebeck et al. (1993).

Evolution of Products

The experimental set-up used for the simulation of lithostatic conditions was not designed to collect all artificially generated products quantitatively. However, after the experiment was finished, one side of the pressure cell was opened to atmospheric pressure. This step led to a release of gaseous as well as highly viscous, liquid products from the system. The liquid products were collected and set to evaporate at ambient temperature. Furthermore, the steel frits of the pressure cell were immersed in a glass beaker filled with dichloromethane. After 24 hours, excess solvent was evaporated and the bitumen-like residue was collected. In order to provide a rapid characterisation of this highly viscous material, it was submitted to py-gc analysis using the same configuration as for Bakken Shale kerogens (ch. 3.3.1).

The results derived from py-gc of products (collected directly from the cell system ("cell") and by solvent extraction of the frits ("frits")) are presented in Fig. 48. For reasons of comparison, pyrograms of whole extracts from Bakken samples of the natural maturity series are given as well (Fig. 49). The "cell" products are characterized by a high proportion of gas-yielding moieties, while medium to long-chain compounds appear to be almost absent. N-alkene/n-alkane doublets

are hardly visible. Alkylbenzenes (e.g. benzene, toluene and meta-/paraxylene) are very prominent. In contrast, the fingerprint of the "frits" products is very similar to a pyrogram derived from a typical high mature type-II Bakken kerogen in that there is a predominance of short to medium-chain n-alkyls paralleled by almost equally abundant aromatic hydrocarbons. The relatively high content of aromatics relative to the n-alkyl hydrocarbons, however, argues against an enhanced level of thermal alteration, as such a feature was associated with low-mature macromolecular organic matter (kerogens) of the Bakken Shale (ch. 4.4). Indeed, the general appearance of the "frits" pyrogram is very close to the fingerprint derived from py-gc analysis of the low-mature extract from well SKA (0.68% R_o).

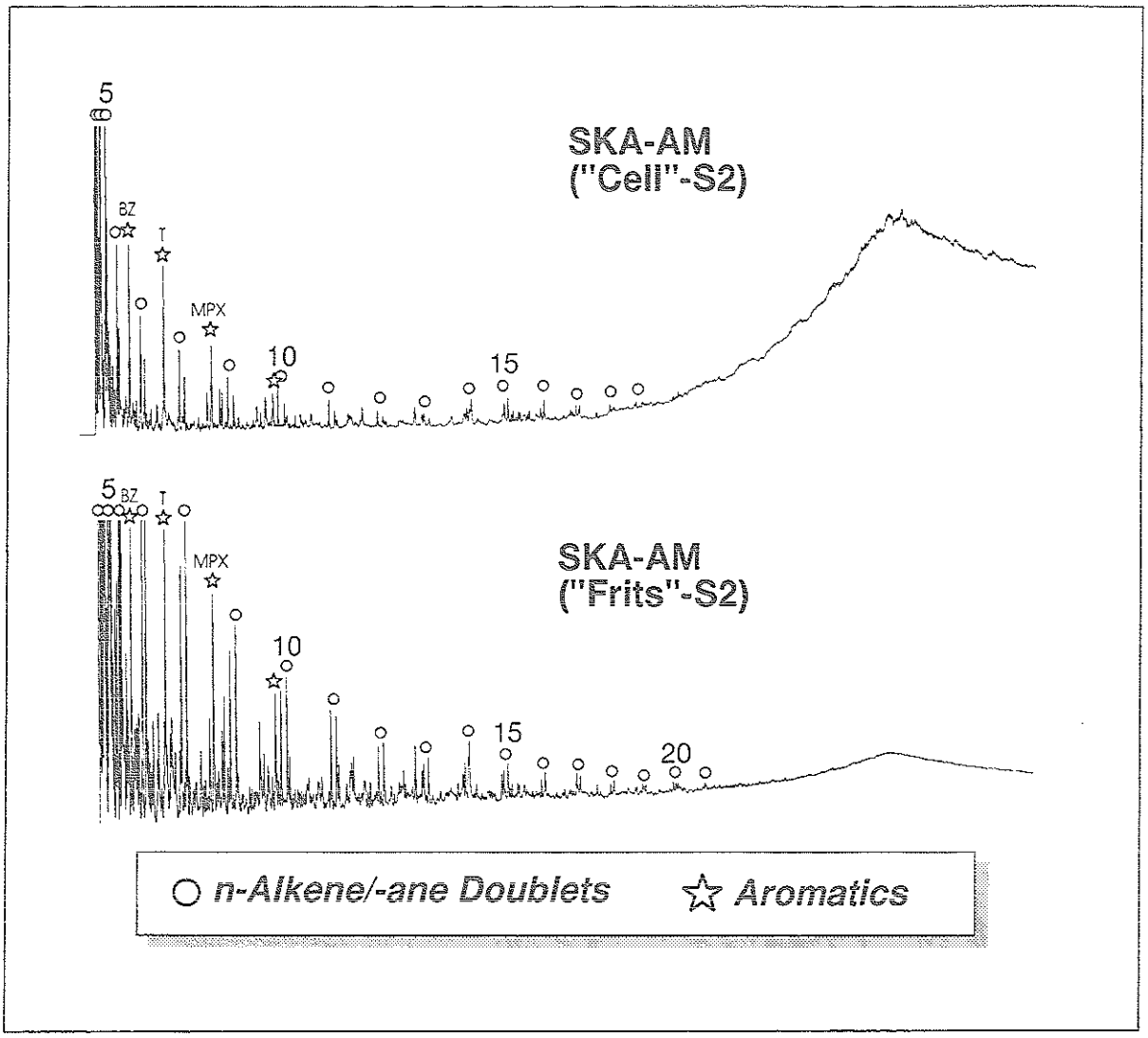

Fig. 48: Fingerprints of pyrolysates as determined by py-gc of the macromolecular matter of products obtained from artificial maturation under constant lithostatic stress and temperature. "Cell" and "Frits" designate organic matter collected directly from the pressure cell system and by solvent extraction of the steel frits, respectively. N-alkyl-doublets are indicated by circles. BZ, T, and MPX refers to benzene, toluene and meta-/paraxylene, respectively.

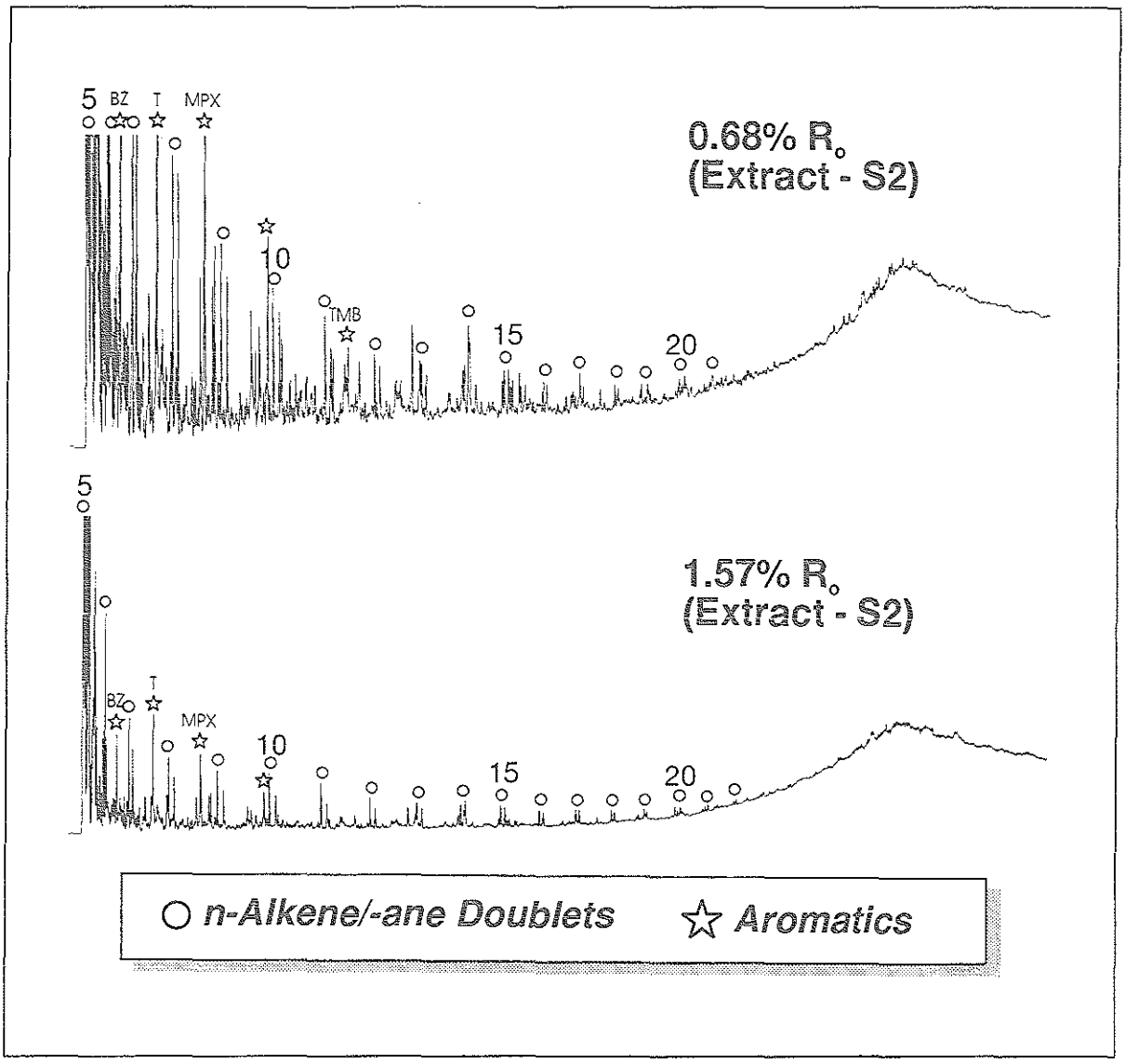

Fig. 49: Two pyrograms as representative for two different levels of thermal evolution (0.68% and 1.57% R_o) were derived from py-gc of whole extracts of samples from the natural maturity sequence. N-alkyl-doublets are indicated by circles, peaks of aromatic compounds by stars. BZ, T, and MPX refers to benzene, toluene and meta-/paraxylene, respectively.

4.8 Permeability

The results derived from permeability measurements using water as the flow through medium (0.95cP viscosity) are compiled in Tab. 13. The datasheets including all parameters which were relevant for calculating permeability are shown in the appendix. Generally, the Bakken shows a very poor permeability (nD range) if measured perpendicular to the bedding plane. All samples

taken from low-mature wells (SKA, 0.68% R_o and TEX, 0.66% R_o) exhibit detectable permeabilities, even perpendicular to the bedding plane. The permeability of one sample of well SKA is highly susceptible to confining pressure.
One mature sample (3185.4m depth) from well FED (0.99% R_o) was measured parallel to the bedding plane and shows a distinct permeability, which is affected by confining pressure.
In contrast, the second sample from well FED (3187.1m depth) appeared to be virtually impermeable after the first run. Further threefold analysis of the same plug revealed an interesting phenomenon: After the direction of the fluid gradient had been reversed, permeability appeared to be ten times higher than before implying that the Bakken Shale has an anisotropic behaviour with respect to fluid transport. Such an inferred "valve effect", however, is difficult to explain in terms of configuration of mineral grains that open up only in one direction but are closed in the other direction. It is more likely that the rheologic behaviour of the rock plug was altered during the first experiment in that preexisting pathways may have been mechanically widened by pressing through water. Moreover, the width of such pathways may also be a result of the flow-through medium dissolving parts of the mineral matrix (e.g. carbonates).

Table 13: Results derived from permeability measurements using water as the flow-through medium. 'pp' refers to perpendicular, 'pl' to parallel plug orientation. Well numbers refer to location of sampled wells in Fig. 6.

Well #	Well name	R_o (%)	Depth (m)	Shale unit	Orient. of plug	Range of permeability (nanoDarcy)	Remarks
*	TEX	0.66	3116.4	lBK	pp	10's	
4	SKA	0.68	2702.9	uBK	pp	10's - 1000's	var. confin. press.
4	SKA	0.68	2705.9	uBK	pp	10's	
4	SKA	0.68	2706.3	uBK	pp	10's	
*	XYZ	0.89	3137.4	uBK	pp	10's	
11	FED	0.99	3185.4	uBK	pl	10's - 100's	var. confin. press.
11	FED	0.99	3187.1	uBK	pp	0 - 100's	

The overall low values for permeability (nanoDarcy range) suggest that the degree of fracturing encountered in the samples, if existent, is not very advanced. If microfractures indeed are a feature of the Bakken Shale (Murray, 1968; Finch, 1969; Meissner, 1978) and they were present in the rock samples submitted here to permeability measurement, then it appears that they are not very efficient for fluid transport perpendicular to the bedding plane.

Normally, the determination of permeability is an important tool to establish migration pathways and, most importantly, to evaluate the quality of a reservoir rock. Hence, corresponding studies focussed mainly on relatively coarse-grained, mostly clastic sediments (e.g. Archer, 1990; Daws & Prosser, 1992).
Determining the permeability of tight, fine-grained source rocks using a triaxial cell which allows the investigation of permeability as a function of confining pressure and fluid pressure is a rather novel method. Thus, equivalent published data are very scarce. In the present contribution, this approach was used in order to seek evidence of the occurrence of fractures in the Bakken Shale.

Clearly, the fact that only a very small number of samples (7 samples from 4 wells) was available for analysis has two major implications as regards interpretation of the data: Firstly, despite the very uniform lithology of the Bakken Shale as elucidated by the present study (ch. 4.4) and related publications (e.g. Webster, 1984), the database is too thin and extrapolation of results on a basin-wide scale is not justified. Secondly, if macrofractures are the dominant fracture type of the Bakken Shale in the subsurface (see discussion of literature data below), it is highly unlikely that such a fracture is "captured" in one of the rock plugs which are submitted to permeability measurements.

Complimentary to the statistical problem, the lithologic/rheologic characteristics of a given Bakken Shale sample may be altered in the course of sample preparation and during analysis. Below, an attempt has been made to address these potential "pitfalls":

- The process of drilling and coring during borehole development, furthermore storage and transportation may induce fracturing (Kulander et al., 1990).
- Drilling, cutting and sawing during preparation of rock plugs for the experiments (ch. 3.3.2) also induces mechanical stress to the sample which may create cracks and fissures. Although the plugs are visually examined prior to mounting them into the triaxial cell, the presence of such voids cannot be excluded.
- Multiple analysis of the same sample (see below) confirmed the poor reproducibility of the analytical set-up.
- Raising of confining pressure may lead to rupture of the rock plug, if very brittle.
- If the sample is not perfectly sealed between the steel frits and the two-layered sleeve, the flow-through medium (water) might "bypass" the plug thence indicating an enhanced (but false) permeability.
- Additional to the uncertainties caused by sample preparation and experimental set-up, the presence of one or more mobile phases (water, oil, gas) in the pore space impedes or enhances transport rates depending on the type of fluid which is used as the flow through medium (Hedberg, 1980; Chapman, 1982). In order to address this issue, the degree of fluid saturation has to be assessed.

  In that context it must be pointed out that the application of a hydrocarbon phase (crude oil or individual compound) as the flow-through medium would even broaden the spectrum of uncertainties: For instance, the combination of excess amounts of low-molecular weight hydrocarbons of a given flow-through medium with a crude oil-like hydrocarbon mixture in the rock would lead to the precipitation of asphaltenes which may reduce permeability (England et al., 1987). On a similar note, the flow-through medium may react with the fluid phase in the rock in terms of dissolution/solution (Price, 1989).

In the light of the above statements, the results of the Bakken Shale analysis (Tab. 13) can only be regarded as a semiquantitative indication of permeability.

4.9 Mineralogy

The results deduced from XRD analyses were used to qualitatively evaluate the mineralogic composition of the Bakken Shale. The bulk rock analyses reveal that all samples are very similar in mineral composition regardless of maturity level of the associated organic matter. Major proportions of the mineral matrix consist of quartz, the second most abundant mineral appears to be illite. Further minerals are in very low concentration.

As regards the clay fraction (<0.5µm) no significant differences could be observed with respect to increasing maturity. A distinctive feature which each spectrum exhibits is a large hump due to high contribution of kerogen which was not removed sufficiently. The major mineral is quartz with less amounts of illite. However, the poor orientation resulting in weak diffraction peaks invalidates an unequivocal evaluation of the clay fraction. Accordingly, the poor quality of the peaks might be due to poor orientation or due to specific illite/smectite structures.

It has to be pointed out that it is crucial to improve sample preparation (i.e. sufficient removal of organic matter) in order to obtain results of better quality. The following sample preparation steps are recommended (J. Francú, written communication):

1. Shorter and coarser grinding of the rock samples to prevent powdering of quartz down to the very fine clay fraction.
2. Application of freeze-drying method to disaggregate the clay minerals (freezing using liquid nitrogen and subsequent removal of water under vacuum).
3. Soft grinding with a rubber stopper in order to obtain fine powder.
4. Thorough removal of organic matter by applying electronic low-temperature ashing (Gluskotter, 1965).
5. For purification purposes, steps 2.-3. are to be repeated at least twice.
6. Dispersing of powder in Na-acetate/acetic acid to remove carbonates and then in distilled and deionized water using ultrasonic probe.
7. Separation of fraction of < 0.2 (0.5)µm using ultracentrifugation.
8. Saturation of the clay with Ca, washing, saturation with glycol. After mounting oriented samples on slides, samples are ready for XRD analyses.

The accurate assessment of abundance and type of clay minerals in a sediment can be important with respect to pressure build-up by the thermal expansion of aqueous fluids. This phenomenon which occurs preferably in rapidly subsiding basins with high sedimentation rates has been called upon to create overpressured zones ("aquathermal pressuring" by Barker, 1972). Such a mechanism requires the isolation of a sediment unit containing water at an early stage of deposition. As burial continues, the pore fluid is submitted to rising temperatures and expands. Therefore it has to be evaluated whether aqueous fluids in the Bakken Shale may be provided by clay mineral interlayer water which could be the crucial agent for overpressuring: Diagenetical smectite dehydration (Bruce, 1984) can result in the release of water from clay minerals. During the alteration of montmorillonite (smectite) to illite, interlayer water is released and becomes free pore water (Powers, 1967). Quantitative meaningful evidence on clay mineralogy of the Bakken Shale, however, is still a subject of uncertainty. Webster (1984) admitted this uncertainty although he carried out XRD analyses. Cramer (1991) was the only one who provided quantitative data on mineralogy of the Bakken Shale. According to these results which were

derived from XRD analysis of two wells from Billings Anticline area, clays make up 28 and 31% of the mineral matrix of the shale units. Unfortunately, he didn't give any details on pretreatment of samples and analytical conditions during XRD. Yet, equivalent analyses performed on samples of the present study revealed that data quality highly depends on appropriate sample pretreatment in order to make unequivocal statements on clay content. This is mainly due to the high proportion of kerogen in the samples. Accordingly, a thorough and elaborate sample preparation program as laid out above involving various steps is required in order to provide results of better quality. Therefore, published quantitative data on clay concentration in the Bakken Shale ought to be judged very carefully, if no detailed information is given on sample preparation and analysis. Thus, it cannot be assessed precisely, if and how much interlayer water may have been released during clay mineral (smectite) diagenesis of the Bakken Shale.

While the presence of water in the pore space of the Bakken Shale as a result of inferred smectite dehydration could only be addressed by a very elaborate and time-consuming analytical effort, related production data from operators in the Bakken play (Hansen, 1991) and from Conoco Inc. provide strong evidence that water is absent in the Bakken petroleum system or produced only in negligible amounts. Hence, hydrocarbons appear to be the only mobile phase in the Bakken Shale in the subsurface.

5 Discussion and Interpretation

5.1 Petroleum Generation

5.1.1 Zonation of Hydrocarbon Formation

In the classical oil window concept, the main stage of liquid hydrocarbon generation is associated with the vitrinite reflectance interval from ca. 0.5% to 1.3% R_o for typical marine source rocks (Tissot & Welte, 1984). Hence, if the generated products do not leave the source rock system, then this particular maturity interval should be characterized by increasing concentrations of mobile organic matter, either thermally releasable (Rock-Eval S1) or solvent extractable (bitumen). In the case of the Bakken Shale, Fig. 15 provides no evidence for an increasing build-up of petroleum in the source rock system. Rather, yields decrease beyond 0.6% R_o or remain roughly constant. For individual wells/samples at 0.9% (MAR) and 0.92% R_o (JEN), however, bitumen contents can rise to very high levels (Fig. 23). This discrepancy for whole extract yields is paralleled by the respective extract fractions (SAT, ARO and RES; Fig. 25). Hence, based on yields of mobile organic matter, the peak of hydrocarbon formation in the Bakken Shale might be assigned to the maturity level 0.9/0.92% R_o. However, due to its mobilisable nature, the concentration of a hydrocarbon phase clearly is not only a function of the generation rate, but can be significantly affected by migration and/or mixing effects with another petroleum phase that enters the source rock system. At a later stage of thermal evolution, the cracking of oil to gas is introduced as a further process (Vassoevich et al., 1970). The extent of expulsion/migration processes in the Bakken Shale will be investigated in ch. 5.2.

In the context of zonation based on vitrinite reflectance, it has to be addressed that the absolute values for vitrinite reflectance determined for strata in the Williston Basin older than early Jurassic (including the Bakken Formation) have been shown to be significantly suppressed (Price et al., 1984). According to these authors, R_o values in the Bakken Shale are suppressed by ca. 0.5-0.6% R_o over the entire maturity range. Hence, by using the inferred unsuppressed "real" values, most of the Bakken Shale in the North Dakota portion would be referred as being beyond the main phase of petroleum generation according to the oil window scheme.
The phenomenon of suppression of vitrinite reflectance is believed to be due to the presence of hydrogen-rich alginite macerals (Hutton & Cook, 1980). In addition, anomalous enhancements of R_o are also known and are considered to be related to oxic depositional conditions (Wenger & Baker, 1987). With that respect, Fang & Jiangyu (1992) concluded that vitrinite reflectance is greatly affected by facies.
Lo (1993), however, provided some evidence that the amount of R_o suppression in the Bakken Shale as concluded by Price et al. (1984) is too high. The model for correcting suppressed R_o values as developed by Lo (1993) utilizes the Rock-Eval Hydrogen Index of the original immature sample in order to determine the maximum true vitrinite reflectance. Hence, the discrepancy between the supposedly suppressed R_o values and the maximum true vitrinite reflectance increases with increasing hydrocarbon potential (HI) of the original sample. This model was applied to the present sample set (0.24% - 1.1%) using an initial HI of 700mg/g TOC.

If these R_o values are considered to be uniformly suppressed, the corrected maximum true vitrinite reflectance according to Lo (1993) would cover a range from ca. 0.8% to 1.7% R_o. Lo (1993) also reported that suppressed and unsuppressed vitrinite particles can be associated together in the same sample. In the light of this finding, the anomaly in R_o measurement for adjacent wells BEH (1.26%) and MAR (0.9%) might reflect a suppressed (well MAR) and unsuppressed (well BEH) stage of Bakken Shale vitrinites. Interestingly, if the measured R_o for MAR (0.9%) is corrected using the method by Lo (1993), it is shifted to a value of ca. 1.25%. Hence, this particular anomaly of the present sample set might indeed indicate that BEH exhibits the true, unsuppressed vitrinite reflectance whereas the R_o values for all other wells in that area were derived from measurement of suppressed vitrinite particles. Such a scenario would imply that all wells of the Nesson and Billings Anticline area which are considered to be in the mainstage of petroleum generation (Webster, 1984; Price et al, 1984) have true R_o values of 1.0% and higher.

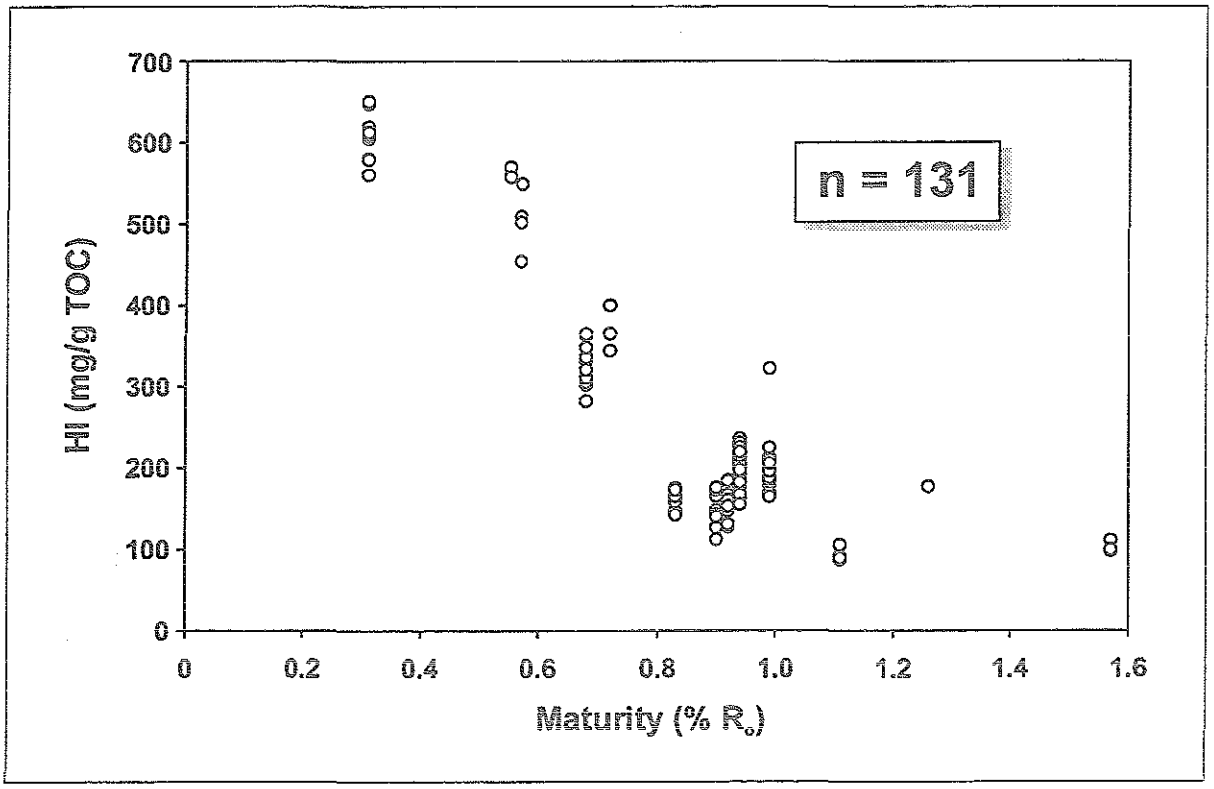

Fig. 50: Evolution of hydrocarbon generation potential (Rock-Eval HI) as a function of proceeding maturation.

Clearly, such a phenomenon bears fundamental implications for petroleum generation and preservation models, in that assessing hydrocarbon generation zones and predicting volumes of generated petroleum on the basis of vitrinite reflectance measurements can be severely misleading (Price & Barker, 1985). Therefore, the vitrinite reflectance data of the present study does not provide an unequivocal measure for maturity. Hence, other criteria have to be evaluated: As generation zonation based on bitumen yields and/or R_o intervals can be potentially misleading, the evolution of the residual kerogen in terms of remaining generation *potential* ought to provide a better and unequivocal insight into petroleum generation. This approach is highly suitable for

the Bakken Shale sample sequence, as strong arguments exist that kerogen quality (type of organic matter) is uniform throughout the basin (ch. 4.1 and 4.4).
Indeed, corresponding Rock-Eval HI data (Fig. 50) delineates a clear decrease from 0.3% to 0.8% R_o which can be attributed to the progressive conversion of kerogen to volatile hydrocarbons. Thus, the onset of petroleum formation in the Bakken Shale appears to occur much earlier than according to the oil window of Tissot & Welte (1984). Also, the trend of HI implies that the principal zone of generation is much narrower, i.e. petroleum formation potential is realized faster. Interestingly, from 0.8% R_o on, the potential of the residual kerogen remains constant despite that R_o still suggests ongoing maturation. Both features, namely early as well as rapid kerogen conversion might as well argue for a very labile organic matter assemblage which requires only a relatively low level of thermal energy to initiate hydrocarbon generation. Kerogen lability and early generation of hydrocarbons will be discussed in ch. 5.1.3.
Based on the results and considerations above it can be stated that the analysed sample suite represents a natural maturation series which incorporates equivalents from all stages of catagenesis.

5.1.2 Quantitative Assessment of Organic Matter Conversion

The combination of a basinwide uniformity in organofacies (ch. 4.4) with a broad spectrum of maturity highly qualifies the Bakken Shale for investigating petroleum generation in quantitative terms as a function of increasing thermal evolution. Variations in hydrocarbon formation potential due to differences in kerogen type (depositional environment) can be considered insignificant.
Cooles et al. (1986) have developed an algebraic scheme which is designed to make quantitative statements on petroleum generation and expulsion in the course of increasing maturation. It is based on Rock-Eval and solvent extract data. These routine geochemical measurements provide useful information on the bulk hydrocarbon generation potential of a given source rock. While the reactive part of the kerogen generates oil and gas at low to moderate maturities (termed "labile" portion) and gas at higher levels of thermal alteration (termed "refractory" portion), it is a key assumption of the model that the concentration of inert kerogen (that portion which is not converted to volatile products due to thermal stress) remains constant during hydrocarbon formation. The model in general and the latter assumption was proven to be applicable to several well-known source rocks, e.g. the Kimmeridge Clay, the Kingak Shale of Alaska and the shale of Lias δ age of the Lower Saxony Basin (Cooles et al., 1986). Still, especially the general validity of the assumption on inert carbon formation has to be carefully considered for the Bakken Shale. For instance, a study on the Cambrian Alum Shale (Horsfield et al., 1992) revealed that, despite an alginite-rich kerogen, predominantly aromatic and branched products are released from the Alum Shale which are - especially under closed system conditions - incorporated into the inert carbon portion of the kerogen, thence increasing its relative concentration in the total kerogen.
In the light of the high abundance of ring structures (cycloalkanes, alkylnaphthalenes) in the thermovaporisation products of the Bakken Shale, this issue will be examined below.

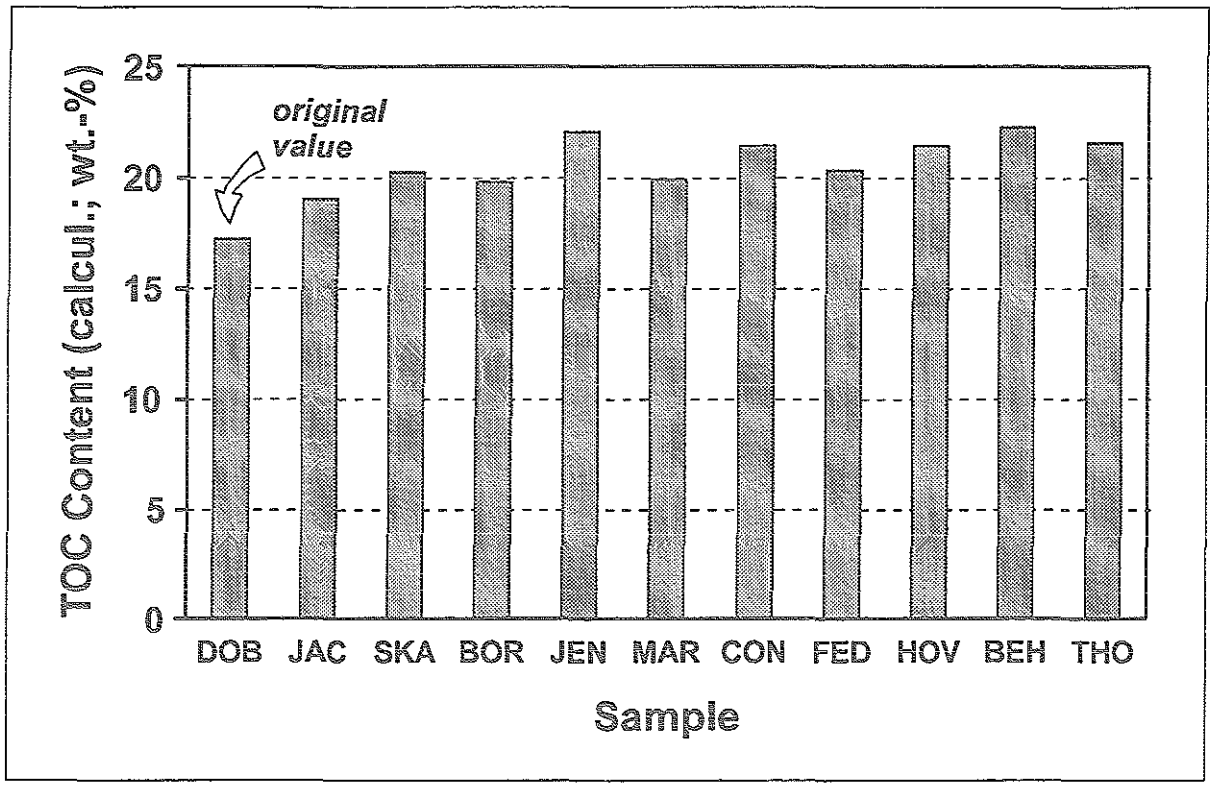

Fig. 51: Calculated *initial* (immature) TOC content for Bakken Shale samples from 10 wells which are in a mature stage at present time. Calculations (average values) are based on the approach by Cooles et al (1986) and refer to well DOB (0.31% R_o).

Fig. 51 depicts the *initial* average TOC content for 10 wells of successively increasing maturity level (% R_o) as calculated using the algebraic scheme proposed by Cooles et al. (1986). For the samples which are at present time in a mature phase of catagenesis, the values represent the samples' organic richness at an immature, *initial* stage of petroleum generation, actually the maturity level of the sample that served as a reference (well DOB). All calculated values range between 19 and 22wt.-% TOC but do not perfectly match the value of the reference sample. This mismatch can be related to the fact that shallow Bakken Shale samples show a high variability for screening parameters (Fig. 12; ch. 4.1). Immature, shallow Bakken Shale cores especially have highly variable TOC contents ranging from ca. 22wt.-% to ca. 3wt.-%. This has also been reported from other studies focussing on organic geochemistry of the Bakken Shale (Webster, 1984; Price et al., 1984). Therefore, it may be quite likely that the samples selected from core DOB for the present study were not representative for the entire core. For more mature, deep cores (e.g. well JEN in Fig. 12; Tab. B, Appendix), the scatter of values is smaller and it is easier to select a representative set of samples. Hence, the average value (17wt.-% TOC) chosen for the immature reference sample (well DOB) may have been too low despite the fact that a relatively high number of values (12) were used to determine the mean value. If the average TOC value for well DOB would have been slightly higher at 19wt.-%, the match of the calculated values for the mature wells would be almost perfect (range from 18 to 20wt.-%; complete data set not shown here). Using a kinetic model for generation and expulsion of petroleum in the Bakken Shale, Sweeney et al. (1992) also calculated initial TOC contents which appear to be slightly lower (up to 18wt.-%) than the values determined in the present study. However, as these authors admitted,

these values might be questionable because of the sensitivity of their model to expulsion-related parameters.

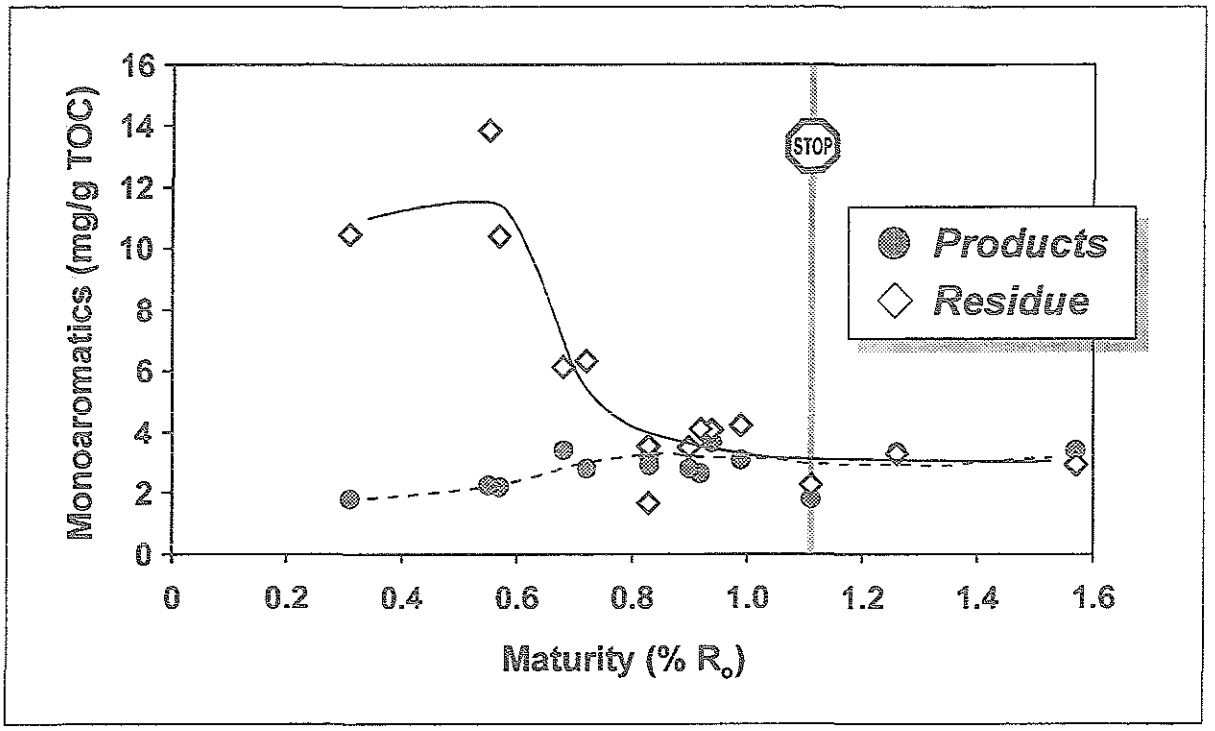

Fig. 52: Relationship of natural products (t'vap-gc) to residual kerogen (py-gc) for aromatic hydrocarbons (average values) as a function of increasing thermal stress. 'Monoaromatics' refers to alkylbenzenes (benzene, toluene, ethylbenzene, meta-/paraxylene, orthoxylene, C_3-benzene and 1,2,3,4-tetramethylbenzene). Curves are drawn according to "eyeball fit". Stop sign indicates end of maturity spectrum as evidenced from other maturity parameters (see ch. 4.1.2).

Two implications arise from these results: Firstly, organic richness was uniformly distributed during deposition of the Bakken Shale in the North Dakota portion of the Williston Basin, serving as a further indicator for uniform organofacies (ch. 4.4). Secondly and most importantly, if more mature samples indeed have distinctively higher (or lower) concentrations of dead carbon than less mature ones, then the *calculation* of *initial* TOC content (Fig. 51) must yield considerably higher (or lower) values than determined for the present sample set.

The arguments as laid out above (decreasing content of organic carbon of the natural maturity sequence, congruence of calculated and measured initial TOC content) allow to conclude that the algebraic mass balancing approach (Cooles et al., 1986) can be applied to the Bakken Shale petroleum system as a tool for evaluating hydrocarbon generation and expulsion. Yet, the fact that calculated initial TOC contents do not perfectly match the TOC values of the natural system, may indicate that mass balancing in the Bakken Shale indeed involves dead carbon formation (5 to ca. 22% overestimation).

Figs. 52 and 53 illustrate the relationship between naturally generated products (t'vap-gc) and the residual kerogen (py-gc) for monoaromatic (alkylbenzenes) and diaromatic (alkylnaphthalenes) hydrocarbons. As regards the residue, both aromatic compound groups exhibit a distinctive decrease in concentration between 0.6% and 0.8% R_o. However, moieties yielding one-ring

aromatic compounds (alkylbenzenes) on pyrolysis are present in higher concentrations than alkylnaphthalene yielding units (ca. 4-fold). The products, in contrast, exhibit a maturity-related evolution which is vice versa: The yield of monoaromatics as well as diaromatics steadily increases as thermal evolution proceeds. The latter appear to be absent below 0.6% R_o. Increasing "aromaticity" of the products paralleled by decreasing "aromaticity" of the residual kerogen as maturation continues, is very surprising. This feature could be a maturation phenomenon and/or related to migration. The likelihood of mixing with an oil that originated from a source other than the Bakken, however, is rather low (Meissner, 1978; Price & LeFever, 1992 and 1994). Therefore, if the observed pattern in the thermovaporisation products is not related to migration, it might be explained by catagenetic formation mechanisms. The precursor-product relationship for aromatic hydrocarbons has been reviewed by Larter & Horsfield (1993). Accordingly, it is believed that the formation of *monoaromatic* alkylbenzene structures typically involves the cleavage of alkyl chains connecting the aromatic ring to the kerogen. For *diaromatic* species, there may be multiple formation mechanisms: For instance, naphthenoaromatic structures like alkylindanes and alkylindenes could have been aromatized in the course of maturation and incorporated into the kerogen as alkylaromatic structures. β cleavage of such structures would result in aromatic products with two or more rings (Van Graas et al., 1980). The diagenetic condensation of unsaturated lipids with unsaturated sites in kerogens has to be considered as well (Larter et al., 1983). Finally, the "artificially" induced aromatization of aliphatic and alicyclic structures during pyrolysis also has to be taken into account, as exemplified by cross-linked algal kerogens (Larter, 1978; Horsfield et al., 1992). Although the Bakken Shale has an organic content (alginite, bituminite, vitrinite precursor material) which is typical for marine source rocks (Tissot & Welte, 1984) it may be plausible that pyrolytically generated diaromatics have contributed to the relatively high yields of alkylnaphthalenes in the thermovaporisation products at $R_o > 0.7\%$ (Fig. 53). This mechanism, however, seems to be less pronounced in case of the monoaromatics (Fig. 52). High concentrations of cycloalkanes in the products (t'vap-gc) especially at low levels of thermal evolution ($< 0.7\%$ R_o) might also be related to condensation processes of originally paraffinic species. Alternatively, cyclic products may be preferentially generated leaving behind a residual kerogen that is enriched in paraffinic hydrocarbons and depleted in aromatics. This unusual product-residue relationship is attributable only to the mature Bakken kerogens (> ca. 0.8% R_o) of the present study. Low mature samples (< ca. 08% R_o) display an analogy which is vice versa, namely overall paraffinic products vs. aromatic residue.

In the context of the present contribution it is relevant that cyclic moieties may be prone to aromatisation and condensation processes and may be incorporated into the inert kerogen portion during natural catagenesis. Condensation reactions of aromatic compounds are known to become increasingly important at higher temperatures (Radke, 1987). Aromatization of paraffins via ring-structured intermediates has also been demonstrated during laboratory experiments involving catalysts (Fogelberg et al., 1967). Consequently, such condensed structures, originally generated from the labile portion of the kerogen, might not be expelled but incorporated into inert carbon. Similar to a disproportionation reaction, a process which is known for both kerogen and crude oil (Connan et al., 1975), bulk aromatization of originally n-alkyl material and condensation may result in the formation of high-molecular-weight macromolecular aromatic sheets (high C/H ratio) which are immobilized and become part of the kerogen structure. The volatile products resulting

from such a disproportionation process could be expected to be enriched in short-chain, low-molecular-weight compounds (low C/H ratio). In the natural system, the aromatization to give a high C/H ratio indeed may also involve the release of a carbon-depleted (CH_4) or carbon-free (H_2) volatile phase (Rullkötter et al., 1988). Although molecular hydrogen is occasionally found as a major component in natural gas (Goebel et al., 1984), this feature does not apply to the Bakken petroleum system.

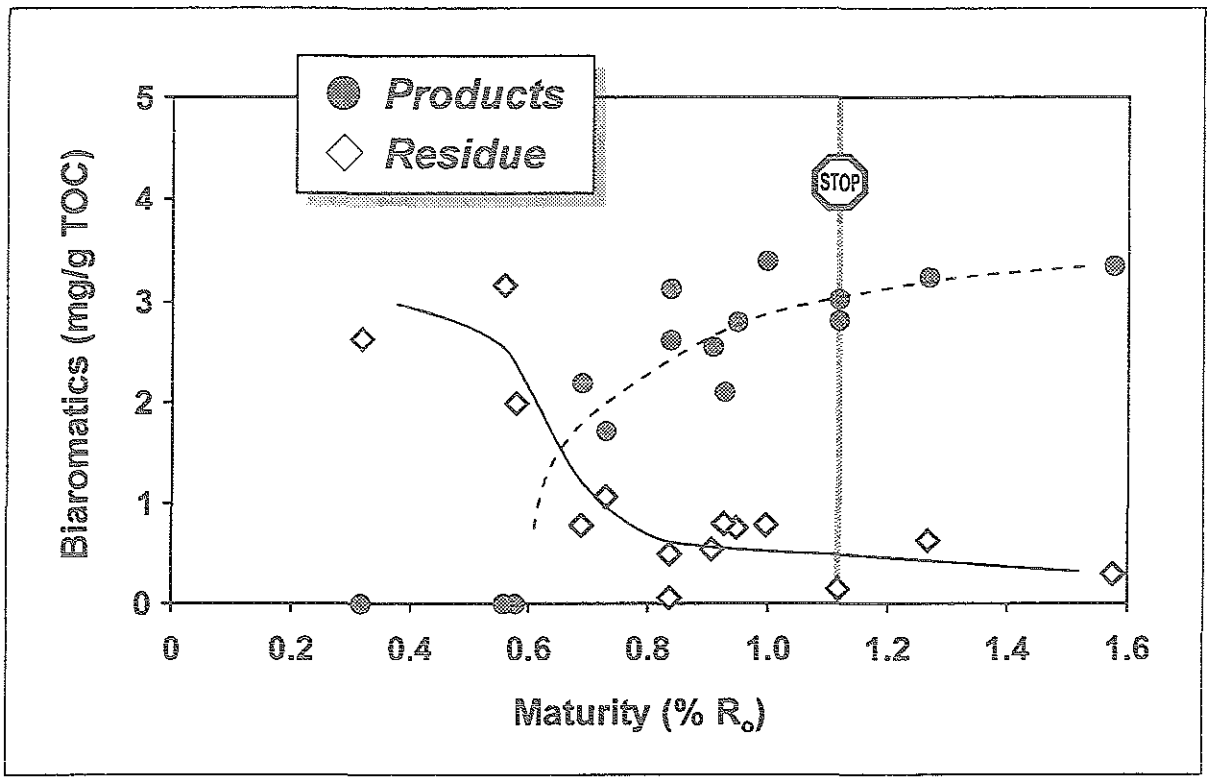

Fig. 53: Relationship of natural products (t'vap-gc) to residual kerogen (py-gc) for aromatic hydrocarbons (average values) as a function of increasing thermal stress. 'Di-aromatics' refers to alkylnaphthalenes (2-methylnaphthalene, 1- methylnaphthalene, dimethylnaphthalenes and trimethylnaphthalenes). Curves are drawn according to "eyeball fit". Stop sign indicates end of maturity spectrum as evidenced from other maturity parameters (see ch. 4.1.2).

If the fate of the Bakken kerogen indeed is associated with cumulative dead carbon formation during organic matter conversion, then the maturity-related evolution of organic richness should reflect this phenomenon, in that TOC content is reduced less than would be anticipated when petroleum is generated from solid organic matter. Fig. 54 addresses this issue: Although the datapoints outline a relatively broad scatter especially at low levels of maturation (< 0.6% R_o), the trend of the average TOC content clearly describes a decrease which is strongest between 0.6% and 0.8% R_o. This R_o interval is associated with enhanced petroleum generation based on the decrease of hydrocarbon generation potential (Rock-Eval HI, Fig. 50). However, all samples beyond 0.8% R_o exhibit uniform average TOC values (ca. 10-11wt.-%), suggesting that kerogen conversion may have come to an end despite continuing maturation up to at least 1.1% R_o (ch. 4.5).

An alternative explanation for the uniformity in TOC values beyond 0.8% R_o would be that TOC content is affected by the high molecular-weight portion of the volatile organic matter (solvent

extractable bitumen) which is still present after sample preparation (evaporation of excess HCl at 100°C) for TOC determination. As Fig. 55 elucidates, reduction in TOC content by solvent extraction is not systematically related to maturity. In other words, the proportion of organic carbon in the extract which is amenable to TOC measurement is principally the same for immature and mature samples. Hence, the inferred constancy in organic richness (TOC) is not due to a heavy oil which is not expelled but remains in-situ.

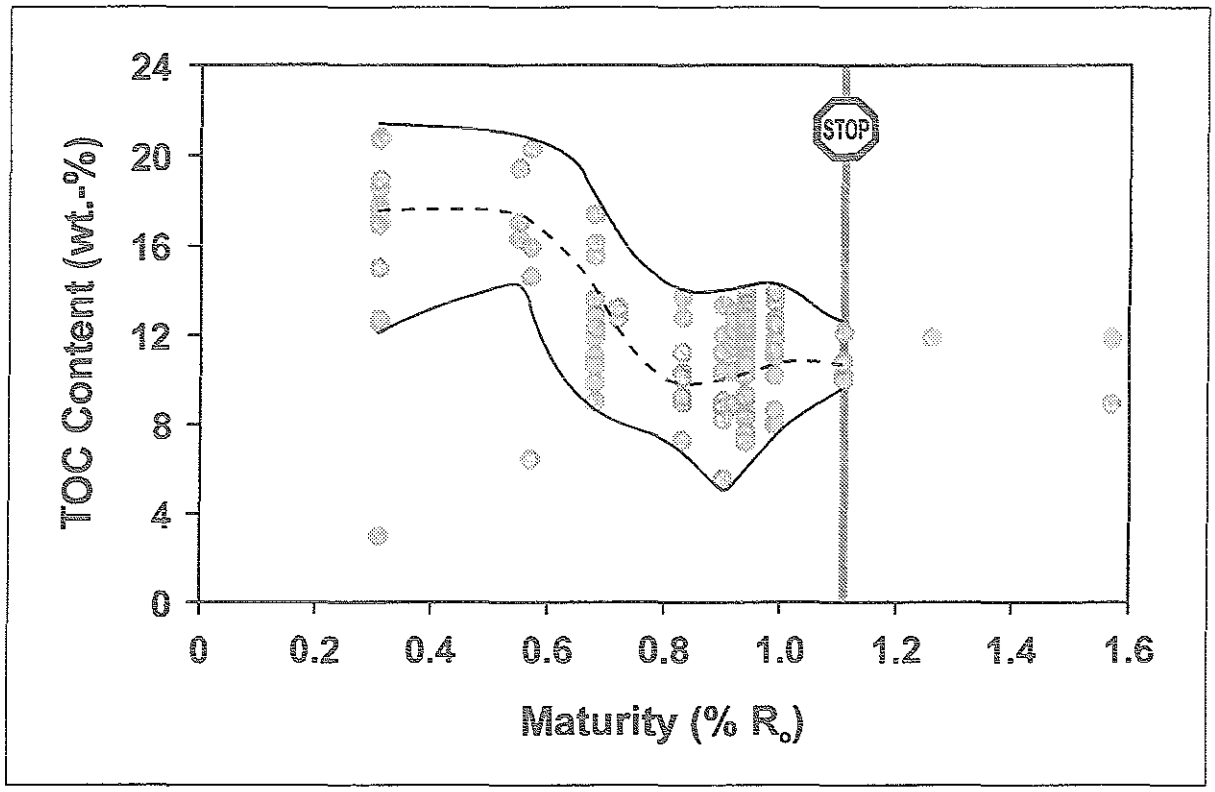

Fig. 54: Evolution of organic richness (TOC content) as a function of maturity for 132 samples from 14 wells. Trend of average TOC indicated by dashed line. Stop sign indicates end of maturity spectrum as evidenced from other maturity parameters (see ch. 4.1.2).

The Petroleum Generation Index (PGI) is an output parameter of the algebraic scheme and indicates the degree of organic matter conversion (Cooles et al., 1986). It divides the amount of generated petroleum (incl. hydrocarbons initially present in the source rock before onset of generation) by the total petroleum potential, the latter including labile and refractory kerogen and initial oil concentration. Accordingly, values range from 0 (no conversion) to 1 (100% conversion). Fig. 56 shows the evolution of PGI as a function of R_o. The curves obtained from calculations on both data sets (Rock-Eval pyrolysis and solvent extract yield) are very close to each other. The interval 0.57% to 0.68% R_o exhibits the most drastic increase in PGI. Beyond 0.7% R_o, only a minor increase can be observed (a step of 0.2 from 0.7% to 0.9% R_o). At maturity levels >0.9% R_o, PGI remains essentially uniform (between 0.8 and 0.9).

The results obtained for the Bakken Shale are similar to other marine type-II source rocks (Kimmeridge Clay, Cooles et al., 1986). High degrees of organic matter conversion within a relatively narrow maturity interval can be associated with enhanced heating rates due to a nearby magmatic intrusion (Rullkötter et al., 1988). The Bakken Shale, however, represents a source

rock system in a slowly subsiding intracratonic basin which appears to be unaffected by enhanced heat flow in the course of its history. Present day heat flow for the Williston Basin lies at ca. 55 mW/m^2 (Sweeney et al., 1992) and, most importantly, kinetic modelling provided evidence that the heat flow was spatially and temporally constant for at least the last 100Ma.

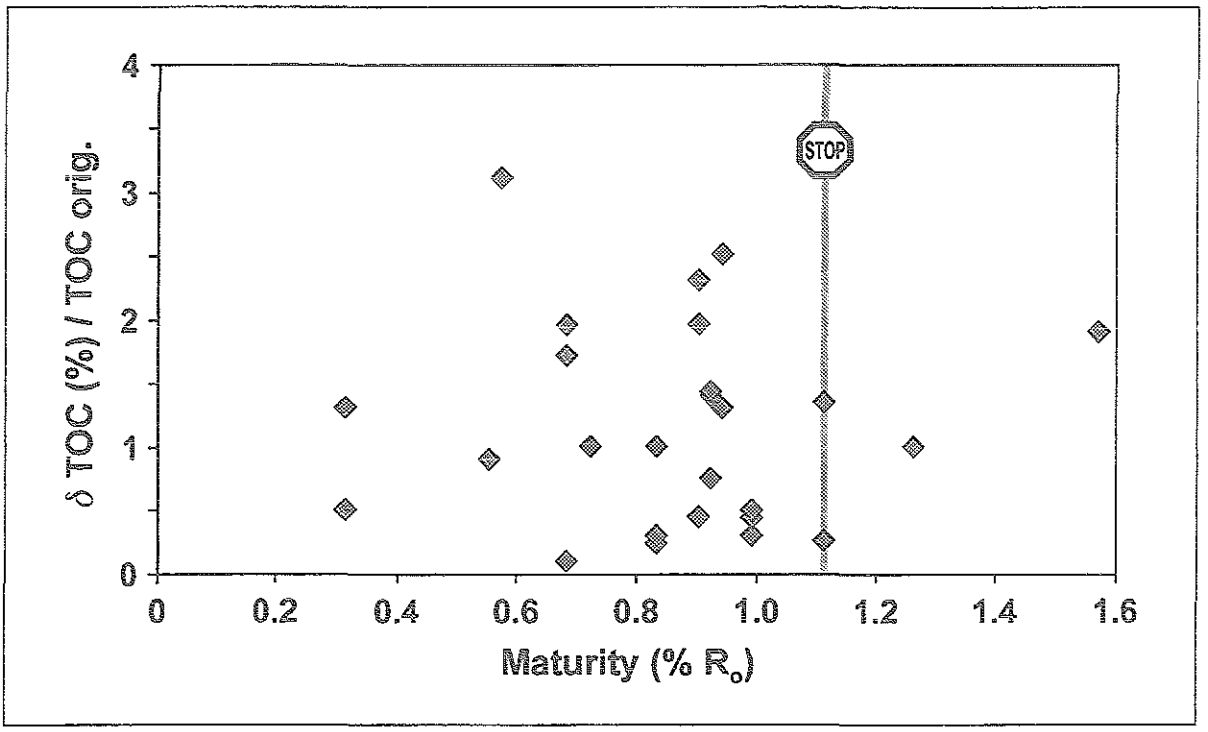

Fig. 55: Maturity related evolution of organic richness for Bakken Shale samples as determined prior to and after solvent extraction. The ratio 'δ TOC / TOC orig.' involves the difference in TOC content between extracted and unextracted sample divided by the TOC value of the original, unextracted sample. Stop sign indicates end of maturity spectrum as evidenced from other maturity parameters (see ch. 4.1.2).

Pyrolysis evolution profiles and kinetic parameters for Bakken Shale samples have been determined (Burnham, 1992) using three different techniques (TG-FTIR, Pyromat-MS and Pyromat-FID). These analyses elucidated that the major proportion of organic matter (85%) is converted within the temperature interval from 100° to 150°C based on a geologic heating rate of 3°C/Ma. At a temperature of ca. 135°C, 50% conversion is reached. These evolution characteristics derived from kinetic experiments are known to be typical for marine source rocks (Burnham, 1992).

As both sets of datapoints (Fig. 56) yielded almost identical trends, the Rock-Eval datapoints were chosen and submitted to spline approximation, and the cumulative curve obtained thereof was differentiated. Both curves are given in Fig. 57. The spline curve clearly elucidates that ca. 50% of the reactive kerogen of the initial organic matter (at 0.31% R_o) is converted within a relatively narrow interval of maturity (from 0.6% to 0.8% R_o). This is in good agreement with kinetic data (Burnham, 1992). As displayed in Fig. 54, this maturity zone is also associated with the most drastic decrease in TOC. Furthermore, the highest increase in alkylnaphthalene abundance in the products is associated with the same maturity zone. Hence, this coincidence

might suggest that the postulated aromatisation and condensation process is induced by thermal energy during maturation of the Bakken kerogen and not related to cyclisation processes forming ring structures from already existing paraffinic compounds, as discussed above.

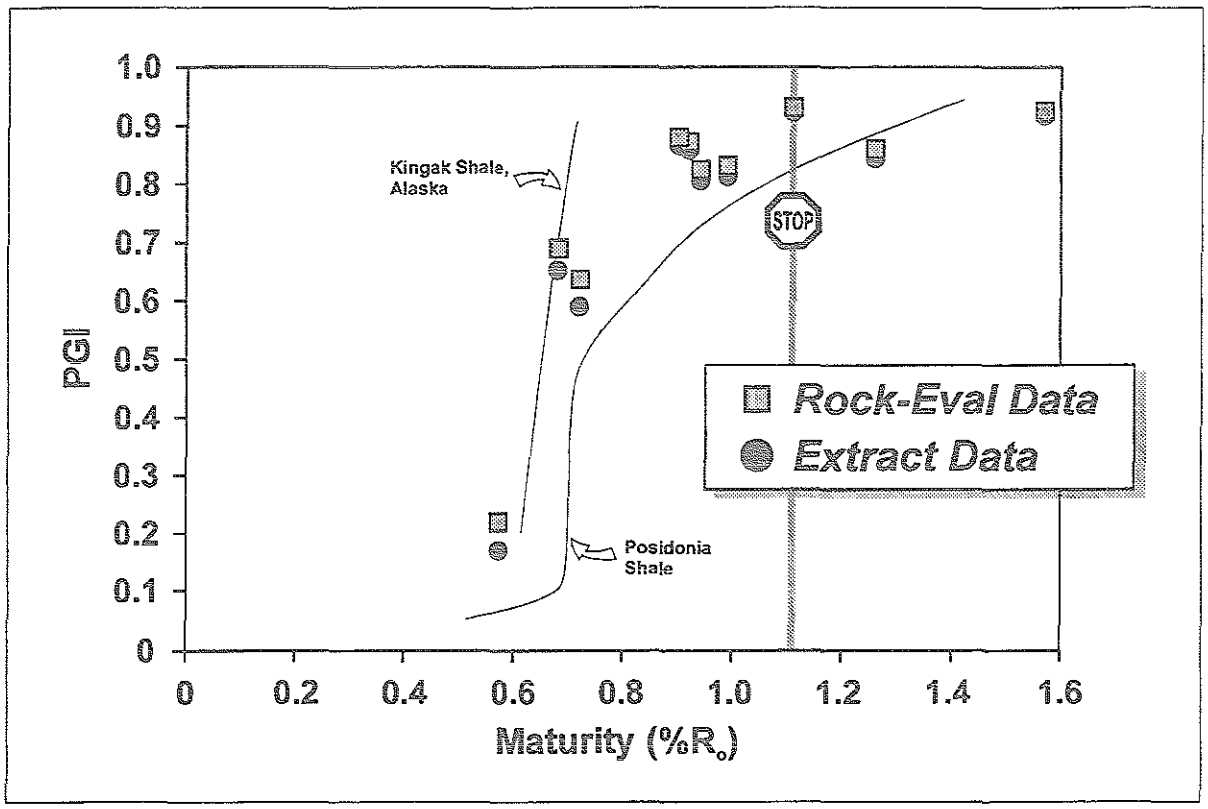

Fig. 56: Maturity-related evolution of Petroleum Generation Index (PGI) as determined from the algebraic mass balance approach by Cooles et al. (1986) using two different data sources (Rock-Eval pyrolysis and solvent extraction). PGI values of 1.0 are indicative of source rocks that have realized their entire hydrocarbon generation potential. Stop sign indicates end of maturity spectrum as evidenced from other maturity parameters (see ch. 4.1.2).

The extent of organic matter conversion, as illustrated by Fig. 57 is very low for all samples beyond 0.8% R_o. This is in good agreement with the observed TOC constancy for samples higher 0.8% R_o (Fig. 54). In other words, the main zone of petroleum formation of the Bakken Shale is bounded by 0.6% and 0.8% R_o, whereas at ca. 0.8% R_o the hydrocarbon generation potential has been exhausted to ca. 80%. According to the terminology of Cooles et al. (1986), the Bakken Shale reactive kerogen appears to consist of predominantly labile, oil-prone structures with only minor contribution of refractory, gas-prone moieties.

The differentiated curve indicates a maximum in the rate of hydrocarbon generation at ca. 0.62% R_o implying that this stage of thermal evolution is associated with maximum amounts of generated products. Thereafter, the petroleum formation rate drops to minimum amounts at ca. 0.85% R_o. The slight bulge of the curve at 1.1% R_o can be considered an artefact of the spline approximation and is therefore negligible. If these results are superimposed on the regional map of the study area (Fig. 58), they suggest that the majority of the producing wells in the North Dakota portion of the Williston Basin (south end of Nesson Anticline and Billings Anticline area)

are in regions where the hydrocarbon generation potential of the corresponding kerogens has grossly been realized and the current rate of generation is very low.

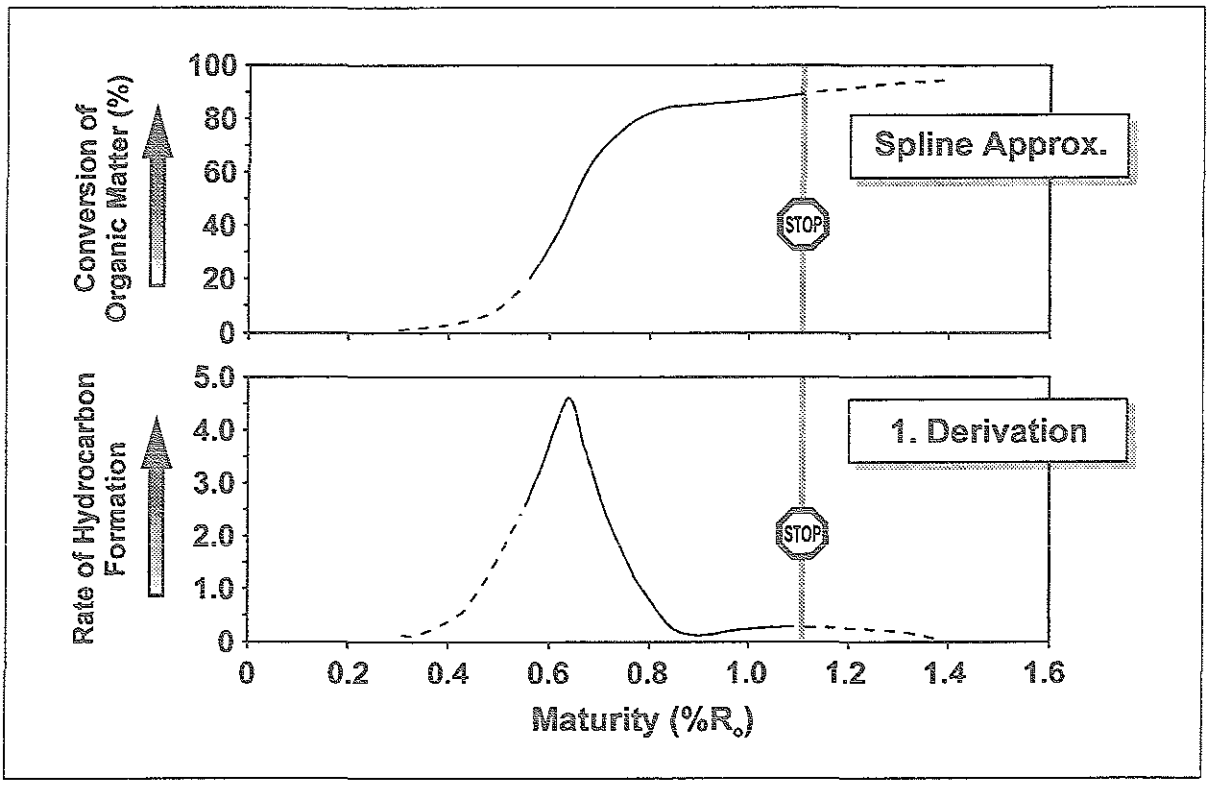

Fig. 57: Top diagram displays spline curve plotted vs. R_o as obtained from Fig. 56 (PGI vs. R_o) for Rock-Eval data set. PGI values were converted to percentage of organic matter conversion. Bottom diagram depicts first derivation of spline curve plotted vs. R_o. Dashed line in both diagrams indicates portion of curve which was extrapolated to reference sample at 0.31% R_o. Stop sign indicates end of maturity spectrum as evidenced from other maturity parameters (see ch. 4.1.2).

Simulation of Lithostatic Conditions

The generation characteristics and the evolution of compaction behaviour of a given Bakken Shale sample under simulated lithostatic conditions (elevated temperature and overburden pressure) was investigated using a triaxial cell experimental set-up (chs. 3.3.2. and 4.7.2). Recently, such an approach is focussed on more frequently (Lafargue et al., 1990; Takeda et al., 1990; Hanebeck et al., 1994) on *intact* rock samples during artificial maturation. With that respect, the Bakken Shale provides a suitable sample material for investigating the role of kerogen as a load-bearing rock component (Palciauskas, 1991), as it is known to contain high volumes of kerogen (ch. 4.4).

Compaction of the Bakken Shale plug as a function of time resulted in a curve (Fig. 47) which is indicative of very slowly proceeding thickness reduction. Hanebeck et al. (1994) have investigated a different marine type II source rock (Lower Toarcian Posidonia Shale) under the same analytical conditions (except for a lower axial stress: 14kN). This experiment revealed a

much more rapid response to elevated temperature and lithostatic pressure than the Bakken (superimposed on Fig. 47). In that case, the equilibrium in compaction was reached after ca. 80h of experiment duration.

These two different evolutionary trends despite the same type of kerogen reflect different degrees of organic matter conversion of the original sample. As laid out in ch. 5.1.2, generation of Bakken products in terms of kerogen transformation is fairly advanced at 0.68% R_o. Mass balancing calculations denoted this maturity level to be associated with ca. 60% of organic matter conversion. Hence, the hydrocarbon generation potential has been realized to an enhanced degree. In contrast, for the Posidonia Shale sample (0.57% R_o) generation of petroleum has just begun (ca. 7% conversion). Therefore, susceptibility of the Bakken kerogen structure of well SKA (0.68% R_o) to lithostatic stress (overburden load and temperature) is low. The fact that the thickness of the rock plug still was considerably reduced in the course of the experiment may have been caused by the loss of parts of the rock material into the steel frits.

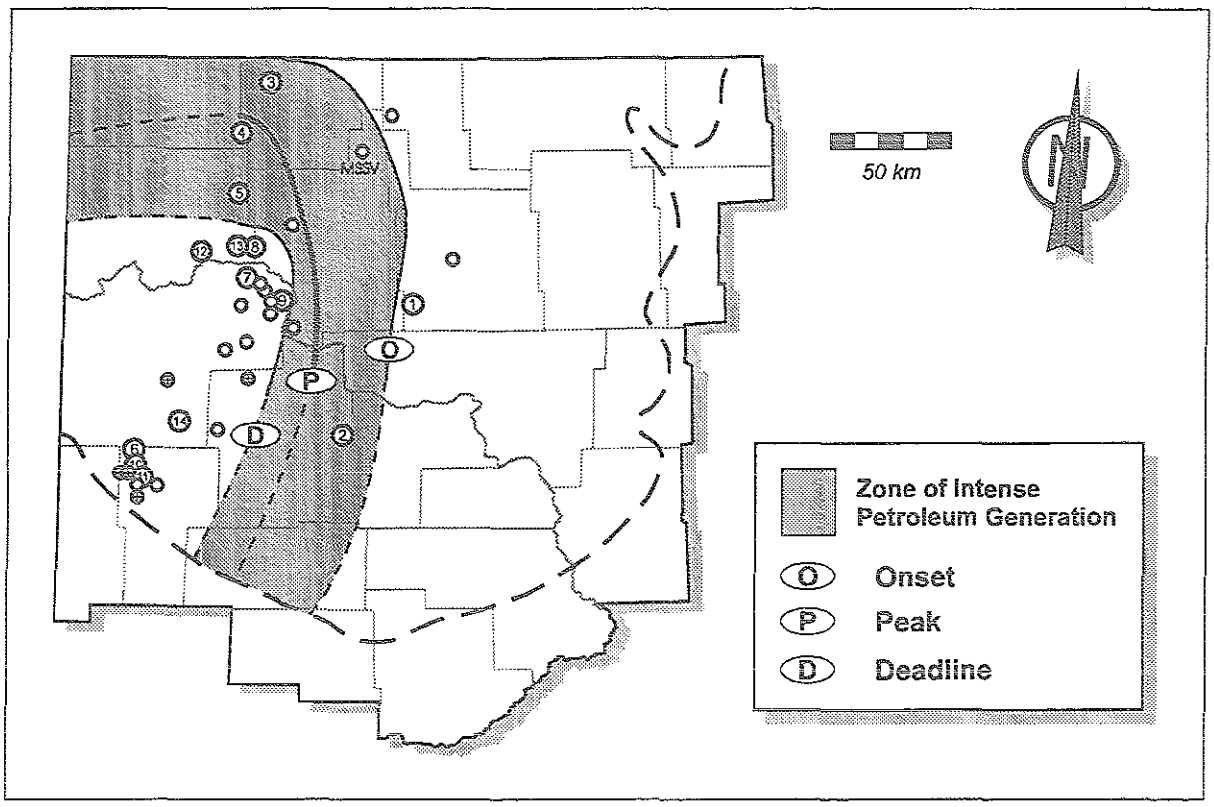

Fig. 58: Map of the study area modified after Webster (1984). Dots refer to well locations of the selected sample set of the present study. Highlighted zone designates maturity interval which is associated with the main stage of organic matter conversion as determined by mass balance calculations (Cooles et al., 1986).

The overall nature of the products, namely low-molecular-weight gases on one side and highly polar, high-molecular-weight viscous matter on the other side may be the result of a disproportionation reaction (Connan et al., 1975), in the course of which originally long-chain material (heavy paraffins) is submitted to bulk aromatization and release of a carbon-depleted short-chain gaseous phase. Indeed, these gaseous products might resemble the light oil, virtually asphaltene-free character of naturally occurring Bakken crude oils (40° to 45° API; Price &

LeFever, 1994) at surface temperature and pressure conditions, i.e. exsolution of gas from a liquid phase leaving behind a viscous, residual phase.

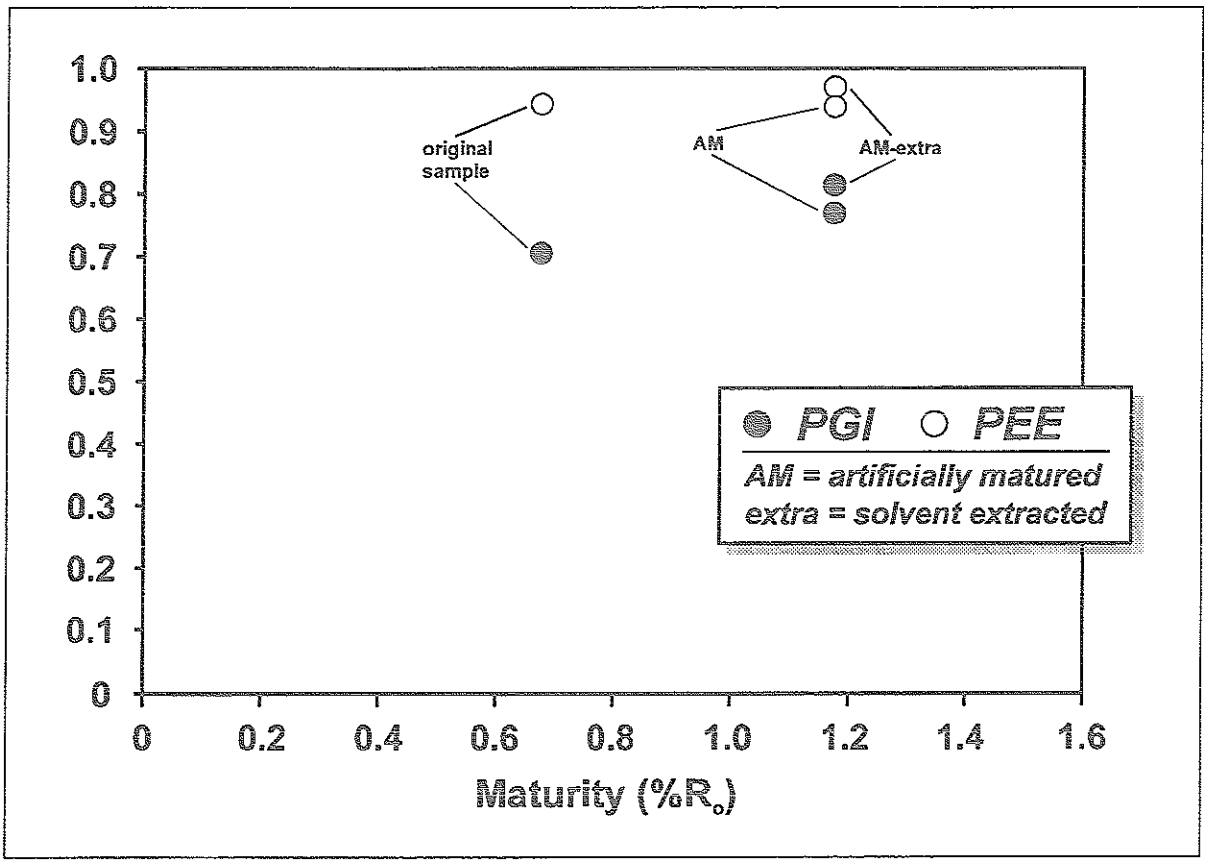

Fig. 59: Evolution of petroleum generation (PGI) and expulsion (PEE) for artificial maturity sequence carried out under simulated lithostatic conditions (elevated temperature and overburden pressure). PGI and PEE indices are determined according to the algebraic scheme by Cooles et al. (1986). Rock-Eval data was used for calculations.

The asphalt-like nature of the liquid products and the phenomenon that parts of the solid rock matrix were forced into the steel frits might indicate that the rock plug adopted a semi-solid, viscous nature in response to simulated elevated temperature and overburden pressure. If this hypothesis is valid, then the asphalt-like products may indeed represent moieties mechanically separated from the kerogen.
However, the level of maturity as determined by fingerprinting of pyrograms ("asphaltenes") of the products (Muscio et al., 1991) gave contradictory results: Compositional features were encountered which can be considered indicative of low and high maturity.

Interestingly, organic richness (TOC content) was significantly reduced during artificial maturation. Such low TOC values (7.8% and 8.5% for extracted and unextracted sample, respectively) are atypical for the Bakken Shale (ch. 4.1). This is even more surprising in the light of the S2 values: The part of the artificially matured kerogen which is amenable to Rock-Eval yielded values that are typical for the high mature natural equivalents (> 0.8% R_o). In other words, Rock-Eval parameters of the sample which was matured in the laboratory suggest a

maturity level similar to the high mature zones of the natural sequence (corroborated by vitrinite reflectance of 1.18% R_o) whereas strongly reduced organic richness implies a degree of organic matter conversion which is further advanced than in nature. This apparent mismatch is investigated below using the algebraic scheme developed by Cooles et al. (1986). Analogous to the natural Bakken Shale maturity sequence, this mass balancing scheme was carried out on the artificial sequence on the basis of screening parameters determined prior to and after the experiment. Immature sample DOB (0.31% R_o) provided the reference data. The theoretical background of the scheme is outlined in ch. 5.1.2.

Fig. 59 depicts PGI and PEE for the untreated (SKA) and artificially matured (SKA-AM and SKA-AM-extra, respectively) as a function of vitrinite reflectance. It must be pointed out that only Rock-Eval data were available for mass balancing, as the yield of solvent extract type products could not be determined (ch. 3.3.2.). Naturally, the artificial maturity sequence consisted only of the two "endmembers", thus representativity is reduced. In comparison to the naturally matured sample suite, only PEE outlines the same pathway (values around 0.95), while organic matter conversion (PGI) increases only slightly from 0.68% to 1.18% R_o. In the natural generation profile, PGI increased from ca. 0.6 to ca. 0.9 elucidating that organic matter conversion still proceeds to a limited extent. The careful examination of both evolution of TOC content and nature of products may provide an explanation to this feature: The liquid products collected from the system had a highly viscous nature implying that they consist of a high proportion of heavy, macromolecular organic matter. Such an asphalt-like material is very different to a typical Bakken Shale solvent extract. Furthermore and importantly, although not solid sensu stricto, it is amenable to TOC determination. Hence, this semi-solid type of product might account for the pronounced loss of organic carbon from the artificially matured kerogen, the TOC content of which was determined *after* removal of the products. However, such high-molecular-weight material is not "captured" in the Rock-Eval-S1. This apparent discrepancy between product nature ("heavy") and type of analysis (sensitive to "light" material) leads to erroneous calculations by the algebraic scheme (Cooles et al., 1986), as the PGI parameter is based on both quantitative evolution of products and residue.
The calculation of *initial* organic richness is also affected by this phenomenon (Fig. 60): Surprisingly, the calculated values for initial TOC content of the artificially matured samples (SKA-AM and SKA-AM-extra) are distinctively lower than the untreated, original sample. In a sample series derived from *natural* thermal evolution, such discrepancies can be explained by local lateral and vertical heterogeneities in organic matter input during deposition. In simulated maturation experiments, however, such a scheme is not valid because the original sample represents a small unit of rock with negligible variations in data of the same kind. Their artificially matured equivalents, in turn, are direct "descendents" to the original "parent" sample in terms of compositional properties. This leads to the conclusion that the calculated initial TOC content has to be equal or higher to the TOC of the "parent" kerogen. The erroneously low values for initial TOC content of SKA-AM and SKA-AM-extra, therefore, are also a result of the phenomenon as laid out above.

The above results and interpretations have the following implications:

- There is some evidence that the experimental simulation of lithostatic subsurface conditions (elevated temperature and overburden pressure) in a triaxial cell modifies the appearance of

the rock sample under consideration in that it adopts a flowable status. Furthermore, liquid products generated during such experiments are considerably different to equivalent products in nature suggesting that organic matter degradation follows different reaction pathways than under *natural* subsurface conditions. Other investigators who have used a similar analytical set-up (Lafargue et al., 1990; Takeda et al., 1990) found products to be similar to natural crude oil. These experiments, however, did not involve axial pressure.

- The algebraic scheme as developed by Cooles et al. (1986) may be of restricted utility for source rock systems that contain unusually high amounts of macromolecular asphalt-like material in their solvent extracts (e.g due to "staining" or impregnation by a migrating heavy petroleum phase). In the case of such a hypothetical scenario the results obtained have to be evaluated and interpreted with great care.

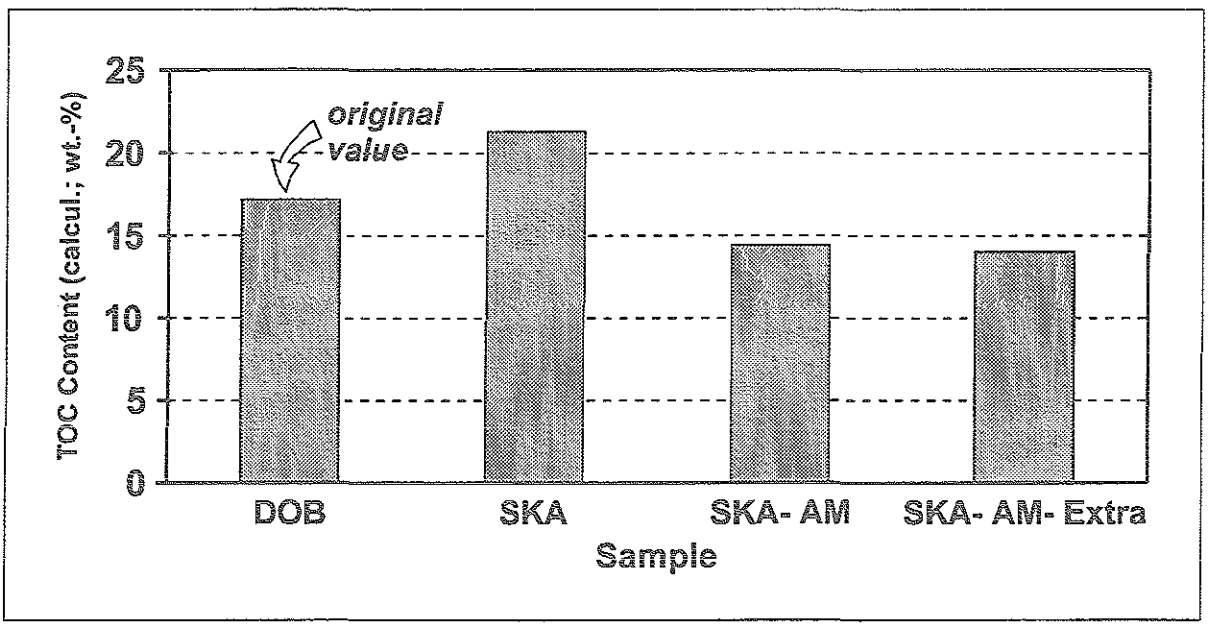

Fig. 60: Calculated *initial* (immature) TOC content for artificially matured Bakken Shale sample (simulated lithostatic conditions). Well DOB (0.31% R_o) provided reference data based on which calculations were performed according to Cooles et al (1986).

5.1.3 Occurrence of Gas

Fig. 36 illustrates that the unusual phenomenon of high gas concentrations in the thermovaporisation compounds of the Bakken Shale is restricted to levels of maturity below 0.7% R_o. At higher levels of thermal evolution (>0.7% R_o) gas yields are significantly reduced. Data derived from mass balance calculations on petroleum generation (ch. 5.1.2) and expulsion/migration (see below, ch. 5.2.2) indicate enhanced hydrocarbon generation and expulsion between 0.6 to 0.7% R_o. Hence, the significant decrease in gas content encountered in Bakken Shales at ca. 0.7% R_o might be related to the two processes of hydrocarbon generation and hydrocarbon expulsion operating together.

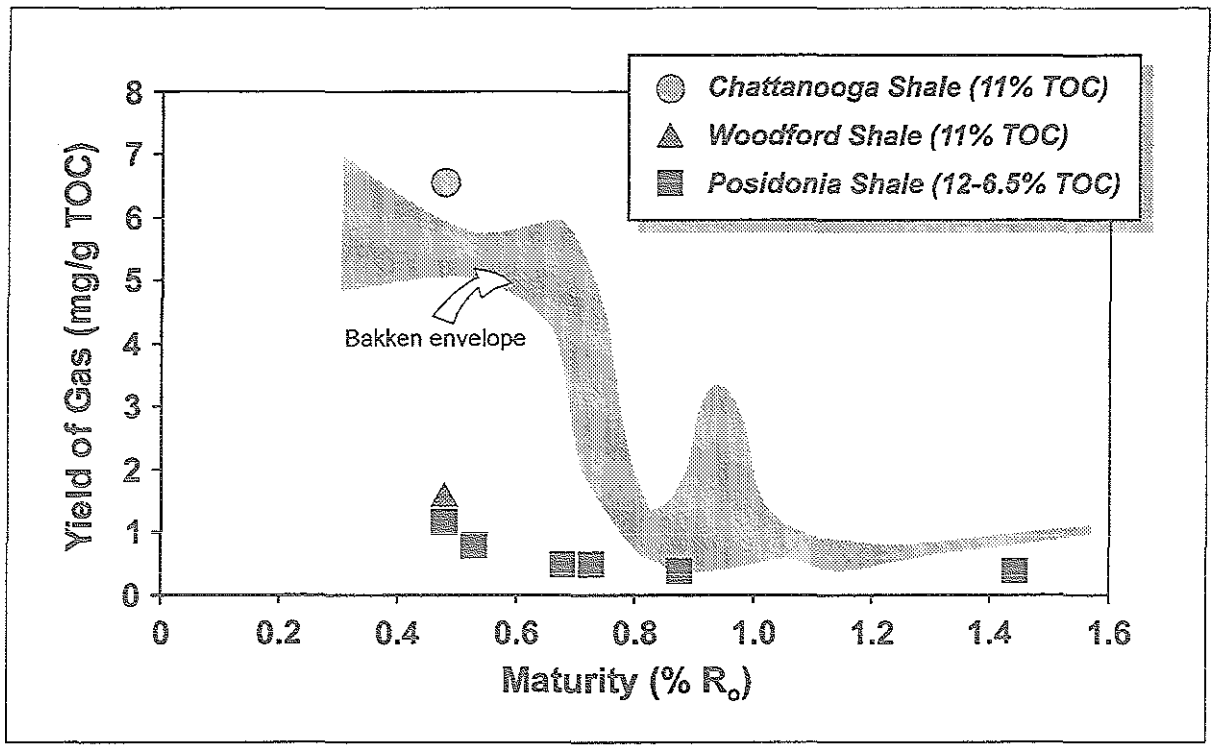

Fig. 61: Yield of gaseous hydrocarbons (C_1-C_5) as determined from t'vap-gc for three type II marine source rocks. Chattanooga and Woodford Shale are stratigraphic equivalents of the Bakken Formation in the Appalachian Basin and Anadarko Basin (U.S.A.), respectively. Posidonia Shale samples (Lower Toarcian) were taken from the Hils Syncline, Northern Germany. For reasons of comparison, the datapoint envelope for Bakken Shale gas yields is shown.

The question, whether such high relative amounts of gas are a feature uniquely associated with the Bakken Shale was evaluated by analysing source rocks of similar kerogen (type II) and TOC content applying the same sample treatment procedure as for thermovaporisation of the Bakken Shale. The results are displayed in Fig. 61. For the Chattanooga and Woodford Shale, only immature samples were available. In the immature zone (<0.7% R_o), only the Chattanooga Shale sample revealed gas contents (6.5mg/g TOC) which are quantitatively similar to the Bakken.
In contrast, the Woodford Shale as well as the Posidonia Shale yielded relatively low amounts of C_1-C_5 material in comparison to the Bakken. The maturity-related evolution of gas yield for the Posidonia Shale shows - apart from overall very low values - a trend which is similar to the Bakken envelope: The most distinct decrease in gas yield is associated with a maturity interval of 0.5% to 0.7% R_o. Based on mass balance calculations, this stage of thermal evolution of the Posidonia Shale is believed to be a phase of considerable organic matter conversion (ca. 30% of the initial amount) and, furthermore, at ca. 0.7% R_o 84% of the generated products are already lost (Rullkötter et al., 1988). Still, however, gas yield for the Woodford as well as the Posidonia Shale appears to be quantitatively rather insignificant in comparison to the Bakken, although bulk elemental kerogen type and TOC content are very similar. The significance of TOC content in relation to the occurrence of gas will be discussed below.

Quantitative investigations of the generation and migration of gases and light hydrocarbons using field studies is difficult. Even if high concentrations of gases are present in the subsurface, their enhanced mobility normally causes sampling problems. If the samples which are collected

directly at the well-site are not sealed in gas-tight containers immediately at the well-site and stored at deep freeze temperatures (Schaefer et al., 1978; Huc & Hunt, 1980), a large portion of the volatile organic products is lost. Using a sampling device which hermetically seals the sample in-situ, Sokolov et al. (1971) have elucidated that the magnitude of gas losses is enormous even during drilling operations while the samples are transported through the borehole to the surface. With this respect, Price (1989) has also pointed out that the presence of large quantities of gaseous hydrocarbons (C_1-C_5) in source rocks at early stages of catagenesis may have gone unrecognized due to sampling problems.
The thermovaporisation of conventionally sampled and stored core samples yields predominantly C_{7+} products (Huc et al., 1981; Price & Wenger, 1992). Hence, quantitative comparisons can only be made to a limited extent, as the sample treatment procedures as applied in the present study and, consequently, quantitative data are not directly compatible to techniques used in related publications.

The formation of significantly high amounts of gaseous hydrocarbons (C_1-C_5) early on in generation is still a subject of controversy. The formerly widely accepted scheme promotes that the occurrence of high amounts of thermogenic gas is related to late catagenetic/metagenetic stages of thermal evolution as various authors have shown, like Evans et al. (1971) and LeTran et al. (1974) for the Western Canada Basin and the Aquitaine Basin, respectively. Other authors have quoted the generation of relatively large quantities of gas under mild thermal conditions, such as below 0.6% R_o (Stahl, 1977; Connan & Cassou, 1980) using head-space analysis-type methods (Huc & Hunt, 1980; Monnier et al., 1983). As light hydrocarbons cannot be related to any specific biological precursor material, Mango (1994), on a completely different perspective, postulates a catalytic origin.

The relative chain length distribution of total gases and resolved n-alkyl-pyrolysates (C_{6-14}, C_{15+}) of the Bakken Shale throughout the R_o range from 0.31% to ca. 1.1% R_o (Fig. 20) illustrates that the kerogen macromolecule predominantly consists of structures which yield more C_{1-5} compounds upon pyrolysis than is typical for marine clastic source rocks. Corresponding field data on API gravity of Bakken produced oils (Price and LeFever, 1994) corroborate that Bakken crude oils are relatively light (40°-45° API) irrespective of maturity of the associated shale. The portion of these light hydrocarbon-yielding (C_{1-5}) moieties (80-90%) clearly exceeds the portion of structures which yield medium- and long-chain n-alkenes and -alkanes on pyrolysis. Increasing thermal stress during the natural maturation of the Bakken Shale apparently does not affect this property with respect to the gross composition. Based on an empirically founded interpretation scheme involving these pyrolysate constituents and natural petroleums, the inferred nature of the petroleum product (Horsfield, 1989) derived from this kerogen would be mostly gas. In contrast, the kerogens of other marine source rocks like the Woodford Shale (Horsfield, 1989), the Posidonia Shale (Muscio et al., 1991) and the La Luna Formation (Ropertz, 1994) are distinctly less gas-rich despite having similar bulk elemental compositions (kerogen type II). Accordingly, the Bakken Shale appears to be much more prone to form gaseous hydrocarbons compared to other kerogens of the same type regardless of maturity (Fig. 20). This finding is even more surprising with respect to the bituminite- and alginite-richness of the Bakken kerogen as revealed by organic petrology. The enhanced tendency to form C_1-C_5 products as revealed by chain length distribution (Fig. 20) is supported by the bulk composition of the pyrolysate based on total yield

of pyrolysis products (Fig. 62): Approximately 20 to 40% of the total pyrolysate consists of gaseous compounds (C_1-C_5). With respect to maturity, two different zonations can be outlined: Immature pyrolysates (up to 0.6% R_o) have low relative contents of C_1-C_5 material while more mature samples (>0.6% R_o) are significantly biased to a gas rich composition. Equivalent data derived from a natural maturation series (0.48% to 1.45% R_o) of the marine type II Posidonia Shale (Muscio et al., 1991) show some overlap with the immature Bakken pyrolysates, however, the overall bulk composition is distinctly less gas rich compared to the Bakken pyrolysate. Consequently, the absolute values for the pyrolysate gas-oil ratio (GOR) (England & MacKenzie, 1989) of the Bakken are also higher than expected for typical organic rich marine kerogens like the Posidonia Shale.

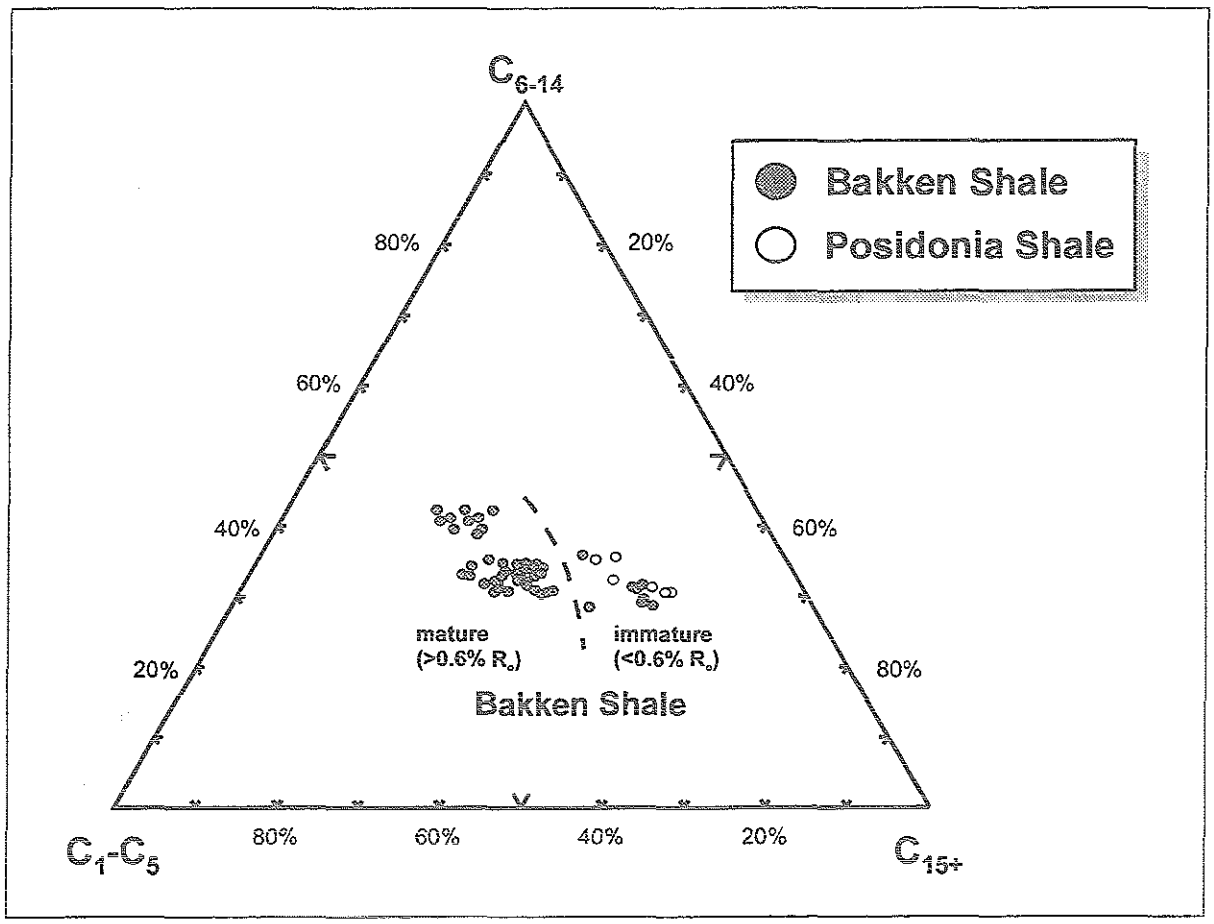

Fig. 62: Ternary diagram as derived from py-gc displaying the relative composition of **total** C_{1-5}, C_{6-14} and C_{15+} pyrolysates for the Bakken Shale. Data from Posidonia Shale kerogens superimposed from Muscio et al. (1991).

Results as provided by closed-system artificial heating of immature Bakken Shale equivalents (Fig. 63) corroborate that the Bakken has a high proneness to form gas relative to that of other kerogens. The relative composition of the artificially generated products in terms of chain length distribution clearly elucidates that low-molecular-weight hydrocarbons (C_{1-5}) are predominant. Interestingly, the tendency to yield gas is not uniform throughout the artificial maturity sequence, as a detailed examination of the data reveals: The relative composition of the products shifts to less gas-rich (C_{1-5}) with increasing heating conditions, indicating a proneness to form gas that is more pronounced at low levels of thermal stress (up to 300°C/5 days). From a certain degree on

(>330°C/1 day) the relative composition of the MSSV products is still overall gaseous but remains essentially constant. This finding implies that the Bakken Shale indeed is able to generate light hydrocarbons predominantly at low stages of thermal evolution. Moreover, this finding matches thermovaporisation results of the present study. Interestingly, hydrous pyrolysis experiments carried out on the Bakken Shale (Price et al., 1984) also yielded gaseous hydrocarbons at relatively low temperatures before the onset of C_{15+}-hydrocarbon generation. Although Price et al. (1984) had no natural evidence for the occurrence of gas early on in maturation as documented in the current contribution, they postulated a migration mechanism (termed gaseous-bulk primary migration) which requires the formation of a dispersed free gas phase before intense hydrocarbon generation takes place. The significance of the occurrence of gas for migration processes will be discussed and evaluated in the following chapter (5.2).

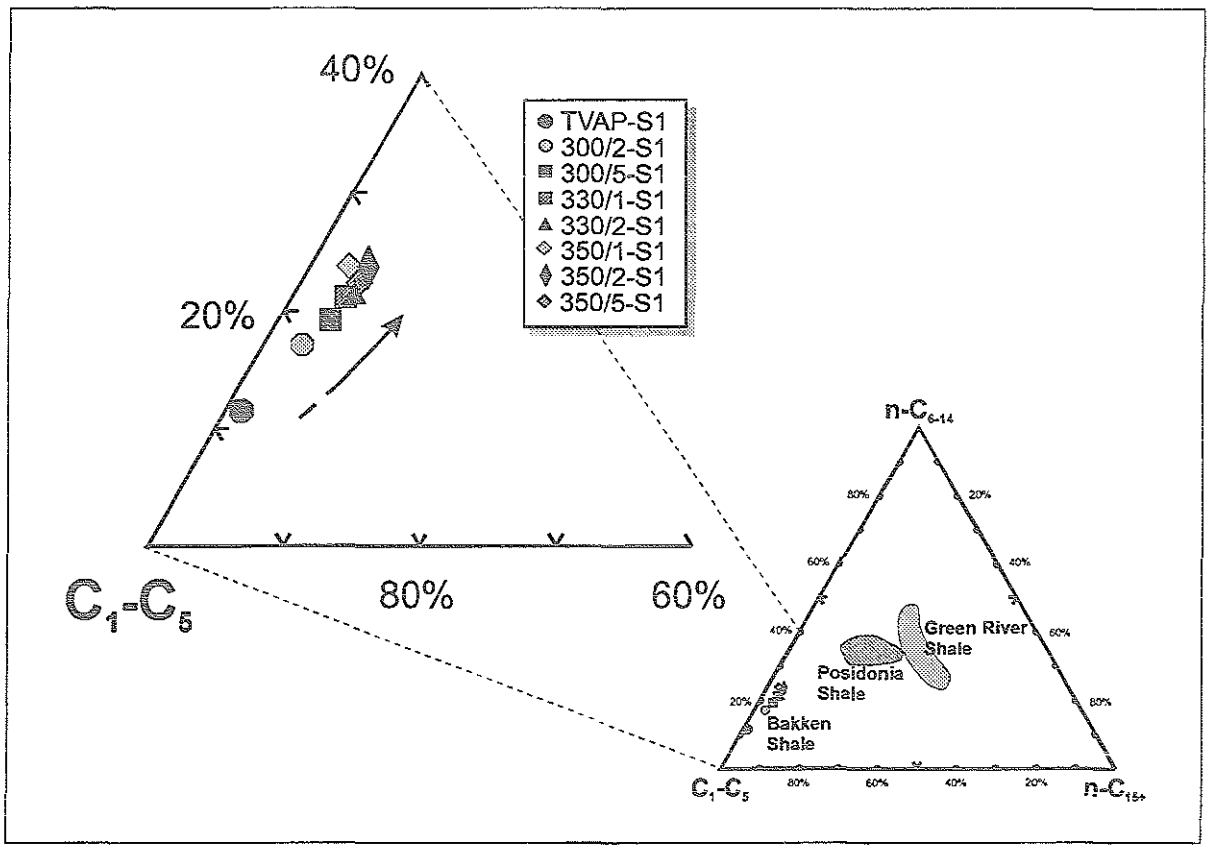

Fig. 63: Ternary diagram displaying the relative composition of short- (C_{1-5}), medium- (C_{6-14}) and long-chain (C_{15+}) n-alkyl-*products* (chain length distribution) of artificially matured Bakken Shale samples (8 different heating conditions). Abbreviation TVAP-S1 refers to products derived from t'vap-gc. Arrow outlines decreasing relative abundance of C_{1-5} components with increasing thermal stress. Data on Posidonia and Green River Shale have been superimposed from Düppenbecker & Horsfield (1990).

The generation of gas in source rocks at high levels of maturity can be explained by the thermal cracking of bitumen and/or kerogen. As an alternative to the temperature-induced cracking of unexpelled oil to gas, gaseous hydrocarbons can also be generated directly from the kerogen throughout catagenesis (Tissot & Welte, 1984). On the other hand, the generation of gas from the Bakken Shale early on in maturation requires that the organic matter structure contains more

weak links than would be anticipated for a marine type-II kerogen and which are supposed to facilitate break up of the kerogen to form gas. The determination of bond energies for specific compounds (Claxton et al., 1993) ought to provide more insight into the lability of the Bakken organic matter. Infrared spectroscopic analysis performed on whole rock Bakken samples of the present study could not provide any evidence pertaining to the presence of oxygen-bearing ester bonds due to mineral matrix interferences. A kerogen macromolecule containing highly branched structures linked to aromatic rings (aryl isoprenoids) which are broken via β-cleavage during pyrolysis (Requejo et al., 1992) might also account for a labile kerogen. Furthermore, the presence of weak heteroatomic bonds incorporating organic sulfur (disulphide bonds) is known to increase the thermal lability of kerogens (Eglinton et al., 1990) and decrease the temperature of product generation (Tegelaar & Noble, 1993). However, py-gc analyses using a sulfur-sensitive detector elucidated that organic sulfur compounds such as alkylthiophenes and alkylbenzothiophenes are quantitatively irrelevant in Bakken kerogens above 0.6% R_o, and below 0.6% R_o are present in very low concentration. The data base of the present study as well as related publications provide no evidence that organic sulfur could account for the generation of gas early on in maturation.

1,2,3,4-tetramethylbenzene as derived from diaromatic carotenoid structures has been shown to be a biomarker candidate for oil-source correlations (Requejo et al., 1992). In the present study, this particular alkylbenzene was identified in the natural products (t'vap-gc; Fig. 34), as well as in the pyrolysates (Fig. 17) and the products derived from MSSV pyrolysis (Fig. 46) of the Bakken Shale. Especially in the artificially generated products 1,2,3,4-tetramethylbenzene is the most prominent individual compound except for the C_{1-5} gaseous hydrocarbons at relatively mild heating conditions (Fig. 46). Hence, the pronounced gas generation potential and gas-retaining potential (see later) of immature Bakken Shales coincides with a kerogen that consists of diaromatic carotenoid structures on a scale larger than normal. Furthermore and importantly, the presence of 1,2,3,4-tetramethylbenzene in both natural and artificially generated products suggests that the gas in the thermovaporisation compounds indeed has been generated from the Bakken organic matter and therefore is indigenous. However, whole oil gas chromatography of the present study (ch. 4.6.3) and data from Price and LeFever (1994) reveals that 1,2,3,4-tetramethylbenzene appears to be absent in Bakken crude oils.

As already indicated by fingerprinting of the pyrograms, Fig. 64 reveals that the aromaticity of the GC-amenable portion of the kerogen is considerably higher in immature samples (<0.7% R_o). The boundary is not clearly defined, as samples at 0.68% R_o cover a broad range from low (0.2) to high (0.53) aromaticity. It has been shown (Horsfield, 1989; reviewed by Larter & Horsfield, 1993), that the aromaticity of the volatilisable substituents of immature to mature kerogens, as determined by py-gc, can be considered representative for the kerogen macromolecule as a whole although being based only on a small portion of the total pyrolysate. The fact that less mature Bakken kerogen pyrolysates are more aromatic than the more mature equivalents has been reported previously by Van Graas et al. (1981) and Solli et al. (1984). In contrast, the aromaticity of a type II kerogen as determined by solid state ^{13}C NMR spectroscopy increases with progressive maturation (Witte et al., 1988 for the Posidonia Shale) due to the elimination of labile functional groups leading to aromatization and polycondensation of the residual kerogen during the process of petroleum generation (Tissot & Welte, 1984). The analysis of the bulk and molecular aromatic composition of the Bakken Shale kerogen therefore provides some evidence

pertaining to the relationship between the early generation of C_1-C_5 compounds and the nature of the parent organic matter.

If the enhanced aromatic nature of immature kerogen in Bakken Shales is considered with respect to the generation of gas at low levels of natural thermal evolution, it is noteworthy that ca. 10-22% of the total sum of aromatic compounds in the pyrolysate consists of 1,2,3,4-tetramethylbenzene (Fig. 19), implying that a large proportion of the immature (<0.6% R_o) kerogen macromolecule is made up of diaromatic carotenoid structures. Therefore, the gas-generative capacity of the Bakken Shale at low natural temperatures might also be a function of the composition of the kerogen in terms of biological precursors. Indeed, the species of green sulfur bacteria might represent a potential biological precursor for the gases encountered in immature Bakken Shales.

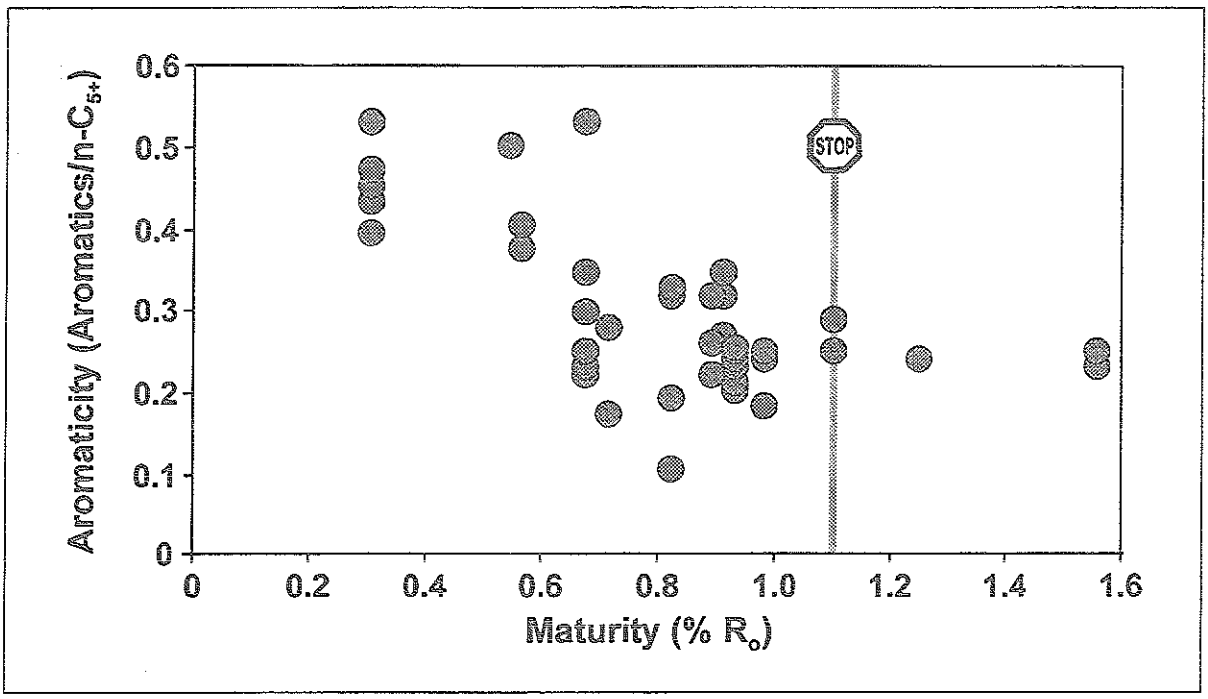

Fig. 64: Aromaticity of the Bakken Shale kerogen as determined from py-gc. The ratio was calculated by dividing resolved aromatics in pyrolysate (benzene, toluene, ethylbenzene, meta-/paraxylene, orthoxylene, C_3-benzenes, 1,2,3,4-tetramethyl-benzene, 2-methylnaphthalene, 1- methylnaphthalene, dimethylnaphthalenes and trimethylnaphthalenes) through the sum of resolved C_{5+} normal alkyls.

Implications from Isotopic Composition

The boundary value in terms of stable carbon isotope ratio which discriminates between biogenic (microbial) and thermogenic (catagenetic) gas lies approximately at -50‰ (Fuex, 1977; Schoell, 1980). Although the results derived from on-line isotope ratio analysis of the thermovaporisation gases and the implications deduced thereof, especially with respect to migration phenomena (direction of transport, see below), have to be evaluated with great caution, it appears to be justified to use them to make statements on their genetic origin. Hence, the isotopic signature of the gases provides clear evidence that the low-molecular-weight compounds encountered in the

Bakken Shale for the complete maturity range are the result of thermally induced breakdown of organic matter and not products of bacterial methanogenesis.

If the stable carbon isotopic compositions of the thermovaporised gases are compared with the corresponding values of the C_{6+}-compounds as derived from standard GC-column equipment (BP-1 fused silica column), the values of the gases are generally rather heavy (Fig. 39). Published data on petroleum distillation fractions indicate that $\delta^{13}C$ ratios increase progressively from methane to the C_6 components while the values for C_{6+}-fractions exhibit only slight variations (Fuex, 1977; Stahl, 1977). Based on this concept, the enrichment of ^{13}C in the gases suggests that the C_{2-5} hydrocarbons may have a different origin from that of the liquid hydrocarbons.

Several scenarios can be envisaged. Gerling et al. (1988) have reported that methane and ethane sampled from potash layers in the North German Zechstein evaporites were extremely enriched in ^{13}C (up to +12.7‰ and +10.7‰, respectively). While the question of the original source of these gases remained unanswered, it can be inferred that the heavy isotopic signature is linked to evaporites. In this context it is noteworthy that the stratigraphic column of the Williston Basin exhibits evaporitic sequences in the Lower Devonian (Prairie salts, Carlson & Anderson, 1965). Accordingly, the natural gases encountered in the Bakken Shales might have originated from the Lower Devonian evaporites. According to Price & LeFever (1992, 1994) such a scenario is rather unlikely due to the lack of efficient vertical migration pathways.
The differences between stable carbon isotope ratios of individual gas compounds are believed to decrease with increasing level of thermal evolution (James, 1983). Interestingly, the values for gases analysed in relatively immature Bakken samples cover a rather narrow range (from -33.7‰ to -28.8‰ for 0.31% R_o and from -32.3‰ to -27.9‰ for 0.68% R_o). This finding might indicate that the gases which are encountered in immature Bakken sediments are more mature than their host. This and the presence of 1,2,3,4-tetramethylbenzene could indicate that the gases were sourced from Bakken equivalents which have already entered the catagenetic stage of gas generation. However, the likelihood of predominantly lateral intraformational migration of highly mobile light hydrocarbons within the overpressured Bakken Formation itself over long distances (tens of kilometres) is rather low. Such a transport mechanism requires a high rate of migration and a carrier system that is effectively sealed to avoid loss of gases. Diffusive transport of gas, however, is considered to be rather slow and quantitatively inefficient (Mackenzie et al., 1988; Krooss et al., 1988). Moreover, the Bakken Formation appears to be laterally very restricted with respect to petroleum migration (ch. 5.2.2). The scenario of lateral long-distance migration of light hydrocarbons can be reconsidered on the basis of implications from artificial maturation (ch. 5.4). These experiments revealed that even under closed-system lab conditions and mild heating the Bakken Shale sample did generate slightly less C_{1-5} material (up to ca. 5mg/g TOC) than encountered in immature equivalents from the natural maturity sequence (ca. 6mg/g TOC) hence supporting the hypothesis that in the latter case the gases consist of in-situ generated immature compounds plus migrated high mature material.
The third possibility is that the values are artefacts of the chromatographic separation method employed for GC-IR-MS analysis. In particular, the coelution of isotopically heavy CO_2 from inorganic sources (e.g. carbonates) with C_2 and C_3 could account for heavy values of the latter two. While the modified analytical approach using a poraplot column yielded equivocal results for hydrocarbon gases, it nevertheless showed that the problematic results are not related to the

mineral matrix and that CO_2 is of biogenic origin. In this regard, the results of Espitalié et al. (1977) have elucidated that the generation of CO_2 from carbonates and clay minerals does not occur before ca. 400°C (siderite) during lab pyrolysis and that carbon dioxide formed below this temperature is of organic origin. Therefore it is difficult to envisage how isotopically heavy CO_2 resulting from mineral matrix effects could be present in the Bakken Shale. Additionally, contribution of inorganic carbon to the products is quantitatively less important in type-II kerogens (Espitalié et al., 1977).

Retention of Light Hydrocarbons

As laid out in the analytical procedure, two steps were taken to prevent potential loss of highly volatile low-molecular-weight hydrocarbons, these being the coarse crushing of the samples immediately followed by sealing of the glass tube containing the sample material. Nevertheless it still remains to be answered why such high yields of gaseous compounds were possible. There must be a very effective retention mechanism for holding gas in samples brought up from 3000m of burial depth. Fig. 65 displays the relationship between TOC content and yield of gas for two different zones of maturity. The boundary (0.7% R_o) between these zones is characterized by a sharp decrease in concentration of C_{1-5} compounds (Fig. 36) and represents an intermediate stage beween minimum and maximum degree of organic matter conversion (Fig. 56). For the immature zone (0.31 - 0.7% R_o), increasing gas yields are paralleled by increasing TOC contents. Beyond 0.7% R_o, gas concentrations are uniformly low although the Bakken Shale still is relatively organic rich (7-14wt.-% TOC). Considering an average TOC content of ca. 15wt.-% for immature Bakken Shales (<0.7% R_o), the total volume of solid organic matter could be as high as ca. 40vol.-% (Price & Clayton, 1992). Analysis of the inorganic rock matrix of the Bakken Shale (Cramer, 1991) revealed that 43vol.-% of the mineral matrix consist of quartz and 29.5vol.-% are made up of clay minerals. Although such quantitative data on the mineral content especially in organic rich sediments has to be considered with great caution (see XRD results of present study, ch. 4.9) adsorption effects of the inorganic rock matrix nevertheless could be possible. However, the good positive correlation between gas yield and organic carbon content strongly suggests that the gas is adsorbed on the kerogen at low maturity or absorbed within the organic matter (Sandvik & Mercer, 1990); low gas yields for >0.7% R_o indicate that the mechanisms controlling such an adsorption effect do not apply to higher levels of maturity. Hence, this might indicate that the reduction in gas yield is related to migration phenomena associated with enhanced hydrocarbon generation (Fig. 56) and/or the loss of gas due to production. In that context, Philippi (1965) proposed that enhanced hydrocarbon generation might exceed the adsorptive capacity of a given source rock. Additionally, the loss of adsorptive capacity might be related to changes of the kerogen structure: Microscopical examination of the Bakken Shale revealed that samples from shallow depths bear organic matter in the form of a horizontally orientated kerogen network while samples from greater depths exhibit a homogeneous texture with no preferred orientation. Furthermore, the intrinsic open 3D aromatic nature of the immature kerogen might enable the entrapment of small hydrocarbon molecules. Such a mechanism has been suggested by Behar & Vandenbroucke (1988) to be dominant in the oil window.

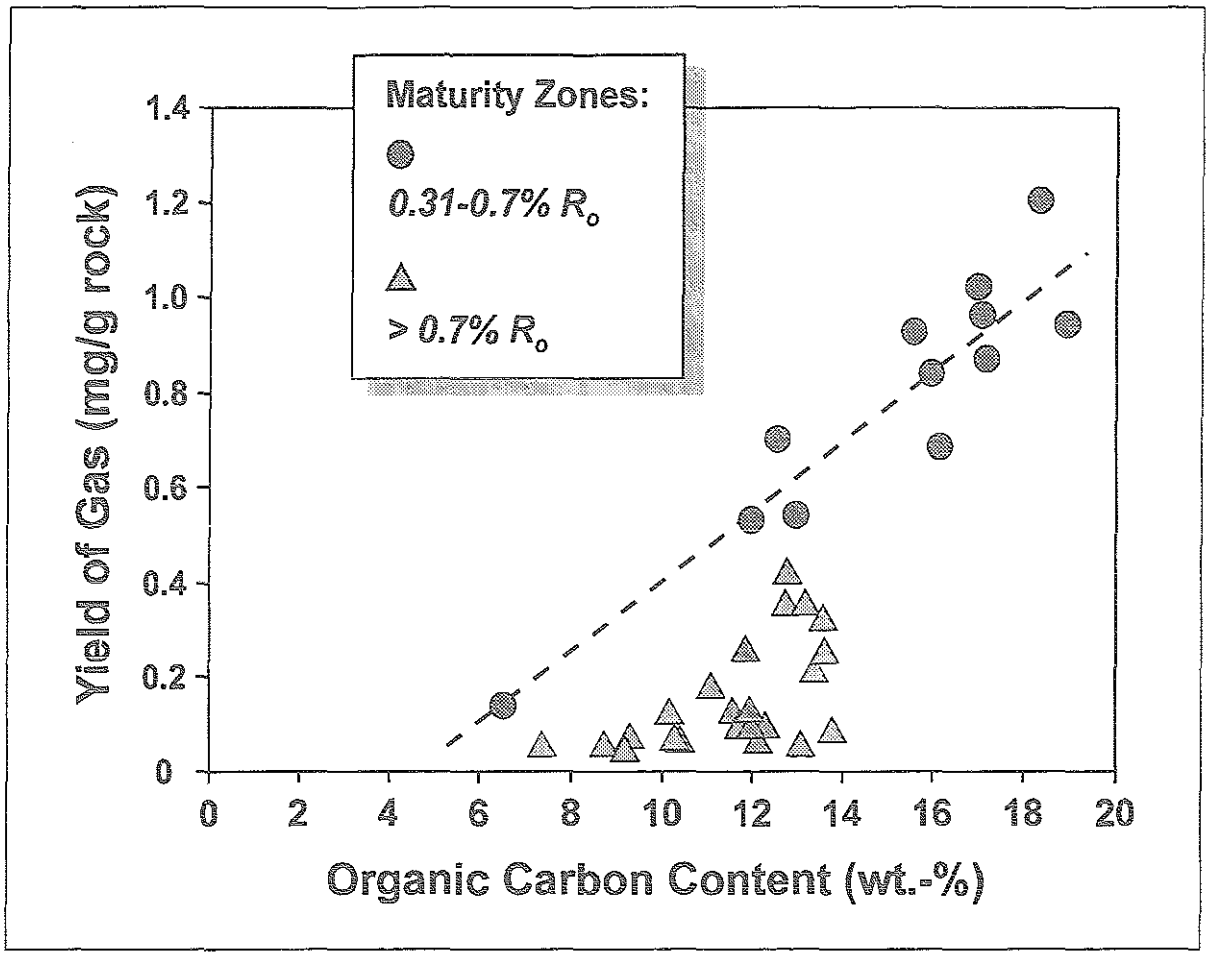

Fig. 65: Relationship of organic richness (TOC content) with gas yield (t'vap-gc) of the Bakken Shale for two different zones of maturity.

5.2 Petroleum Expulsion and Migration

5.2.1 Maturity of Crude Oils

The Bakken crude oil samples investigated in the present study were all produced from reservoirs within the Bakken Formation. Principally, they are derived from two regions in the North Dakota portion of the Williston Basin (Fig. 6): One sample stems from the south end of the Nesson Anticline (sample LB), 3 samples were derived from the Billings Anticline area (samples ER-1, -2, -3). The fifth sample (BY) cannot be associated with either of these regions, as it was produced from the northern extension of the Billings Anticline.
Compositional characteristics in terms of MPLC fractions (Fig. 24), ratios as calculated from saturates fraction (Fig. 29: CPI, LHCPI, Pri/n-$C_{17:0}$, Pri/Phy) and aromatic fraction (Fig. 31: TNR-2, MPR-3, MPI-1) as well as biomarker data (Fig. 33) corroborate that the crude oils compositionally are very alike, except for sample BY. The latter differs from the other oils as regards the following parameters: LHCPI (higher), Pri/Phy (lower), TNR-2 (lower), MPR-3 (lower), MPI-1 (higher). Additionally, the API gravity for this individual oil is - atypical for Bakken crude oils (Price & LeFever, 1992 and 1994) - relatively low (38.4°). While high density can be related to relative high proportions of resins and asphaltenes (Tissot & Welte, 1984), this is not reflected by the bulk composition (Fig. 24). Indeed, the saturates fraction of sample BY indicates a preponderance of light, short-chain compounds (distribution pattern, LHCPI). Unpublished analytical data provided by Conoco Inc. reveal a slightly enhanced sulfur content (0.16wt.-% in comparison to ca. 0.04wt.-% for typical Bakken oils) and, surprisingly, a high concentration of asphaltenes (ca. 50% vs. ca. 30% for the other oils).
The exceptional nature of sample BY is also exemplified with respect to relative maturity: High relative maturity is denoted by high values for MPI-1. On the contrary, a relatively low MPR-3 argues for a low relative maturity.
In view of the puzzling and contradictory results for sample BY as laid out above (especially the lack of asphaltenes as determined from the precipitation procedure applied in the present study (ch. 4.5.2) vs. ca. 50% asphaltene yield by Conoco Inc.), its compositional data as obtained for the present study has to be considered carefully.

In order to evaluate expulsion and migration phenomena for crude oils, it is essential to correlate them with their source rocks in terms of the corresponding level of maturity. Chapter 4.5 elucidated that only a few of the molecular parameters which are considered to be sensitive to maturation, indeed are directly associated with increasing thermal evolution: Ratios calculated from the saturates fraction showed only minor (Pri/n-$C_{17:0}$) or no relationship (CPI, Pri/Phy) to maturity (R_o). This feature is known for marine organic matter consisting predominantly of algae and deposited in anoxic environments (Philippi, 1965; Powell & McKirdy, 1973). For ca. 70% of the samples of the present study, biomarker ratios determined for crude oils and source rock extracts had already reached their equilibrium values (ch. 4.5.4). Thus, the aromatic hydrocarbon fraction provided the most useful data for establishing a maturity-sensitive oil-source rock correlation. Furthermore and importantly, Leythaeuser et al. (1988) have studied effects on aromatic maturity parameters associated with hydrocarbon expulsion in a natural sample sequence and found no evidence that these parameters are affected by fractionation. However,

simulation experiments involving the mixing of an oil with large amounts of gas at controlled pressure and temperature conditions suggested that for instance biomarker ratios and also methylphenanthrene indices (MPI) indeed are altered during migration (Larter & Mills, 1991; England et al., 1991).

Fig. 66 illustrates that the source rock maturity "window", in which the crude oils may have been released from the source rock, can be defined between ca. 0.8% and 1.1% R_o. For TNR-2, the Billings Anticline crude oils (ER-1, -2, -3) appear to have been expelled in the late zone of this "window" while oil LB refers to the early stage. As regards MPI-1, LB as well as ER-1, ER-2 and ER-3 suggest an early level of expulsion (close to 0.8% R_o). The correlation of oil data with corresponding solvent extract data using MPR-3 implies an even higher maturity level for petroleum expulsion for samples LB, ER-1, ER-2 and ER-3, as the isolines for these oils do not intersect with the trend line for the solvent extract datapoints. Sample BY, however, elucidates a correlation with the source rock bitumen at ca. 0.8% R_o.
Based on the approach above, the determination of a maturity "window" during which the oils have left the source rock system can only be considered an approximation. Clearly, the correlation of crude oil with solvent extract data as depicted in Fig. 66 designates the **minimum** maturity zone in which oil expulsion might have occurred. This is due to the rather broad outline of datapoints deduced from solvent extract analysis. Nonetheless, Fig. 66 implies that the oils were *not* expelled *before* ca. 0.8% R_o. These data, however, have to be evaluated in the light of the experiments by England et al. (1991) who, as already mentioned above, revealed that e.g. MPI ratios are fractionated by phase changes in the course of migration. These authors measured changes in MPI values of +10 to -16%. Such a sensitivity of MPI to fractionation clearly can have some bearing on oil expulsion timing with respect to maturity for the present Bakken oils. The following scenario, for instance, would result in a shifting of the minimum maturity zone for oil expulsion to lower R_o levels: The MPI values determined for the *solvent extract* subfraction are considered to be unaffected by migration-induced fractionation but the values for the *oil* subfractions are considered to be too *high* ("real" values are lower) due to fractionation effects. This would mean that the Bakken oils indeed fall within the maturity zone which is also associated with the main phase of expulsion, as will be discussed below. Nonetheless, there are other strong indications for a high level of maturity of the oils, such as TNR-2 and MPR-3 ratios, API gravity, distribution pattern of saturates and relative composition of cycloalkanes (see below)
Further evidence for a relatively high level of maturity of the crude oils is provided by the relative composition of the cycloalkanes methylcyclopentane, dimethylcyclopentane and methylcyclohexane. These three species belong to the most prominent individual compounds in the thermovaporisation products (Fig. 34) as well as in the crude oils (ch. 4.6.3). Fig. 67 illustrates that the Bakken light ends (t'vap-gc) outline a clear maturity zonation with respect to their relative cycloalkane composition. Equivalent datapoints for the crude oils fall very close to each other indicating that their relative composition in terms of cycloalkanes is almost identical despite the fact that they were produced from fields which regionally are distant to each other. Furthermore and importantly, they plot close to and within, respectively, the high mature field (> 0.8% R_o) of the light ends. Hence, this approach corroborates, what already has been implied from the aromatic parameters MPI-1 and TNR-2 (Fig. 66), namely that Bakken crude oils indeed have not been expelled before 0.8% R_o.

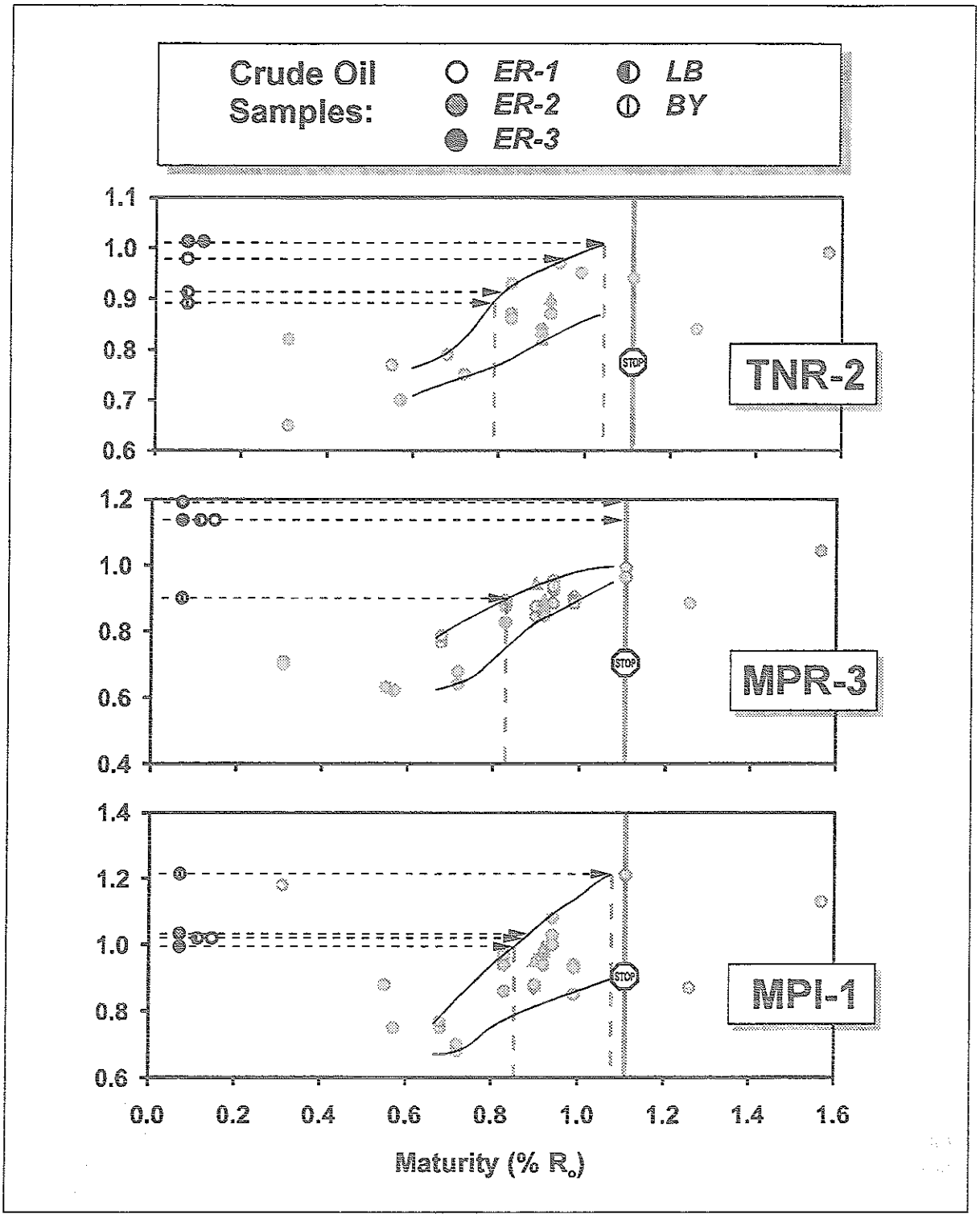

Fig. 66: Maturity-sensitive oil-source rock correlation based on three aromatic maturity parameters (TNR-2, MPR-3 and MPI-1). Arrowlines indicate values of corresponding maturity parameter for crude oils. Dashed vertical lines designate **minimum** maturity interval during which oils may have been expelled from the source rock. Stop sign indicates end of maturity spectrum as evidenced from other maturity parameters (see ch. 4.1.2).

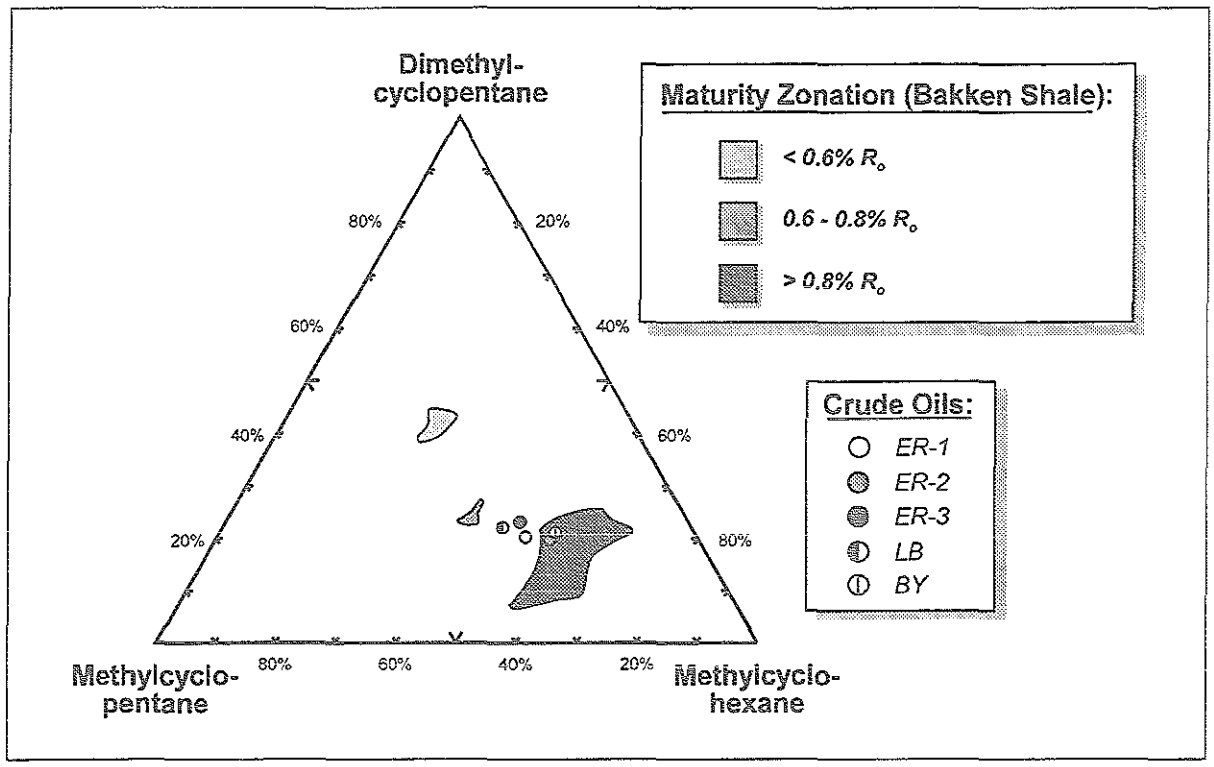

Fig. 67: Composition of thermovaporisation products and Bakken crude oils in terms of relative abundance of cycloalkanes. While the light ends exhibit a clear maturity zonation, the composition of the crude oils remains uniform.

With respect to the correlation approach as outlined above (aromatics, cycloalkanes), it must be pointed out that *post*-generation alteration effects, namely mixing with an oil from a different source like e.g. the Ordovician-Silurian Winnipeg-Red River system of the Williston Basin (Dow, 1974) or in-situ maturation could yield misleading results. However, the Bakken crude oils do not exhibit a distinctive odd-even-predominance of the n-alkanes (Fig. 41) which is known for Ordovician sourced oils (Fowler et al., 1986; Hoffmann et al., 1987). While mixing effects by non-Bakken-sourced petroleum appear to be unlikely in view of the isolated nature of the Bakken petroleum system (Price & LeFever, 1992), the *post*-generation thermal alteration of oils (Connan et al., 1975) would lead to a significant overestimation of the maturity level of the source rock at the time of expulsion. This aspect is evaluated in ch. 5.3.

A larger data base on Bakken oils by Price & LeFever (1994) was examined with respect to oil-maturity and maturity-related oil-source rock correlation. The 14 samples cover a regional area from the Antelope Anticline (township 152) to Billings Anticline area, hence also covering a relatively broad spectrum of source rock maturity (ca. 0.8% to 1.1% R_o). Although Price & LeFever (1994) did not include parameters based on the relationship of individual aromatic hydrocarbons equivalent to the ones of the present study and which have shown to be valuable maturity indicators, it can be stated that their parameters (depicted in Fig. 68) based on molecular characterisation of the saturates fraction (from 0.95 to 0.55 for Pri/n-$C_{17:0}$ and 0.75 to 0.35 for Phy/n-$C_{18:0}$) generally designate an enhanced level of maturation for the oils (Tissot et al., 1971; Tissot & Welte, 1984). A more detailed examination defines certain groups of samples characterised by almost identical Pri/n-$C_{17:0}$ and Phy/n-$C_{18:0}$ ratios. These groups are congruent with oil fields/adjacent oil fields, implying that uniformity in composition and maturity level is

associated with a limited regional/local area, i.e. the outline of an oil field. However, the oils produced from Bicentennial Field (McKenzie/Golden Valley Co.) show relatively high values for Pri/n-$C_{17:0}$ and Phy/n-$C_{18:0}$ ratios (0.81 to 0.96 and 0.62 to 0.75, respectively), suggesting that they were generated at a relatively early level of thermal evolution. According to Price & LeFever (1994) and Price et al. (1984), equivalent Bakken Shale samples from this field revealed very high Rock-Eval HI values (491-535mg/g TOC). Although such an inferred low maturity level of the source rock would explain the low maturity level of the corresponding crude oil, it must be considered a local anomaly as Bakken Shale maturity determinations designate this area as being a high mature zone at ca. 1.0% R_o (Webster, 1984 and present study).

Accordingly, the findings above corroborate what has already been evidenced from the limited sample set of the present study, namely that Bakken crude oils which are regionally associated with the south end of Nesson Anticline, as well as Antelope and Billings Anticline exhibit a uniformly enhanced degree of thermal alteration.

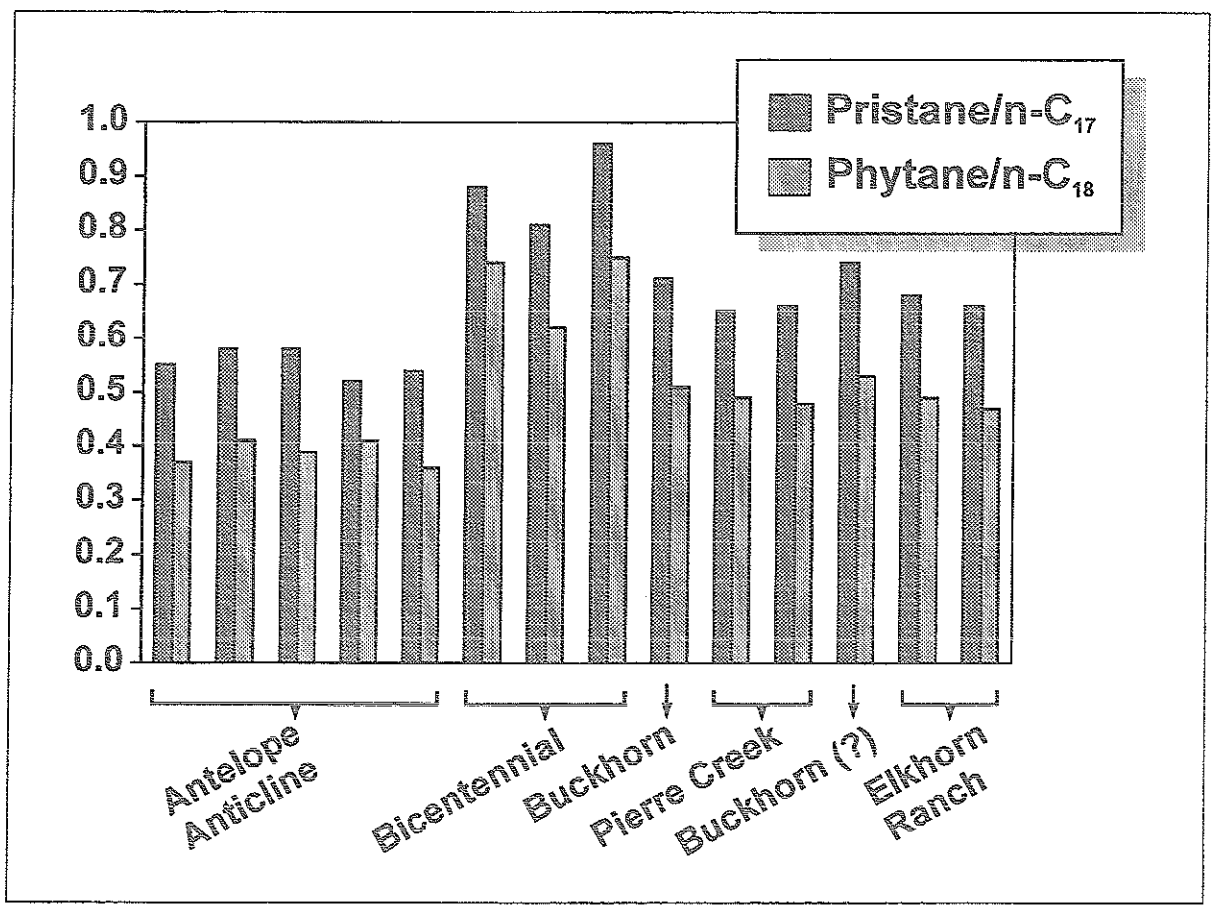

Fig. 68: Compositional data on Bakken crude oils by Price & LeFever (1994). Oilfields cover a regional area from township 152 to the depositional limit of the Bakken Shale in SW North Dakota.

5.2.2 Expulsion Efficiency

The generation of hydrocarbons in thermally mature source rocks is known to be accompanied by its expulsion out of the source rock system. Hence, the concentration - quantitatively as well as qualitatively - of mobile hydrocarbons present in the source rock represent the net result of both processes. At very high levels of thermal evolution, the cracking of oil to gas is introduced as an additional process. In order to assess the extent of expulsion phenomena, its efficiency - both in absolute and relative terms - has to be evaluated.

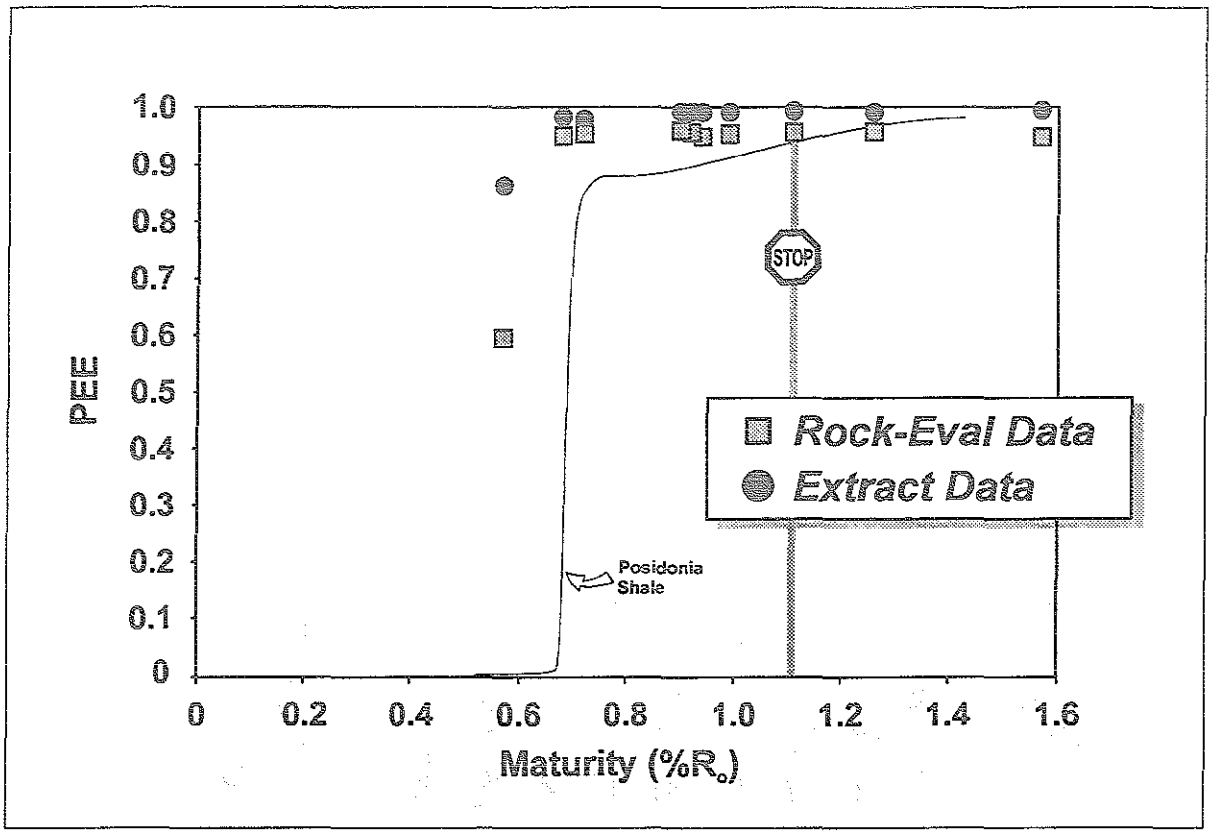

Fig. 69: Maturity related evolution of Petroleum Expulsion Efficiency (PEE) as determined from the algebraic mass balance approach by Cooles et al. (1986) using two different data sources (Rock-Eval pyrolysis and solvent extraction). PEE values of 1.0 are indicative of source rocks which have lost all the hydrocarbons they have generated. Stop sign indicates end of maturity spectrum as evidenced from other maturity parameters (see ch. 4.1.2).

Absolute Expulsion Efficiency

The algebraic mass balancing approach by Cooles et al. (1986) enables conclusions regarding the maturity-controlled degree of organic matter conversion to be drawn. This aspect as well as the general applicability of the model has been dealt with in ch. 5.1. It has been shown that generally the model is valid but it cannot be excluded that yields may be overestimated by max. 22%. The same model also provides quantitative results on the expulsion of generated petroleum ("Petroleum Expulsion Efficiency PEE") based on the concentration of volatile organic matter (Rock-Eval S1 and solvent extract yield, respectively). Fig. 69 illustrates the relationship of PEE

as a function of increasing Bakken Shale catagenesis. Analogous to the PGI plot (Fig. 56), the trends outlined for both types of data (Rock-Eval and solvent extract) are very similar. For the sample at 0.55% R_o, however, PEE is distinctly higher for the extract data set. At maturity levels higher than 0.6% R_o, the expulsion efficiency expressed as PEE appears to be uniformly high (ca. 0.95).

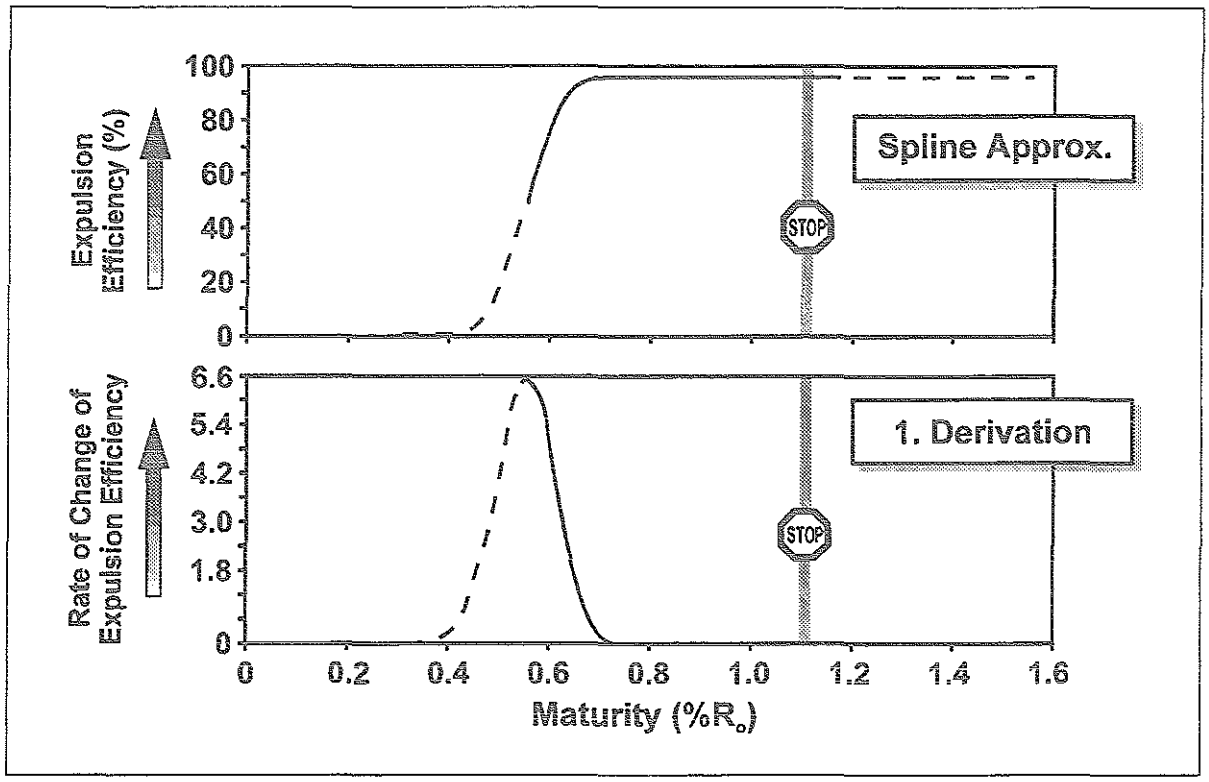

Fig. 70: Top diagram displays spline curve plotted vs. R_o as obtained from Fig. 69 (PEE vs. R_o) for Rock-Eval data set. Bottom diagram depicts first derivation of spline curve plotted vs. R_o. Curve is equivalent to rate of hydrocarbon expulsion. Dashed line in both diagrams indicates portion of curve which was extrapolated to reference sample at 0.31% R_o. Stop sign indicates end of maturity spectrum as evidenced from other maturity parameters (see ch. 4.1.2).

Analogous to the PGI data, the spline curve for PEE datapoints from the Rock-Eval data set was determined and, in a second step, this curve was differentiated (Fig. 70). Although the overall shape of both curves appears to be very similar to the ones based on PGI data (Fig. 57), their relationship to level of thermal evolution bears significant differences: Firstly, expulsion efficiency has reached 95% at ca. 0.6% R_o implying that 95% of the mobile hydrocarbons initially present have been lost due to expulsion. Hence, the efficiency of releasing mobile organic matter increases drastically over a short range of maturation. Beyond 0.6% R_o, only a very small amount of the generated compounds (ca. 5%) are not expelled but remain in the source rock system. It must be noted, however, that the slope of the spline curve cannot be assessed accurately for the maturity interval 0.31% R_o (reference well) to 0.55% R_o due to the lack of further samples (indicated by dashed line). Secondly, the rate of change of petroleum expulsion efficiency was highest at ca. 0.55% R_o. Beyond that level of maturity, the rate decreases rapidly to values close to zero (at ca. 0.7% R_o), i.e. uniformly very high efficiencies. If these results are correlated with well location (Fig. 71), it becomes apparent that Bakken Shales sampled from wells in the

Nesson Anticline (incl. Antelope Anticline) and Billings Anticline area must have lost ca. 95% of the total oil generated, as they are already beyond the stage of active and efficient removal of products. This is consistent with results presented by Cooles et al. (1986) for other source rocks who found that high expulsion efficiencies are associated with high *initial* organic richness. Sweeney et al. (1992), who made a similar calculation using Rock-Eval S1 data, also came to the conclusion that expulsion is extremely efficient in the Bakken Shale.

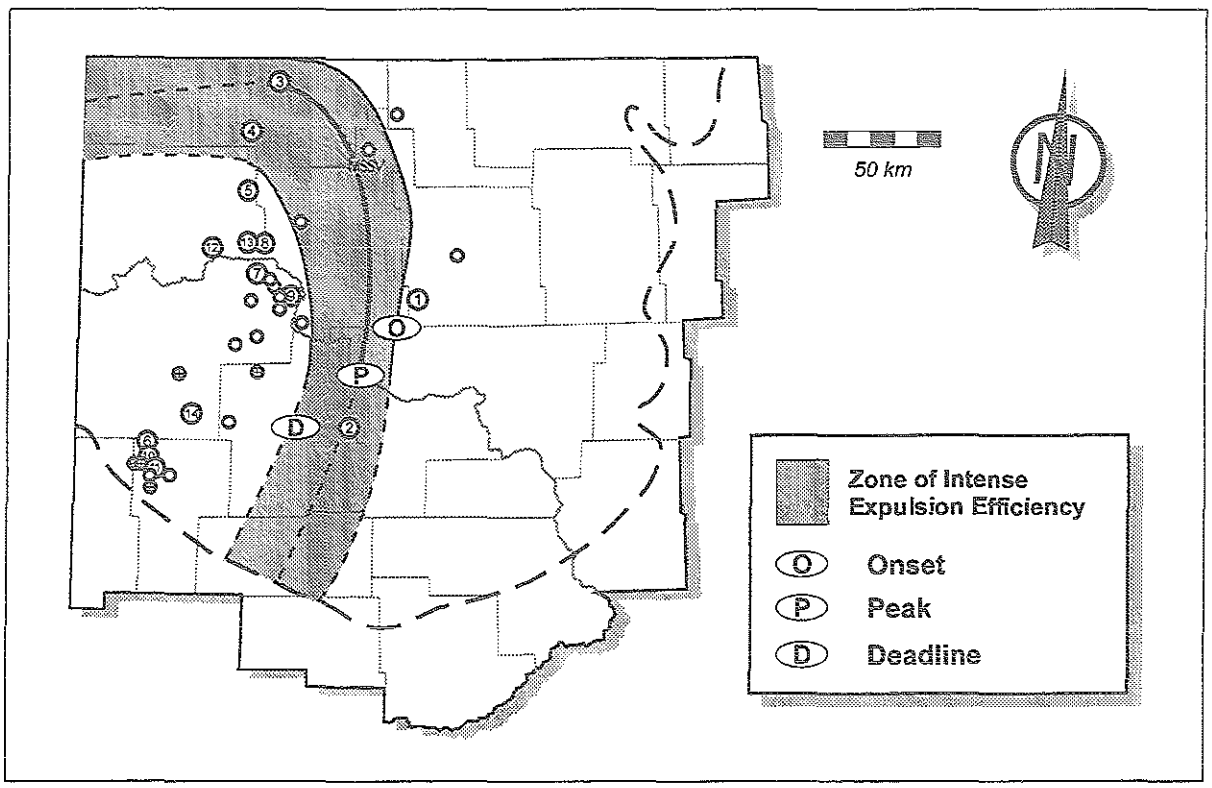

Fig. 71: Map of the study area modified after Webster (1984). Dots refer to well locations of the selected sample set of the present study. Highlighted zone designates maturity interval which is associated with the main stage of petroleum expulsion as determined by mass balance calculations (Cooles et al., 1986).

Fig. 72 elucidates the relationship of expulsion efficency (PEE) to organic matter conversion (PGI). Interestingly, the diagram shows that despite a low level of petroleum generation (PGI of ca. 0.2 ≅ 20% organic matter transformation), expulsion already is very efficient (PEE of ca. 0.6 and 0.85 ≅ 60 and 85% expulsion efficiency). In contrast, the source rock sequences as investigated in Cooles et al. (1986) (e.g. Kimmeridge Clay, North Sea) showed high degrees of petroleum expulsion only at enhanced levels of organic matter transformation.
The extent of petroleum expulsion efficiency in the Bakken source rocks was also investigated by Burrus et al. (1994a; 1994b) using a 2d basin modeling package: These simulations also showed that expulsion efficiency from the Bakken Shale can be very high (0.85). These authors have related this phenomenon to the low Bakken matrix porosity (Ropertz, 1994), i.e. the low storage capacity and hence provide an alternative to the recent proposal by Price & LeFever (1992) who postulated that the mismatch between petroleum generation potential of the Bakken source rock and actually discovered reserves is due to petroleum losses during drilling operations.

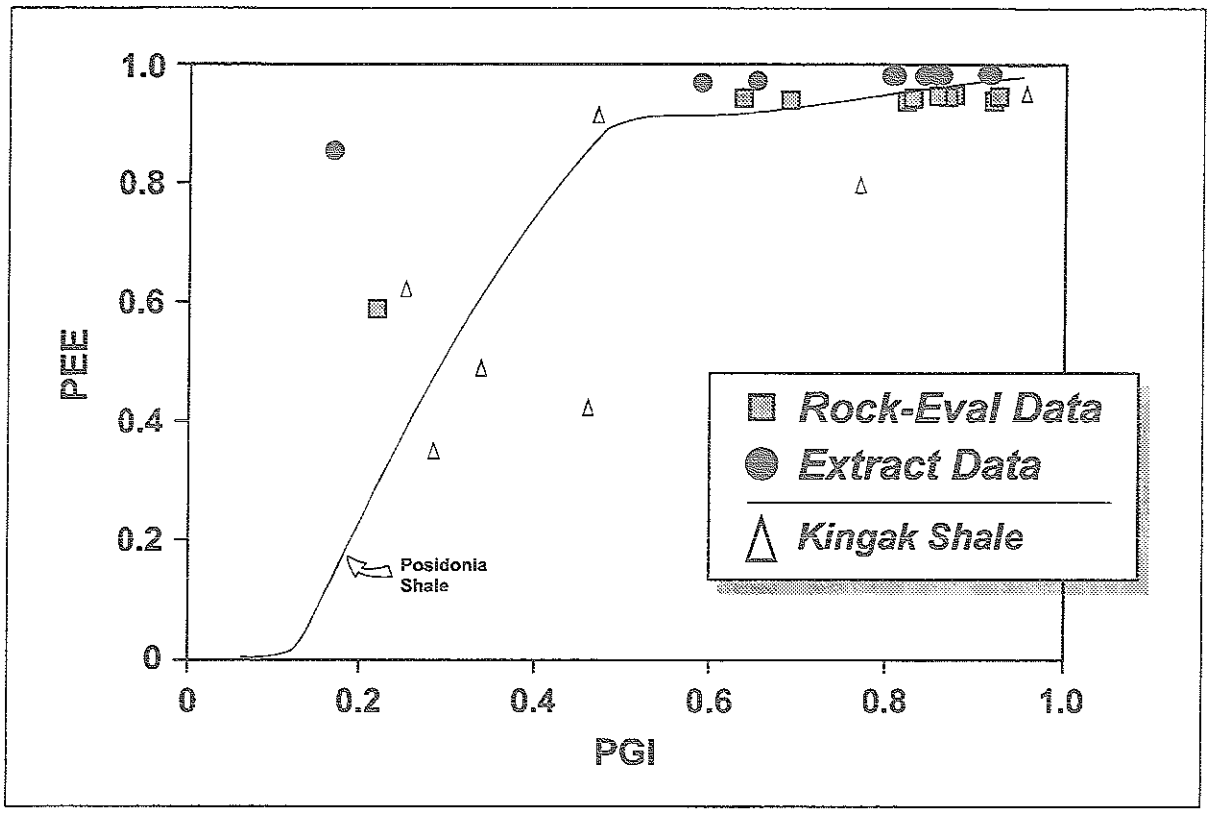

Fig. 72: Relationship of expulsion efficiency (PEE) to degree of organic matter conversion (PGI) based on the algebraic approach by Cooles et al. (1986).

Clearly, such an efficient removal of newly formed products can only be achieved by the combination of suitable migration pathways and/or type of mechanism. The fundamentally important question is: What kind of combination of pathway and mechanism is efficient enough to set the scene for comprehensive and rapid release of petroleum? This issue is evaluated at the end of this section.

As laid out above, calculations using the algebraic scheme developed by Cooles et al. (1986) are based on quantitative analytical data representing *average* values of individual wells. However, as regards solvent extractable organic matter, individual wells are characterised by a high variability of data (Fig. 23). For instance, samples from the lower shale units of wells MAR and JEN (0.9% and 0.92% R_o, respectively) yielded considerably higher amounts of extract than equivalents from the upper shale of the same well. Thus, averaging such data would not take into account characteristics associated with either of the two strata of these particular wells and, most importantly, expulsion efficiencies would be overestimated.

In order to address this issue, calculations were performed on individual samples using the mass balancing program PROSPECT ANALYZER® that is principally based on the work of Larter (1985). Similar to the model by Cooles et al. (1986), the program utilizes standard organic geochemical analytical data (Rock-Eval, solvent extract yield) in order to predict, amongst other parameters, masses of petroleum expelled from source rocks (expulsion efficiency). In order to evaluate the comparability of the two models, calculations were performed using the PROSPECT ANALYZER® with the same input data set (averaged values) as used for the Cooles model. These test runs yielded basically the same results with only negligible discrepancies. Tab. 14 gives expulsion

efficiency for selected individual Bakken Shale samples from wells of different maturity levels as calculated by PROSPECT ANALYZER®. For most of the samples, expulsion efficiency is very high (ca. 85% to 95%). This is consistent with the results deduced from the model by Cooles et al. (1986). Two samples from the lBK of wells MAR and JEN, however, have markedly lower expulsion efficiencies (63% and 75%, respectively), as could be expected from their atypically high extract yields. Hence, the results derived from the PROSPECT ANALYZER® mass balancing indicate differences in expulsion/migration phenomena between the two shale units which could not be assessed by an approach using averaged data.

Table 14: Results derived from mass balancing using the PROSPECT ANALYZER® (reverse mode) for Rock-Eval and solvent extract input data. EOM refers to 'extractable organic matter'. Well numbers refer to location of sampled wells in Fig. 6.

Well name (#)	FED (11)	THO (14)	MAR (8)	MAR (8)	JEN (9)	JEN (9)
R_o (%)	0.99	1.57	0.9	0.9	0.92	0.92
Sample ID, shale unit	(average, uBK)	(E 34362, uBK)	(E 34328, lBK)	(E 34322, uBK)	(E34455, lBK)	(E 34449, uBK)
TOC (wt.-%)	11.2	11.9	8.2	13.3	8.9	10.4
S2 (mg/g rock)	23.1	11.7	9.2	19.0	11.6	16.8
S1 (mg/g rock)	3.9	5.2	4.4	4.4	4.9	4.6
EOM (mg/g TOC)	150.0	80.0	360.0	140.0	270.0	100.0
S1/EOM	0.0	0.1	0.0	0.0	0.0	0.1
Results (pyrolysis):						
expelled petroleum (mg/g rock)	103.5	136.3	89.4	142.6	93.1	104.2
expulsion efficiency (%)	96.1	96.1	95.0	96.8	94.7	95.5
Results (EOM):						
expelled petroleum (mg/g rock)	95.3	155.6	43.3	138.1	64.2	114.0
expulsion efficiency (%)	86.4	94.7	63.4	89.1	75.3	92.3

Fig. 73 addresses this phenomenon from a different point of view, as it displays solvent extract yield as a function of genetic potential (Rock-Eval HI) of solvent extracted Bakken Shale samples. Although the hydrocarbon generation potential of the residual kerogen, as expressed in HI, is essentially the same for both shale strata from wells MAR and JEN (between 112 and 148mg/g TOC for MAR and from 131 to 161mg/g TOC for JEN), bitumen concentrations are highly variable. With the prerequisite that kerogen quality and, consequently, hydrocarbon formation potential were uniform during deposition of the Bakken Shale (ch. 4.4), this phenomenon implies that expulsion and migration occurred preferably in the upper member of a given well, whereas in the lower member, it remained in-place. Alternatively, as both wells are from the Nesson Anticline area, where Bakken crude oil is produced predominantly from the Sanish Sandstone directly underlying the lBK (Meissner, 1978), high extract contents in the latter could also be the result of impregnation by hydrocarbons reservoired in the Sanish.

Whatever the reason is for this occurrence, it clearly bears important implications with respect to the Bakken oil play and its postulated "in-source reservoir" character (Price & LeFever, 1992). If the phenomenon of an in-source reservoiring indeed can be attributed to the *lower* Bakken Shale and this hypothesis could be extended on a basinwide scale, then the lower shale unit might be designated the principal exploration and production target in the Bakken Formation. In order to test the validity of such a hypothesis, however, a larger and specific sample set is required.

In summary, the generalized rule of high expulsion rates on a regional scale has to be questioned in the light of locally restricted occurrences of accumulation of petroleum in the Bakken Shale. The feature of locally enhanced yields of products in the source rock will be reconsidered in ch. 5.3.

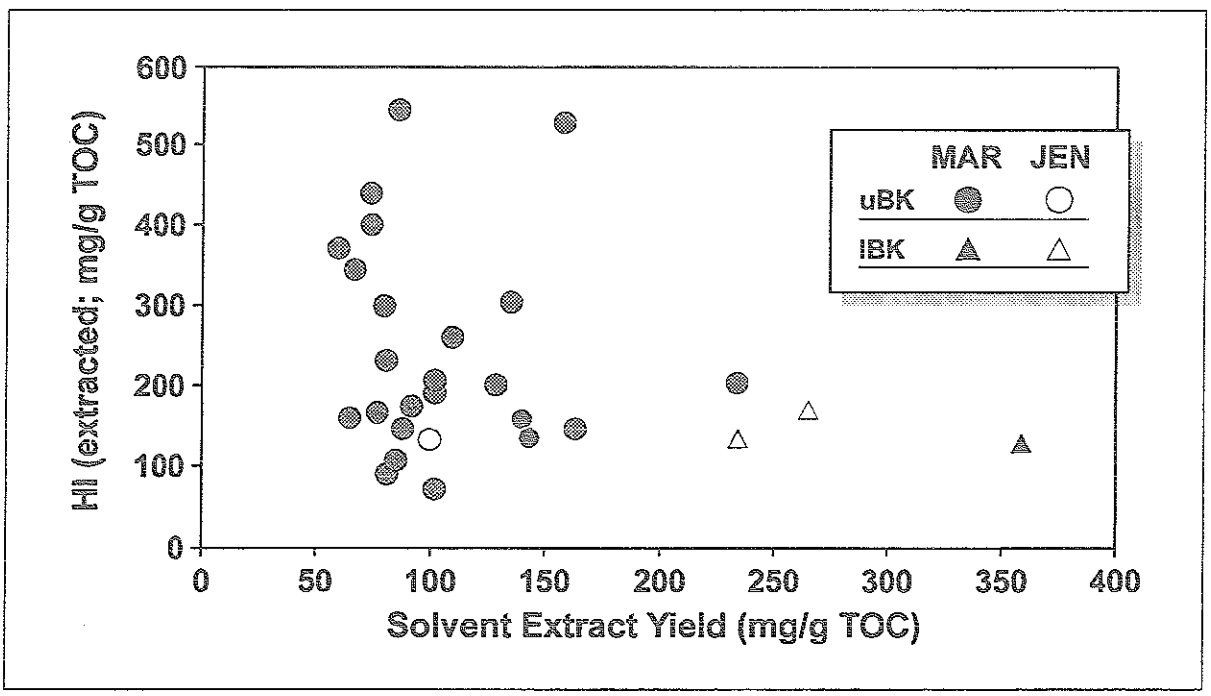

Fig. 73: Cross-plot of hydrocarbon generation potential of Bakken Shale kerogens (Hydrogen-Index) vs. content of mobile organic matter (solvent extract). Triangles refer to lower shale unit of a given well, circles to the upper unit (solid: well MAR, 0.9% R_o; hollow: well JEN, 0.92% R_o). For other wells, samples were available only for either of the two shale strata.

Relative Expulsion Efficiency

Expulsion efficiencies as determined by a quantitative comparison of one or more samples with a reference sample of the same kerogen type is a valuable tool to recognize, in relative terms, migration mechanisms and fractionation effects associated with petroleum expulsion (Mackenzie et al., 1983; Leythaeuser et al., 1984). In several studies, this approach mostly has been applied to sedimentary sequences where organic rich shales of variable thickness are interbedded with sandstone strata. In contrast to the method by Cooles et al. (1986), where all calculations are referred to the concentration of inert kerogen, which, in turn, is assumed to be a constant datum

during hydrocarbon generation, the scheme of Relative Expulsion Efficiency (REE) involves the selection of a reference sample which appears to be relatively untouched by expulsion and fractionation effects, on a bulk as well as on a molecular level. All other samples ("SAMPLE") are related to this reference sample ("REFERENCE") in the following way (Mackenzie et al., 1983), yielding relative expulsion efficiencies in %:

$$\frac{REFERENCE - SAMPLE}{REFERENCE} \times 100$$

Accordingly, positive values for REE can be interpreted as relative expulsion (i.e. depletion), negative values as accumulation (i.e. enrichment). Clearly, it is assumed that all differences observed between the unmodified reference sample and the sample under study are related to expulsion and not to other phenomena (variations in generation potential, maturity, mixing effects etc.).

Although the approach of relative expulsion efficiency is applicable to total extract, extract fractions as well as individual compound groups and compounds, hence proving its versatility, meaningful results deduced thereof highly depend on the selection of the correct reference sample. On the bulk compositional level, criteria such as absolute extract yield, bulk composition of extract (e.g. ratio of hydrocarbons to nonhydrocarbons) as well as the evaluation of local petrophysical characteristics of the corresponding rock sample (porosity, permeability) which may enhance or impede expulsion processes, have to be carefully considered. On a molecular level, the concentration of individual compounds and the distribution pattern ("completeness") of a gas chromatogram (light vs. heavy range) are additional features which have to be taken into account. In the present study, the proper selection of the reference sample was difficult. In some cases, samples which could be considered "unmodified" on a bulk compositional level (e.g. solvent extract yield), exhibited characteristics on a molecular level qualifying them as "depleted/enriched". Therefore it was not possible to select *one* reference sample for all types of sample material (total extract, subfractions and compound groups/compounds. Moreover, in related publications (e.g. Leythaeuser & Schwarzkopf, 1986; Leythaeuser et al., 1988; Mackenzie et al., 1988), this scheme was applied mostly to directly adjacent source rock/reservoir sequences, which had been sampled at frequent intervals in the vertical direction. In these studies it was crucial that samples from the reservoir unit were also available in order to establish vertically orientated depletion pathways. Unfortunately, the sample set of the present study neither includes Bakken Shale samples of the boundary zone close to the adjacent strata (Devonian Three Forks, mBK, Mississippian Lodgepole) nor enough equivalents from the latter. Therefore, it might be too speculative to interpret the results of this approach in terms of expulsion directions. However, solvent extract data on a single Bakken Shale core (Price, 1989) has shown no detectable concentration gradient of resins or asphaltenes towards the contact zones of the shale members with the over- and underlying units.

In the present study, the approach of relative expulsion efficiency was applied to the n-alkane and aromatic compound group (GC traces) of Bakken Shale solvent extracts. The results are displayed in Figs. 74 to 75.

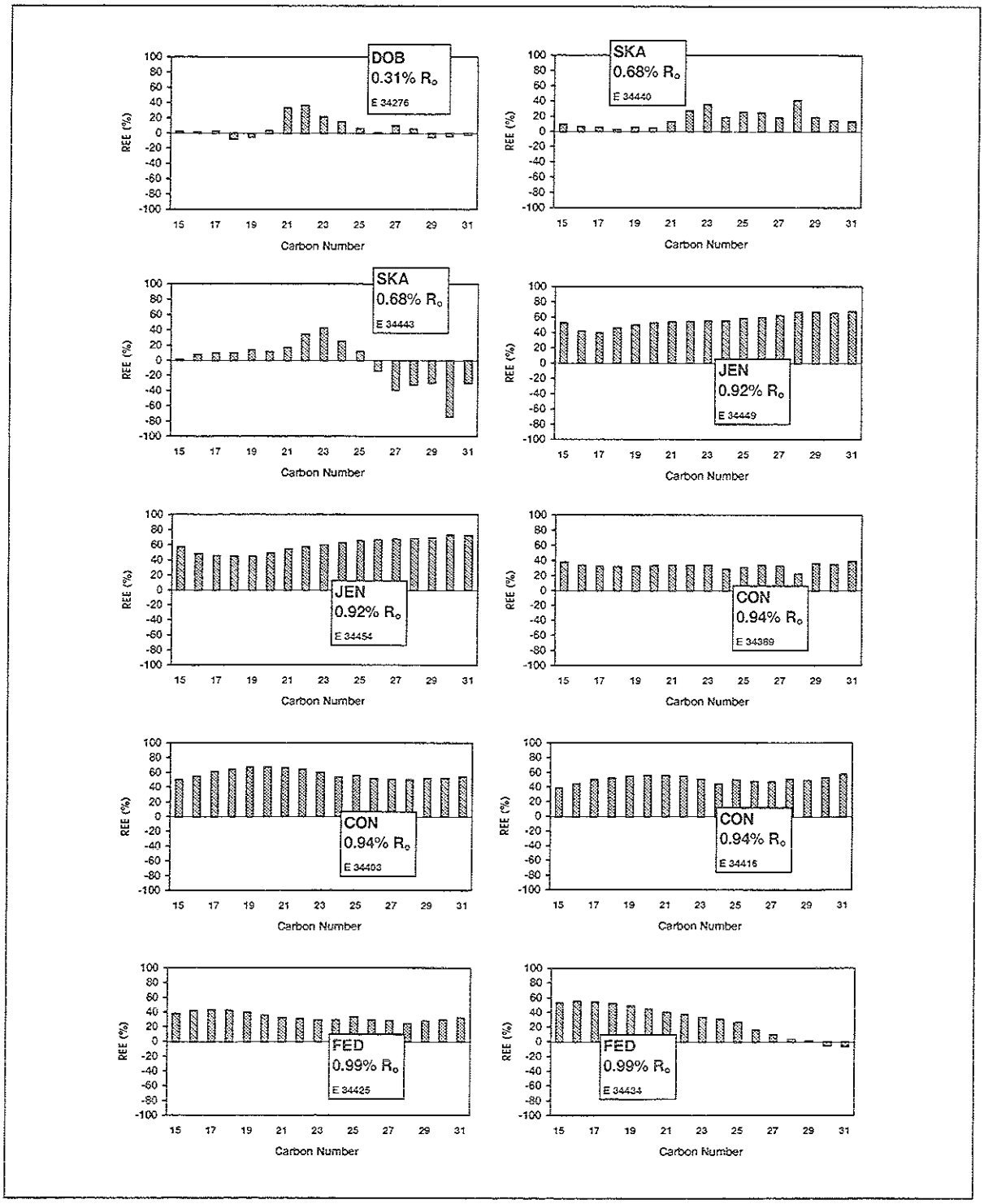

Fig. 74: Relative Expulsion Efficiency (REE; Mackenzie et al., 1983) for straight chain hydrocarbons as derived from solvent extracts of wells covering the entire maturity spectrum. Positive REE values represent relative expulsion, negative relative accumulation. Note the change in distribution pattern between 0.68% (SKA) and 0.92% R_o (JEN). CON (0.94% R_o) represents a horizontal well.

Fig. 74 shows the relative expulsion efficiency (REE) of n-alkanes as determined for individual samples of a given well/maturity level. Clearly, only those wells were selected for which at least two samples were available. Based on the distribution pattern, two groups of samples/wells,

equivalent to two maturity zones, can be discriminated: The first category includes samples from wells up to 0.7% R_o (DOB, 0.31% R_o and SKA, 0.68% R_o). The patterns exhibit considerable internal variability indicating that, relative to the reference sample, expulsion as well as accumulation varies. For the carbon number range 15 to 20, values are close to zero, implying that neither relative depletion nor enrichment has occurred for medium-weight n-alkanes. For long-chain hydrocarbons ($>C_{20}$), relative expulsion efficiencies reach maximum and minimum values of +50% and -50%, respectively. In summary, the low maturity zone (0.31% to 0.68% R_o) is characterised by redistribution phenomena affecting specific narrow carbon number ranges ($C_{15\text{-}20}$, $C_{21\text{-}25}$, $C_{26\text{-}31}$).

The second category incorporates more mature samples/wells (>0.9% R_o): Here the values for REE range between ca. 30% to 70% implying that quantitative redistribution occurs on a relatively large scale within individual wells of this maturity zone. Furthermore and importantly, compound-specific fractionation effects seem to be negligible in this zone of thermal evolution, as all n-alkanes of a given sample have principally the same values for REE. One sample of well FED, however, reveals a slight decrease in expulsion efficiency with increasing chain-length, indicating that C_{15} to C_{25} n-alkanes are preferentially expelled relative to the reference sample. The patterns of well CON are supposed to shed some light on lateral redistribution features, as these samples are derived from the *horizontal* portion of well CON. Hence, while these samples reveal the same compositional features (medium to high expulsion efficiencies, no major compound-specific fractionation effects) as samples from vertical wells, it may be justified to conclude that expulsion-related effects are similar in lateral as well as in vertical directions.

Corresponding distribution patterns for aromatic hydrocarbons (Fig. 75) don't suggest the maturity zonations as evidenced for the straight-chain alkanes: Here, relative expulsion efficiencies for any level of maturation appear to be rather low (20 to 30%), except for a few individual compounds. The sample from the most immature well (0.31% R_o), however, outlines a relatively heterogeneous pattern in that relative expulsion/accumulation varies significantly from one individual aromatic to the other. Except for this sample, the aromatic hydrocarbons of the Bakken Shale apparently were not submitted to major redistribution processes. Aromatic hydrocarbons therefore appear to have remained in the source rock system relative to n-alkanes which have been released preferably. This has also been observed for the Brae field area in the North Sea (Leythaeuser et al., 1988).

This difference in expulsion preference indeed is reflected by the bulk/molecular composition of the thermovaporisation products vs. Bakken crude oils. The thermally released mobile phase contains relatively high concentrations of aromatic hydrocarbons (Figs. 34 and 38) especially at low maturity levels. In contrast, the bulk composition of crude oils produced from Bakken reservoirs reveals a rather low abundance of aromatics in the the C_{15+} material (Fig. 24) as well as in the light fraction (Fig. 42).

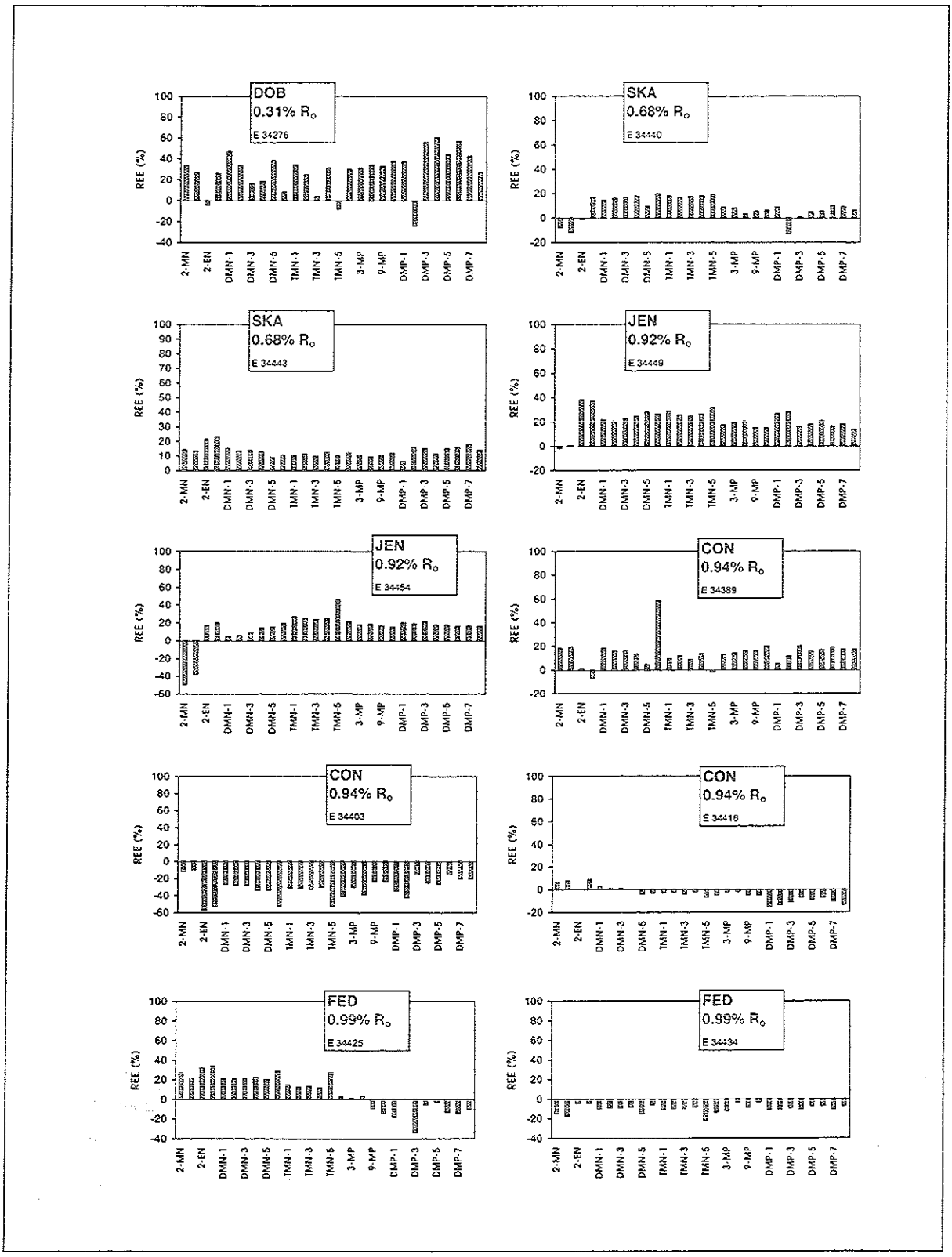

Fig. 75: Relative Expulsion Efficiency (REE; Mackenzie et al., 1983) for aromatic hydrocarbons as derived from solvent extracts of wells covering the entire maturity spectrum. Positive REE values represent relative expulsion, negative relative accumulation. CON (0.94% R_o) represents a horizontal well.

The quantitative determination of the effects of expulsion/migration in a natural source rock system is always very difficult because it typically represents an open system. Mass balance approaches involving the volatile, mobilisable organic matter constituents are affected by removal of the latter during migration. Furthermore, expulsion/migration is a dynamic process and its quantitative dimension varies in the course of natural maturation. Although the material loss from the system during migration can be overcome by the closed system pyrolysis approach applied in the laboratory for artificially maturing organic matter (Monthioux et al., 1985; Horsfield et al., 1989), additional information is required for accurately predicting composition and *quantitative concentration* of newly formed hydrocarbons and residual kerogen in a source rock for a given level of maturity. That means that a maturity sequence artificially created in the lab ought to be applied to the framework of the natural maturity sequence.
Such a concept is especially favorable in the Bakken petroleum system, as it exhibits important features (ch. 1.1): Uniformity in kerogen type is accompanied by a broad natural maturity spectrum. Additional to these attributes there is strong evidence that the Bakken petroleum system is unaffected by petroleum fluids from sources other than the Bakken Shale. Furthermore, the unusual occurrence of high amounts of inferred adsorbed gas (ch. 5.1.3) was introduced as a further interesting feature in the course of the present study. The latter enables the comparison of artificial with natural products in terms of bulk molecular composition of light ends.

In the natural sequence (thermovaporisation products), selected evolutionary trends and/or compositional features have been shown to be diagnostic for a specific level of maturity: (1) Evolution of aromaticity of the residual kerogen (Fig. 64); here, a sharp drop in the ratio of aromatics vs. C_{6+} n-alkanes is associated with vitrinite reflectance of ca. 0.6%. (2) Product-residue relationship as regards yield of monoaromatics (Fig. 52); in this case, both trends cross-over at ca. 0.8% R_o.
If such maturity-sensitive parameters derived from natural maturation can be detected in the maturity sequence created in the laboratory, they may be useful in order to calibrate the latter. Accordingly, Fig. 76 depicts both parameters for the artificial maturation sequence. As regards aromaticity, the MSSV pyrolysis residue indeed exhibits a significant decrease between the two stages of 300°C/2 days and 300°C/5 days. For the rest of the series the value for aromaticity remains essentially constant.
With respect to the yield of monoaromatics for MSSV pyrolysis products and residues (Fig. 76, bottom), the curves for both datapoint groups merge together between the artificial maturation levels 350°C/1 day and 350°C/2 days. Clearly, the significance of this parameter is not unambiguous, as its assessment in the natural system involves data from the products which may have been perturbed by expulsion and migration processes. This finding is of particular importance in the light of high expulsion efficiencies encountered in the Bakken Shale. Nonetheless, it may be justified to relate the artificial maturity zone ranging from 350°C/1 day to 350°C/2 days to a stage of natural thermal evolution of ca. 0.8% R_o. Hence, by using the *aromaticity* parameter for low levels of maturation (deflection in trend for both systems at 0.6% R_o and 300°C/2-5 days, respectively) and the *product/residue* parameter for higher stages of maturation (cross-over in both systems at 0.8% R_o and 350°C/1-2 days), one is able to define the

calibration scheme in Tab. 15 (maturity zonation ①, ② and ③) which, of course, should only be considered an approximate framework.

Table 15: Maturity zonation approach defined by maturity level specific parameters common in both the natural and artificial system of the Bakken Shale.

	Natural Maturation		*Simulated Maturation*
Zone ①	0.3% to 0.6% R_o	⇨	RT to 300°C/2-5 days
Zone ②	0.6% to 0.8% R_o	⇨	300°C/2-5 days to 350°C/1-2 days
Zone ③	> 0.8% R_o	⇨	> 350°C/1-2 days

Before using this framework for quantitative prediction of products, its validity is tested against the evolution of the *natural* residual kerogen (py-gc). Fig. 77 displays the corresponding diagrams for total yield of pyrolysate and its subfractions (C_{1-5}, C_{6-14} and C_{15+}). Range of equivalent values of artificially heated kerogens (MSSV) are superimposed for each maturity zone. As regards the total yield of pyrolysate, there is indeed a rather good match between absolute yields for the natural and artificial series suggesting that the inferred boundaries for the maturity zones are correct and the approach is valid. However, it must be stated that this good agreement is less pronounced for the gaseous hydrocarbons (C_{1-5}) whereby the naturally matured kerogens consist of more gas-yielding moieties than the artificially heated ones. This is especially true for the first two maturity zones. Nonetheless, the general maturity trend of the natural system indeed is traced by the laboratory system: In the course of natural thermal evolution, the gas yielding proportion of the Bakken kerogen is submitted to the lowest degree of transformation of all subfractions, as evidenced by an only gradually decreasing amount of equivalent pyrolysate. This phenomenon is also reflected by the MSSV pyrolysis residues. The medium and heavy pyrolysates, finally, reveal a good to moderate congruency of natural and laboratory system.

As laid out above, the natural and the artificial maturity sequence of the Bakken Shale residual kerogen (py-gc) have quantitative as well as qualitative bulk compositional properties in common which allow to calibrate the artificially heated series and define maturity zones adopted from natural thermal evolution. This serves as a further indication that the method of MSSV-type simulated maturation (Horsfield et al., 1989) indeed mimics naturally occurring thermal degradation of kerogen, although excess water was not involved during pyrolysis. A large excess volume of water ("hydrous pyrolysis", Lewan et al., 1979) or confinement of reactants and products ("confined medium pyrolysis", Monthioux et al., 1985) were believed to be a prerequisite for successful simulation of natural reaction pathways.

With respect to the products, there are considerable discrepancies in concentration of products between the natural (inferred open system) and the lab system (closed system), especially in the high mature zones, as shown by Fig. 78: For the low mature zone, however, there is good agreement between both systems for total response (C_{1+}). As maturation proceeds in both systems, however, evolutionary trends follow different pathways: In the closed system, yields drastically rise, whereas in nature the average concentration remains virtually constant with a high

variability of data. Interestingly, the "endmember" of the simulated maturity sequence exhibits a yield which is almost three times as high as the highest concentration of products in the natural sequence (well FED at 0.99% R_o). The pattern is similar for the subfractions: Both trends diverge significantly from 0.6% R_o on. The latter feature is even more pronounced for the gases (C_{1-5}) as their yield is submitted to a sharp drop in the second maturity zone (0.6% to 0.8% R_o). The distribution pattern is almost identical for the medium (C_{6-14}) and high molecular weight (C_{15+}) material. Here, natural Bakken Shale products are characterized by uniformly high yields throughout maturation, while yield in the lab system increases continuously.

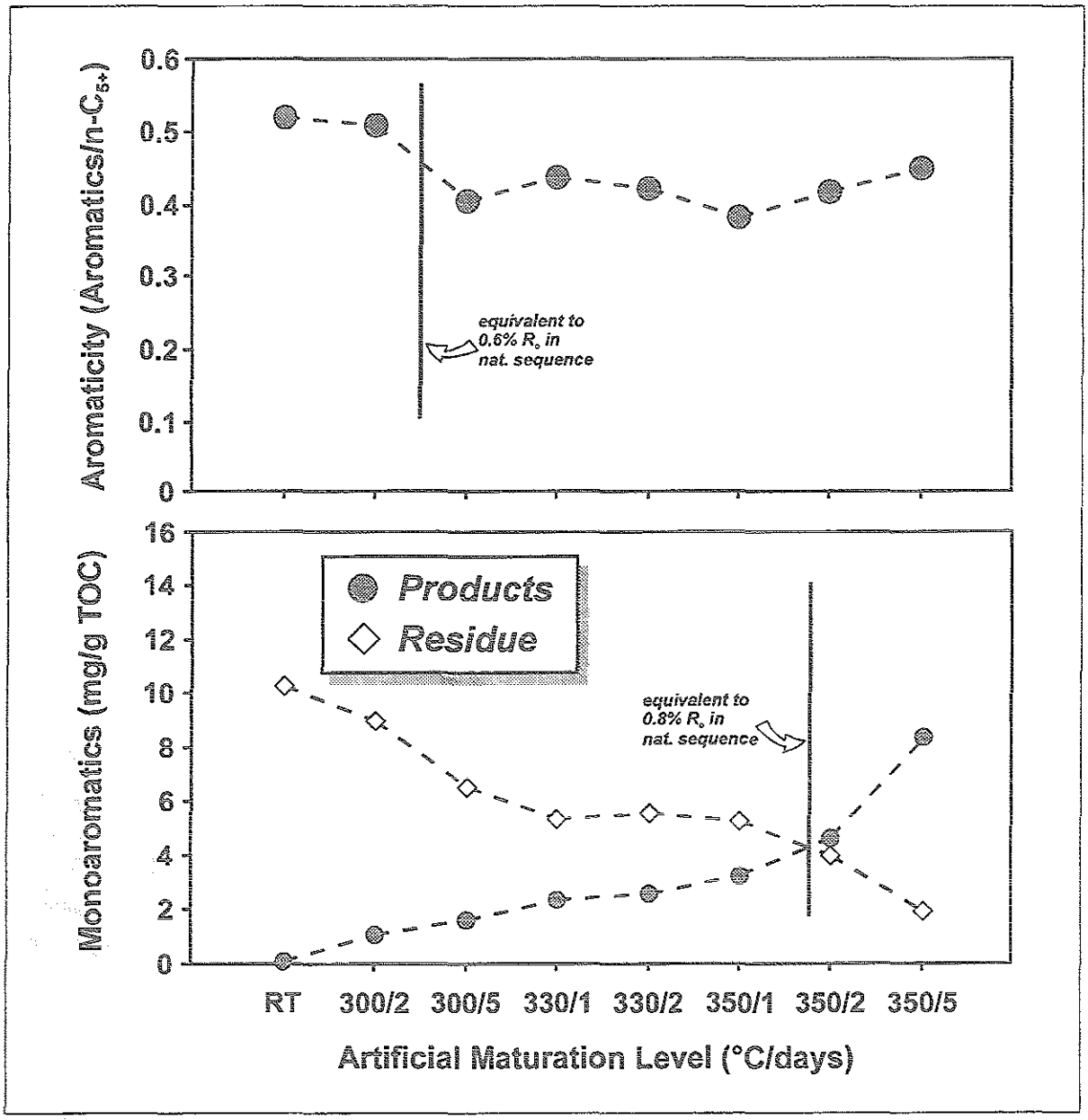

Fig. 76: Compositional evolution of artificial maturity sequence (MSSV approach) for two parameters. Top diagram shows fate of aromaticity of the residual kerogen as a function of level of artificial maturation. The ratio "aromaticity" was determined as in Fig. 64. Bottom diagram depicts product/residue relationship with respect to yield of monoaromatics (sum of benzene, toluene, ethylbenzene, meta-/para-xylene, orthoxylene, C_3-benzene and 1,2,3,4-tetramethylbenzene).

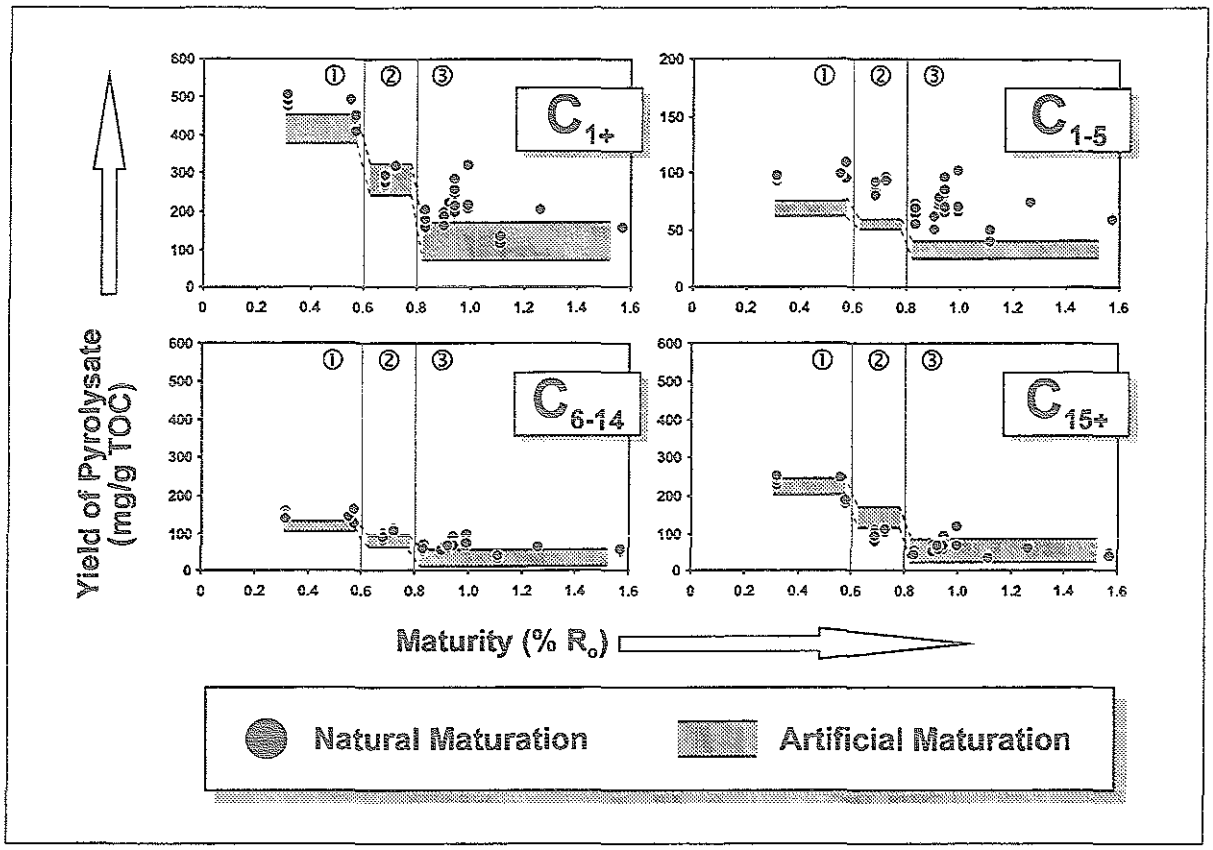

Fig. 77: Yield of total pyrolysate (C_{1+} and subfractions C_{1-5}, C_{6-14} and C_{15+}) of natural Bakken Shale maturity sequence (py-gc) as a function of thermal evolution (% R_o). Shaded areas denote range of equivalent data derived from analysis of artificially matured Bakken kerogen. Approximate boundaries for maturity zones are determined using maturity sensitive parameters of Fig. 76.

The maturity zone during which natural and artificial maturity trends diverge is coincident with the main phase of hydrocarbon generation and expulsion in the natural system. This serves as a further indicator that the zonation approach is valid. Hence, it may be justified to calculate the amount of generated products which actually have been removed from the source rock system by subtracting the concentration of naturally present hydrocarbons from the amount of artificially formed ones. Clearly, such a relative mass balancing approach can only be carried out for each maturity zone. Furthermore, for each zone one has to select that sample of the natural system which revealed the highest yield of products. This sample is considered being the least depleted equivalent of the respective natural maturity zone. The corresponding value is balanced against the lowest value of the corresponding artficial maturity sequence. Choosing the lowest value for the closed system sample is of particular importance for high levels of simulated maturation: As already outlined above, there is some evidence that the products derived from the most severe stages of artificial maturation have been modified by secondary cracking reactions in that oil-like components are cracked to gaseous compounds (Fig. 45). The drastic increase in gas yield (30 times as much than at the starting level) paralleled by a more smooth increase of "oil" (5 times as much C_{6+} material than at the starting level) may also illustrate that effect.

In that way, one obtains the **minimum** difference between the natural and artificial system for each maturity zone. Analogous to the approach by Mackenzie et al. (1983), the following

equation can be used in order to determine the minimum extent of removal (abbreviated in the following as "EXR"):

$$\frac{CLOSEDSYSTEM_{min} - NATURALSYSTEM_{max}}{CLOSEDSYSTEM_{min}} \times 100$$

The results are listed in Tab. 16. For the total yield of products, the immature zone (zone ①) of the natural system is enriched in products relative to the closed system. The other two zones which are associated with comprehensive generation and release of hydrocarbons in nature, indeed reflect a difference in masses between both systems (33.7% for zone ② and 45.5% for zone ③).

Table 16: Results from mass balancing of the natural and artificial system using maturity zonation approach for bulk compound groups. CS_{min} refers to the minimum yield of the respective compound group of the artificial (closed) system, NS_{max} to the maximum yield of the respective compound group of the natural system. EXR is calculated according to the equation as displayed in the text.

Fraction	Zone	CS_{min}	NS_{max}	EXR (%)
C_{1+}	zone ①	49.6	83.0	-67.3
	zone ②	82.9	55.0	33.7
	zone ③	172.8	94.1	45.5
C_{1-5}	zone ①	2.3	6.9	-200.0
	zone ②	7.5	6.0	20.0
	zone ③	29.3	3.3	88.7
C_{6-14}	zone ①	8.9	47.0	-428.1
	zone ②	23.5	31.3	-33.2
	zone ③	70.5	50.3	28.7
C_{15+}	zone ①	38.4	30.7	20.1
	zone ②	51.9	19.8	61.8
	zone ③	73.0	43.2	40.8

This pattern is similar for the subfractions. Zone ① is characterised by an enrichment of naturally generated products relative to the artificial maturation sequence. This is most pronounced for the medium boiling range (C_{6-14}). A noteworthy feature can be observed for the gaseous products: Here, the high mature zone (zone ③) exhibits the highest value for EXR, indicating that discrepancy between the two systems is most enhanced for gaseous compounds at high levels of maturity. This phenomenon may be explained by differences in formation mechanisms for gases as a function of maturity level. As illustrated in Fig. 45, it is very likely that the yield of gaseous products in the lab system at high artificial maturation stages (> 350°C/1 day including zone ③) has a significant contribution from "oil" (C_{6+}) to gas cracking. It must be pointed out, however, that it is difficult to determine which would be the equivalent *natural* maturity stage of the endmember of the artificial maturity sequence, as there is no suitable parameter for this.

Therefore, in the course of closed system maturation in the lab the stage of metagenetic gas generation indeed has been entered in contrast to the natural system.

In the following, the maturity zonation scheme was utilized in order to correlate amounts and bulk composition of *products* derived from the closed system (MSSV) with the natural system (Fig. 78).

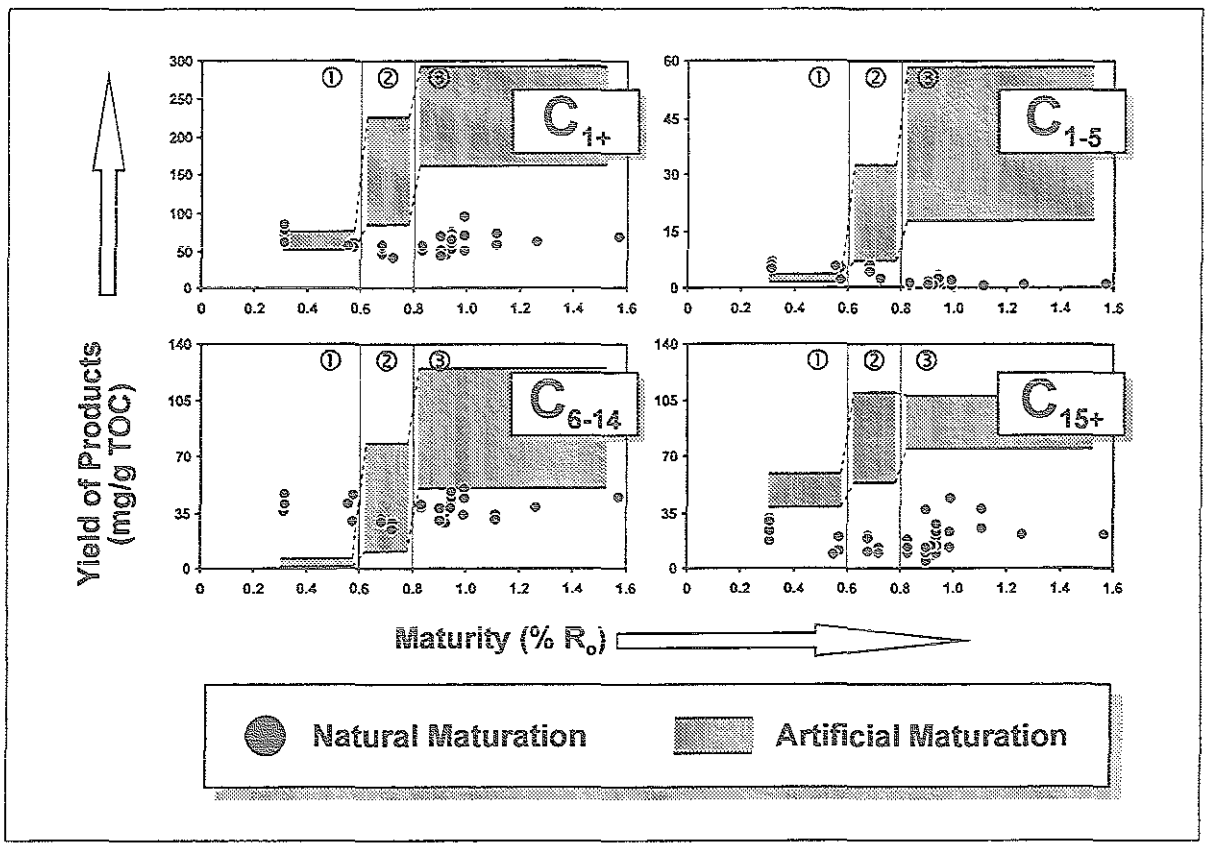

Fig. 78: Yield of total volatilisable products (C_{1+} and subfractions C_{1-5}, C_{6-14} and C_{15+}) of natural Bakken Shale maturity sequence (t'vap-gc) as a function of thermal evolution (% R_o). Shaded areas denote range of equivalent data derived from analysis of artificially matured Bakken kerogen. Approximate boundaries for maturity zones are determined using maturity sensitive parameters of Fig. 76.

The scheme as outlined in Tab. 16 suggests that the extent of quantitative discrepancy between the natural and artificial maturity sequence is not only a function of level of thermal evolution but also of boiling range. The phenomenon that the yield of C_{1-5} and C_{6-14} material is higher in zone ① of the natural system is surprising. In case of the gaseous subfraction, this may be explained by the retention capability of the Bakken Shale for gas. During thermovaporisation analysis, it was evidenced that coarsely crushed samples revealed high concentrations of gas while powdered ones yielded lower amounts. For MSSV experiments, powdered samples were utilized. Therefore, the gas yields in the closed system may have been affected by sample treatment in that the amount of gas initially present prior to the heating procedure was less than in the samples which were submitted to natural thermal evolution.
Alternatively, this mismatch might indicate that the natural gas encountered in the low mature zone (zone ①) is not a result of thermal degradation of the host source rock but was derived from

another maturity zone by lateral intraformational migration processes. This scenario has already been called upon based on compound specific isotope analysis (ch. 5.1.3).
However, such a hypothesis is only valid with the prerequisite that the maturity zonation approach between natural and lab system indeed is applicable and that both systems are comparable in terms of identical reaction pathways. Nonetheless, the results as deduced from quantitative comparison of artificial and natural thermal evolution imply that intraformational migration may have contributed to the unusually enhanced concentrations of gaseous hydrocarbons in the immature zone of the Bakken Shale. This was also implied by the isotopic composition of the thermovaporisation products (ch. 5.1.3).

Migration Mechanism

The observations as laid out above (see section on relative expulsion efficiency, p. 117) allow to make statements on the migration mechanism (Leythaeuser et al., 1984). In the case of the Bakken Shale petroleum system, the type of migration mechanism appears to be related to maturity. Samples/wells of the mature zone (>0.9% R_o) show features which are considered to be caused by flow of a bulk hydrocarbon phase: The molecular composition of the C_{15+} saturates does not bear any evidence for major compound specific fractionation effects. These characteristics have to be evaluated on the basis of their relationship to the main stages of petroleum generation and expulsion in the Bakken petroleum system. In the Bakken Shale, these processes have been shown to be essentially completed at 0.8% and 0.7% R_o, respectively. It follows that the compositional characteristics encountered in the samples/wells of the mature class (>0.9% R_o) represent a *post*-generation and *post*-expulsion stage.
In contrast, the mobile hydrocarbon phase of well SKA (0.68% R_o) might represent the stage of active present-day expulsion and generation (ch. 5.1). Here, compound-specific fractionation effects are prevailing, leading to a random distribution pattern. Interestingly, such compositional disequilibrium is known for early maturation and is thought to be an indicator for currently occurring expulsion (Young & McIver, 1977). Unfortunately, there was not sufficient sample material available in the R_o range 0.31% and 0.68% (wells JAC and NEG of the present study) to enable solvent extraction of more than one sample per well. Due to the coincidence of their rank (0.55% and 0.57% R_o, respectively) with peak of expulsion efficiency (between 0.55% and 0.62% R_o), samples from these wells are supposed to give some better insight into the effects of current expulsion. Therefore, it must be taken into account that the compositional characteristics observed in well SKA may be the result of declining expulsion efficiency. Moreover, as generation in terms of organic matter conversion is still actively continuing at this stage, the influence from the latter process may be larger.
Investigations on an actively expelling Kimmeridge Clay source rock revealed that high expulsion efficiencies are achieved by the pressure-driven flow of a discrete oil-rich phase (Leythaeuser et al., 1988; Mackenzie et al., 1988) after a certain degree of oil-saturation of the pore space has been reached. Such bulk flow is characterised by the virtual absence of compound-specific fractionation effects. The heterogeneous pattern of well SKA is not consistent with such a mechanism and, according to Leythaeuser et al. (1982), points to diffusion as the migration mechanism. Although compositional heterogeneities observed for well SKA cannot unequivocally be related to either generation or expulsion phenomena, there is some evidence that bulk flow of

hydrocarbons in the Bakken Shale may have been impeded by insufficient oil saturation as a result of the extremely efficient removal of newly generated products, as elucidated by the efficiency of expulsion rates which precedes peak generation of petroleum. Hence, despite overall low porosity (ca. 2-3%, Ropertz, 1994) and high initial hydrocarbon generation potential (Rock-Eval-S2 of ca. 11kg/ton rock) of the Bakken Shale, conditions apparently were not favorable for the onset of bulk phase flow.

The process of diffusion, however, is preferably associated only with low-molecular-weight hydrocarbons and relatively short transport distances (Mackenzie et al., 1988; Krooss et al., 1988). In the Bakken petroleum system, the t'vap-gc results of the present study have revealed that, unlike many other marine type-II source rocks, gaseous hydrocarbons are present in relatively high concentrations (ch. 5.1.3), especially at immature stages. Therefore, by using the same approach as for the C_{15+} n-alkanes (see above) the data on light hydrocarbons (C_{1-14}) serves as a means to evaluate to what extent diffusion is relevant for expulsion in the Bakken Shale. The corresponding results (Fig. 79) are discussed in the following.

Except for one high mature sample (well FED, 0.99% R_o), where uniformly high values for REE (75% to 100%) argue for bulk hydrocarbon phase flow, all other samples show features which are associated with selective diffusive transport of compound groups: For instance both samples of well MAR (0.9% R_o) elucidate enhanced relative expulsion of C_1-C_8 n-alkanes, whereas C_{10}-C_{15} species are relatively enriched. In the lateral direction, exemplified by the samples from horizontal well CON (0.94% R_o), intra-compound-class fractionation effects seem to be even more pronounced. With respect to the evolution of relative expulsion efficiency patterns with increasing maturity, the diagrams of Fig. 79 suggest a maturity zonation: At low levels of maturity (well DOB, 0.31% R_o), quantitatively only minor redistribution seems to take place, as evidenced by relatively low values of REE. As laid out above, wells NEG and SKA are of peculiar importance as regards generation/expulsion related characteristics. The individual sample of well NEG (0.57% R_o) displays major compound class specific depletion/enrichment suggesting large-scale fractionation effects. In the case of well NEG, however, only two samples were available for analyses, one of which (selected as reference sample here) appeared to be Bakken atypical as regards TOC content (6.44wt.-%). Results as outlined in ch. 5.1.3 provide evidence that the abundance of low-molecular weight compounds may be a function of organic richness (adsorption) for levels of maturity below 0.7% R_o. Therefore, it appears to be more likely that the difference beween the two samples of well NEG are not related to relative expulsion effects.

The results for the low-molecular-weight hydrocarbons as laid out above indicate that the diffusive transport of the light proportions of petroleum (C_{15-}) occurs in the Bakken Shale at all stages of catagenesis. Most importantly, it can also be associated with higher maturity levels, thence accompanying bulk phase flow of heavy proportions (C_{15+}) of petroleum. Usually, compositional fractionation as created by diffusive expulsion is believed to be a phenomenon of predominantly early stages of catagenesis (Leythaeuser et al., 1987). Interestingly, Talukdar et al. (1991) postulated that particularly in early phases of Bakken oil generation hydrocarbons migrated via diffusion through the kerogen.

If the distribution patterns for samples of a given well (e.g. well CON) are examined, it is noteworthy that a given compound group (for instance C_2-C_7) may be relatively expelled as well

as accumulated, depending which sample is regarded. Such a finding might elucidate that diffusive equilibrium is not yet achieved.

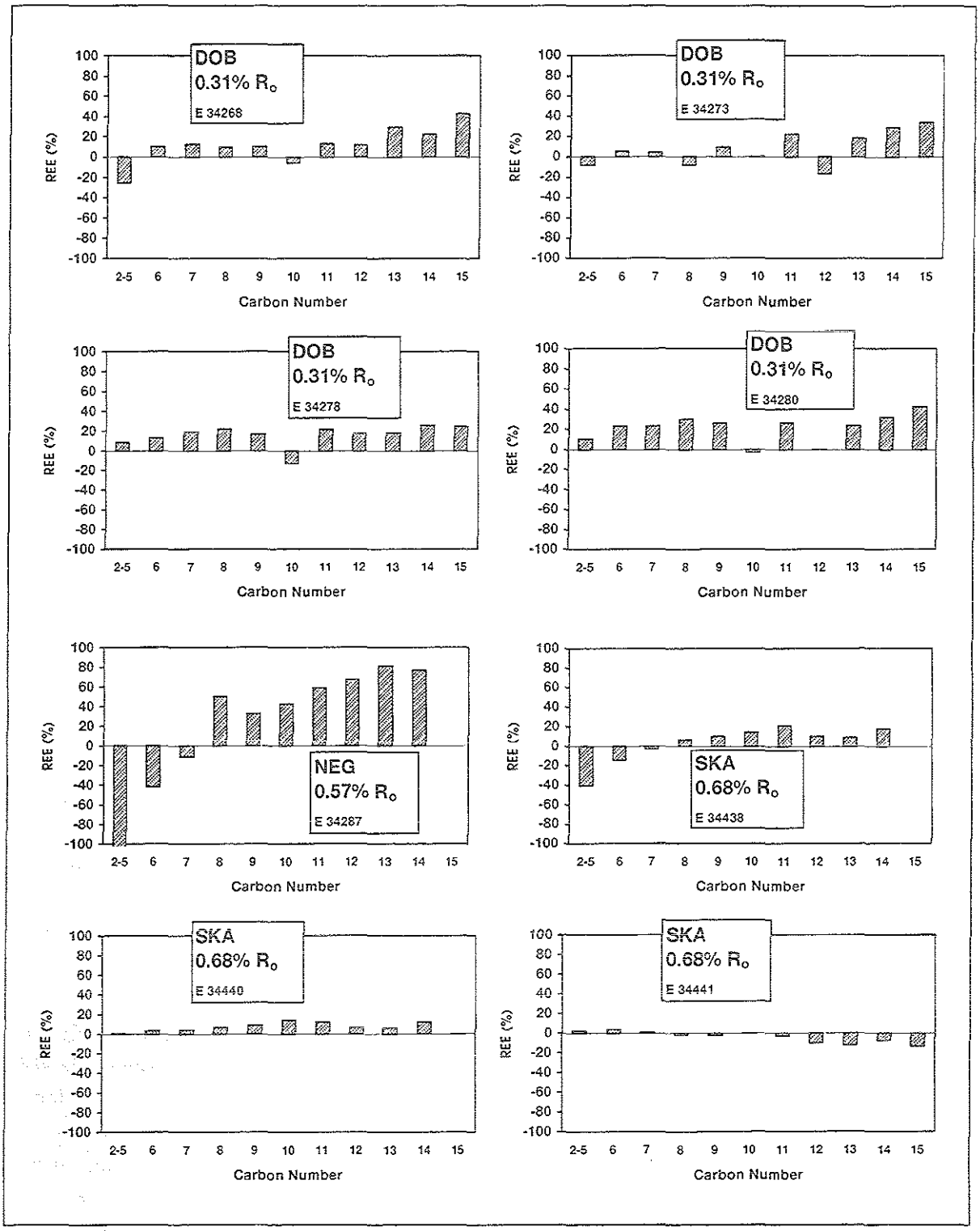

Fig. 79: Relative Expulsion Efficiency (REE; Mackenzie et al., 1983) for straight chain hydrocarbons as derived from thermovaporisation of wells covering the entire maturity spectrum. Positive REE values represent relative expulsion, negative relative accumulation. CON (0.94% R_o) represents a horizontal well.

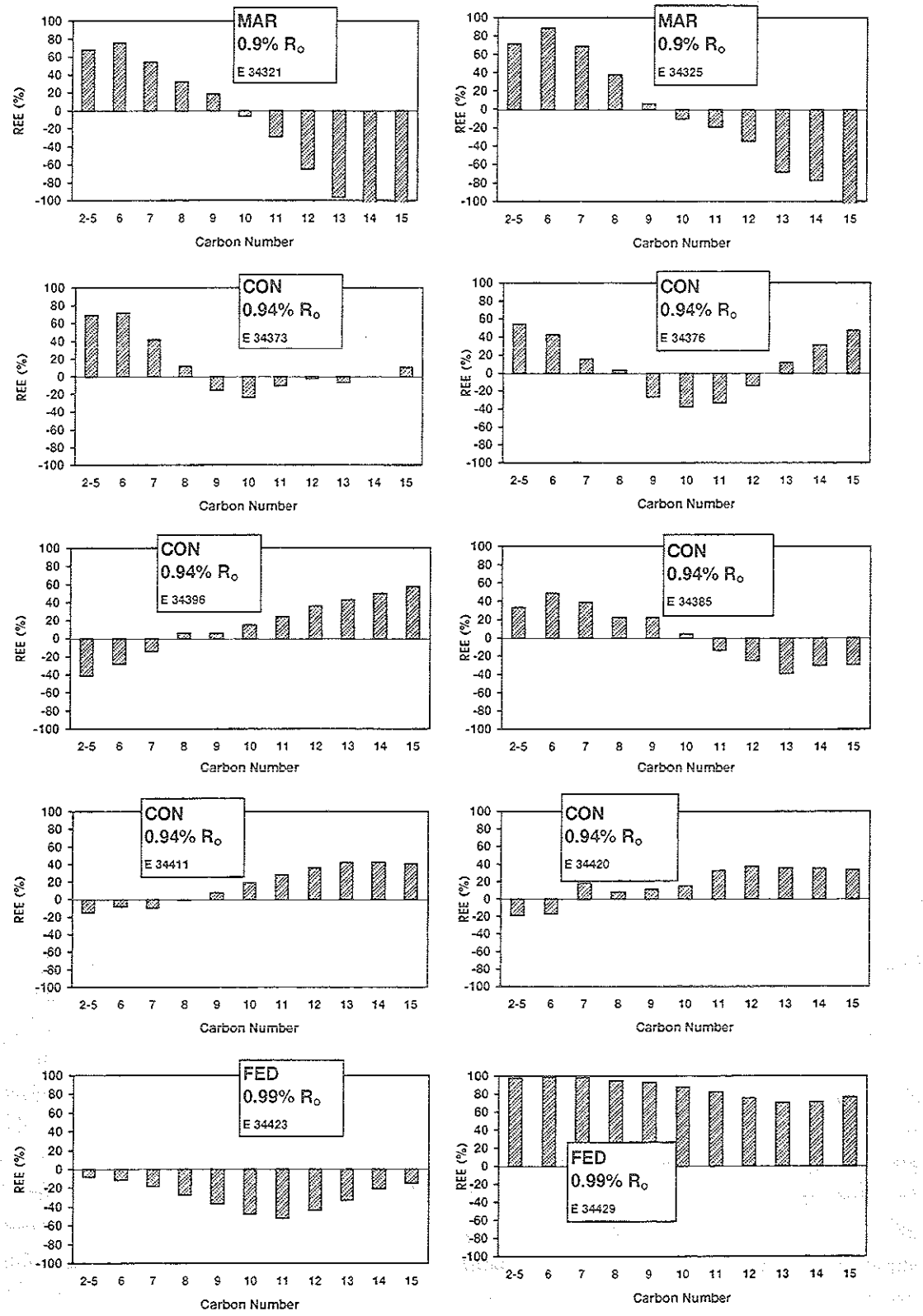
MAR
0.9% Ro
E 34321
MAR
0.9% Ro
E 34325
CON
0.94% Ro
E 34373
CON
0.94% Ro
E 34376
CON
0.94% Ro
E 34396
CON
0.94% Ro
E 34385
CON
0.94% Ro
E 34411
CON
0.94% Ro
E 34420
FED
0.99% Ro
E 34423
FED
0.99% Ro
E 34429
REE (%)
Carbon Number
2-5 6 7 8 9 10 11 12 13 14 15

Fig. 79 (cont.)

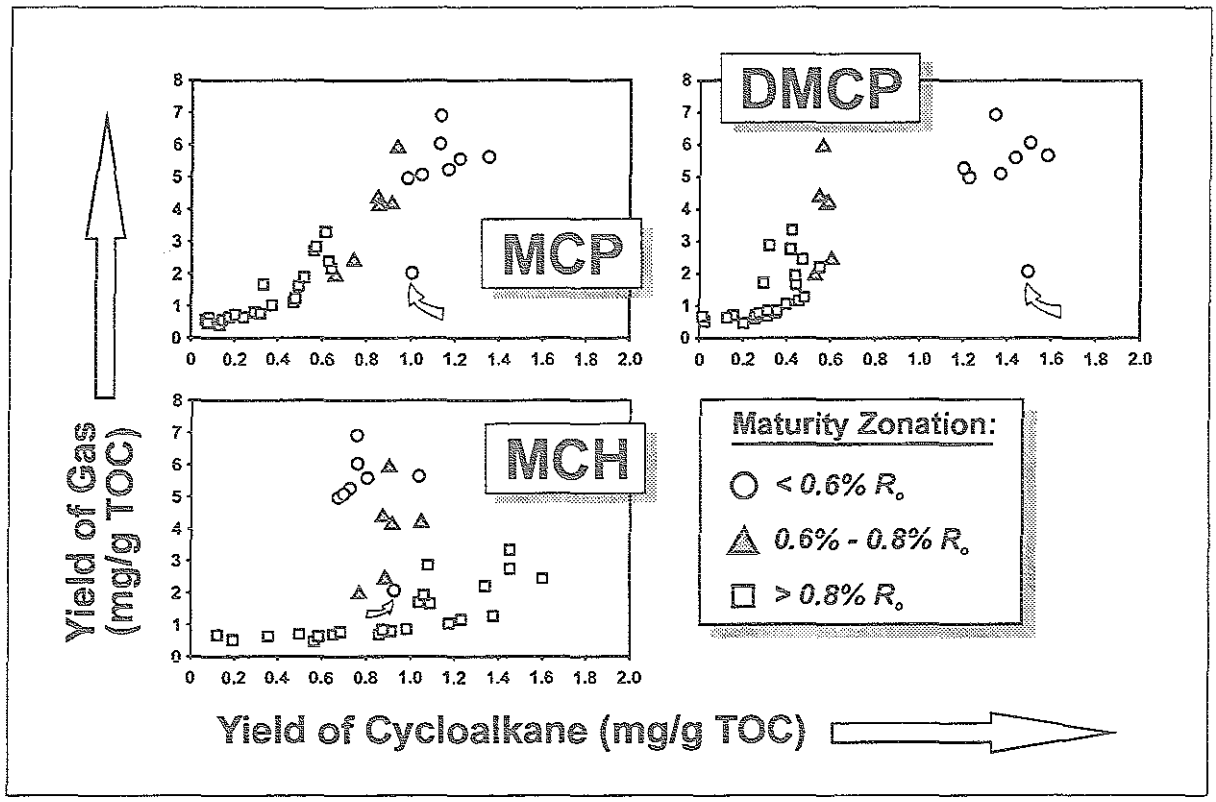

Fig. 80: Correlation of cycloalkanes with concentration of C_{1-5} hydrocarbons (gas) as deduced from t'vap-gc. X-axis designates abundance of methylcyclopentane (MCP), dimethylcyclopentane (DMCP) and methylcyclohexane (MCH) in mg/g TOC. Arrow marks individual sample with Bakken-atypically low TOC content (see ch. 4.6).

Various ratios based on light C_{1-7} paraffins (cycloalkanes, n-and iso-alkanes) have been shown to be diagnostic for maturation (Philippi, 1975; Thompson, 1979) and migration (Whelan et al., 1986). Mostly, such parameters involve the sum of several isomers of the same carbon number, e.g. alkylcycloalkanes vs. alkylated branched alkanes (Thompson, 1979) or, alternatively, the ratio comprises of individual compounds (Whelan et al., 1986). For the present data set, however, the conditions for GC-analysis of the thermovaporisation products were not set up in order to resolve individual hydrocarbon isomers in the C_{1-5} material. Hence, it was not possible for the author to use individual compounds of the C_{1-5} range for calculation of such parameters. Nonetheless, the evolution of the three most abundant cycloalkanes (methylcyclopentane, dimethylcyclopentane and methylcyclohexane) as a function of maturity and yield of gas is investigated below. Fig. 80 elucidates that the concentration of methylcyclopentane and, to a lesser extent, dimethylcyclopentane parallels the amount of gas present in the Bakken across the entire maturity sequence. In other words, both alkylcyclopentanes appear to be removed to the same degree as the gases. However, this is not true for methylcyclohexane. The maturity independent, uniformly high yields of methylcyclohexane relative to decreasing concentrations of the other two cycloalkanes as shown earlier in Fig. 67 is depicted quantitatively in Fig. 81. This feature reveals that both cyclopentane species may be suitable to establish maturation effects in the Bakken, similar to other types of source rocks (Thompson, 1979; Whelan et al., 1986).

In contrast, the concentration of methylcyclohexane appears to be controlled by a different mechanism, although the boiling point and hence the elution position in the GC trace are very close to the former two compounds (MCP: 71.8°C; DMCP: 103.5°C; MCH: 100.9°C).

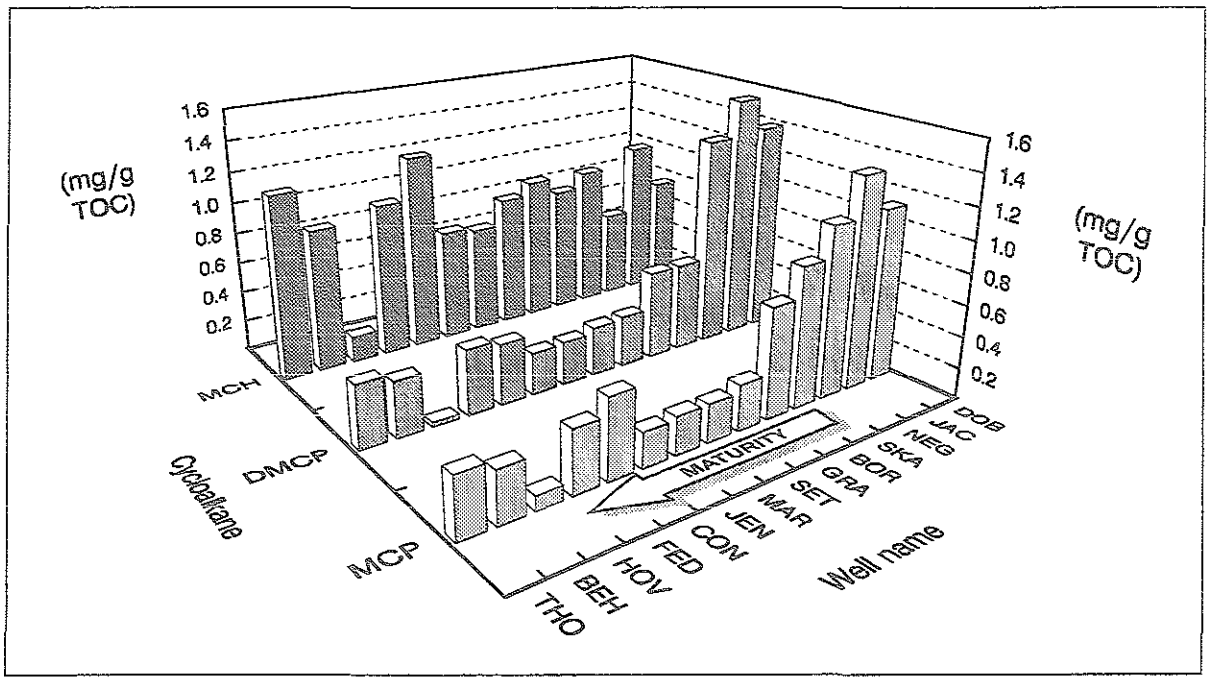

Fig. 81: Concentration of methylcyclopentane (MCP), dimethylcyclopentane (DMCP) and methylcyclohexane (MCH) as a function of increasing thermal evolution (% R_o) indicates relative enrichment of methylcyclohexane, while the samples become relatively depleted in cyclopentanes (methylcyclopentane and dimethylcyclopentane).

Fig. 82 displays the evolution of two ratios incorporating cyclopentanes and corresponding n-alkanes. These ratios are equivalent to paraffin index 1 by Thompson (1979). Clearly, neither ratio suggests any correlation with level of catagenesis. Although regression analysis defined a linear decrease of both MCP/n-$C_{6:0}$ and DMCP/n-$C_{7:0}$ with increasing maturation, the overall pattern expresses a high degree of maturity-independence. According to Thompson (1979), such a random distribution can be observed in areas where active redistribution of generated hydrocarbons has taken place. Furthermore and importantly, if redistribution distances are short to intermediate (range of meters), as is the case in the Bakken petroleum system, then such phenomena can be interpreted to result from diffusion (Thompson, 1979). Indeed, this particular maturity interval is associated with a considerable scatter in values of Fig. 82. This serves as a further argument that diffusive transport of low-molecular-weight hydrocarbons contributes to the process of expulsion in the Bakken petroleum system.

The equivalent cycloalkane/n-alkane ratios as determined for the Bakken crude oils show generally low values (Fig. 82). By using the same oil-source rock correlation approach as applied in Fig. 66, Fig. 82 designates a high level of maturity for the oils. Although this can be considered a further argument for a high degree of thermal alteration of the oils, the trends outlined by the source rock datapoints are not well defined, so as to enable an unequivocal correlation and maturity zonation.

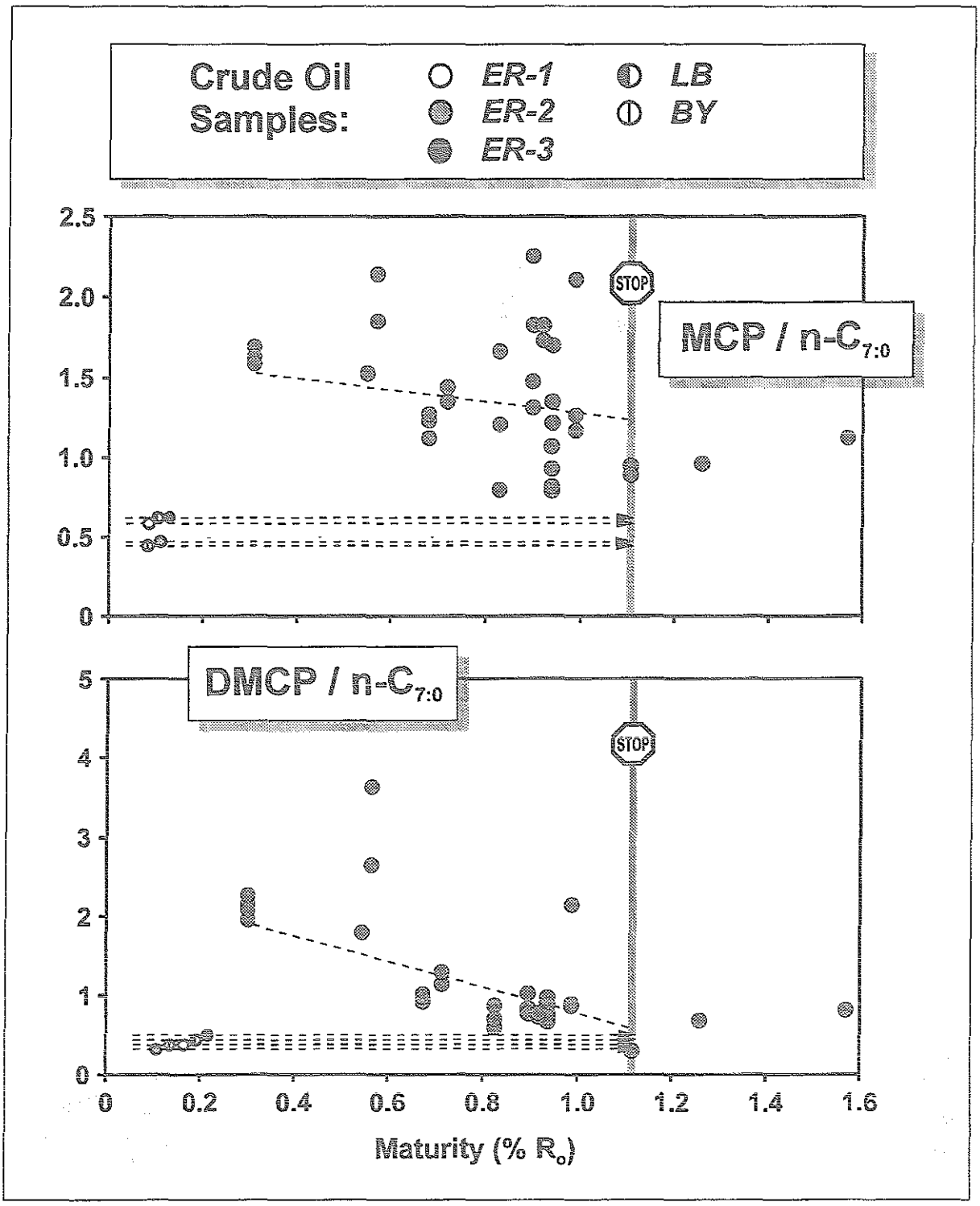

Fig. 82: Assessment of maturity trend for Bakken light ends using the ratio of methylcyclohexane vs. n-heptane (MCH / n-$C_{7:0}$) and dimethylcyclopentane vs. n-heptane (DMCP/n-$C_{7:0}$). Dashed line was determined by regression analysis. Stop sign indicates end of maturity spectrum as evidenced from other maturity parameters (see ch. 4.1.2).

A further concept, termed 'evaporative fractionation', was presented by Thompson (1988): Here, high-molecular-weight compounds are dissolved in gas and removed via evaporation. The residual petroleum phase is enriched in light aromatics and cycloalkanes. In the present study, this

scheme indeed would be matched by the high abundance of equivalent aromatic and cycloalkane species in the thermovaporisation products.

As already laid out further above, the concept of relative expulsion efficiency (Mackenzie et al., 1983) may not be applicable to the Bakken petroleum system for investigating and assessing expulsion directions because it was not possible to sample the cores in close vertical intervals as well as retrieve samples from the boundary zone to the adjacent strata. The lack of apparent depletion/enrichment avenues can be explained by the intimate association of source and reservoir rock in a constrained system. Nonetheless, the results derived from the relative expulsion efficiency concept as outlined above allow to make conclusions on the mechanism *how* hydrocarbons are redistributed in the Bakken Shales. With that respect, the interrelationship of migration mechanism and migration pathway has to be considered. In the light of the results as outlined above and the rather short vertical distances in the Bakken petroleum system between source rock and potential reservoir (see discussion in ch. 5.3), hydrocarbon removal (expulsion) via diffusion may be much more pronounced in the Bakken Shale than expected. The argument that diffusion is predominantly associated with light hydrocarbons and is less applicable to rather heavy oil-like components (Mackenzie et al., 1988) has to be evaluated in the light of the composition of an extract/saturate fraction from the maturity zone of extensive expulsion (e.g. wells NEG, JAC and SKA): The straight-chain hydrocarbon GC-fingerprint of samples from those wells are characterised by relatively short chain lengths (between C_{13} and C_{22}). Hence, the light oil character of Bakken petroleum may facilitate transport by diffusion.

Stainforth & Reinders (1990) postulated a thermally activated diffusive transport of bitumen through 3-dimensional organic matter networks as a rate-limiting migration process. This mechanism does not require the active participation of fluids, as it occurs via polymeric solid kerogen and adsorbed organic matter. The efficiency of this procedure is enhanced for low-molecular-weight molecules in comparison to heavy ones. Accordingly, this mechanism governs both retention and release of products.

However, in the same publication (Stainforth & Reinders, 1990) it was also stated that such a diffusion mechanism becomes progressively less efficient with increasing degree of aromaticity (polyaromatic cross-linking) of the kerogen. The geometry of the kerogen network (2d vs. 3d orientation, size of aromatic sheets) is also believed to be crucial. Equivalent results from py-gc (ch. 4.4), however, have revealed that low-mature Bakken Shale kerogens (< 0.7% R_o) exhibit a mainly labile monoaromatic nature. The latter feature therefore might restrict the effectivity of activated diffusion for the Bakken Shale.

Thomas & Clouse (1990a) have found that diffusion via an organic matter network is relevant in source rocks which are unable to achieve sufficient oil saturation of the pore space due to leaner quality (low TOC), relatively high porosity and/or during early maturity levels and slow rates of generation. Clearly, the attributes of low TOC content and high porosity are not applicable to the Bakken Shale. However, as these authors pointed out in an accompanying publication (Thomas & Clouse, 1990b), the efficiency of such a transport mechanism increases with the quality of the organic matter network. The most decisive factor with that respect seems to be connectivity and extension of the kerogen network (Thomas & Clouse, 1990b) in order to provide a continuous avenue for diffusion. Such requirements are perfectly met by Bakken Shale kerogens of shallow depths (2000 to ca. 2900m below surface), equivalent to the maturity zone below 0.7% R_o, as revealed by organic petrology (ch. 4.1.1). SEM images on isolated kerogens from two different

stages of thermal evolution (0.49% and 0.68% R_o) designate the Bakken kerogen as being highly continuous (Ropertz, 1994) although the more mature one consisted of thinner sheets and was more wide-meshed.

As laid out above, transport via diffusion may be a plausible migration mechanism for *low-molecular-weight* hydrocarbon species. Indeed, the combination of a well-developed organic matter network facilitating diffusive transport with the presence of high concentrations of gaseous hydrocarbons (ch. 5.1.3) is highly favorable for a migration mechanism postulated by Price (1989) in the course of which also *high-molecular-weight* species are involved. He provided evidence that C_{5-15} n-alkanes are preferentially dissolved in C_{1-5} hydrocarbons and removed via migration ("gaseous solution"). As the hydrocarbon solution capacity of gas increases with increasing temperature and pressure (catagenesis), it may also dissolve high-molecular-weight resins and asphaltenes thus forming light crude oil microdroplets which can migrate more easily. Such a migration mechanism is called upon to explain the compositional differences between reservoired crude oils and solvent extractable bitumen of the parent source rock (ratio of hydrocarbons vs. non-hydrocarbons). Such a migration mechanism is interesting with respect to the high expulsion efficiencies at $R_o > 0.7\%$ and the concomitant decrease in gas concentration (t'vap-gc) of the Bakken Shale. This feature might be due to the solubilisation of high-molecular-weight compounds in the light hydrocarbon fraction and the subsequent release of this hydrocarbon phase from the source rock according to the scheme proposed by Price (1989).

With respect to compound-specific redistribution (expulsion) processes it is noteworthy that the n-hexane-insoluble asphaltene fraction represents the only compound class of the solvent extractable organic matter which shows a good relationship to maturation over the entire spectrum of vitrinite reflectance (Fig. 25). This phenomenon may imply that asphaltenes are not affected by redistribution processes like saturates and aromatics. The fact that residual solvent extracts from the Bakken Shale samples bear significant amounts of asphaltene material is of particular interest in view of the highly asphaltene-depleted nature of the Bakken crude oils. Such a feature may be interpreted as an indication that n-hexane-insoluble polar material does not leave the source rock system during expulsion but is retained. Therefore, their yield is primarily controlled by catagenesis.
Resins, in contrast, are also a fraction of Bakken crude oils. Moreover, their distribution pattern in the course of thermal evolution of the extracts (Fig. 25) exhibits a gross analogy to the pattern of saturates and aromatics. This is particularly true for the two wells where samples could be analysed from both shale strata. The significance of this irregular yield of asphaltenes on one side and saturates, aromatic and resin fraction on the other side for crude oil migration mechanism is discussed in ch. 5.3.

Migration Pathways

As reviewed recently by Ropertz (1994), additional to primary migration via organic matter network the following two basic concepts on migration pathways are discussed in the literature: Primary migration (1) via the pore space and (2) via microfractures. The applicability of these principles to the Bakken Shale is outlined in the following:

Migration through the *pore network* is rather unlikely in view of the constrained pore geometry of the Bakken Shale (Ropertz, 1994): The small pore radii of the Bakken Shale are associated with enormously high capillary pressures. In order to initiate migration, the pore pressure has to overcome capillary pressure. Postulated bulk volume flow, therefore, would have to exceed these pressures in order to establish a continuous fluid flow (McAuliffe, 1980; Tissot & Welte, 1984).
The formation of *microfractures*, which serve as possible conduits for expulsion, was considered to be caused by volume expansion of organic matter during the main phase of hydrocarbon generation in the Posidonia Shale (Düppenbecker & Welte, 1991). Based on this theory, the same authors developed a numerical model which indicated that microfractures parallel to the bedding plane may be formed with the prerequisite that fracturing threshold of the source rock is achieved. Permeability measurements parallel to the bedding plane (Ropertz, 1994) showed that the Bakken Shale indeed is laterally several orders of magnitude more permeable than vertically. This enhanced permeability may be indicative of microfractures oriented parallel/subparallel to the bedding plane of the Bakken Shale, allowing hydrocarbon fluids to move laterally and to set up a continuous fluid network. However, this might also be a primary feature of the Bakken Shale rock matrix as has been observed during microscopic examination (ch. 4.1).
Nonetheless, the question still remains how to move the petroleum in the vertical direction, i.e. into the overlying/underlying strata. Hence, the understanding and accurate appraisal of fracture characteristics in general and *vertical* fracturing in particular is crucial for optimum exploration and production in the Bakken petroleum system. Even if the fractured reservoir model is considered valid, controversial discussions on the magnitude, orientation and frequency of fractures are still a subject of ongoing debate in related publications. The lack of unequivocal data as derived from visual examination of cores led to the development of more refined methods and technologies. Skopec (1992) recommended to drill a vertical pilot hole in a new field prior to extensive horizontal drilling. Thereafter, the core section of the target interval is analysed in field tests as well as in the laboratory providing information on parameters like the orientation of present-day stress and fracture pressure.
The following literature overview includes the most recent studies pertaining especially to the nature of vertical fracturing in the Bakken petroleum system:

- ⇨ Price & LeFever (1992) - These authors have coined the term of the "Bakken in-source reservoir system" and postulated vertical fracturing to extend into the three units adjacent to the Bakken Shales (Mississippian Lodgepole, mBK and Devonian Three Forks).
- ⇨ Freisatz (1991) - This comprehensive study adds a new facet to the fracture issue: The author examined Landsat-derived surface lineament maps in order to identify fracture patterns on a regional scale. In the absence of major tectonic activity in the relatively stable, intracratonic Williston Basin, he proposed a surface expression of Bakken Formation fractures (closest lineament spacing: 1.44m). This hypothesis was verified by a positive linear correlation between proximity of wells to lineament traces and the percentage of high initial shut-in pressures (> 10mpa) which are believed to be indicative of fracturing. The fractures are genetically related to basement block tectonics. The evaluation of surface lineaments with respect to subsurface fractures reservoirs was also applied to the San Juan Basin (Dart, 1992).
- ⇨ Eric Michael (Conoco, written communication) - Production data indicate that wells drilled parallel to the main fracture network as deduced from principle stress analysis are poor producers. Yet only those horizontal wells are economic producers which are drilled

perpendicular to the main fracture network, as they intersect more fractures. Hence, experience from production seems to support that fractures are relatively widely spaced (10s to 100s of feet) and regularly orientated.

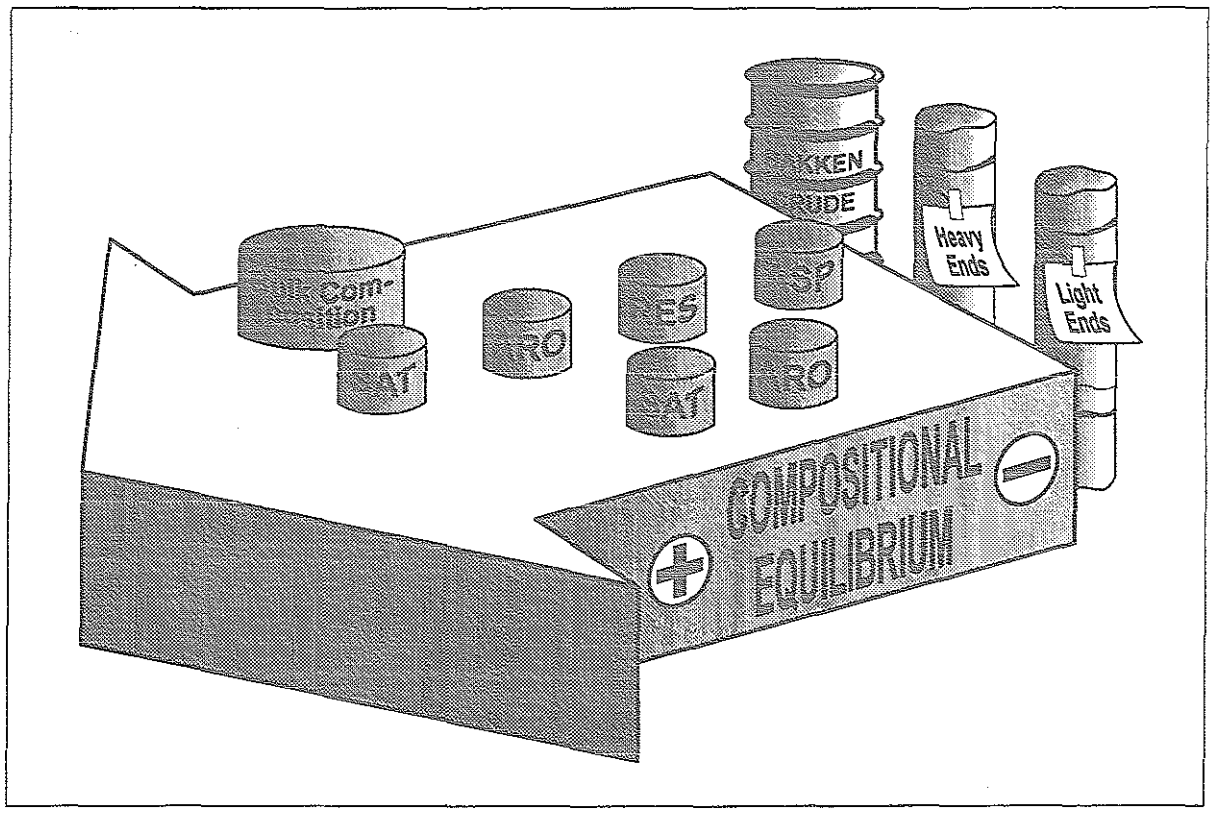

Fig. 83: Compositional interrelationship of Bakken light ends (C_{1-14}), heavy ends (C_{15+}) and crude oils as a function of compound class. 'Compositional equilibrium' refers to uniformity of individual compound class with respect to geographic distribution in the study area. Most enhanced compositional equilibrium corresponds to maturity independence.

Summary

- While the validity of highly efficient removal of newly formed products from Bakken Shales between 0.4% and 0.7% R_o seems to be established and confirmed by mass balance calculations, the mechanism *how* expulsion takes place remains less clear. Contrary to the widespread scheme of bulk phase flow as the predominant expulsion mechanism for organic rich, dense source rocks, kerogen geometry and compositional characteristics of the saturated hydrocarbon fraction of the Bakken Shale provide some evidence that diffusive expulsion via a well-connected kerogen network may be regarded as a quantitative meaningful process during the main phase of petroleum expulsion from the Bakken source rock. Thermovaporisation analyses indeed revealed that gaseous hydrocarbons are present in abundant concentrations and could act as a migration "vehicle" for dissolving C_{15+} compounds. In addition, the lack of bulk, compound-unspecific redistribution processes during the main stage of petroleum release provides evidence that *bulk hydrocarbon phase flow* is less dominant in that maturity zone, but prevails after the main phase of hydrocarbon

generation and expulsion (> 0.8% R_o) whereas diffusion - reflected by compound-specific enrichment/depletion - is uniformly active throughout maturation.
This hypothesis, however, requires the examination of a comprehensive sample set including more samples from maturity interval 0.4% to 0.8% R_o.

- Migration/expulsion related compositional characteristics appear to be a function of compound class and, to a limited degree, type of mobile organic matter (low- vs high-molecular-weight species) of Bakken petroleum. With respect to compositional equilibrium, the thermovaporisation products and the crude oils represent the minimum and maximum end members, respectively, while the solvent extracts have a medium position. Within the latter compound class, the degree of maturity-independence and migration/expulsion sensitivity increases with mobility of the compound classes, namely in the order asphaltenes - resins - aromatics - saturates. This interrelationship is illustrated in Fig. 83.

5.3 Bakken Petroleum Generation and Redistribution in Space and Time

Mass balance calculations have shown that the gross amount of reactive Bakken kerogen is efficiently converted to mobile petroleum within a relatively short interval of catagenesis. This process is accompanied by equally high expulsion rates. In other words, onset, peak and deadline of quantitatively significant hydrocarbon generation as well as expulsion occupy only a rather narrow period of thermal evolution of the Bakken Shale. Additional to their high rates, both generation and migration overlap in the course of Bakken evolution (Fig. 84). The C_{15+} compounds of the residual petroleum phase (solvent extractable organic matter) from this specific maturity interval display major compound-specific fractionation effects relative to each other. Corresponding light species (t'vap-gc) of the same catagenetic stage principally show a similar behaviour, although expulsion-induced compositional variations are less severe. These arguments elucidate that processes associated with highly efficient expulsion (diffusion, discrete oil phase flow) of Bakken petroleum apparently have removed compositional properties inherited from the process of hydrocarbon generation, i.e. generation effects cannot be discriminated from migration effects.

Nonetheless, accumulation of petroleum in the *source rocks* of the maturity zone >0.8% R_o seems to take place, but this feature was observed only on a local scale and could only be attributed to the lower Bakken Shale. If these findings are extrapolated throughout the study area, it becomes evident that most of the Bakken oil fields lie in areas which, at present-time, are in a static, equilibrated stage with respect to petroleum generation and expulsion. This regional scheme has major impact on petroleum generation and migration models of the Bakken Formation: (1) Long-distance migration vs. in-situ maturation of Bakken petroleum. (3) Cause of overpressuring in the Bakken reservoir system (Meissner, 1978).

Long-distance migration vs. in-situ maturation of Bakken petroleum

The Bakken crude oils studied here exhibit bulk as well as molecular characteristics which reflect an enhanced degree of maturity (e.g. predominance of paraffins paralleled by a preference of short-chain saturates, high values for aromatic maturity parameters). Such ongoing thermal maturation of mobile hydrocarbon phases requires that the petroleum, once it is generated, resides in rock units which are submitted to increasing maturation, i.e. rising temperature. If the sedimentary column exhibits avenues/pathways which allows long-distance migration of the crude oil, then it may be able to move to more shallow parts of the basin and "escape" from further maturation. Therefore it is important to evaluate the areal extent and quality of potential migration conduits for Bakken petroleum.
Maturity-specific oil-source rock correlations suggest that the *minimum* level of maturity, at which the oils have been expelled, was ca. 0.8% R_o. However, the peak of hydrocarbon expulsion in the Bakken Shale was already reached at ca. 0.6% R_o. Thereafter, oil release decreased drastically and was grossly completed at ca. 0.7% R_o. Simultaneous to this highly efficient expulsion process, hydrocarbon generation was essentially completed at ca. 0.8% R_o. Hence,

most of the entire volume of crude oil accumulated in the Bakken petroleum system including the samples which are examined in the present study should reflect that period of thermal evolution, during which expulsion was most efficient, i.e. from 0.4% to 0.7% R_o. This apparent mismatch suggests that post-generation maturation effects may have altered the maturity level inherited from the source rock at the time of expulsion. However, it cannot be unequivocally ruled out that the aromatic maturity parameter MPI, which was used in the present study amongst other parameters to designate oil-source rock correlation (ch. 5.2.1), is not suitable for such approaches as laboratory experiments suggest that this parameter is altered during migration (England et al., 1991).

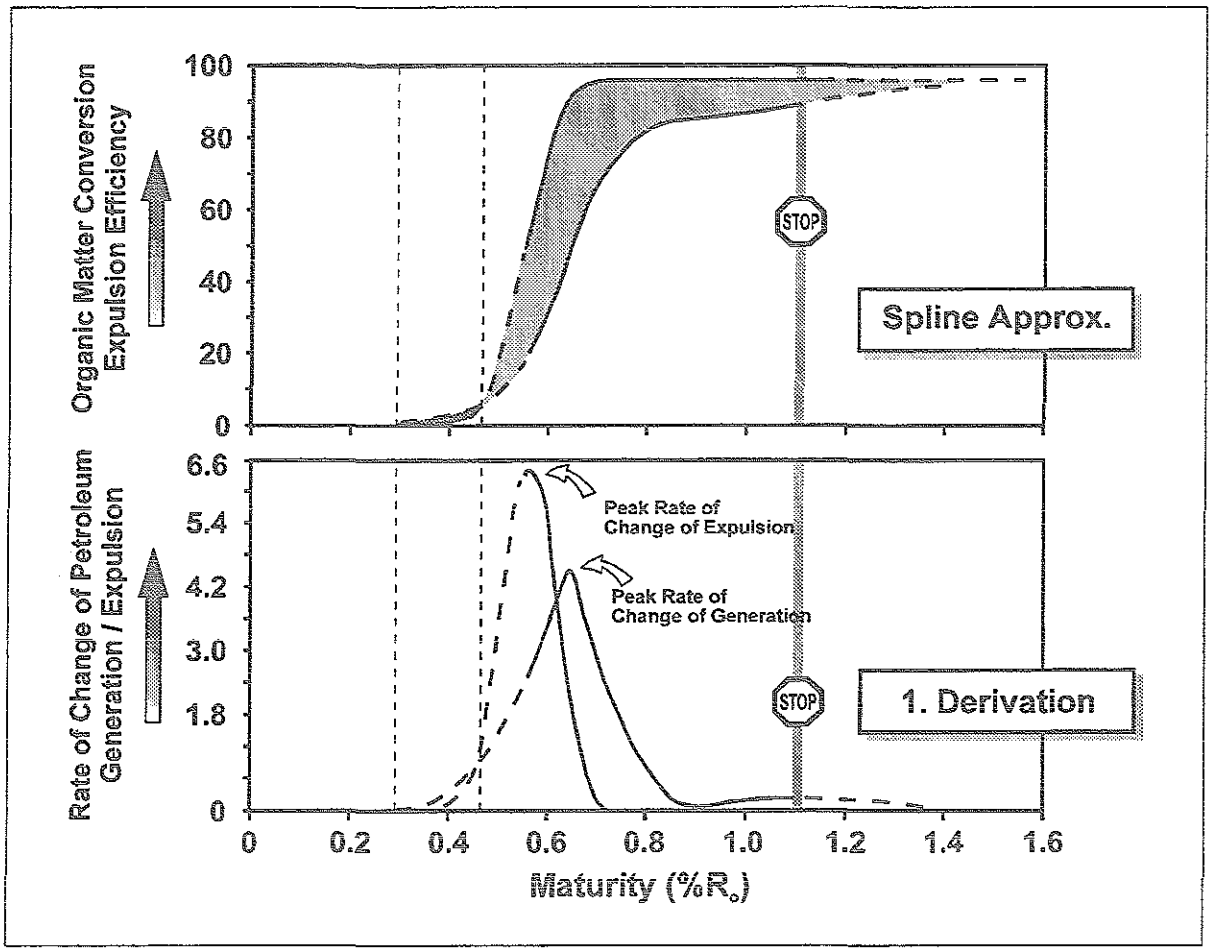

Fig. 84: Relationship of petroleum generation and expulsion in the course of thermal evolution of the Bakken Shale. Data is provided from mass balance calculations as carried out in chs. 5.1.2 and 5.2.2. Interval bounded by dashed lines designates maturity zone during which generation rate may have been higher. Stop sign indicates end of maturity spectrum as evidenced from other maturity parameters (see ch. 4.1.2).

In-situ thermal alteration of Bakken petroleum may be facilitated in the vertically constrained nature of the Bakken petroleum system, in which migration of the generated hydrocarbon phase as well as entrapment are vertically restricted. Hence, predominantly vertically oriented expulsion/migration pathways can theoretically only be as wide as the maximum thickness of the Bakken Formation (from 50m in the depocenter to zero at the depositional edge). In other

hydrocarbon basins, the potentially available expulsion/migration avenues - and consequently the timespan covered between expulsion and reservoiring of a given crude oil - within a source rock/reservoir system are vertically much higher, often encompassing several geologic periods (Klemme & Ulmishek, 1991). In contrast, in the Bakken system the timespan between generation of hydrocarbons and their entrapment in the reservoir can be considered to be relatively short. Therefore, if the mobile hydrocarbon phase is not submitted to efficient, predominantly laterally oriented migration processes within the Bakken Formation, then the nature of the oil should be expected to reflect the same thermal history as its source rock from which it originated.
If predominantly laterally orientated migration of expelled Bakken petroleum indeed takes place, it requires an efficient conduit. Equivalent permeability data (LeFever et al., 1991) on the mBK which is sandwiched between the two shale members might indicate that this stratum indeed may be able to transport hydrocarbons over long distances. However, in view of the highly heterogeneous and variable lithology of this sediment (Webster, 1984; LeFever et al., 1991), it may not be justified to extrapolate its good carrier rock quality, which is based only on a limited number of wells, on a regional scale. The unequivocal evaluation of the carrier/reservoir rock quality of the mBK requires the analysis of a much larger sample set. Furthermore and importantly, a lithologically and petrophysically heterogenous rock unit like the mBK clearly affects a migrating fluid in terms of varying adsorption phenomena (Seifert & Moldowan, 1981) and modifies its composition. However, such postulated "geochromatographic" effects don't seem to apply to the Bakken crude oils, as outlined in the following.

Compositional data on Bakken crude oils of the present study, confirmed by related data from Price & LeFever (1994), indicates that oils from the same oil field are very similar. This might suggest that hydraulic connectivity of the Bakken carrier/reservoir rocks is laterally very limited (in the order of magnitude of several kilometers). Furthermore, the extent of how far the products are redistributed in the source rock system (solvent extractable organic matter and thermovaporisation products) seems to be linked to compound class and mobility, respectively. Highly mobile paraffins are transported farthest. Aromatics migrate to a lesser extent than saturates. High-molecular-weight asphaltenes appear to be essentially immobile. Low-molecular-weight species are redistributed only within a very small volume of rock.
Hence, long-distance migration may not have occurred in the past geologic time since the onset of petroleum generation. Indeed, the compositional characteristics of the crude oils which are currently produced from the Bakken Formation appear to be predominantly the result of post-generation in-situ maturation effects which have ruled out compositional fractionations associated with migration and generation/expulsion. There is some evidence that the product (crude oil) and its residue (source rock) are spatially closely associated with each other. This implies that both 'components' have undergone the same thermal history during basin development.
With respect to compound class-specific, relative homogeneity of Bakken crude oils the influence of in-reservoir mixing processes has to be evaluated. Lateral variations in petroleum composition can result from reservoir filling processes (England & Mackenzie, 1989): Mechanical equilibrium of the reservoir fill is achieved rather rapid (within 10's Ma) after the filling process has come to an end. The latter may be relevant for those Bakken reservoirs which are associated with high mature host source rocks.

Reservoir pressures in the Bakken Formation have been reported to be distinctly higher than normal hydrostatic and to be congruent with mature areas of the Bakken Shale (Meissner, 1978). This situation of overpressuring is believed to be created by high hydrocarbon generation rates which are paralleled by the inability of the newly formed petroleum to escape due to extremely impermeable rocks in the underlying and overlying formations (Meissner, 1978). Results of the present study, however, elucidate that the highest generation rates are restricted to a short maturity interval, i.e. ca. 0.5% to 0.8% R_o. This period of drastic, thermally induced kerogen breakdown is accompanied by highly efficient release of the products. Fig. 84 illustrates the present day relationship: Although the corresponding curves had to be extrapolated for levels below 0.55% R_o, it is evident that there is only a very narrow "slice" of thermal evolution in the Bakken during which expulsion may not have been efficient enough to remove the generated hydrocarbons. If this maturity "slice" from ca. 0.3 to 0.48% R_o is superimposed on the map of the study area (Fig. 85), it covers only a small portion of the abnormally high pressured area according to Meissner (1978). These results corroborate that, apart from local anomalies (ch. 5.2.2), the degree of overpressuring in the mature Bakken Shales (> 0.6% R_o) at present time is much lower than during active generation. Computerized basin modelling with special emphasis laid on generation rate-induced pressure history also revealed that reservoir pressures must have decreased to the recent level (Burrus et al., 1994a).

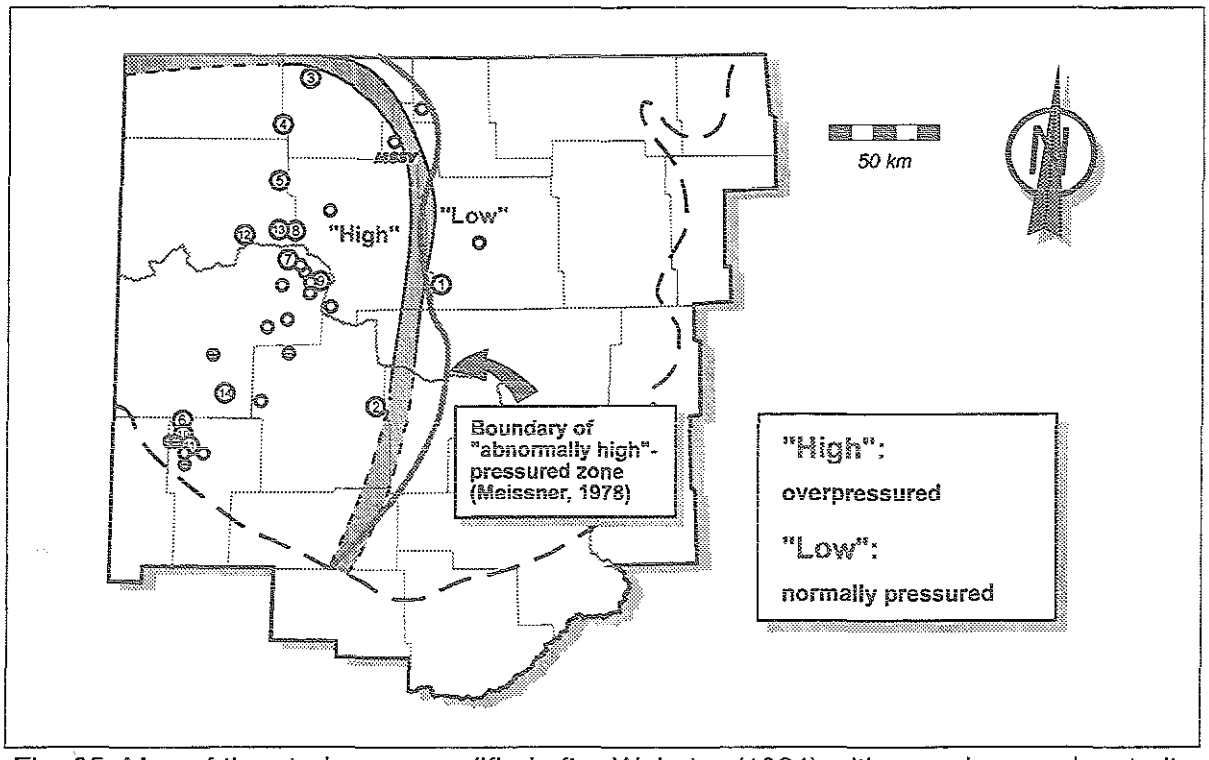

Fig. 85: Map of the study area modified after Webster (1984) with superimposed maturity zones of the Bakken Shale and overpressured zones according to Meissner (1978). Highlighted narrow zone refers to maturity interval during which the rate of petroleum generation is believed to exceed the rate of petroleum expulsion based on mass balancing calculations of the present study.

In the light of high expulsion efficiencies of the Bakken Shale source rock system and negligible generation of petroleum in mature (> 0.8% R_o) regions of the basin, the question still remains whether overpressuring is a basinwide phenomenon, whether it incorporates all members of the Bakken *Formation* and whether it is exclusively caused by petroleum generation in the past. In the following, an attempt is made to provide answers to the questions above on the basis of a conceptual model. This model of pressure build-up as a consequence of combined early efficient expulsion, constrained lateral and vertical migration, progressive burial and reimpregnation is illustrated in Fig. 86. The model is subdivided into four stages:

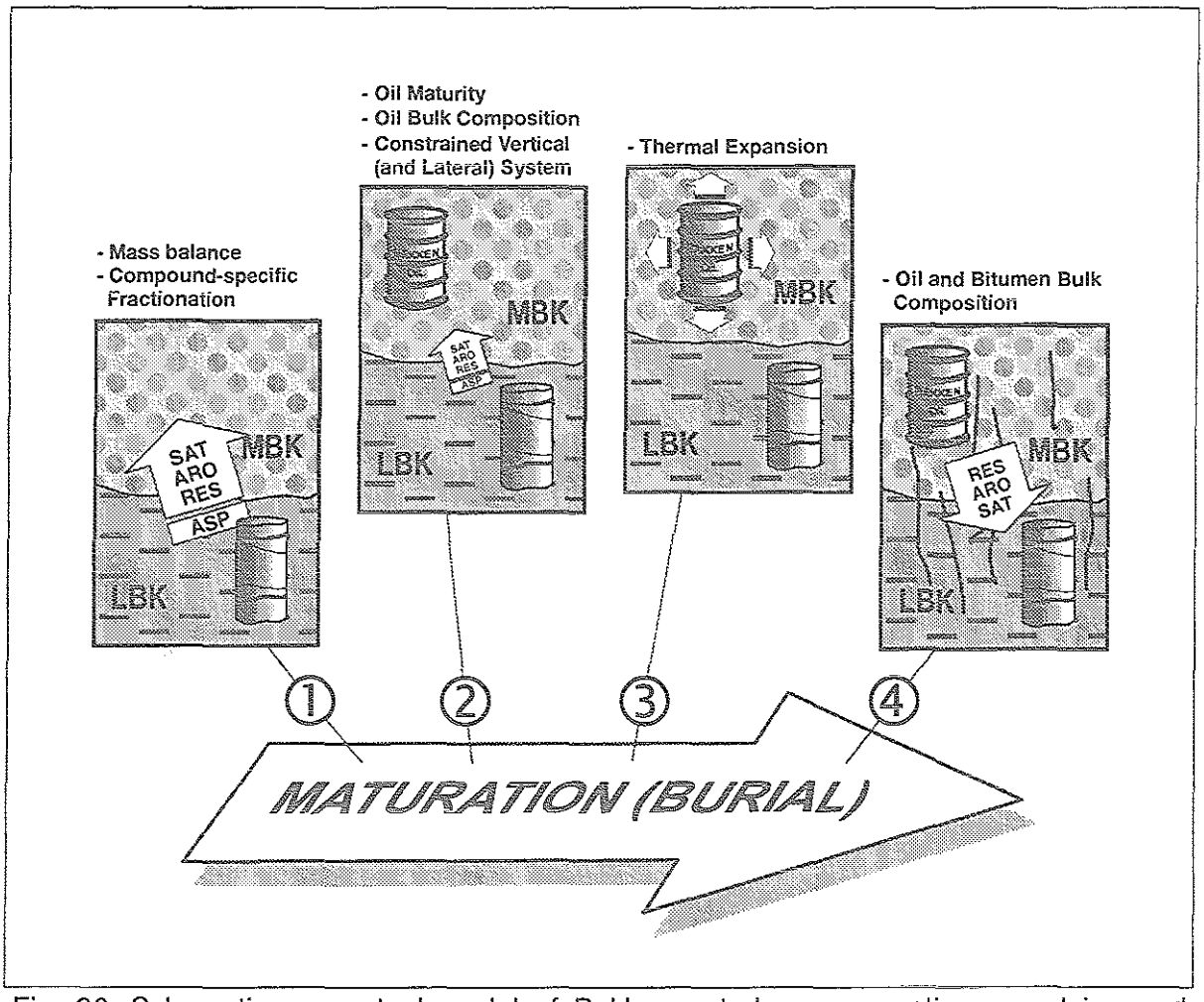

Fig. 86: Schematic conceptual model of Bakken petroleum generation, expulsion and redistribution as a function of maturity interval. In the text, this scenario is outlined as a potential mechanism for local pressure build-up in the North Dakota portion of the Williston Basin.

❑ Stage 1 - Efficient expulsion of petroleum from the source rock into the reservoir

This stage includes the conversion of organic matter to mobile compounds and their removal from the source rock system. The results of mass balance calculations pertaining to organic matter conversion and expulsion were discussed in detail in ch. 5.1 and 5.2. This approach showed that generation and expulsion occur rather early in maturation (0.4% - 0.8% R_o) and that the latter process is very efficient. The diffusive transport of hydrocarbons along a well-connected kerogen network apparently has contributed to a greater extent to bulk flow

expulsion than normal. The differences in bulk composition between source rock solvent extracts (containing polar asphaltenes) and produced Bakken crude oil (asphaltene-free except for one sample) are believed to be indicative of a compound-specific fractionation process, during which mobile, less polar species (saturates, aromatics and resins) are removed from the source rock while the high-molecular-weight asphaltenes are retained.
This asphaltene-depleted petroleum phase then enters a reservoir. The Sanish Sandstone (DTF) as well as the middle Siltstone Member (mBK) may serve as a suitable reservoir. The Sanish Sandstone is believed to be only locally important (Finch, 1969; Meissner, 1978). Thence, its regional relevance may be negligible. In a detailed study including core analysis and determination of petrophysical parameters, LeFever et al. (1991) focussed on the mBK in particular in terms of reservoir potential. Analysis of 12 North Dakota wells elucidated that reservoir quality reflects the variable lithology in that porosity and permeability range from 0.02 to 15.8%, and 0.01 to 109md, respectively (LeFever et al., 1991). Such properties qualify the mBK as a good reservoir rock (Muskat, 1981) and especially its basinwide distribution may designate it as the *principal* reservoir for Bakken oil in the North Dakota portion of the Williston Basin.

❑ Stage 2 - Post-generation/-expulsion in-situ maturation of Bakken crude oil

This stage refers to the evolution of the Bakken petroleum system after generation and expulsion of petroleum has been grossly completed (0.8% R_o), but maturation (burial) still continues. With the prerequisite that the oil cannot migrate very far (neither vertically nor laterally) it undergoes the same fate as its parent source rock, namely progressive thermal alteration. The latter leads to changes in compositional characteristics of the oils and the molecular parameters such as aromatic ratios are modified to reflect high levels of maturity (ch. 5.2.1). Such a prolonged thermal maturation of oils within the Bakken reservoir itself was also considered by Talukdar et al. (1991) to result in high API gravity crude oils. For instance, the bulk composition (GOR) is shifted to higher contents of low-molecular-weight compounds (England & Mackenzie, 1989). However, cracking of oil to gas at ca. 0.9% R_o conflicts with the classical oil window scheme (Tissot & Welte, 1984). Nonetheless it may still be feasible in the case of the Bakken petroleum system because here the mainstage of hydrocarbon generation is also shifted to rather early ranges of vitrinite reflectance (ch. 5.1.1). In the same chapter, the limited applicability of the classical R_o approach for delineating hydrocarbon generation zones for the Bakken has been pointed out. Hence, the process of in-situ maturation appears to be one strong controlling factor for the high-quality, light oil character of Bakken petroleum. Furthermore, the unusual high concentrations of gaseous and other low-molecular-weight compounds in the Bakken source rock as revealed by t'vap-gc (ch. 5.1.3) might not only be a result of direct and early generation from the kerogen, but also derived from cracking reactions.

❑ Stage 3 - Thermal expansion of reservoired crude oil

In this phase of evolution, Bakken crude oil is considered to increase its volume as a consequence of thermal stress. Timewise, it directly adds to stage 2. The petroleum fluid may react by thermal expansion similar to the aquathermal pressuring scheme proposed by Barker (1972) for aqueous subsurface fluids. In the case of the Bakken petroleum system, there is strong evidence that hydrocarbons are the only present fluid. Although the results derived

from mineralogic analysis were not unequivocal, interlayer water originating from smectite-illite alteration can be considered to be of minor importance in the Bakken Shale (ch. 4.9)
The density of a given petroleum fluid decreases with increasing temperature (Muskat, 1981) but the specific volume increases and it tends to expand. The maximum rate of thermal expansion for petroleum is reported to be ca. 5%/Ma (Chapman, 1980). If the rate of overburden pressure (mechanical compression) is not reduced (e.g. as a consequence of erosion/uplift) and permeability is not significantly improved, then the resistance to thermal expansion increases and pressure build-up is initiated (Chapman, 1980).
The latter is also enhanced by the limited storage capacity of the principal reservoir, i.e. the mBK. Although a given rock volume of mBK represents a good reservoir rock (Muskat, 1981; see stage 1), the total volume of mBK which is available for reservoiring Bakken Shale generated oil is relatively low. This is due to the fact that thickness of the mBK decreases gradually from a maximum of ca. 27m in the basin center to zero at the depositional edge (Webster, 1984). Based on a simple calculation incorporating the total volume of mBK with an average thickness of 15m and an average porosity of 10% covering an area in North Dakota where the Bakken *Shale* is considered mature (areas B, C, D and E from Webster, 1984), the total volume of pore space in the mBK available to hold petroleum equals ca. 18 billion bbls. Yet, estimations of the amount of crude oil generated by the Bakken Shale of the same area are in the order of magnitude of 100 billion bbls (Webster, 1984) or 150 billion bbls (Price & LeFever, 1994). Thus, there may be a significant discrepancy between reservoir capacity of the mBK and volume of petroleum generated from the Bakken Shales. That means that the pore space of the mBK may not be sufficient to take up all the Bakken petroleum and that further storage capacity is required. Clearly, such calculations bear some uncertainties and results thereof should only be regarded as an order of magnitude, as they are only based on estimations and average parameters. Furthermore, this approach assumes that the total amount of petroleum is quantitatively uniformly distributed throughout the entire area under consideration. However, as laid out further above, lateral hydraulic connectivity may be valid only within very short distances.
The considerations above imply that, when a certain trigger value (threshold) is reached, the volume of the petroleum may exceed the limited storage capacity of the reservoir rock unit (mBK) in which it resides.

❑ Stage 4 - Reimpregnation of petroleum from the reservoir back into the source rock

This step follows directly stage 3 and provides an explanation for the enhanced solvent extract yields (lower Bakken Shale samples of wells MAR and JEN) in the mature zone (Fig. 23) and for the different concentration patterns obtained for asphaltenes and resins in those samples associated with locally enhanced extract yields (Fig. 25). The enhanced concentrations of petroleum could be due to locally higher generation potentials and/or impeded expulsion. However, the basinwide uniformity in Bakken Shale kerogen type (ch. 4.4) and the fairly constant distribution of organic richness (TOC) and Rock-Eval-HI in a given mature well (> 0.7% R_o) as exemplified by well JEN (Fig. 12) argue for uniformity in hydrocarbon generation potential. As regards expulsion, it can never be ruled out unequivocally that local "spots" exist in the Bakken where expulsion avenues (fractures, kerogen network) are not sufficiently well-developed and/or continuous.

Nonetheless, there is some evidence that the observed solvent extract yield anomalies are a result of reimpregnation of petroleum from overlying and underlying strata (DTF and mBK). The direction of transport from inferred reservoir to source is substantiated by migration-sensitive Pri/n-$C_{17:0}$ (Leythaeuser & Schwarzkopf, 1986) and Phy/n-$C_{18:0}$ values, which are *lower* for Bakken Shales than for adjacent strata of the same well (Ropertz, 1994; Eric Michael, written communication; see Tab. 17).

Table 17: Distribution of values for two selected molecular parameters (saturated hydrocarbon fraction) for both shale members and their over- and underlying units.

Parameter	Unit	Reference	
		Ropertz (1994)	*Michael (1993)*
Pri/n-$C_{17:0}$	LP	0.68	0.4
	uBK	0.55	0.35
	mBK	0.75	0.3 - 0.6
	lBK	0.51	--
	DTF	0.70	--
Phy/n-$C_{18:0}$	LP	0.62	--
	uBK	0.55	--
	mBK	0.71	--
	lBK	0.50	--
	DTF	0.61	--

In the context of an inferred transport of petroleum from reservoir to source as laid out in this section it is interesting that the concept of "activated diffusion" (Stainforth & Reinders, 1990), which was discussed as a potentially meaningful migration mechanism for the Bakken system in ch. 5.2.2, also incorporates such reversed diffusive transport back into the source rock system.

With respect to the different concentration patterns obtained for asphaltenes and resins in those samples associated with locally enhanced extract yields (Fig. 25) it may be plausible that this feature is also due to a reverted direction of transport: The asphaltenes are retained in the source rock and represent a portion of the residual extract, while the resins as well as the saturates and aromatic fraction represent a portion of the crude oil that first leaves the source rock system (stage 1) but then re-enters it again after stage 3. Consequently, the locally enhanced yields of solvent extracts in the lower shale units of well MAR and JEN exhibit the same distribution patterns as the saturate and aromatic fraction of the oils. During reimpregnation the crude oil, consisting mainly of saturates, aromatics and resins is added to the originally present bitumen in the rock, which in turn is enriched in polar compounds (asphaltenes).
Based on this concept, a mass balance was developed for the solvent extractable organic matter for the lBK samples of wells MAR and JEN based on the solvent extract yield distribution as a function of maturity as depicted in Fig. 23. These individual samples with maximum contents of bitumen were considered to be affected by reimpregnation, while the

averaged extract yield of all other samples > 0.8% R_o was believed to be representative for the original situation after the main stage of generation and expulsion and thence acted as a reference similar to the relative expulsion efficiency approach in ch. 5.2.2. Tab. 18 elucidates that the asphaltene concentration for MAR and JEN remains almost unmodified, while the other fractions are submitted to considerable variations. According to this approach, it is proposed that ca. 70% of the bitumen of well MAR is derived from reimpregnation processes, while well JEN appears to be less influenced (ca. 50 to 60%).

Table 18: Results of mass balance calculations for hypothesized reimpregnation process from reservoir back into the source rock. Approach is explained in text.

Fraction	Portion derived from Reimpregnation (%)		
	MAR (0.9% R_o) E 34328	JEN (0.92% R_o) E 34454	JEN (0.92% R_o) E 34455
Whole extract	68.60	57.51	51.90
SAT	72.52	55.14	67.89
ARO	67.90	61.86	43.02
RES	68.18	68.02	45.26
ASP	4.99	-2.59	5.14

The 4-stage scenario as laid out above may finally lead to pressure build-up: (a) In the absence of corresponding pathways from reservoir to source rock, release of the oil is inhibited. In this case, overpressuring would be restricted to the reservoir (mBK). (b) The petroleum is drained along appropriate pathways (e.g. fractures), but storage capacity of the shales, which can be considered a function of the macrofracture network density, is rapidly exceeded. Here, anomalously high pressures could be encountered in shales and adjacent members of the Bakken Formation.

The theory presented above implies that the overpressured situation encountered in the Bakken petroleum at present-day time is a *local* phenomenon and cannot be extrapolated on a basinwide scale. Controlling factors are reservoir quality (storage capacity) of the sediments adjacent to the shales and availability of appropriate pathways for the reverse migration. Overpressuring is caused by the restricted nature of the petroleum system in terms of long-distance vertical and lateral migration.

Furthermore, the postulate of a Bakken Shale in-source reservoir (Price & LeFever, 1992) may have to be redefined. Results of the present study strongly suggest that in some regions the source rock (Bakken Shale) can be clearly separated from the reservoir rock (primarily mBK, secondary Sanish Sandstone).

6 Conclusions

- The nature of Bakken petroleum is governed by efficient expulsion and subsequent in-situ maturation. The latter process is the controlling factor for the high-quality, light oil character of Bakken crude oil.

- The Bakken Shale shows an enhanced capability of generating gaseous products throughout maturation. These low molecular weight hydrocarbons might play a vital role in expulsion mechanisms.

- There is some evidence that the mechanism of diffusive transport of products contributes to a high degree to the rapid and efficient expulsion of petroleum in the Bakken Formation. A well-developed and continuous organic matter network may provide the suitable expulsion/migration pathway.

- Highly efficient expulsion and, most importantly, post-generation in-situ maturation effects have overprinted compositional properties of the Bakken crude oils inherited from the process of hydrocarbon generation.

- Compositional features which are common in both the natural and artificial maturation sequence are useful for calibrating the latter in terms of maturity zones. This maturity zonation approach can be utilized for predicting the quantitative and qualitative evolution of natural products without the fractionating interferences of expulsion and migration.

- Abnormally high reservoir pressures encountered in the Bakken Formation apparently are a local phenomenon. Overpressuring may have been caused by thermally-induced volume expansion of crude oil stored in Bakken Shale over- and underlying strata. The phenomenon of reimpregnation of petroleum from the reservoir back into the source rock system may account for locally enhanced concentrations of crude oil in the Bakken Shale. Therefore, the generalized postulate of an in-source reservoir has to be reconsidered.

7 References

ABELLA, C.; MOUTESINOS, E. AND GUERRERO, R. (1980) Field Studies on the Competition Between the Purple and Green Sulfur Bacteria for Available Light. - Dev. Hydrobiol. 3, pp. 173-181.

AHERN, J.L. AND MRKVICKA, S.R. (1984) A Mechanical and Thermal Model for the Evolution of the Williston Basin. - Tectonics, Vol. 3, No. 1, pp. 79-102.

ALBRECHT, P.; VANDENBROUCKE, M. AND MANDENGUÉ, M. (1976) Geochemical Studies on the Organic Matter from the Douala Basin (Cameroon) - I. Evolution of the Extractable Organic Matter and the Formation of Petroleum. - Geochim. Cosmochim. Acta, 40, pp. 791-799.

ANDERSON, S.B.; GERHARD, L.C. AND LEFEVER, J.A. (1983) Structural and Sedimentologic History of Nesson Anticline. - In: AAPG Rocky Mountain Section Meeting, Billings, Montana, 1983.

ARCHER, J.S. (1990) Heterogeneity of Permeability in Oil Reservoirs.- In: Seventy-five Years of Progress in Oil Field Science and Technology (ed. by Ala, M.A. et al.), Balkema, Rotterdam, pp. 169-176.

BARKER, C. (1972) Aquathermal Pressuring - Role of Temperature in Development of Abnormal-Pressure Zones. - Bull. Am. Assoc. Petrol. Geol., v. 56, No. 10, pp. 2068-2071.

BÉHAR, F. AND VANDENBROUCKE, M. (1988) Characterization and Quantification of Saturates Trapped Inside Kerogen: Implications for Pyrolysate Composition. - In: Advances in Organic Geochemistry 1987 (ed. by Mattavelli, L. and Novelli, L.). pp. 335-341, Pergamon Press, Oxford.

BLUEMLE, J.P.; ANDERSON, S.B.; ANDREW, J.A.; FISCHER, D.W. AND LEFEVER, J.A. (1986) Williston Basin Stratigraphic Nomenclature Chart. - In: North Dakota Geological Survey Miscellaneous Series No. 6, Sheet 1.

BRAY, E.E. & EVANS, E.D. (1961) Distribution of N-Paraffins as a Clue to Recognition of Source Beds. - Geochim. Cosmochim. Acta, 31, pp. 2389-2397.

BROOKS, P.W.; SNOWDON, L.R. AND OSADETZ, K.G. (1987) Families of Oils in Southeastern Saskatchewan. - In: Proceedings of the Fifth International Williston Basin Symposium (ed. by Carlson, C.G. and Christopher, J.E.), Bismarck, North Dakota, June 15-17. Saskatchewan Geological Society, Special Publication No. 9, pp. 253-263.

BRUCE, C.H. (1984) Smectite Dehydration - Its Relation to Structural Development and Hydrocarbon Accumulation in Northern Gulf of Mexico Basin. - Bull. Am. Assoc. Petrol. Geol., v. 68, No. 6, pp. 673-683.

BUISKOOL TOXOPEUS, J.M.A. (1983) Selection Criteria for the Use of Vitrinite Reflectance as a Maturity Tool. - In: Petroleum Geochemistry and Exploration of Europe (ed. by Brooks, J.), pp. 295-307, Oxford, Blackwell Scientific Publications.

BURNHAM, A.K. (1992) Pyrolysis Kinetics for the Bakken Shale. - In: LLNL Report UCRL. ID-109622.

BURRUS, J.; OSADETZ, K.G.; WOLF, S.; DOLIGEZ,B.; VISSER, K. AND DEARBORN, D. (1994a) Re-Evaluation of Williston Basin Petroleum Systems Using Two-Dimensional Basin Modelling. - (submitted to AAPG Bulletin).

BURRUS, J.; OSADETZ, K.G.AND WOLF, S. (1994b) Geochemical and Numerical Modelling Constraints on Oil Expulsion and Accumulation from Bakken and Lodgepole Petroleum Systems in Williston Basin. - (submitted to CSPG Bulletin).

CARDOTT, B.J. AND LAMBERT, M.W. (1985) Thermal Maturation by Vitrinite Reflectance of Woodford Shale, Anadarko Basin, Oklahoma.- Bull. Am. Assoc. Petrol. Geol., v. 69, pp. 1982-1988.

CARLISLE, J. (1991) The Bakken Formation of the Williston Basin: Deposition, Maturation And Fracturing. - In: 1991 Guidebook to Geology and Horizontal Drilling of the Bakken Formation (ed. by Hansen, W.B.), Montana Geological Society, pp. 89.

CARLSON, C.G. AND ANDERSON, S.B. (1965) Sedimentary and Tectonic History of North Dakota Part of Williston Basin. - Bull. Am. Assoc. Petrol. Geol. v. 49, No. 11, pp. 1833-1846.

CHAPMAN, R.E. (1980) Mechanical Versus Thermal Cause of Abnormally High Pore Pressures in Shales. - Bull. Am. Assoc. Petrol. Geol., v.64, No. 12, pp. 2179-2183.

CHAPMAN, R.E. (1982) Effects of Oil and Gas Accumulation on Water Movement. - Bull. Am. Assoc. Petrol. Geol., v.66, No. 3, pp. 368-378.

CLAXTON, M.J.; PATIENCE, R.L. AND PARK, P.J.D. (1993) Molecular Modelling of Bond Energies in Potential Kerogen Sub-units. - 16th International Meeting on Organic Geochemistry, Stavanger Sept 1993, pp. 198-201, (ed. by Øygard, K.).

CONNAN, J.; LE TRAN, K. AND VAN DER WEIDE, B. (1975) Alteration of Petroleum in Reservoirs. - In: Proc. 9th World Petroleum Congress, v. 2, pp. 171-178.

CONNAN, J. AND CASSOU, A.M. (1980) Properties of Gases and Petroleum Liquids Derived from Terrestrial Kerogen at Various Maturation Levels. - Geochim. Cosmochim. Acta 44, pp. 1-23.

COOLES, G.P.; MACKENZIE, A.S. AND QUIGLEY, T.M. (1986) Calculation of Petroleum Masses Generated and Expelled from Source Rocks. - In: Advances in Organic Geochemistry 1985 (ed. by Leythaeuser, D. and Rullkötter, J.), Org. Geochemistry 10, pp. 235-245, Pergamon Press, Oxford.

CRAMER, D.D. (1991) Results of Stimulation Treatment in the Bakken Formation: Implications for Horizontal and Vertical Completions. - In: Montana Geological Society 1991 Guidebook to Geology and Horizontal Drilling of the Bakken Formation (ed. by W.B. Hansen), pp. 117-140.

DART, S.W. (1992) Evaluation of San Juan Basin Fractured Reservoirs from Surface Data. - In: Geological Studies Relevant to Horizontal Drilling: Examples from Western North America (ed. by Schmoker, J.W. et al.), Rocky Mountain Association of Geologists, pp. 95-112.

DAWS, J.A. AND PROSSER, D.J. (1992) Scales of Permeability Heterogeneity within the Brent Group. - Journal of Petroleum Geology, v. 15, pp. 397-418.

DOW, W.G. (1974) Application of Oil Correlation and Source Rock Data to Exploration in Williston Basin. - Bull. Am. Assoc. Petrol. Geol., v. 58, pp. 1253-1262.

DOW, W.G. (1977) Kerogen Studies and Geological Interpretations. - Journal of Geochemical Exploration, v. 7, pp. 79-99.

DÜPPENBECKER, S.J. AND HORSFIELD, B. (1990) Compositional Information for Kinetic Modelling and Petroleum Type Prediction. - In: Advances in Organic Geochemistry 1989 (ed. by Béhar, F. and Durand, B.), Org. Geochem. 16, Nos. 4-6, pp. 259-266, Pergamon Press, Oxford.

DÜPPENBECKER, S.J. AND WELTE, D.H. (1991) Petroleum Expulsion from Source Rocks - Insights from Geology, Geochemistry and Computerized Numerical Modelling. - In: Preprints of the 13th World Petroleum Congress, Topic 3, The Interplay of Petroleum Generation and Migration.

EGLINTON, T.I.; SINNINGHE DAMSTÉ, J.S.; KOHNEN, M.E.L.; DE LEEUW, J.W.; LARTER, S.R. AND PATIENCE, R.L. (1990) Analysis of Maturity-Related Changes in the Organic Sulfur Composition of Kerogens by Flash Pyrolysis-gaschromatography. - In: Geochemistry of Sulfur in Fossil Fuels (ed. by Orr, W.L. & White, C.M.), ACS Washington D.C., pp. 529-565.

ENGLAND, W.A.; MACKENZIE; A.S.; MANN, D.M. AND QUIGLEY, T.M. (1987) The Movement and Entrapment of Petroleum Fluids in the Subsurface. - J. Geol. Soc., 144, pp. 326-347.

ENGLAND, W.A. AND MACKENZIE, A.S. (1989) Some aspects of the Organic Geochemistry of Petroleum Fluids. - Geologische Rundschau 78/1, pp. 291-303, Stuttgart.

ENGLAND, W.A.; ANDREWS, S.R. AND RÜCKHEIM, J. (1991) Experimental Simulation of Gas-Phase Migration: Results and Interpretations. - In: 15th International Meeting on Organic Geochemistry, Manchester Sept 1991, Advances and Applications in Energy and the Natural Environment (ed. by Manning, D.), pp. 146-150.

ESPITALIÉ, J.; LAPORTE, J.L.; MADEC, M.; MARQUIS, F.; LEPLAT, P.; PAULET, J. AND BOUTEFEU, A. (1977) Méthode Rapide de Caractérisation des Roches Mères de Leur Potential Pétrolier et de Leur Degré d'Évolution. - Rev. Inst. Fr. Pétr., v.32, pp. 23-42.

ESPITALIÉ, J.; MADEC, J.M. AND TISSOT, B. (1980) Role of Mineral Matrix in Kerogen Pyrolysis: Influence on Petroleum Generation and Migration. - Bull. Am. Assoc. Petrol., v. 64, pp. 59-66.

ESPITALIÉ, J.; DEROO, G. AND MARQUIS, F. (1985) La Pyrolyse Rock-Eval et Ses Applications. - Rev. Inst. Fr. Pétr., v. 40, pp. 563-579 and p. 755-784.

EVANS, C.R., ROGERS, M.A. AND BAILEY, N.J.L. (1971) Evolution and Alteration of Petroleum in Western Canada. - Chem. Geol., 8, pp. 147-170.

FANG, H. AND JIANYU, C. (1992) The Cause and Mechanism of Vitrinite Reflectance Anomalies. - Journal of Petroleum Geology, v. 15 (4), pp. 419-434.

FINCH, W.C. (1969) Abnormal Pressure in the Antelope Field, North Dakota. - Journal of Petroleum Technology, v. 21, pp. 821-826.

FOGELBERG, L.-G., GORE, R. AND RÅNBY, B. (1967) Aromatization of Paraffin Hydrocarbons. - Acta. Chem. Scand., v. 21, No. 8, pp. 2041-2049.

FOWLER, C.M.R. AND NISBET, E.G. (1985) The Subsidence of the Williston Basin. - Ca. J. Earth Sci. 22, pp. 408-415.

FOWLER, M.G.; ABOLINS, P. AND DOUGLAS, A.G. (1986) Monocyclic Alkanes in Ordovician Organic Matter. - In: Advances in Organic Geochemistry 1985 (ed. by Leythaeuser, D. and Rullkötter, J.), Org. Geochemistry 10, pp. 815-823, Pergamon Press, Oxford.

FRANCÚ, J. (1993) written communication (November 12th, 1993)

FREISATZ, W.B. (1991) Fracture-enhanced Porosity and Permeability in the Bakken Formation, Williston Basin, Western North Dakota. - Univ. of North Dakota Msc. Thesis, Grand Forks, North Dakota, 81 p.

FUEX, A.N. (1977) The Use of Stable Carbon Isotopics in Hydrocarbon Exploration. - Journal of Geochemical Exploration, v. 7, pp. 155-188.

GERHARD, L.C.; ANDERSON, S.B.; LEFEVER, J.A. AND CARLSON, G.C. (1982) Geological Development, Origin, and Energy Mineral Resources of Williston Basin, North Dakota. - Bull. Am. Assoc. Petrol. Geol. v. 66, No. 8, pp. 989-1020.

GERLING, P.; WHITICAR, M.J. AND FABER, E. (1988) Extreme Isotope Fractionation of Hydrocarbon Gases in Permian Salts. - In: Advances in Organic Geochemistry 1987 (ed. by Mattavelli, L. and Novelli, L.). pp. 335-341, Pergamon Press, Oxford.

GLUSKOTTER, H.J. (1965) Electronic Low-temperature Ashing of Bituminous Coals. - Fuel, v.44, pp. 285-291.

GOEBEL, E.D.; COVENEY JR., R.M.; ANGINO, E.E.; ZELLER, E.J. AND DRESCHHOFF, G.A.M. (1984) Geology, Composition, Isotopes of Naturally Occurring H_2/N_2 Rich Gas From Wells Near Junction City, Kans. - Oil Gas J., 82 (19), pp. 215-222.

GOSNOLD, W.D., JR., (1991) Stratabound Geothermal Resources in North Dakota and South Dakota. - In: Final Report for DOE Geothermal Technology Division, 214 p.

HALL, K.; HORSFIELD, B. AND MILLS, N. (1993) On the Feasibility of Coupling Microscale Sealed Vessel (MSSV) Pyrolysis, Gas Chromatography and Isoptope Mass Spectrometry for Studying the Thermal Degradation of Crude Oils into Natural Gas. - In: 16th International Meeting on Organic Geochemistry, Stavanger Sept. 1993, (ed. by Øygard, K.).

HANEBECK, D.; KROOSS, B.M. AND LEYTHAEUSER, D. (1993) Experimental Investigation of Petroleum Generation and Expulsion from Source Rock under Lithostatic Conditions. - In: Proceedings of the 4th International Symposium on Hydrothermal Reactions (ed. by Cuney, M. and Cathelineau, M.), Nancy, pp. 71-74.

HANEBECK, D.; KROOSS, B.M. AND LEYTHAEUSER, D. (1994) Laboratory Simulation of Petroleum Generation and Expulsion from Source Rocks under Lithostatic Stress. - CSEG & CSPG Joint National Convention, May 9-12, 1994, Calgary, Alberta.

HANSEN, W.B (1991) 1991 Guidebook to Geology and Horizontal Drilling of the Bakken Formation. - Montana Geological Society, 1991, 197 p.

HANSEN, W.B. AND LONG, G.I.W. (1991a) Bakken Production and Potential in the U.S. and Canada: Can the Fairway be Defined? - In: 1991 Guidebook to Geology and Horizontal Drilling of the Bakken Formation (ed. by Hansen, W.B.), Montana Geological Society, pp. 69-88.

HANSEN, W.B. AND LONG, G.I.W. (1991b) Criteria for Horizontal and Vertical Prospect Generation in the Bakken Formation, Montana and North Dakota. - In: 1991 Guidebook to Geology and Horizontal Drilling of the Bakken Formation (ed. by Hansen, W.B.), Montana Geological Society, pp. 151-164.

HAYES, M.D. AND HOLLAND, F.D. (1983) Conodonts of the Bakken Formation (Devonian and Mississippian), Williston Basin, North Dakota. - Bull. Am. Assoc. Petrol. Geol., v. 67, pp. 1341-1342.

HEDBERG, H.D. (1980) Methane Generation and Petroleum Migration. - In: Problems of Petroleum Migration (ed. by Roberts, W.H. & Cordell, R.J.). AAPG Studies in Geology, 10, pp. 179-206.

HOFFMANN, C.F.; FOSTER, C.B.; POWELL, T.G. AND SUMMONS, R.E. (1987) Hydrocarbon Biomarkers from Ordovician Sediments and the Fossil Alga *Gloeocapsomorpha Prisca* Zalessky 1917. - Geochim. Cosmochim. Acta, v. 51. pp. 2681-2697.

HORSFIELD, B. AND DOUGLAS, A.G. (1980) The Influence of Minerals on the Pyrolysis of Kerogens. - Geochim. Cosmochim. Acta, v. 44. pp. 1110-1131.

HORSFIELD, B. (1989) Practical Criteria for Classifying Kerogens: Some Observations from Pyrolysis-Gas Chromatography. - Geochim. Cosmochim. Acta 53, pp. 891-901.

HORSFIELD, B.; DISKO, U. AND LEISTNER, F. (1989) The Microscale Simulation of Maturation: Outline of a New Technique and its Potential Applications. - Geol. Rund. 78, pp. 361-374.

HORSFIELD, B. AND DÜPPENBECKER, S.J. (1991) The Decomposition of Posidonia Shale and Green River Shale Kerogens Using Microscale Sealed Vessel (MSSV) Pyrolysis. - Journal of Analytical and Applied Pyrolysis, 20, pp. 107-123.

HORSFIELD, B.; BHARATI, S.; LARTER, S.R.; LEISTNER, F; LITTKE, R., SCHENK, A.J. AND DYPVIK, H. (1992) On the Atypical Petroleum-Generating Characteristics of Alginite in the Cambrian Alum Shale. - In: Early Organic Evolution: Implications for Mineral and Energy Resources (ed. by M. Schidlowski et al.), pp. 257-266, Springer-Verlag Berlin Heidelberg 1992.

HUANG, W.Y. AND MEINSCHEIN, G. (1979) Sterols as Ecological Indicators. - Geochim. Cosmochim. Acta, 43, pp. 739-745.

HUC, A.Y. and HUNT, J.M. (1980) Generation and Migration of Hydrocarbons in Offshore South Texas Gulf Coast Sediments. - Geochim. Cosmochim. Acta, 10, pp. 1081-1089.

HUC, A.Y.; HUNT, J.M. and WHELAN, J.K. (1981) The Organic Matter of a Gulf Coast Well Studied by a Thermal Analysis-Gas Chromatography Technique. - Journal of Geochemical Exploration, v. 15, pp. 671-681.

HUTTON, A.C. AND COOK, A.C. (1980) Influence of Alginite on the Reflectance of Vitrinite from Joadja, NSW, and some other Coals and Oil Shales Containing Alginite. Fuel, v. 59, pp. 711-714.

HUTTON, A.C.; KANTSLER, A.J.; COOK, A.C. AND MCKIRDY, D.M. (1980) Organic Matter in Oil Shales. - Aust. Pet. Explor. Assoc., v. 20. p. 44-67.

JAMES, A.T. (1983) Correlation of Natural Gas by Use of Carbon Isotopic Distribution Between Hydrocarbon Components. - Bull. Am. Assoc. Petrol., v. 67 (7), pp. 1176-1191.

KALKREUTH, W. AND MACAULEY, G. (1984) Organic Petrology of Selected Oil Shale Samples from Lower Carboniferous Albert Formation, New Brunswick, Canada. - Bull. Can. Petrol. Geol., v. 32, pp. 38-51.

KLEMME, H.D. AND ULMISHEK, G.F. (1991) Effective Petroleum Source Rocks of the World: Stratigraphic Distribution and Controlling Depositional Factors. - Bull. Am. Assoc. Petrol., v. 75, No. 12, pp. 1809-1851.

KROOSS, B.M.; LEYTHAEUSER, D. AND SCHAEFER, R.G. (1988) Light Hydrocarbon Diffusion in a Caprock. - Chemical Geology, v. 71, pp. 65-67.

KULANDER, B.R.; DEAN, S.L. AND WARD JR., B.J. (1990) Fractured Core Analysis - Interpretation, Logging and Use of Natural and Induced Fractures in Cores. AAPG.

LAFARGUE, E.; ESPITALIÉ, J.; JACOBSEN, T. AND EGGEN, S. (1990) Experimental Simulation of Hydrocarbon Expulsion. - In: Advances in Organic Geochemistry 1989, (ed. by Béhar, F. & Durand, B.), Org. Geochem. 16, Nos. 4-6, pp. 121-131, Pergamon Press.

LARTER, S.R. (1978) A Geochemical Study of Kerogens and Related Material. - Ph.D. Thesis, University of Newcastle upon Tyne.

LARTER, S.R. AND DOUGLAS, A.G. (1980) A Pyrolysis-gas Chromatographic Method for Kerogen Typing. - In: Advances in Organic Geochemistry 1979 (ed. by Douglas, A.G. and Maxwell, J.R.), pp. 579-584, Pergamon Press, Oxford.

LARTER, S.R.; SOLLI, H. AND DOUGLAS, A.G. (1983) Phytol Containing Melanoidins and their Bearing on the Fate of Isoprenoid Structures in Sediments. - In: Advances in Organic Geochemistry 1981 (ed. by Bjorøy et al.), pp. 513-521, John Wiley, Chichester, England.

LARTER, S.R. (1985) Integrated Kerogen Typing and the Quantitative Evaluation of Petroleum Source Rocks. - In: Thomas, B.M. et al. (eds.) Petroleum Geochemistry in Exploration of the Norwegian Shelf. Graham and Trotman, pp. 269-286.

LARTER, S.R. AND MILLS, N. (1991) Phase Controlled Fractionations in Migrating Petroleum Charges. - In: Petroleum Migration (ed. by England, W.A. & Fleet, A.J.), Geol. Soc. Spec. Pub., v. 59, pp. 137-147.

LARTER, S.R. AND HORSFIELD, B. (1993) Determination of Structural Components of Kerogens by the Use of Analytical Pyrolysis Methods. - Organic Geochemistry (ed. by Engel, M.H. & Macko, S.A.), Plenum Press, New York, 1993.

LECKIE, D.A.; KALKREUTH, W.D. AND SNOWDON, L.R. (1988) Source rock Potential and Thermal Maturity of Lower Cretaceous Strata: Monkman Pass Area, British Columbia. - Bull. Am. Assoc. Petrol., v. 72, No. 7, pp. 820-838.

LEENHEER, M.J. (1984) Mississippian Bakken and Equivalent Formations as Source Rocks in the Western Canadian Basin. - Org. Geochem., v. 6, pp. 521-532.

LEFEVER, J.A. (1991) History of Oil Production from the Bakken Formation, North Dakota. - In: Montana Geological Society 1991 Guidebook to Geology and Horizontal Drilling of the Bakken Formation (ed. by W.B. Hansen), pp. 3-18.

LEFEVER, J.A.; MARTINIUK, C.D.; DANCSOK, E.F.R. AND MAHNIC, P.A. (1991) Petroleum Potential of the Middle Member, Bakken Formation, Williston Basin . - In: Sixth International Williston Basin Symposium (ed. by Christopher, J.E and Haidl, F.M.), Saskatchewan Geological Society Spec. Publ. 11, Regina, pp. 74-94.

LETRAN, K., CONNAN, J. AND VAN DER WEIDE, B. (1974) Diagenesis of Organic Matter and Occurrence of Hydrocarbons and Hydrogen Sulfide in the SW Aquitaine Basin (France). - Bull. Centre Rech., Pau-SNPA, 8, pp. 111-137.

LEWAN, M.D.; WINTERS, J.C. AND MCDONALD, J.H. (1979) Generation of Oil-like Pyrolysates from Organic-rich Shales. - Science, 203, pp. 897-899.

LEYTHAEUSER, D; SCHAEFER, R.G. AND YÜKLER, A. (1982) Role of Diffusion in Primary Migration of Hydrocarbons. - Bull. Am. Assoc. Petrol., v. 66, No. 4, pp. 408-429.

LEYTHAEUSER, D.; MACKENZIE, A.S.; SCHAEFER, R.G. AND BJORØY, M. (1984) A Novel Approach for Recognition and Quantification of Hydrocarbon Migration Effects in Shale-Sandstone Sequences. - Bull. Am. Assoc. Petrol. Geol. 68, pp. 196-219.

LEYTHAEUSER, D. AND SCHWARZKOPF, T. (1986) The Pristane/n-heptadecane Ratio as an Indicator for Recognition of Hydrocarbon Migration Effects. - Org. Geochem., v. 10, pp. 191-197.

LEYTHAEUSER, D.; SCHAEFER, R.G. AND RADKE, M. (1987) On the Primary Migration of Petroleum. - In: Proc. 12th World Petroleum Congress, v. 2, pp. 227-236.

LEYTHAEUSER, D.; RADKE, M. AND WILLSCH, H. (1988) Geochemical Effects of Primary Migration of Petroleum in Kimmeridge Source Rocks from Brae Field Area, North Sea. II: Molecular Composition of Alkylated Naphthalenes, Phenanthrenes, Benzo- and Dibenzothiophenes. - Geochim. Cosmochim. Acta, v. 52, pp. 2879-2891.

LIJMBACH, G.W.M. (1975) On the Origin of Petroleum. - In: Proc. on the 9th World Petroleum Congress, v. 2, pp. 357-369.

LITTKE, R.; BAKER, D.R. AND LEYTHAEUSER, D. (1988) Microscopic and Sedimentologic Evidence for the Generation and Migration of Hydrocarbons in Toarcian Source Rocks of Different Maturities. - Org. Geochem. v. 13, Nos. 1-3, pp. 549-559.

LO, H.B. (1993) Correction Critera for the Suppression of Vitrinite Reflectance in Hydrogen-rich Kerogens: Preliminary Guidelines. - Org. Geochem. v. 20, No. 6, pp. 653-657.

LOUIS, M.C. AND TISSOT, B.P. (1967) Influence de la Température et de la Pression sur la Formation des Hydrocarbures dans les Argiles à Kérogene. - In: Proceedings of the 7th World Petroleum Congress, v. 2, pp. 47-60.

MACKENZIE, A.S.; PATIENCE, R.L.; MAXWELL, J.R.; VANDENBROUCKE, M. AND DURAND, B. (1980) Molecular Parameters of Maturation in the Toarcian Shales, Paris Basin, France. I. Changes in the Configurations of Acyclic Isoprenoid Alkanes, Steranes and Triterpanes. - Geochim. Cosmochim. Acta, v. 44, pp. 1709-1721.

MACKENZIE, A.S.; LEYTHAEUSER, D.; SCHAEFER, R.G. AND BJORØY, M. (1983) Expulsion of Petroleum Hydrocarbons from Shale Source Rocks. - Nature, v. 301, pp. 506-509.

MACKENZIE, A.S.; PRICE, I.; LEYTHAEUSER, D.; MÜLLER, P.; RADKE, M. AND SCHAEFER, R.G. (1988) The Expulsion of Petroleum from Kimmeridge Clay Source Rocks in the Area of the Brae Oil Field, UK Continental Shelf. - In:

Petroleum Geology of Northwest Europe (ed. by Brooks, J. and Glennie, K.) pp. 865-877, Graham and Trotman, London.

MANGO, F.D. (1991) The Stability of Hydrocarbons under the Time-Temperature Conditions of Petroleum Genesis. - Nature 352, pp. 146-148.

MANGO, F.D. (1994) The Origin of Light Hydrocarbons in Petroleum: Ring Preference in the Closure of Carbocyclic Rings. - Geochim. Cosmochim. Acta 58, No. 2, pp. 895-901.

MARTINIUK, C.D. (1988) Regional Geology and Petroleum Potential of the Bakken Formation, Southwestern Manitoba. - In: Manitoba Energy and Mines, Petroleum Open File Report POF 8-88.

MCAULIFFE, C.D. (1980) Oil and Gas Migration: Chemical and Physical Constraints. - In: AAPG Studies in Geology No. 10, Problems of Petroleum Migration (ed. by Roberts III, W.H. and Cordell, J.R.), Tulsa, Oklahoma, pp. 89-107.

MEISSNER, F.F. (1978) Petroleum Geology of the Bakken Formation, Williston Basin, North Dakota and Montana. - In: Williston Basin Symposium, pp. 207-227, Montana Geological Society.

MICHAEL, E. (1993) written communication (September 13th, 1993)

MICHAEL, E. (1994) written communication (April 25th, 1994)

MOLDOWAN, J.M.; SEIFERT, W.K. AND GALLEGOS, E.J. (1985) Relationship Between Petroleum Composition and Depositional Environment of Petroleum Source Rocks. - Bull. Am. Assoc. Petrol. Geol., v. 69, pp. 1255-1268.

MONNIER, F.; POWELL, T.G. AND SNOWDON, L.R. (1983) Qualitative and Quantitative Aspects of Gas Generation During Maturation of Sedimentary Organic Matter. Examples from Canadian Frontier Basins. - In: Advances in Organic Geochemistry 1981 (ed. by Bjorøy, M.), pp. 487-495, John Wiley and Sons, New York.

MONTHIOUX, M.; LANDAIS, P. AND MONIN, J.-C. (1985) Comparison between Natural and Artificial Maturation Series of Humic Coals from the Mahakam Delta, Indonesia. - Organic Geochemistry, v. 8, No. 4, pp. 275-292.

MOREL-À-L'HUISSIER, P.; GREEN, A.G.; JONES, A.G.; LATHAM, T.; MAJOROWICZ, J.A.; DRURY, M.J. AND THOMAS, M.D. (1990) The Crust Beneath the Intracratonic Williston Basin from Geophysical Data. - In: The Potential of Deep Seismic Profiling for Hydrocarbon Exploration (ed. by Pinet, B. and Bois, C.), Éditions Technip, Paris 1990, pp. 141-160.

MURRAY JR., G.H. (1968) Quantitative fracture study - Sanish Pool, McKenzie County, North Dakota. - Bull. Am. Assoc. Petrol. Geol., v. 52, No. 1, pp 57-65.

MUSCIO, G.P.A.; HORSFIELD, B. AND WELTE, D.H. (1991) Compositional Changes in the Macromolecular Organic Matter (Kerogens, Asphaltenes and Resins) of a Naturally Matured Source Rock Sequence from Northern Germany as Revealed by Pyrolysis Methods. - In: 15th International Meeting on Organic Geochemistry, Manchester Sept 1991, Advances and Applications in Energy and the Natural Environment (ed. by Manning, D.), pp. 447-449.

MUSKAT, M. (1981) Physical Principles of Oil Production. 922 pp., McGraw-Hill Book Co., Inc.

MYCKE, B.; HALL, K. AND LEPLAT. P. (1994) Carbon Isotopic Composition of Individual Hydrocarbons and Associated Gases Evolved from Micro-Scale Sealed Vessel (MSSV) Pyrolysis of High Molecular Weight Organic Material. - Org. Geochem. (accepted)

NEUZIL, C.E. (1993) Low Fluid Pressure Within the Pierre Shale: A Transient Response to Erosion. - Water Resources Research, v. 29, No. 7, pp. 2007-2020.

NORTH, F.K. (1985) Petroleum Geology. 607 pp., Allen & Unwin, Boston.

OSADETZ, K.G.; SNOWDON, L.R.; BROOKS, P.W. AND RYGH, M.E. (1990) Progress Identifying Oil Families and Effective Sources in Williston Basin. - Bull. Am. Assoc. Petrol. Geol., v. 74, pp. 1340.

OSADETZ, K.G.; SNOWDON, L.R. AND BROOKS, P.W. (1991) Relationships Amongst Oil Quality, Thermal Maturity and Post-Accumulation Alteration in Canadian Williston Basin (Southeastern Saskatchewan and Southwestern Manitoba). - In: Proceedings of the Sixth International Williston Basin Symposium (ed. by Christopher, J.E. and Haidl, F.), Saskatchewan Geological Society, Special Publication No. 11, pp. 293-311.

OSADETZ, K.G.; BROOKS, P.W. AND SNOWDON, L.R. (1992) Oil Families and Their Sources in Canadian Williston Basin, (Southeastern Saskatchewan and Southwestern Manitoba). - Bull. Can. Petrol. Geol., v. 40, pp. 254-273.

OTTENJANN, K.; WOLF, M. UND WOLFF-FISCHER, E. (1982) Das Fluoreszenzverhalten der Vitrinite zur Kennzeichnung der Kokungseigenschaften von Steinkohlen. - Glückauf-Forschungshefte 43 (1982) H. 4.

PALCIAUSKAS, V.V. (1991) Source and Migration Processes and Evaluation Techniques. - In: AAPG Treatise Petrol. Geol. Handbook Petrol. Geol. (ed. by Merrill, R.K.), pp. 13-22.

PHILIPPI, G.T. (1965) On the Depth, Time and Mechanism of Petroleum Generation. - Geochim. Cosmochim. Acta, v. 29, pp. 1021-1049.

PHILIPPI, G.T. (1975) The Deep Subsurface Temperature Controlled Origin of the Gaseous and Gasoline-range Hydrocarbons of Petroleum. - Geochim. Cosmochim. Acta, v. 39, pp. 1353-1373.

POWELL, T.G. AND MCKIRDY, D.M. (1973) Relationship between Ratio of Pristane to Phytane, Crude Oil Composition and Geological Environment in Australia. - Nature Physical Science, v. 243, pp. 37-39.

POWELL, T.G. AND MCKIRDY, D.M. (1975) Crude Oil Composition in Australia and Papua-New Guinea. - In: Bull. Am. Assoc. Petrol. Geol., v. 59, pp. 1176-1197.

POWERS, M.C. (1967) Fluid-Release Mechanisms in Compacting Marine Mudrocks and their Importance in Oil Exploration. - Bull. Am. Assoc. Petrol. Geol., v. 51, pp. 1240-1254.

PRICE, L.C.; GING, T.; DAWS, T., LOVE, A.; PAWLEWICZ, M. AND ANDERS, D. (1984) Organic Metamorphism in the Mississippian-Devonian Bakken Shale North Dakota Portion of the Williston Basin. - Hydrocarbon Source Rocks of the Greater Rocky Mountain Region (ed. by Woodward J. et al.), pp. 83-133, R.M.A.G.

PRICE, L.C. AND BARKER, C.E. (1985) Suppression of Vitrinite Reflectance in Amorphous Rich Kerogen - A Major Unrecognized Problem. - Journal of Petroleum Geology, v. 8, pp. 59-84.

PRICE, L.C. (1989) Primary Petroleum Migration from Shales with Oxygen-rich Organic Matter. - J. Petrol. Geol., v. 12, pp. 289-324.

PRICE, L.C. AND CLAYTON, J.L. (1992) Extraction of Whole Versus Ground Source Rocks: Fundamental Petroleum Geochemical Applications Including Oil-Source Rock Correlation. - Geochim. Cosmochim. Acta, Vol. 56, pp. 1213-1222, Pergamon Press.

PRICE, L.C. AND WENGER, L.M. (1992) The Influence of Pressure on Petroleum Generation and Maturation as Suggested by Aqueous Pyrolysis. - In: Advances in Organic Geochemistry 1991 (ed. by Eckardt, C.), Org. Geochem., v. 19, Nos. 1-3, pp. 141-159, 1992.

PRICE, L.C. AND LEFEVER, J.A. (1992) Does Bakken Horizontal Drilling Imply Huge Oil-Resource Bases in Fractured Shales ? - In: Geological Studies Relevant to Horizontal Drilling: Examples from Western North America (ed. by Schmoker et al.).

PRICE, L.C. AND LEFEVER, J.A. (1994) Dysfunctionalism in the Williston Basin: The Mid-Madison/Bakken Petroleum System. - Bull. Can. Petrol. Geol., v. 42, pp. 187-218.

RADKE, M.; SITTARDT, H.G. AND WELTE, D.H. (1978) Removal of Soluble Organic Matter from Rock Samples with a Flow-through Extraction Cell. - Anal. Chem. 50, pp. 663-665.

RADKE, M.; WILLSCH, H. AND WELTE, D.H. (1980a) Preparative Hydrocarbon Group Type Determination by Automated Medium Pressure Liquid Chromatography. - Anal. Chem. 52, pp 406-424.

RADKE, M.; SCHAEFER, R.G. AND LEYTHAEUSER, D. (1980b) Composition of Soluble Organic Matter in Coals: Relation to Rank and Liptinite Fluorescence. - Geochim. Cosmochim. Acta, v. 44, pp. 1787-1800.

RADKE, M.; WILLSCH, H.; LEYTHAEUSER, D. AND TEICHMÜLLER, M. (1982) Aromatic Components of Coal: Relation of Distribution Pattern to Rank. - In: Geochim. Cosmochim. Acta, v.46, pp. 1831-1848.

RADKE, M. AND WELTE, D.H. (1983) The Methylphenanthrene Index (MPI): A Maturity Parameter Based on Aromatic Hydrocarbons. - In: Advances in Organic Geochemistry 1981 (ed. by Bjorøy, M. et al.), pp. 504-512. Wiley, Chichester.

RADKE, M.; WELTE, D.H. AND WILLSCH, H. (1986) Maturity Parameters Based on Aromatic Hydrocarbons: Influence of the Organic Matter Type. - In: Advances in Organic Geochemistry 1985 (ed. by Leythaeuser, D. and Rullkötter, J.), Org. Geochemistry 10, pp. 51-63, Pergamon Press, Oxford.

RADKE, M. (1987) Organic Geochemistry of Aromatic Hydrocarbons. - In: Advances in Petroleum Geochemistry, v. 2, (ed. by Brooks, J. & Welte, D.H.), Academic Press, London.

RAY, J.E.; OLIVER, K.M. AND WAINWRIGHT, J.C. (1982) The Application of the IATROSCAN TLC Technique to the Analysis of Fossil Fuels. - In: Petroanalysis 81, IP Symposium, London, pp. 361-388, Heyden & Son, London.

REQUEJO, A.G.; ALLAN, J.; CREANEY. S.; GRAY, N.R. AND COLE, K.S. (1992) Aryl Isoprenoids and Diaromatic Carotenoids in Paleozoic Source Rocks and Oils from the Western Canada and Williston Basins. - In: Advances in Organic Geochemistry 1991 (ed. by Eckardt, C.), Org. Geochem. v. 19, Nos. 1-3, pp. 245-264.

ROPERTZ, B. (1994) Wege der primären Migration: Eine Untersuchung über Porennetze, Klüfte und Kerogennetzwerke als Leitbahnen für den Kohlenwasserstofftransport. Berichte des Forschungszentrums Jülich - Nr. 2875, Diss. T.H. Aachen.

RULLKÖTTER, J. AND MARZI, R. (1988) Natural and Artificial Maturation of Biological Markers in a Toarcian Shale from Northern Germany. - In: Advances in Organic Geochemistry 1987. (ed. by Mattavelli, L. and Novelli, L.), pp. 639-645, Pergamon Journals, Oxford.

RULLKÖTTER, J.; LEYTHAEUSER, D.; HORSFIELD, B.; LITTKE, R.; MANN, U.; MÜLLER, P.J.; RADKE, M.; SCHAEFER, R.G.; SCHENK, H.-J.; SCHWOCHAU, K.; WITTE, E.-G. AND WELTE, D.H. (1988). Organic Matter Maturation Under the Influence of a Deep Intrusive Heat Source: a Natural Experiment for Quantitation of Hydrocarbon Generation and Expulsion from a Petroleum Source Rock. (Toarcian Shale, Northern Germany). - In: Advances in Organic Geochemistry 1987. (ed. by Mattavelli, L. and Novelli, L.), pp. 847-856, Pergamon Journals, Oxford.

SANDVIK, E.I. AND MERCER, J.N. (1990) Primary Migration by Bulk Hydrocarbon Flow. - In: Advances in Organic Geochemistry 1989 (ed. by Béhar, F. and Durand, B.), Org. Geochem. 16, Nos. 1-3, pp. 83-89, Pergamon Press, Oxford.

SCHAEFER, R.G.; WEINER, B. and LEYTHAEUSER, D. (1978) Determination of Sub-nanogram per Gram Quantities of Light Hydrocarbons (C_2-C_9) in Rock Samples by Hydrogen Stripping in the Flow System of a Capillary Gas Chromatograph.- Analytical Chemistry, v. 50, No. 13, pp. 1848-1854.

SCHENK, H.J.; WITTE, E.G.; MÜLLER, P.J. AND SCHWOCHAU, K. (1986) Infrared Estimates of Aliphatic Kerogen Carbon in Sedimentary Rocks. - In: Advances in Organic Geochemistry 1985 (ed. by Leythaeuser, D. and Rullkötter, J.), Org. Geochemistry 10, pp. 1099-1104, Pergamon Press, Oxford.

SCHENK, H.J.; WITTE, E.G.; LITTKE, R. AND SCHWOCHAU, K. (1990) Structural Modifications of Vitrinite and Alginite Concentrates During Pyrolytic Maturation at Different Heating Rates. A Combined Infrared, ^{13}C NMR and Microscopical Study. - In: Advances in Organic Geochemistry 1989, (ed. by Béhar, F. & Durand, B.), Org. Geochem. 16, Nos. 4-6, pp. 943-950, Pergamon Press.

SCHOELL, M. (1980) Genetic Characterisation of Natural Gases. - Bull. Am. Assoc. Petrol. Geol., v. 67, pp. 2225-2238.

SEARS, J.W. AND ALT, D. (1990) Impact Origin of Large Intracratonic Basins, the Stationary Proterozoic Crust, and the Transition to Modern Plate Tectonics. 8th International Conference on Basement Tectonics.

SEIFERT, W.K. AND MOLDOWAN, J.M. (1981) Paleoreconstruction by Biological Markers. - Geochim. Cosmochim. Acta, v. 45, pp. 783-794.

SKOPEC, R.A. (1992) Evaluating Naturally Fractured Reservoirs Targeted for Horizontal Drilling. - In: Geological Studies Relevant to Horizontal Drilling: Examples from Western North America (ed. by Schmoker, J.W. et al.), Rocky Mountain Association of Geologists, pp. 37-46.

SLOSS, L.L. (1963) Sequences in the Cratonic Interior of North America. - Geol. Soc. America Bull. , v. 74, pp. 93-114.

SOKOLOV, V.A.; GEODEKYAN, A.A.; GRIGORYEV, C.G.; KREMS, A.; STROGANOV, V.A.; ZORKIN, L.; ZEIDELSON, M.I. AND VAINBAUM, S.Ja. (1971) The New Methods of Gas Surveys, Gas Investigations of Wells and Some Practical results. - Geochemical Exploration (ed. by Boyle, R.W.), sp. vol., 11, Can. Inst. Min. and Met., pp. 538-544.

SOLLI, H.; VAN GRASS, G.; LEPLAT, P. AND KRANE, J. (1984) Analysis of Kerogens of Miocene Shales in a Homogeneous Sedimentary Column. A Study of Maturation Using Flash Pyrolysis Techniques and Carbon-13 CP-MAS NMR. - Org. Geochem. v. 6, pp. 351-358, Pergamon Press.

SOLLI, H. AND LEPLAT, P. (1986) Pyrolysis-gas Chromatography of Asphaltenes and Kerogens from Source Rocks and Coals - A Comparative Structural Study. - In: Advances in Organic Geochemistry 1985 (ed. by Leythaeuser, D. and Rullkötter, J.), Org. Geochemistry 10, pp. 313-329, Pergamon Press, Oxford.

SPEIGHT, J.G., LONG, R.B. AND TROWBRIDGE, T.D. (1983) Factors Influencing the Separation of Asphaltenes from Heavy Petroleum Feedstocks. - Fuel, v. 63, pp. 616-620.

SPERR, J.T. (1990) Exploration Models for Bakken Shale Reservoirs, Williston Basin, North Dakota. - Bull. Am. Assoc. Petrol. Geol. v. 74, No. 8, p. 1345.

STACH, E.; MACKOWSKY, M.-TH.; TEICHMÜLLER, M.; TAYLOR, G.H.; CHANDRA, D. AND TEICHMÜLLER, R. (1982) Stach's Textbook of Coal Petrology. 535 pp. Borntraeger, Stuttgart.

STAHL, W.J. (1977) Carbon and Nitrogen Isotopics in Hydrocarbon Research and Exploration. - Chem. Geol., v. 20, pp. 121-149.

STAINFORTH, J.G. AND REINDERS, J.E.A. (1990) Primary Migration of Hydrocarbons by Diffusion through Organic Matter Networks, and its Effect on Oil and Gas Generation. - In: Advances in Organic Geochemistry 1989, (ed. by Béhar, F. & Durand, B.), Org. Geochem. 16, Nos. 1-3, pp. 61-74, Pergamon Press.

STEARNS, D.W. (1971) Mechanisms of Drape Folding in the Wyoming Province. - In: Wyoming Geological Association Guidebook, 23rd Annual Field Conference, pp. 125-143.

SWEENEY, J.J.; GOSNOLD, W.D.; BRAUN, R.L. AND BURNHAM, A.K. (1992) A Chemical Kinetic Model of Hydrocarbon Generation from the Bakken Formation, Williston Basin North Dakota. - LLNL Report UCRL-ID-112038.

TAKEDA, N.; SATO, S. AND MACHIHARA, T. (1990) Study of Petroleum Generation by Compaction Pyrolysis. - I. Construction of a Novel Pyrolysis System With Compaction and Expulsion of Pyrolysate from Source Rock. - In: Advances in Organic Geochemistry 1989, (ed. by Béhar, F. & Durand, B.), Org. Geochem. 16, Nos. 4-6, pp. 143-153, Pergamon Press.

TALUKDAR, S.C.; DOW, W.G. AND CASTAÑO, J.R. (1991) Oil Expulsion in Organic-rich Type II Source Rocks. - In: 15th International Meeting on Organic Geochemistry, Manchester Sept 1991, Advances and Applications in Energy and the Natural Environment (ed. by Manning, D.), pp. 169-170.

TEGELAAR, E.W. AND NOBLE, R.A. (1993) Kinetics of Hydrocarbon Generation as a Function of the Macromolecular Structure of Kerogen. - In: Advances in Organic Geochemistry 1993 (ed. by Øygard, K.) (in press).

THOMAS, M.M. AND CLOUSE, J.A. (1990a) Primary Migration by Diffusion Through Kerogen: I. Model Experiments with Organic-Coated Rocks. - Geochim. Cosmochim. Acta, v. 54, pp. 2775-2779.

THOMAS, M.M. AND CLOUSE, J.A. (1990b) Primary Migration by Diffusion Through Kerogen: II. Hydrocarbon Diffusivities in Kerogen. - Geochim. Cosmochim. Acta, v. 54, pp. 2781-2792.

THOMPSON, K.F.M. (1979) Light Hydrocarbons in Subsurface Sediments. - Geochim. Cosmochim. Acta, v. 43, pp. 657-672.

THOMPSON, K.F.M. (1988) Gas-Condensate Migration and Oil Fractionation in Deltaic Systems. - Mar. Petrol. Geol. 5, pp. 237-246.

THRASHER, L.C. (1985) Macrofossils and Biostratigraphy of the Bakken Formation (Devonian and Mississippian) in western North Dakota. Master's Thesis, University of North Dakota, Grand Forks, North Dakota, 292p.

TISSOT, B.P.; CALIFET-DEBYSER, Y.; DEROO, G. AND OUDIN, J.L. (1971) Origin and Evolution of Hydrocarbons in Early Toarcian Shales, Paris Basin, France. - Bull. Am. Assoc. Petrol. Geol., v. 55, pp. 2177-2193.

TISSOT, B.P.; PELET, R; ROUCHACHÉ, J. AND COMBAZ, A. (1977) Utilisation des alcanes comme fossiles géochimiques indicateurs des environnements géologiques. - In: Advances in Organic Geochemistry 1975, (ed. by Campos, R. & Goni, J.), Madrid, 1977.

TISSOT, B.P. AND WELTE, D.H. (1984) Petroleum Formation and Occurrence. 2nd ed., 699 pp., Berlin, Springer-Verlag.

TISSOT, B.P. AND UNGERER, P. (1990) In: Advances in Organic Geochemistry, a Narrow Path Between Fundamental Interest and Industry Needs. - Org.Geochem. 16, XXV-XLV.

VAN GRAAS, G.; DE LEEUW, J.W.AND SCHENCK, P.A. (1980) Analysis of Coals of Different Rank by Curie Point Pyrolysis-Gas Chromatography and Curie Point Pyrolysis-Mass Spectrometry. - In: Advances in Organic Geochemistry 1979, (ed. by Douglas, A.G. & Maxwell, J.R..), pp. 485-497, Pergamon Press, Oxford.

VAN GRAAS, G.; DE LEEUW, J.W.; SCHENCK, P.A. AND HAVERKAMP, J. (1981) Kerogen of Toarcian Shales of the Paris Basin. A Study of its Maturation by Flash Pyrolysis Techniques. - Geochim. Cosmochim. Acta, v. 45, pp. 2465-2474.

VASSOEVICH, N.B. ; KORCHAGINA, YU. I.; LOPATIN, N.V. AND CHERNYSHEV, V.V. (1970) Principal Phase of Oil Formation. - Int. Geol. Rev., v. 12, 11, pp. 1276-1296.

VOLKMAN, J.K. (1986) A Review of Sterol Markers for Marine nad Terrigenous Organic Matter. - Org. Geochem. v. 9, pp. 83-99, Pergamon Press.

WAPLES, D.H. AND MACHIHARA, T. (1991) Biomarkers for Geologists - a Practical Guide to the Application of Steranes and Triterpanes in Petroleum Geology. AAPG Methods in Exploration, 9.

WEBSTER, R.L. (1984) Petroleum Source Rocks and Stratigraphy of the Bakken Formation in North Dakota. - In: Hydrocarbon Source Rocks of the Greater Rocky Mountain Region (Edited by Woodward J. et al.) 57-81, R.M.A.G.

WELTE, D.H. AND YÜKLER, M.A. (1981) Petroleum Origin and Accumulation in Basin Evolution - A Quantitative Model. - Bull. Am. Assoc. Petrol. Geol., v. 65, pp. 1387-1396.

WENGER, L.M. AND BAKER, D.R. (1987) Variations in Vitrinite Reflectance with Organic Facies - Examples from Pennsylvanian Cyclothems of the MidContinent, USA. - Org. Geochem. 11, pp. 411-416.

WHELAN, J.K.; FARRINGTON, J.W. AND TARAFA, M.E. (1986) Maturity of Organic Matter and Migration of Hydrocarbons in two Alaskan North Slope Wells. - In:

Advances in Organic Geochemistry 1985 (ed. by Leythaeuser, D. and Rullkötter, J.), Org. Geochemistry 10, pp. 207-219, Pergamon Press, Oxford.

WILLIAMS, J.A. (1974) Characterization of Oil Types in Williston Basin. Bull. Am. Assoc. Petrol. Geol., v. 58, pp. 1243-1252.

WITTE, E.G.; SCHENK, H.J.; MÜLLER, P.J. AND SCHWOCHAU, K. (1988) Structural Modifications of Kerogen During Natural Evolution as Derived from ^{13}C CP/MAS NMR, IR Spectroscopy and Rock-Eval Pyrolysis of Toarcian Shales. - In: Advances in Organic Geochemistry 1987, (ed. by Mattavelli, L. and Novelli, L.), pp. 847-856, Pergamon Journals, Oxford.

WOLF, M. (1993) written communication (September 6th, 1993)

YOUNG, A. AND MCIVER, R.D. (1977) Distribution of Hydrocarbons Between Oils and Associated Fine-Grained Sedimentary Rocks - Physical Chemistry Applied to Petroleum Geochemistry, II. - Bull. Am. Assoc. Petrol. Geol. 61, pp. 1407-1436.

Appendix

Equations Used for the Calculation of Molecular Parameters

CPI-1 = $$\frac{2(C23+C25)}{(C22+2C24+C26)}$$

LHCPI = $$\frac{2(C17+C18+C19)}{(C27+2C28+C29)}$$

TNR-2 = $$\frac{1,3,7-TMN+2,3,6-TMN}{1,3,5-TMN+1,3,6-TMN+1,4,6-TMN}$$

MPI-1 = $$\frac{1,5(2-MP+3-MP)}{P+1-MP+9-MP}$$

MPR-3 = $$\frac{3-MP}{P}$$

TMN - trimethylnaphthalene
MP - methylphenanthrene
P - phenanthrene

20S/(20S+20R) = $$\frac{20S}{20S+20R}$$ of C_{29}, 5α(H), 14α(H), 17α(H)-steranes

ββ/ (αα+ββ) = $$\frac{2(14\beta(H),17\beta(H)20R+S)}{2(2(14\beta(H),17\beta(H),20R+S)+14\alpha(H),17\alpha(H),20R+S}$$ of C_{29} steranes

Ts/(Tm+Ts) = $$\frac{18\alpha(H)-trisnorneohopane}{17\alpha(H)-trisnorneohopane+18\alpha(H)-trisnorneohopane}$$

Hop/(Hop+Mor) = $$\frac{17\alpha(H),21\beta(H)-hopane}{17(H),21\beta(H)-hopane+17\beta(H),21\alpha(H)-hopane}$$

Tab. A-1: Background information on sampled cores/crude oils used in the present study. Data on well status was provided by the North Dakota Industrial Commision.

Abbrev.	Well # (Fig. 6)	NDGS core #	Location	County	Operator	Well name	Field	Dry	Producing	Producing Formation
Cores										
DOB	1	8177	18-151-87	Ward	Marathon Oil	Dobrinski		x		
JAC	2	2618	SWSE 15-145-91	Dunn	Pan Amer. Pet. Corp	Jacob Huber #1		x		
NEG	3	9001	NWNE 21-163-093	Burke	Clarion Resources Inc.	Negaard #1		x		
SKA	4	--	1-160-95	Divide	Conoco	Skarphol D-5	Stoneview		x	Madison
BOR	5	5656	SWSW 03-157-095	Williams	Texakota Inc.	H. Borstad #1	West Tioga		x	Bakken
GRA	6	8474	NESW 15-144-102	Billings	Tenneco	Graham USA #1-15	Buckhorn		x	Bakken
SET	7	2602	SWNE 06-153-095	McKenzie	Texaco	Seth A. Garland #5	Charlson		x	Devonian (?)
MAR	8	4340	SWSW 02-154-095	Williams	Pan Amer. Pet. Corp	Clifford Marmon #1	Hofflund	x	x	
JEN	9	1202	SWNW 06-152-094	McKenzie	Amerada	Jens Strand 1	Antelope		x	Sanish/Madison
CON	10	12886	27-144N-102W	Billings	Shell	Connell #24-27	Buckhorn		x	Bakken
FED	11	--	12-143-102	Billings	Conoco	Federal 12-1	Elkhorn Ranch		x	Bakken
HOV	12	2828	NWNW 15-154-098	Williams	Texaco	L.J. Hovde #1		x		
BEH	13	4297	SWNW 02-154-095	Williams	Pan Amer. Pet. Corp	B.E. Hove #1	Hofflund		x	Bakken
THO	14	12748	SWSW 05-145-099	McKenzie	Texaco	Thompson Unit #5-1	Whitetail	x		
PIE	*	8637	SENE 18-161-87	Renville	Clarion Resources Inc.	Pierce #1-18		x		
WAS	*	105	SWNE 02-153-085	Ward	Stanolind	Walter & Ingeberg		x		
FOR	*	4113	SENW 04-150-093	Mountrail	Texaco Inc.	Fort Berthold Allottee 437 #A1		x		
GIL	*	1254	SWSE 17-152-094	McKenzie	Amerada	Gilbert T. Rohde 1	Antelope		x	Sanish/Madison
HHS	*	1606	NESW 35-150-097	McKenzie	Amerada	H.H. Shelvic Tract 1 #1	North Fork		x	Dev.
REE	*	1748	NWNE 06-152-094	McKenzie	Amerada	Reed-Norby Unit #1	Antelope		x	Sanish
JOH	*	1886	NWSE 33-153-094	McKenzie	Amerada	John Dinwoodie #1	Antelope		x	Sanish/Madison
TEX	*	5088	NENW35-156-093	Mountrail	Shell	Texel 21-35		x		
ASW	*	2967	NWSE 03-152-096	McKenzie	Texaco	A.S.Wisness #2	Keene		x	Madison
MIN	*	1858	NWNE 25-150-096	McKenzie	Amerada	Minnie Kummer TI #1		x		
UST	*	2226	SWNW 18-153-094	McKenzie	Amerada	U.S.A. Thomas #1				
WEB	*	6082	SENW 18-145-097	Dunn	Gulf	Martin Weber #1-18-1C	Little Knife		x	Madison
XYZ	*	8363	NWNE 23-143-102	Billings	Coastal Oil & Gas	23-143-102 BN #1	Elkhorn Ranch		x	Bakken
MOI	*	12162	NWSW 21-143-101	Billings	Meridian Oil	MOI #13-21	Elkhorn Ranch		x	Bakken
Oils										
BY			21-148N-100W	Dunn	Conoco	Federal A-4	Bully			
LB			10-148N-96W	McKenzie	Conoco	Wiser Com. 1	Lost Bridge			
ER-1			10-143N-102W	Billings	Conoco	Federal No. 2	Elkhorn Ranch			
ER-2			3-142-102	Billings	Maxus Energy	Rauch Shapiro Fee 22-9R	Roosevelt			
ER-3			143-102	Billings	Conoco	Federal No. 1	Elkhorn Ranch			

Tab. A-2: Input data sheet for permeability measurements for samples of well SKA. Note increasing confining pressure.

Sample: SKA (E34435)
Sample thickness 11.04 mm
Sample diameter 28.15 mm
Sample cross-section 6.22E-04 m²

Pressure difference 2.73E+06 Pa 27.3 bar
Pressure gradient 2.47E+08 Pa/m

Temperature (T) 23 °C 296.15 K
Water viscosity 9.50E-01 cP 9.50E-04 Pa s
Calculation of flowrate
Start of exp.: 03. Feb 94 10:39

Date	Time	Volume [ml]	Time [h]	Flow Rate [m³/s]	Confining Pressure [MPa]	Flux [m/s]	Permeability [m²]	Darcy	nDarcy
03. 02	10:39	0.00	0.0		8				
03. 02	10:45	0.10	0.1	2.78E-10	8	4.46E-07	**1.7E-18**	1.71E-06	1713.78
03. 02	10:51	0.2	0.2	2.78E-10	8	4.46E-07	**1.7E-18**	1.71E-06	1713.78
03. 02	11:04	0.4	0.4	2.56E-10	8	4.12E-07	**1.6E-18**	1.58E-06	1581.95
03. 02	11:22	0.6	0.7	1.85E-10	8	2.98E-07	**1.1E-18**	1.14E-06	1142.52
average flow				2.49E-10		4.01E-07	**1.5E-18**	1.54E-06	1538.01
integral flow				2.33E-10		3.74E-07	**1.4E-18**	1.43E-06	1434.79

Sample: SKA (E34435)
Sample thickness 7.76 mm
Sample diameter 28.15 mm
Sample cross-section 6.22E-04 m²

Pressure difference 2.73E+06 Pa 27.3 bar
Pressure gradient 3.52E+08 Pa/m

Temperature (T) 23 °C 296.15 K
Water viscosity 9.50E-01 cP 9.50E-04 Pa s
Calculation of flowrate
Start of exp.: 03. Feb 94 12:28

Date	Time	Volume [ml]	Time [h]	Flow Rate [m³/s]	Confining Pressure [MPa]	Flux [m/s]	Permeability [m²]	Darcy	nDarcy
03. 02	12:28	0.00	0.0		10				
03. 02	12:42	0.12	0.2	1.43E-10	10	2.30E-07	**6.2E-19**	6.20E-07	619.52
03. 02	12:51	0.2	0.4	1.48E-10	10	2.38E-07	**6.4E-19**	6.42E-07	642.46
03. 02	13:03	0.3	0.6	1.39E-10	10	2.23E-07	**6.0E-19**	6.02E-07	602.31
03. 02	14:10	0.82	1.7	1.29E-10	10	2.08E-07	**5.6E-19**	5.61E-07	560.96
03. 02	14:20	0.9	1.9	1.33E-10	10	2.14E-07	**5.8E-19**	5.78E-07	578.22
average flow				1.39E-10		2.23E-07	**6.0E-19**	6.01E-07	600.69
integral flow				1.34E-10		2.15E-07	**5.8E-19**	5.81E-07	580.80

Sample: SKA (E34435)
Sample thickness 7.76 mm
Sample diameter 28.15 mm
Sample cross-section 6.22E-04 m²

Pressure difference 2.73E+06 Pa 27.3 bar
Pressure gradient 3.52E+08 Pa/m

Temperature (T) 23 °C 296.15 K
Water viscosity 9.50E-01 cP 9.50E-04 Pa s
Calculation of flowrate
Start of exp.: 04. Feb 94 14:28

Date	Time	Volume [ml]	Time [h]	Flow Rate [m³/s]	Confining Pressure [MPa]	Flux [m/s]	Permeability [m²]	Darcy	nDarcy
04. 02	14:28	0.00	0.0		12				
04. 02	15:21	0.06	0.9	1.89E-11	12	3.03E-08	**8.2E-20**	8.18E-08	81.82
04. 02	16:27	0.16	2.0	2.53E-11	12	4.06E-08	**1.1E-19**	1.10E-07	109.51
04. 02	17:19	0.23	2.9	2.24E-11	12	3.60E-08	**9.7E-20**	9.73E-08	97.30
average flow				2.22E-11		3.56E-08	**9.6E-20**	9.62E-08	96.21
integral flow				2.24E-11		3.60E-08	**9.7E-20**	9.72E-08	97.21

Data sheet for permeability measurement

Sample: SKA (E34435)
Sample thickness 7.76 mm
Sample diameter 28.15 mm
Sample cross-section 6.22E-04 m²

Pressure difference 3.40E+06 Pa 34 bar
Pressure gradient 4.38E+08 Pa/m

Temperature (T) 23 °C 296.15 K
Water viscosity 9.50E-01 cP 9.50E-04 Pa s

Calculation of flowrate
Start of exp.: 06. Feb 94 12:30

Date	Time	Volume [ml]	Time [h]	Flow Rate [m³/s]	Confining Pressure [MPa]	Flux [m/s]	Permeability [m²]	Darcy	nDarcy
06. 02	12:30	0.00	0.0		20				
07. 02	08:15	0.27	19.7	3.80E-12	20	6.10E-09	**1.3E-20**	1.32E-08	13.22
07. 02	12:28	0.33	24.0	3.95E-12	20	6.35E-09	**1.4E-20**	1.38E-08	13.76
07. 02	13:49	0.35	25.3	4.12E-12	20	6.61E-09	**1.4E-20**	1.43E-08	14.33
average flow				3.96E-12		6.35E-09	**1.4E-20**	1.38E-08	13.77
integral flow				3.84E-12		6.17E-09	**1.3E-20**	1.34E-08	13.37

Sample: SKA (E34443)
Sample thickness 7.76 mm
Sample diameter 28.15 mm
Sample cross-section 6.22E-04 m²

Pressure difference 5.00E+06 Pa 50 bar
Pressure gradient 6.44E+08 Pa/m

Temperature (T) 23 °C 296.15 K
Water viscosity 9.50E-01 cP 9.50E-04 Pa s

Calculation of flowrate
Start of exp.: 18. Mär 94 14:15

Date	Time	Volume [ml]	Time [h]	Flow Rate [m³/s]	Confining Pressure [MPa]	Flux [m/s]	Permeability [m²]	Darcy	nDarcy
18. 03	14:15	0.00	0.0		10				
18. 03	14:40	0.02	0.4	1.33E-11	10	2.14E-08	**3.2E-20**	3.16E-08	31.57
19. 03	13:40	0.21	23.4	2.29E-12	10	3.69E-09	**5.4E-21**	5.43E-09	5.43
20. 03	17:10	0.38	50.9	1.72E-12	10	2.76E-09	**4.1E-21**	4.07E-09	4.07
20. 03	21:05	0.41	54.8	2.13E-12	10	3.42E-09	**5.0E-21**	5.04E-09	5.04
21. 03	08:45	0.48	66.5	1.67E-12	10	2.68E-09	**3.9E-21**	3.95E-09	3.95
21. 03	09:45	0.49	67.5	2.78E-12	10	4.46E-09	**6.6E-21**	6.58E-09	6.58
average flow				3.99E-12		6.40E-09	**9.4E-21**	9.44E-09	9.44
integral flow				2.02E-12		3.24E-09	**4.8E-21**	4.77E-09	4.77

Sample: SKA (E34444)
Sample thickness 9.89 mm
Sample diameter 28.05 mm
Sample cross-section 6.18E-04 m²

Pressure difference 5.00E+06 Pa 50 bar
Pressure gradient 5.06E+08 Pa/m

Temperature (T) 23 °C 296.15 K
Water viscosity 9.50E-01 cP 9.50E-04 Pa s

Calculation of flowrate
Start of exp.: 22. Mär 94 11:25

Date	Time	Volume [ml]	Time [h]	Flow Rate [m³/s]	Confining Pressure [MPa]	Flux [m/s]	Permeability [m²]	Darcy	nDarcy
22. 03	11:25	0.00	0.0		10				
22. 03	12:15	0.04	0.8	1.33E-11	10	2.16E-08	**4.1E-20**	4.05E-08	40.52
22. 03	13:55	0.1	2.5	1.00E-11	10	1.62E-08	**3.0E-20**	3.04E-08	30.39
22. 03	15:15	0.15	3.8	1.04E-11	10	1.69E-08	**3.2E-20**	3.17E-08	31.66
22. 03	17:10	0.2	5.8	7.25E-12	10	1.17E-08	**2.2E-20**	2.20E-08	22.02
22. 03	19:15	0.27	7.8	9.33E-12	10	1.51E-08	**2.8E-20**	2.84E-08	28.37
23. 03	08:40	0.63	21.2	7.45E-12	10	1.21E-08	**2.3E-20**	2.27E-08	22.65
average flow				9.63E-12		1.56E-08	**2.9E-20**	2.93E-08	29.27
integral flow				8.24E-12		1.33E-08	**2.5E-20**	2.50E-08	25.03

Tab. A-3: Input data sheet for permeability measurements for samples of well TEX.

Sample:	TEX (E34333)		
Sample thickness	*6.47*	mm	
Sample diameter	28.41	mm	
Sample cross-section	6.339E-04	m²	
Confining pressure	1.70E+07	Pa	
Pressure difference	8.00E+06	Pa	80 bar
Pressure gradient	1.24E+09	Pa/m	
Temperature (T)	*23*	°C	296.15 K
Water viscosity at T °C	9.50E-01	cP	9.50E-04 Pa s

Calculation of flowrate

Start of exp.: 27. Mai 93 15:11

Date	Time	Volume [ml]	Time [h]	Flow Rate [m³/s]	Confining Pressure [MPa]	Flux [m/s]	Permeability [m²]	Darcy	nDarcy
27.05.1993	15:11	0.00	0.0		17				
27.05.1993	16:00	0.20	0.8	6.80E-11	17	1.07E-07	**8.2E-20**	8.24E-08	82
27.05.1993	17:45	0.52	2.6	5.08E-11	17	8.01E-08	**6.2E-20**	6.15E-08	62
28.05.1993	08:05	2.12	16.9	3.10E-11	17	4.89E-08	**3.8E-20**	3.76E-08	38
28.05.1993	10:10	2.20	19.0	1.07E-11	17	1.68E-08	**1.3E-20**	1.29E-08	13
28.05.1993	11:45	2.40	20.6	3.51E-11	17	5.54E-08	**4.3E-20**	4.25E-08	43
28.05.1993	15:15	2.70	24.1	2.38E-11	17	3.76E-08	**2.9E-20**	2.88E-08	29
28.05.1993	16:50	2.84	25.6	2.46E-11	17	3.87E-08	**3.0E-20**	2.98E-08	30
average flow				3.49E-11		5.50E-08	**4.2E-20**	4.22E-08	42
integral flow				3.08E-11		4.85E-08	**3.7E-20**	3.73E-08	37

Tab. A-4: Input data sheet for permeability measurements for samples of well XYZ

Sample:	XYZ (E34355)		
Sample thickness	*6.76*	mm	
Sample diameter	28.46	mm	
Sample cross-section	6.362E-04	m²	
Confining pressure	1.70E+07	Pa	
Pressure difference	8.00E+06	Pa	80 bar
Pressure gradient	1.18E+09	Pa/m	
Temperature (T)	*29*	°C	302.15 K
Water viscosity at T °C	8.32E-01	cP	8.32E-04 Pa s

Calculation of flowrate

Start of exp.: 26. Mai 93 15:30

Date	Time	Volume [ml]	Time [h]	Flow Rate [m³/s]	Confining Pressure [MPa]	Flux [m/s]	Permeability [m²]	Darcy	nDarcy
26.05.1993	15:30	0.00	0.0		12				
26.05.1993	16:55	0.29	1.4	5.69E-11	12	8.94E-08	**6.3E-20**	6.29E-08	63
26.05.1993	18:30	0.50	3.0	3.68E-11	12	5.79E-08	**4.1E-20**	4.07E-08	41
27.05.1993	08:15	1.60	16.7	2.22E-11	12	3.49E-08	**2.5E-20**	2.46E-08	25
27.05.1993	09:45	1.79	18.2	3.52E-11	12	5.53E-08	**3.9E-20**	3.89E-08	39
27.05.1993	12:00	2.10	20.5	3.83E-11	12	6.02E-08	**4.2E-20**	4.23E-08	42
average flow				3.79E-11		5.95E-08	**4.2E-20**	4.19E-08	42
integral flow				2.85E-11		4.47E-08	**3.1E-20**	3.15E-08	31

Tab. A-5: Input data sheet for permeability measurements for samples of well FED. Note increasing confining pressure.

Sample: FED (E34423)
Sample thickness 5.09 mm
Sample diameter 28.07 mm
Sample cross-section 6.19E-04 m²

Pressure difference 2.46E+06 Pa 24.6 bar
Pressure gradient 4.83E+08 Pa/m

Temperature (T) 23 °C 296.15 K
Water viscosity 9.50E-01 cP 9.50E-04 Pa s
Calculation of flowrate
Start of exp.: 22. Feb 94 14:46

Date	Time	Volume [ml]	Time [h]	Flow Rate [m³/s]	Confining Pressure [MPa]	Flux [m/s]	Permeability [m²]	Darcy	nDarcy
22. 02	14:46	0.05	0.0		8				
22. 02	15:21	0.22	0.6	7.86E-11	8	1.27E-07	**2.5E-19**	2.49E-07	249.44
22. 02	15:37	0.28	0.8	6.77E-11	8	1.09E-07	**2.1E-19**	2.15E-07	214.96
22. 02	15:55	0.355	1.2	6.94E-11	8	1.12E-07	**2.2E-19**	2.20E-07	220.47
average flow				7.19E-11		1.16E-07	**2.3E-19**	2.28E-07	228.29
integral flow				7.37E-11		1.19E-07	**2.3E-19**	2.34E-07	233.89

Sample: FED (E34423)
Sample thickness 5.09 mm
Sample diameter 28.07 mm
Sample cross-section 6.19E-04 m²

Pressure difference 2.46E+06 Pa 24.6 bar
Pressure gradient 4.83E+08 Pa/m

Temperature (T) 23 °C 296.15 K
Water viscosity 9.50E-01 cP 9.50E-04 Pa s
Calculation of flowrate
Start of exp.: 23. Feb 94 10:15

Date	Time	Volume [ml]	Time [h]	Flow Rate [m³/s]	Confining Pressure [MPa]	Flux [m/s]	Permeability [m²]	Darcy	nDarcy
23. 02	10:15	0.00	0.0		14				
23. 02	10:43	0.04	0.5	2.38E-11	14	3.85E-08	**7.6E-20**	7.56E-08	75.59
23. 02	11:08	0.08	0.9	2.67E-11	14	4.31E-08	**8.5E-20**	8.47E-08	84.66
23. 02	11:27	0.11	1.2	2.63E-11	14	4.25E-08	**8.4E-20**	8.35E-08	83.55
23. 02	12:34	0.23	2.3	2.99E-11	14	4.82E-08	**9.5E-20**	9.48E-08	94.77
23. 02	13:00	0.28	2.7	3.21E-11	14	5.18E-08	**1.0E-19**	1.02E-07	101.75
23. 02	13:12	0.3	3.0	2.78E-11	14	4.49E-08	**8.8E-20**	8.82E-08	88.19
average flow				2.77E-11		4.48E-08	**8.8E-20**	8.81E-08	88.08
integral flow				2.82E-11		4.56E-08	**9.0E-20**	8.97E-08	89.68

Sample: FED (E34423)
Sample thickness 5.09 mm
Sample diameter 28.07 mm
Sample cross-section 6.19E-04 m²

Pressure difference 2.46E+06 Pa 24.6 bar
Pressure gradient 4.83E+08 Pa/m

Temperature (T) 23 °C 296.15 K
Water viscosity 9.50E-01 cP 9.50E-04 Pa s
Calculation of flowrate
Start of exp.: 23. Feb 94 13:15

Date	Time	Volume [ml]	Time [h]	Flow Rate [m³/s]	Confining Pressure [MPa]	Flux [m/s]	Permeability [m²]	Darcy	nDarcy
23. 03	13:15	0	0.0		16				
23. 03	14:02	0.04	0.8	1.42E-11	16	2.29E-08	**4.5E-20**	4.50E-08	45.03
23. 03	15:09	0.12	1.9	1.99E-11	16	3.22E-08	**6.3E-20**	6.32E-08	63.18
23. 03	15:36	0.145	2.3	1.54E-11	16	2.49E-08	**4.9E-20**	4.90E-08	48.99
23. 03	16:14	0.185	3.0	1.75E-11	16	2.83E-08	**5.6E-20**	5.57E-08	55.70
average flow				1.68E-11		2.71E-08	**5.3E-20**	5.32E-08	53.22
integral flow				1.72E-11		2.78E-08	**5.5E-20**	5.47E-08	54.69

Sample: FED (E34423)
Sample thickness 5.09 mm
Sample diameter 28.07 mm
Sample cross-section 6.19E-04 m²

Pressure difference 2.46E+06 Pa 24.6 bar
Pressure gradient 4.83E+08 Pa/m

Temperature (T) 23 °C 296.15 K
Water viscosity 9.50E-01 cP 9.50E-04 Pa s
Calculation of flowrate
Start of exp.: 23. Feb 94 16:25

Date	Time	Volume [ml]	Time [h]	Flow Rate [m³/s]	Confining Pressure [MPa]	Flux [m/s]	Permeability [m²]	Darcy	nDarcy
23. 02	16:25	0.00	0.0		18				
23. 02	17:25	0.07	1.0	1.94E-11	18	3.14E-08	6.2E-20	6.17E-08	61.73
average flow				1.94E-11		3.14E-08	6.2E-20	6.17E-08	61.73
integral flow				1.94E-11		3.14E-08	6.2E-20	6.17E-08	61.73

Sample: FED (E34433)
Sample thickness 16.96 mm
Sample diameter 28.14 mm
Sample cross-section 6.22E-04 m²

Pressure difference 5.22E+06 Pa 52.15 bar
Pressure gradient 3.07E+08 Pa/m

Temperature (T) 30 °C 303.15 K
Water viscosity 8.15E-01 cP 8.15E-04 Pa s
Calculation of flowrate
Start of exp.: 26. Jul 94 11:37

Date	Time	Volume [ml]	Time [h]	Flow Rate [m³/s]	Confining Pressure [MPa]	Flux [m/s]	Permeability [m²]	Darcy	nDarcy
26. 07	11:37	0.00	0.0		14				
26. 07	15:30	0.03	3.9	2.15E-12	14	3.45E-09	9.1E-21	9.14E-09	9.14
26. 07	17:45	0.06	6.1	3.70E-12	14	5.96E-09	1.6E-20	1.58E-08	15.78
27. 07	10:50	0.53	23.2	7.64E-12	14	1.23E-08	3.3E-20	3.26E-08	32.56
27. 07	13:30	0.64	25.9	1.15E-11	14	1.84E-08	4.9E-20	4.88E-08	48.83
27. 07	15:00	0.73	27.4	1.67E-11	14	2.68E-08	7.1E-20	7.10E-08	71.02
average flow				8.32E-12		1.34E-08	3.5E-20	3.55E-08	35.47
integral flow				7.41E-12		1.19E-08	3.2E-20	3.16E-08	31.55

Sample: FED (E34433) reverse flow direction!!
Sample thickness 16.96 mm
Sample diameter 28.14 mm
Sample cross-section 6.22E-04 m²

Pressure difference 5.86E+06 Pa 58.55 bar
Pressure gradient 3.45E+08 Pa/m

Temperature (T) 30 °C 303.15 K
Water viscosity 8.15E-01 cP 8.15E-04 Pa s
Calculation of flowrate
Start of exp.: 28. Jul 94 14:10

Date	Time	Volume [ml]	Time [h]	Flow Rate [m³/s]	Confining Pressure [MPa]	Flux [m/s]	Permeability [m²]	Darcy	nDarcy
28. 07	14:10	0.00	0.0		14				
28. 07	15:45	0.29	1.6	5.09E-11	14	8.18E-08	1.9E-19	1.93E-07	193.10
28. 07	16:50	0.5	2.7	5.38E-11	14	8.66E-08	2.0E-19	2.04E-07	204.36
28. 07	18:20	0.82	4.2	5.93E-11	14	9.53E-08	2.2E-19	2.25E-07	224.91
average flow				5.47E-11		8.79E-08	2.1E-19	2.07E-07	207.46
integral flow				5.47E-11		8.79E-08	2.1E-19	2.07E-07	207.48

Table B: Data as derived from organic carbon determination and Rock-Eval analysis. Well # refers to location of wells in study area (Fig. 6).

Sample ID	Well name (#)	TOC (wt.-%)	S1 (mg HC /g rock)	T_{max} (°C)	HI (mg HC /g TOC)	OI (mg CO_2 /g TOC)	Shale Unit	
E34257	PIE*	1.15	0.44	414	117	11		IBK
E34258		2.61	0.39	421	124	8		IBK
E34259		3.22	0.72	423	92	4		IBK
E34260		3.69	1.13	424	142	4		IBK
E34261		3.15	1.17	421	131	2		IBK
E34262		3.62	0.7	424	103	3		IBK
E34267	DOB (1)	2.98	0.56	425	142	23	uBK	
E34268		17.7	7.75	419	605	13	uBK	
E34269		17.8	7.72	421	648	12	uBK	
E34270		12.5	5.25	421	580	18	uBK	
E34271		18.5	6.18	419	612	13	uBK	
E34272		20.8	8.2	417	561	19	uBK	
E34273		16.9	5.93	424	619	12	uBK	
E34275		15	5.6	421	606	14	uBK	
E34276		12.7	5.19	419	579	19	uBK	
E34277		17.6	6.76	421	610	13	uBK	
E34278		17.1	7.77	418	610	14	uBK	
E34279		20.7	8.13	419	613	13	uBK	
E34280		18.9	8.39	420	651	13	uBK	
E34283		4.34	0.83	422	182	18		IBK
E34284		3.7	0.69	419	121	15		IBK
E34285		3.14	0.67	425	133	12		IBK
E34286		3.35	0.78	422	12	1		IBK
E34263	JAC (2)	17	7.78	430	559	7		IBK
E34264		19.4	9.08	424	570	1		IBK
E34265		16.3	6.85	428	558	14		IBK
E34287	NEG (3)	15.9	5.35	433	509	11	uBK	
E34288		20.3	8.23	430	502	8	uBK	
E34289		14.6	4.85	432	549	12	uBK	
E34290		6.44	1.86	432	454	17	uBK	
E34291	WAS*	10.1	2.28	421	484	36		IBK
E34292		3.47	0.59	429	318	28		IBK
E34293		13.4	3.92	415	545	24		IBK
E34294		18.3	4.72	416	531	22		IBK
E34295		13.2	3.84	414	525	25		IBK
E34296		8.99	1.75	417	504	34		IBK
E34299	FOR*	11.6	4.96	435	231	13		IBK
E34300		1.06	3.27	436	255	13		IBK
E34301		15.1	3.71	441	256	9		IBK
E34302	GIL*	14.9	3.99	446	154	9		IBK
E34303		13.1	4.31	445	161	13		IBK
E34304	HHS*	13	3.78	453	121	9	uBK	
E34305	REE*	14.3	4.4	449	142	8		IBK

Sample ID	Well name (#)	TOC (wt.-%)	S1 (mg HC /g rock)	T_{max} (°C)	HI (mg HC /g TOC)	OI (mg CO_2 /g TOC)	Shale Unit	
E34435	SKA (4)	9.87	2.1	445	282	1	uBK	
E34436		11.1	2.64	440	302	8	uBK	
E34437		10.6	2.31	444	306	8	uBK	
E34438		15.5	4.1	439	332	4	uBK	
E34439		17.4	4.02	441	363	5	uBK	
E34440		11.9	3.25	439	311	7	uBK	
E34441		12.9	3.83	439	321	5	uBK	
E34442		13.6	4.67	439	336	4	uBK	
E34443		16.1	5.13	438	364	4	uBK	
E34444		12.3	3.38	442	348	8	uBK	
E34445		9.01	2.65	435	321	7	uBK	
E34306	BOR (5)	13.1	2.38	443	344	12	uBK	
E34307		12.7	2.89	437	365	11	uBK	
E34308		13.2	3.4	443	400	1	uBK	
E34317	JOH*	12.8	3.83	445	135	18		IBK
E34318		12.6	6.25	441	121	1		IBK
E34319		4.62	2.49	445	122	15		IBK
E34332	TEX*	2.95	2.67	435	192	15		IBK
E34333		7.57	3.38	442	317	11		IBK
E34334	ASW*	11.1	5.06	446	121	14		IBK
E34335		13.1	5.14	442	92	7		IBK
E34336		11.1	4.78	449	117	11		IBK
E34337	MIN*	14.3	4.74	445	157	8		IBK
E34338		11.9	4.42	441	117	11		IBK
E34342	SET (7)	8.97	4.92	441	165	15		IBK
E34343		12.8	5.39	440	147	7		IBK
E34344		13.7	5.79	440	159	7		IBK
E34345		11.2	3.71	441	158	7		IBK
E34364	GRA (6)	9.25	3.55	441	165	1	uBK	
E34365		7.3	2.7	446	175	9	uBK	
E34366		10.3	3.12	441	142	11	uBK	
E34368		10.1	1.29	442	173	109	uBK	
E34320	MAR (8)	9.06	2.43	447	165	18	uBK	
E34321		10.3	3.8	440	148	21	uBK	
E34322		13.3	4.39	437	143	11	uBK	
E34323		10.4	3.22	444	173	6	uBK	
E34324		11.2	3.56	444	175	12	uBK	
E34325		8.74	3.24	439	142	16	uBK	
E34326		12	3.64	443	176	1	uBK	
E34327		5.43	1.82	437	127	13		IBK
E34328		8.24	4.44	441	112	7		IBK
E34330		5.54	2.79	438	140	24		IBK

Table B (cont.)

Sample ID	Well name (#)	TOC (wt.-%)	S1 (mg HC /g rock)	T_{max} (°C)	HI (mg HC /g TOC)	OI (mg CO_2 /g TOC)	Shale Unit
E34310	JEN (9)	12.2	3.66	443	174	13	uBK
E34311		11.4	3.71	441	167	11	uBK
E34312		13	3.75	439	184	9	uBK
E34313		11.8	4.39	440	147	6	uBK
E34316		12.2	4.63	440	168	19	uBK
E34449		10.4	2.87	444	161	1	lBK
E34454		12.6	1.5	443	153	7	lBK
E34455		8.87	4.01	442	131	11	lBK
E34353	WEB*	8.48	4.25	444	142	9	uBK
E34354		11.2	6.1	441	134	11	uBK
E34355	XYZ*	10.9	3.23	445	194	5	uBK
E34356		10	3.51	442	204	8	uBK
E34357	MOI*	9.54	3.66	448	121	7	lBK
E34358		9.54	3.7	442	111	12	lBK
E34372	CON (10)	12.3	4.25	444	191	13	uBK
E34373		11.6	4.39	440	164	9	uBK
E34374		9.17	3.5	445	166	15	uBK
E34375		9.31	4.11	440	167	13	uBK
E34376		11.5	4.04	444	184	12	uBK
E34377		12.1	4.54	442	176	8	uBK
E34378		8.45	3.85	449	163	4	uBK
E34379		10.9	3.72	440	186	9	uBK
E34380		11.1	3.97	440	186	1	uBK
E34381		12.7	4.19	446	211	7	uBK
E34382		11.1	3.89	441	209	6	uBK
E34383		10.2	4.22	440	167	7	uBK
E34384		8.31	3.12	446	186	13	uBK
E34385		11	4.44	440	188	9	uBK
E34386		12.2	3.98	445	210	9	uBK
E34387		7.63	4.48	439	155	13	uBK
E34388		12.6	4.59	446	209	9	uBK
E34389		12.8	5.29	442	236	5	uBK
E34390		12.5	3.8	445	211	1	uBK
E34391		12.3	3.72	440	204	7	uBK
E34392		7.2	3.51	439	182	11	uBK
E34393		12.5	3.64	445	218	9	uBK
E34394		10.7	4.12	438	192	7	uBK
E34395		9.24	3.26	445	182	13	uBK
E34396		12.7	4.12	437	215	8	uBK
E34397		12.6	4.04	445	229	8	uBK
E34398		13	4.22	441	201	8	uBK
E34399		13.8	5.03	440	220	1	uBK
E34400		13.4	3.75	445	231	8	uBK
E34401		13.5	3.82	441	217	9	uBK
E34402		13.5	3.52	444	228	6	uBK
E34403	CON	13.6	4.58	438	217	6	uBK
E34404	(cont.)	13.4	3.75	445	231	8	uBK
E34405		12.6	3.86	439	206	1	uBK
E34406		13.8	4.26	438	221	9	uBK
E34407		13.4	4.34	442	231	7	uBK
E34408		13.1	4.47	437	203	1	uBK
E34409		12.9	3.82	446	225	8	uBK
E34410		12.6	4.28	446	201	1	uBK
E34411		13.1	5.13	438	200	4	uBK
E34412		12.9	3.46	442	213	8	uBK
E34413		12.8	3.88	445	199	5	uBK
E34414		13	3.64	441	213	8	uBK
E34415		12.4	4.12	445	209	6	uBK
E34416		13.1	3.68	440	220	7	uBK
E34417		12.7	4.05	445	204	7	uBK
E34418		12.8	4.1	439	207	9	uBK
E34419		12.8	3.24	438	214	8	uBK
E34420		12.7	3.53	445	197	7	uBK
E34421		12.7	4	441	219	7	uBK
E34422	FED (11)	12.4	3.57	447	199	7	uBK
E34423		11.8	4.84	438	178	1	uBK
E34424		12.7	4.41	437	184	6	uBK
E34425		12.5	3.88	443	186	6	uBK
E34426		11	4.36	442	188	6	uBK
E34427		8.62	3.2	441	169	9	uBK
E34428		7.99	3.47	449	213	6	uBK
E34429		8.65	3.85	442	164	11	uBK
E34430		10.2	3.87	444	196	9	uBK
E34431		11.3	3.21	446	208	9	uBK
E34432		13.5	3.69	442	322	6	uBK
E34433		11.3	3.03	445	206	7	uBK
E34434		13.9	4.85	440	224	3	uBK
E34347	HOV (12)	10.2	4.53	443	87	7	lBK
E34348		10.2	3.84	446	105	5	lBK
E34349		10.8	4.88	443	92	5	lBK
E34350		12.1	4.25	447	106	5	lBK
E34351		10	4.03	442	89	5	lBK
E34331	BEH (13)	11.9	4.03	444	177	2	uBK
E34360	TIO (14)	11.8	5.38	445	98	2	uBK
E34361		8.95	3.96	451	111	6	uBK
E34362		11.9	5.19	444	99	3	uBK
E34339	UST*	1.16	0.79	417	87	47	lBK
E34340		6.07	4.76	445	118	13	lBK
E34341		5.14	3.3	443	122	6	lBK

Tab. C: Spreadsheet with input data and results derived from mass balancing of Bakken Shale maturity sequence using calculations according to Cooles et al. (198

Cooles MassBalance		
	W	0.85
	Zv	0.3

immature reference sample: DOB (uBK, average values)

		TOC	S1 mg(HC)/g(rock)	S2 mg(HC)/g(rock)	S1C g(HC)/g(Corg)	HI g(HC)/g(Corg)	m(inert ker)/ m(Corg)	PGI(RE)	PEE(RE)	m(inert ker)/ m(rock)	TOC initial	% Rm
DOB	**average of 12 samples**	**17.18%**	**6.91**	**104.76**	**0.0488**	**0.5183**	0.4328			0.074	**17%**	0.31
JAC	average of 3 samples	17.57%	7.90	98.82	0.0546	0.4781	0.4673	0.22	0.59	0.082	**19%**	0.57
SKA	average of 11 samples	12.75%	3.46	42.08	0.0330	0.2805	0.6865	0.69	0.95	0.088	**20%**	0.68
BOR	average of 3 samples	13.00%	2.89	48.09	0.0270	0.3144	0.6586	0.64	0.95	0.086	**20%**	0.72
JEN	average of 9 samples	11.67%	4.17	19.10	0.0434	0.1391	0.8175	0.87	0.95	0.095	**22%**	0.92
MAR	average of 8 samples	10.41%	3.59	16.20	0.0419	0.1323	0.8258	0.88	0.96	0.086	**20%**	0.90
CON	average of 50 samples	11.96%	4.47	25.37	0.0454	0.1803	0.7743	0.82	0.95	0.093	**21%**	0.94
FED	average of 13 samples	11.22%	3.86	23.10	0.0418	0.1750	0.7832	0.83	0.95	0.088	**20%**	0.99
HOV	average of 5 samples	10.66%	4.31	10.25	0.0491	0.0817	0.8692	0.93	0.95	0.093	**21%**	1.11
BEH	average of 1 samples	11.90%	4.03	21.04	0.0411	0.1503	0.8086	0.86	0.95	0.096	**22%**	1.26
THO	average of 3 samples	10.88%	5.02	11.15	0.0560	0.0871	0.8569	0.92	0.95	0.093	**22%**	1.57

		TOC	TSE mg(HC)/g(rock)	TSE g(C)/g(Corg)	m(inert ker)/ m(Corg)	PGI(Ex)	PEE(Ex)	TOC initial	% Rm
DOB	**average of 12 samples**	**17.18%**	10.56	0.0128	0.4689			**17%**	0.31
JAC	average of 3 samples	17.57%	11.23	0.0136	0.5083	0.17	0.86	**19%**	0.57
SKA	average of 11 samples	12.75%	8.61	0.0105	0.7090	0.65	0.98	**19%**	0.68
BOR	average of 3 samples	13.00%	8.72	0.0106	0.6750	0.59	0.98	**19%**	0.72
JEN	average of 9 samples	11.67%	7.2	0.0087	0.8521	0.86	0.99	**21%**	0.92
MAR	average of 8 samples	10.41%	7.32	0.0089	0.8588	0.86	0.99	**19%**	0.90
CON	average of 50 samples	11.96%	7.02	0.0085	0.8112	0.80	0.99	**21%**	0.94
FED	average of 13 samples	11.22%	7.2	0.0087	0.8163	0.81	0.99	**20%**	0.99
HOV	average of 5 samples	10.66%	7.43	0.0090	0.9092	0.92	0.99	**21%**	1.11
BEH	average of 1 samples	11.90%	7.73	0.0094	0.8403	0.84	0.99	**21%**	1.26
THO	average of 3 samples	10.88%	6.77	0.0082	0.9047	0.92	0.99	**21%**	1.57

FORSCHUNGSZENTRUM JÜLICH GmbH

Jül-3094
July 1995
ISSN 0944-2952